Operation of Falling Film Evaporator involving Viscous Liquid

By

Chong Xun (Lawrence) Quek

A thesis submitted in fulfilment of the requirements for the degree

Doctor of Philosophy

at

Department of Chemical Engineering
Monash University
Clayton, Victoria 3800, Australia

March 2011

Copyright Notices

Notice 1

Notice 2

DECLARATION

This thesis contains no material that has been accepted for the awards of any other degree or diploma in any educational institution and, to the best knowledge and belief, it contains no materials published or written by another person, except where due reference is made in the text of the thesis.

Signed: _____ Date: _____

Chong Xun (Lawrence) Quek

ACKNOWLEDGEMENTS

This thesis arose in parts out of years of research that has been done since I came to the Biotechnology and Food Engineering Group in Monash University (Clayton Campus). By that time, I have worked with a great number of people whose contribution in assorted ways to the research project deserved special mention.

I would like to dedicate this PhD to my loving parents, Quek Seng Long and Tan Geok Bee. This thesis and my education until now would not have been possible with their support and encouragement. I will forever be in their debt for their love, support and faith in me.

I wish to express my sincerest appreciation and gratitude to my supervisor, Professor Xiao Dong Chen, who has supported me throughout my thesis with his patience and knowledge whilst allowing me the room to work in my own way. I would also wish to extend my appreciation to Dr Sean Lin who has assisted me with the design, construction and commission of the experimental rigs. His technical expertise with process equipments has made the operation of the experimental rigs a breeze.

My gratitude goes to Dairy Innovation Australia Limited for their generous financial support for my PhD project. Special thanks to Dr Mike Weeks, Mark Schleyer and Nicole Barnes from Dairy Innovation Australia Limited for their constructive suggestions and technical supports.

I sincerely thank the staff on the Chemical Engineering Department in Monash University (Clayton Campus) for their assistance. I would also like to mention the pleasant company and memorable moments by my fellow post-graduate colleagues during the course of this project.

ABSTRACT

In this thesis, the working principles of falling film evaporator used in dairy industries in relation to the evaporation of skim milk have been explored with a focus on the effect of milk solids content. The changes in rheological behaviour of skim milk and heat transfer within the evaporator during the concentration process have been investigated. With the better understanding of the rheological behaviour of skim milk and the operation of a falling film evaporator, the possibility of improving the performance of commercial falling film evaporator from its current configuration can be assessed.

The use of falling film evaporator is a common and economical practice in the food and beverage industries to remove water from liquid products, e.g. juices, milk, etc., especially when the product is temperature sensitive. In dairy industries, falling film evaporators are used to evaporate water from dairy products such as milk, protein concentrate, etc. Falling film evaporator is a well established technology but the understanding of rheological influence of milk on the performance and operation of falling film evaporator remains relatively unexplored which formed the motivation of this project.

In milk powder production, milk is normally concentrated from around 10wt% to 50wt% or 52wt% (this depends on the type of milk) using multi-effect falling film evaporator prior to the spray drying process. The viscosity changes of milk during the concentration process are evident, especially the exponential rise in viscosity as solids level reaches 50wt%. With the increase in viscosity, the flowing characteristics of the milks within the tubes in the evaporator change with the concentration of milk. Consequently, the performance of the evaporator, in terms of heat transfer, is considerably affected. The current research project has been divided into 3 main parts into context of viscosity and evaporation of milk using falling film evaporator. Firstly, viscosity models of milk are established based on stringent viscosity measurement procedures that ensure the repeatability and reliability of the measurements. These models are used for process simulation, model based control and production planning. The second part is to evaluate the performance of falling film evaporator under the

influences of various operation conditions. In the last part, findings from the first two sections are merged into a pilot evaporator mathematical model that is able to predict the solid content, flow characteristics and residence time of milk concentrate in a falling film evaporator.

The viscosity of milk is influenced by several factors such as solids content, temperature, ageing and shearing, etc. The focus in this thesis is on the instantaneous milk viscosity during the operation of the falling film evaporator. Therefore, viscosity measurements and modelling of the milk viscosity have been mainly focused on only on the effect of solids content, temperature and, to some extend, shear rate. A 2m steam-heated pilot evaporator was designed and constructed to commercial grade based on a falling film evaporator design. This pilot evaporator is able to operate under vacuum conditions (up to -85kPa gauge) in both shell and tube side so as to mimic the operation conditions in the dairy industries. The viscosity models in this thesis are predominately formulated based on the fresh and reconstituted medium heat-treated skim milk, unless otherwise stated. A comparison of viscosity models were made between the reconstituted and fresh skim milk. Significant differences were found and reported between the two types of milks.

The heat transfer coefficient (HTC), a common method of quantifying the performance of an evaporator, was measured based on temperature difference between the heat transfer surface and the processed fluid (e.g. milk) and the energy transfer within the evaporator. Another 1m electric-heated pilot evaporator was designed and built to facilitate the measurement at such temperatures and to have known power inputs which was not accessible in the steam-heated device. The influence of different operating conditions, such as varying heat flux, flow characteristics (e.g. Re number) and protein content, on the heat transfer coefficient is thoroughly investigated in this thesis. The study into the HTC on the product side found that the HTC measured from the evaporation of reconstituted skim milk is unresponsive to some of the operating conditions it was subjected to as compared to the fresh skim milk. Generally, HTC improves with greater Re number, heat flux and protein content (milk protein concentrate was added). Visual examination of the evaporation conditions within the

evaporator also indicates that the amount of bubble formed during the evaporation process appears to increase with increasing flow rate, heat flux and protein content.

During the formulation of the pilot evaporator model in this thesis, the viscosity models and heat transfer coefficients established in the current project were incorporated so as to model the steam-heated batch pilot evaporator. Several assumptions were introduced in order to create a working model. The pilot evaporator model has been verified against the actual experimental data and is proven to be accurate. This model is able to predict the solids content of the skim milk at any given time provided that the operating conditions are available. This model can also be applied onto a commercial falling film evaporator with minor modification to the calculation sequence. A scale-up version has been developed but due to commercial nature, it is not reported in this thesis.

The research into the operation of falling film evaporator has been seen to enhance the knowledge of the mechanisms and interactions between the process fluid and the evaporator. Some of the results obtained here have already benefited an industrial operation.

CONTENTS

LIST OF FIGURES

LIST OF TABLES

CHAPTER ONE: INTRODUCTION

1.0 INTRODUCTION

Milk, a good source of calcium, protein, vitamin A and B-12, potassium, phosphorous, niacin and riboflavin, is the first food ingested by young mammals, including human infants. Being a highly nutritional diet and extremely perishable product, it is desirable to preserve milk for later consumption. One of the most effective ways of preservation used today is drying. The moisture content in milk powder ranged from 2.5 to 5wt% and such low moisture content inhibits the growth of bacteria. With the advancement of technology, it is possible to turn milk into powder without scarifying its nutritional value. Besides preservation, another major benefit of converting milk into powder lies in the considerable reduction in transport and storage cost. However, owing to the thermal requirements, such as evaporation, spray drying, pasteurization and ultra-high temperature treatment, dairy processing consumes a considerable amount of energy despite of the utilization of more energy efficient technologies. In fact, there is no other process in the dairy industry that has a higher energy demand per tonne of finished product. Being an energy intensive industry, reduction in energy usage throughout the milk powder production is becoming progressively more important with the aim of protecting profitability with the rising fuel prices (Walton, 2005). For reference, Figure 1.1 shows the flow chart of various dairy products.

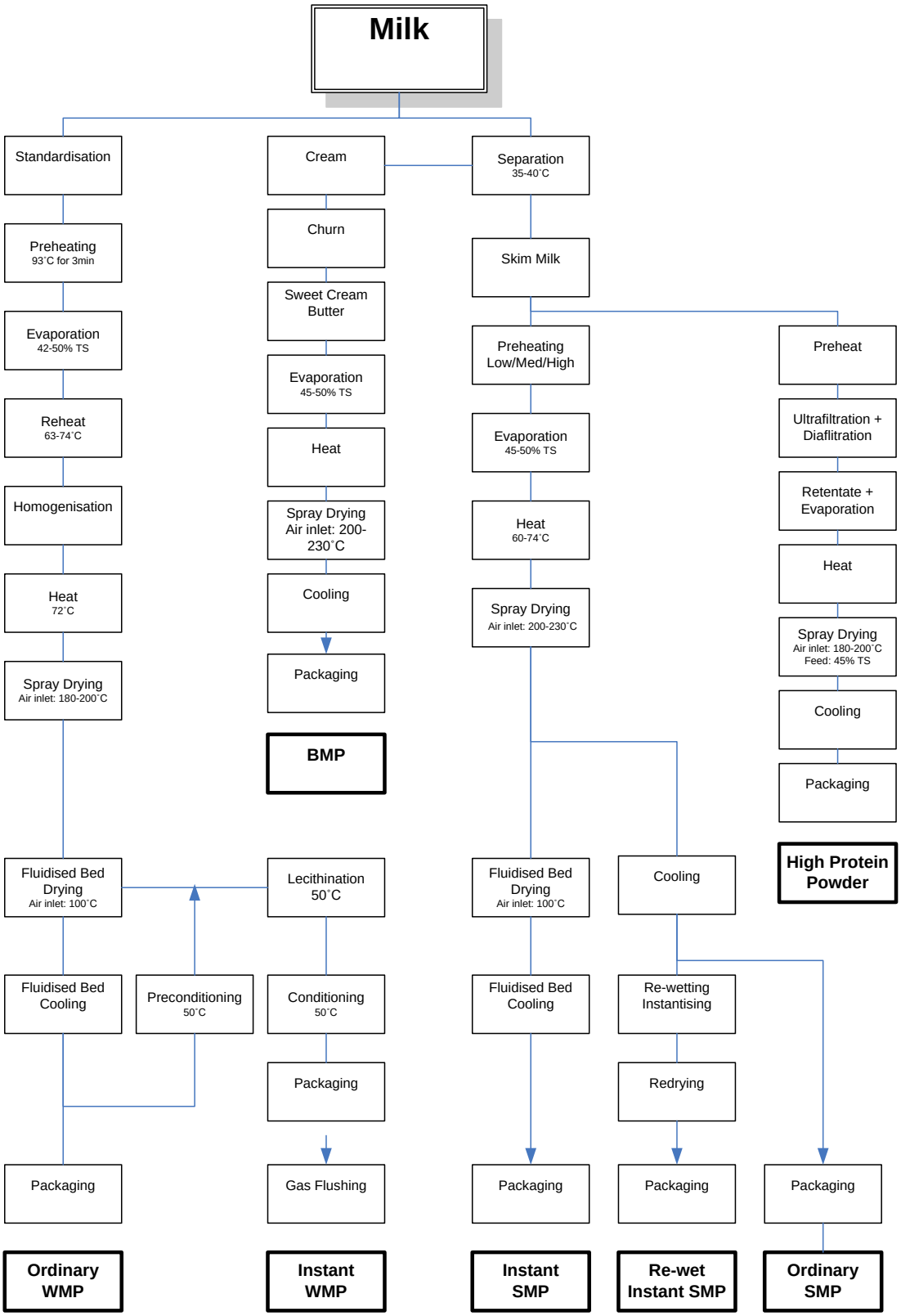

Figure 1.1. Flow chart of milk powder production

Evaporation is an important process in milk powder manufacturing. Milk is usually concentrated using multi-effect falling film evaporator to around 48 to 52 wt% depending on the type of milk being processed. After which, the concentrate is sent to the spray dryer for further processing. The fact that the multi-effect falling film evaporator is a lot more energy efficient than the spray dryer, it is desirable to remove as much water during the evaporation process as possible so that the drying load for thermal dryer in the subsequent processing is reduced. However, the limitation of doing so lies on the physical property of milk. At high concentration (above 45wt%), the viscosity for concentrated milk increases exponentially and the recommended operating viscosity of the falling film evaporator should not exceed 100 mPa.s to prevent excessive fouling and like wise for the spray dryer. Therefore, the viscosity is a crucial physical property when it comes to removal of water from milk.

The primary objective of this research project is to improve the quantitative understanding the mechanism and interaction between the process fluid (milk) and the falling film evaporator. Emphasis of this research work is on the establishment of robust viscosity models for milk and to investigate the factors that would influence the heat transfer within an evaporator. Thereafter, with the appropriate results gathered, evaluate the viability of improving the performance of commercial evaporator in their current configurations.

1.1 Outline of the Thesis

Chapter 2 provides an overview of the composition and physical properties of milk. These properties are the foundation of an evaporator model. Furthermore, they also provide insights to some of the phenomena observed during the experiments conducted.

Chapter 3 presents a detail study of milk viscosity and their models used by various previous authors. The design process of the steam-heated pilot evaporator and experimental work on the viscosity measurements are also documented. Comparisons in viscosity are made on the reconstituted and fresh skim milk and the factors that influence the milk viscosity are analysed. Mathematical models of skim milk viscosity are formulated in relation to total solids, temperature and shear rate (to some extents).

Chapter 4 presents the fundamental working principles of another falling film evaporator built in the current work. The design process of the electric-heated pilot evaporator and experimental work on the heat transfer coefficient (HTC) measurement are also reported. The relationship between HTC and Reynolds number (Re) is established.

Chapter 5 describes a falling film evaporator model based on the fundamental heat and mass transfer principles to predict the total solids in milk at any given time or position based on the type of evaporator used (batch or continuous).

Overall conclusions and summary of the present research work and general recommendations for future work are described in chapter 6.

CHAPTER TWO:
MILK COMPOSITIONS AND PROPERTIES

2.0 MILK COMPOSITIONS AND PROPERTIES

2.1 Introduction to the Composition of Milk

Milk is the fluid secretion by female mammals which primary purpose is to feed their young before they can digest other types of food. Milk provides neonate with energy, vital amino acids, fatty acids, vitamins and water (Fox, 2003). Therefore, milk is naturally packed full of essential nutrients that are beneficial for the well-being of new born mammals. The nutritional content varies from mammal to mammal due to the specific requirements by difference species. Composition variation also occurs in cows of different breed, stage of lactation, illness of cow and food to which the cow feed on. The main focus of this thesis is the milk of healthy cows, unless otherwise stated. The composition of cow's milk is complex and the main constituent includes proteins, fats, lactose and water. The detail compositions of milk are listed in Table 2.1.

Table 2.1 Approximate composition of milk (Walstra et al., 2006d)

Component	Average Content in Milk (wt%)	Range (wt%)	Average Content in Dry Matter (wt%)
Water	87.1	85.3 – 88.7	-
Solids-not-fat	8.99	7.9 – 10.0	-
Fat in dry matter	31	22 – 38	-
Lactose	4.6	3.8 – 5.3	36
Fat	4.0	2.5 – 5.5	31
Protein	3.3	2.3 – 4.4	25
Casein	2.6	1.7 – 3.5	20
Mineral substances	0.7	0.57 – 0.83	5.4
Organic acids	0.17	0.12 – 0.21	1.3
Miscellaneous	0.15	-	1.2

2.1.1 Milk proteins

The two types of protein that can be found in milk are whey proteins (aka serum proteins) and caseins. Caseins constitute about 80% of the total protein of milk. However, the ratio of caseins to whey protein varies with the stage of lactation.

2.1.1.1 Caseins

Approximately 95% of caseins in milk are presented in a colloidal form known as the micelles and it consists of water, protein and salts. Cations, mainly calcium and magnesium, are bind on casein micelles. The voluminous nature of micelles is highly hydrated which holds more water than dry matter (around 2 grams water per gram protein). To large extent, they are responsible for the rheological properties of concentrated milk products. The shape of casein micelles appears to be roughly spherical under electron microscope with diameter ranging 50 to 500 nm (average ~ 150nm). The white colour appearance of milk is largely owe to the light scattering capability of the micelles. Once the micelles structure is disrupted, the while colour is lost. Casein molecules are also resistant to denaturation as they have little secondary and tertiary structure.

There are four subclasses of caseins, namely, α_{s1}-, α_{s2}-, β-, κ- caseins and their molar ratio is about 11:3:10:4 (Walstra *et al.*, 2006c). They are concentrated at different sites of casein micelle and many variation of casein micelle model proposed (Waugh *et al.*, 1970; Payens, 1966; Rose and Colvin, 1966; Morr, 1967).

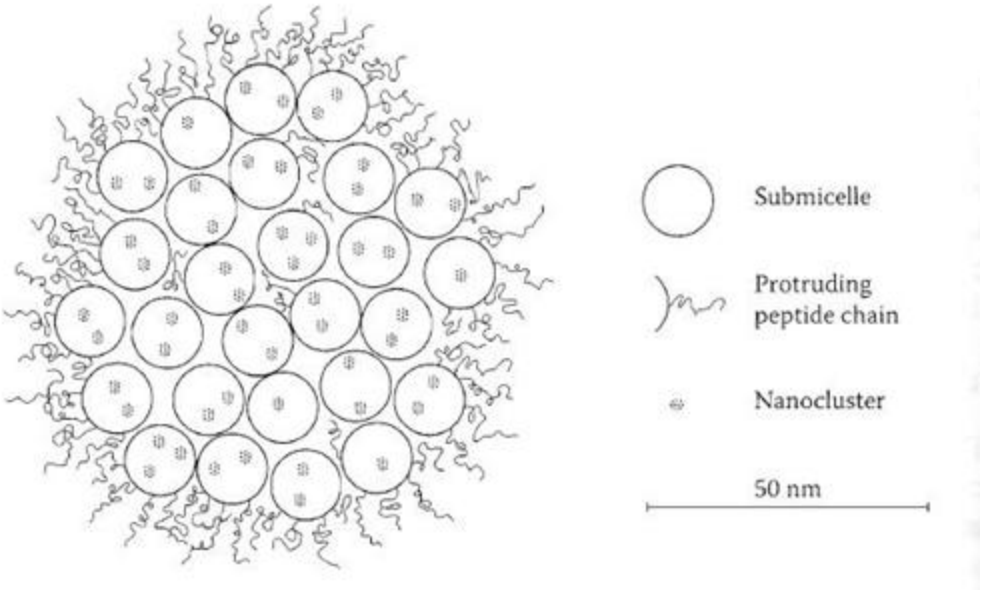

Figure 2.1 Cross section through a casein micelle (Walstra *et al.*, 2006a)

The model of a casein micelle in Figure 2.1 was proposed by Morr.(1967) It shows that the micelle is made up of a collection of submicelles of 10 to 15 nm in size bond together by colloidal calcium phosphate (CCP) and other forces, e.g. hydrophobic and hydrogen bonds. The grouping of submicelles results in an open and porous structure which is able to hold a lot of water within. Roughly the same amounts of α_s- and β-casein are located at the core of micelle while the outer layer consists of equal parts of κ- and α_s- casein with trace of β-casein. Since the κ-casein can only be found on the surface of a casein micelle, its concentration is proportional to the surface area of the micelles.(Walstra *et al.*, 2006a).

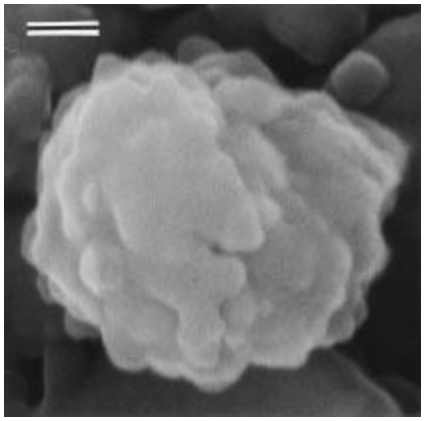

Figure 2.2 Stereo pair of scanning electron micrograph of casein micelle adsorbed on a ceramic membrane. Sample was coated with 2-nm layer of iridium before imaging at a magnification of 70,000. Bar = 100 nm.

(McMahon and McManus, 1998)

Although the model concurs with most of casein micelles' properties, some workers (Visser, 1992; Holt *et al.*, 1992; McMahon and McManus, 1998) remains sceptical about the existence of submicelles. The appearance of a submicellar structure was suggested by the raspberry-like structure from electron microscopy. However, the appearance on electron microscopy is subjected to the preparation technique of casein micelles like fixation, exchanging of water for ethanol, air-drying or metal coating of The cryopreparation method of casein micelles for TEM stereo imaging by McMahon and McManus (1998) suggest no indication of a submicellar structure or the submicelles is less densely packed than previously assumed to appear to be individual proteins.

Nevertheless, there are a few features of casein micelles that are generally agreed upon. The surface of casein micelles is covered by a 5-10 nm thick layer of highly hydrated "hairs". They are made up of C-terminal region of κ-casein (Walstra, 1990; Walstra, 1999) and some non-κ-casein macropeptide chains. The hairs are hydrophilic and negatively charged and they are also responsible for micelle stability according to Hill and Wake (Hill and Wake, 1969). The mobility of the hair increases steadily with temperature. Casein micelles are held up together by

calcium phosphate nanocluster cross-linking polypeptide chains and hydrophobic bonds.

The influence of temperature affects the structural behaviour of casein micelles. At low temperature (around 4 °C), the weakened of hydrophobic bonds which held the casein micelle together dissolves away β-casein from the micelles. A thicker hairy layer is formed and β-casein chains may extend further beyond the micelle surface. This improves the steric repulsion. Other caseins are also dissociated but to a lesser extent. Furthermore, those loosen β-casein chains which are not totally dissociated increases the voluminosity of the micelles, hence increasing the viscosity. There are also evident that suggests the dissolution of colloidal calcium phosphate which further weakens the binding force with the micelles. Generally, the colloidal stability of casein micelles enhances with decreasing temperature. At high temperatures, part of κ-casein dissolves and the C- terminals of β-casein become adhesive, hence causing the shrinkage of micelles. The pH also governs the reaction that will occur. For instance, at room temperature, milk coagulates at pH 4.9 oppose to 4.3 at 0°C (De Kruif and Roefs, 1996) and at 100°C, the dissolution of κ-casein is almost complete at pH 7.2 while nothing occurs below pH 6.2 (Walstra *et al.*, 2006a).

2.1.1.2 Whey proteins or serum protein.

Whey proteins are globular proteins found in the milk serum. They consist of compactly folded peptide chains with most of the hydrophobic residues hidden in the interior of the molecule. Therefore, in native state, whey proteins do not interact or aggregate strongly with others proteins. Whey proteins consist of two types of proteins of significant proportions and they are α-lactalbumin and β-lactoglobulin.

The role of α-lactalbumin is to act as a coenzyme that regulates and catalyses the synthesis of lactose. They are bind together by very strong calcium at specific hidden sites. Although calcium is not essential for the enzymatic activity (Kronman *et al.*, 1981; Musci and Berliner, 1985), it helps to stabilise the molecule. (Ikeguchi

et al., 1986) When the calcium is removed or the pH is reduced to about 4, parts of α-lactalbumin starts to unfold and transformed into a molten globule state. In this state, the protein is vulnerable against irreversible denaturation at relatively low temperatures. (Walstra *et al.*, 2006c) On the other hand, the presence of calcium will promote the refolding process of denatured α-lactalbumin by at least two orders of magnitude, provided the disulfide bonds are still intact (Kumwajima *et al.*, 1989; Forge *et al.*, 1999).

β-lactoglobulin is a globular protein and accounts for 50% of total whey protein and around 12% of the total protein in milk. Therefore, it dominates the properties of whey protein, particularly the reactions associated with heat treatment. The real biological function of β-lactoglobulin remains unknown. However, there are several hypothesis proposed by workers. The possible role as a retinol (vitamin A) transporter or up take enhancer was suggested by Papiz *et al*. (Papiz et al., 1986) based on the identification of specific receptors in the intestine of neonatal calf. Furthermore, the enhancement of retinol absorption in the jejunum, a middle section of small intestine, shown by Said et al (1989) strengthened the hypothesis. Besides retinol, Wang *et al*. (1997) indicated that vitamin D_2 also binds tightly to β-lactoglobulin. Perhaps β-lactoglobulin has a more general role as a vitamin absorption enhancer.

2.1.2 Fat globules

In the composition of full cream milk, fat (in dry mater) takes up around 30% of the total mass and almost 99.975% are found as small globules. Hence, milk can be considered as an oil-in-water emulsion. The composition of fat globules is predominantly constituted of triacylglycerols, generally known as triglycerides (98%). Details fat compositions are listed in Table 2.2 they are data reported by Bitman and Wood. (Bitman and Wood, 1990) They are high in energy, about 37 kilojoules per gram, and easy to digest regardless of the physical form (natural, homogenised fat globules or butter) they are in. The size of fat globules varies from 0.1 to 15 μm in diameter, however, the size can be altered by treatment, e.g. homogenisation (Section 3.1.4). Every individual fat globule is covered by a layer of

membrane with an average thickness of 15 nm but varies from about 10 to 20nm and the membrane helps to avoid the fat globules from coalescence.

Table 2.2 Lipids in milk

Lipid Class	% of total lipids (g/100g)
Phospholipid	1.1
Cholesterol	0.46
Triacylglycerol	95.80
1,2-Diacylglycerol	2.25
Free fatty acids	0.28
Monoacylglycerol	0.08
Cholesteryl ester	0.02

Ye et al. (2004a; 2004b) has shown that throughout preheat treatment and evaporation, changes were observed in the fat globules and fat globule surface proteins. When whole milk under goes preheat treatment by direct steam injection (DSI), fat globule becomes smaller and the concentration of surface protein increases to about 1.8mg/m^2 due to the absorption of casein micelles at the fat globules surface. Similarly, during evaporation process, the size of fat globules decrease while the total surface proteins increase with the number of effect the milk has gone through in a multi-effect evaporator.

During homogenisation, the average size (d_{43}) of fat globules decrease and the degree of shrinkage depends on the pressure used by the homogeniser. The average fat globule size decreases from ~ 1.80 µm to ~ 1.3 µm at 4 MPa and ~ 1.1 µm at 7 MPa respectively. Also, the surface protein composition on the fat globule varies with the preheat treatment prior to homogenisation. At low preheated concentrate (70 °C), whey proteins accounted for < 5% of the total surface protein, however, with the preheat treatment increase to 90 °C, the proportion of whey protein on the fat globule surface increased to > 20%. Similar results were observed with heat treatment after homogenisation (Ye *et al.*, 2008).

2.1.3 Lactose

Lactose is the primary carbohydrate of milk in most mammals and they are commonly called milk sugar. The synthesis of lactose is made possible by the presence of α-lactalbumin in the Golgi vesicles. α-lactalbumin modifies a common enzyme called galactosyltransferase, the modified enzyme catalyse the reaction between uridine-diphosphate-galactose and glucose to form disaccharide, lactose. This disaccharide account for 4.5 to 5.0% of the total content in milk and 50-52% of total solids-non-fat (Feely *et al.*, 1975; Nickerson, 1978; Scrimshaw and Murray, 1988a). The main role of lactose is to provide neonate with energy (17kJ per gram of lactose) although the caloric content is not as high as the fat globules (37 kJ per gram fat). Also, the lactose gives a sweet taste to milk. Like other components in milk, the lactose content subjected to animal's health, breed and season of the year (Potter, 1986). The absorption of lactose is not straight forward, as it cannot be taken up into the blood. The lactose has to be broken down into glucose and galactose by enzyme lactase (β-galactosidase) and the reaction happens rather slowly. This will prevent the sudden surge of glucose level of the blood after drinking milk. (Walstra *et al.*, 2006c) However, it is estimated that 60% of the world population over 4 years old has low lactase activity (5 - 10%), resulting in poor lactose metabolism. Lactose can be extracted by crystallising them in concentrated whey solution and separated by centrifugation. To get higher yield and purity, it is advisable to deproteinise and demineralise whey first before commencing the extraction (Holsinger, 1992). The applications of lactose are broad. In food processing sector, lactose is commonly used instead of commercial sugar because they are not as sweet. With this in mind, it is use to alter the viscosity and texture of food product as well. Lactose also acts as a coating agent for pills and tablets in the pharmaceutical industries. It helps to seal in the contents and makes them easy to handle.

2.2 Physical Properties of Milk

2.2.1 Density

Density is given by mass per unit volume which can be expressed in kg/m^3 (SI units). It is sensitive to the temperature and composition. Milk, being a mixture of components, can have its density derived from

$$\frac{1}{\rho} = \sum \left(\frac{m_x}{\rho_x}\right) \tag{2.1}$$

where m_x is the mass fraction of component x, and ρ_x its apparent density in the mixture. The apparent densities (at 20 °C) of the major components in milk are listed below in Table 2.3.

Table 2.3 Apparent density of major components in milk

Components	Apparent Density (kg/m^3)
Water	998.2
Fat	918
Protein	1400
Lactose	1780
Residual components	1850

Apparent densities of each component (except for fat) above were measure in aqueous solution as dissolution will cause contraction, particularly components with low molecular mass. In general, the degree of contraction increases with concentration. Also, the crystallisation of fat increases the density.

The average density of whole milk at 20 °C is about 1030 kg/m^3 and varies from 1027 to 1033 kg/m^3 depending on the fat content (Walstra and Jenness, 1984). During the concentration process of milk, the measurement of density gives a quick means of measuring the total solids (Jenness and Patton, 1959) .

Specific gravity (SG), also known as relative density, is used to quantify density in a dimensionless form in relation to water at a specific temperature. SG is define as

$$SG^{\theta} = \frac{\rho_{product}}{\rho_{water}} \tag{2.2}$$

where θ is the measurement temperature (°C).

Specific gravity has much lower temperature dependence then density and the numerical value is independent of the units for density. On average, the $SG^{15.5}$ for skim milk is 1.036 (Sherbon, 1988) .

Temperature is another important factor that affects the density and specific gravity of milk. Rambke and Konrad (1970) has suggested the following equation that incorporates both total solids and temperature for whole milk.

$$\rho = 1002.7 - 3.62X + 0.018X^2 - 0.365T - 0.0025X\,T \tag{2.3}$$

where X is the total solids (wt%) and T is temperature (°C). The validity of Equation (2.3) range 5 – 85°C for total solids of 10 – 45 wt%. However, fat, being the component with lowest density in milk, has the most influence on density. The lack of fat content factor in Equation (2.3) is compensated by the following equation recommended by Bertsch *et al.* (1982).

$$\rho = -2.307 \times 10^{-3}T^2 - 0.2655T + 1040.51 - F(-47.8 \times 10^{-6}T^2 + 9.69 \times 10^{-3}T + 0.967) \tag{2.4}$$

where F is the amount of fat (wt%), ranging 6 – 15.5 wt% and T is temperature (°C) ranging 65 – 140 °C

2.2.2 Viscosity

Bertsch and Cerf have investigated the influence of temperature and fat content on the viscosity of UHT skim and homogenised milk and cream. The amount of fat tested ranged from 0.03 to 15.5 wt% and the rate of shearing tested was between 200 – 1000 s^{-1}. They have found that milk viscosity increases with fat content. The relationship can be represented by the following equation:

$$\ln\mu = 3.92 \times 10^{-5}T^2 - 1.951 \times 10^{-2}T + 0.666 + F(-9.53 \times 10^{-6}T^2 + 1.674 \times 10^{-3}T - 4.37 \times 10^{-2}) + F^2(9.75 \times 10^{-7}T^2 - 1.739 \times 10^{-4}T + 9.83 \times 10^{-3}) \quad (2.5)$$

where μ is viscosity (mPa.s), *F* is the amount of fat (wt%) and *T* is temperature (°C) range 70 – 135 °C. For more details on milk viscosity, refer to Chapter 3.

2.2.3 Heat capacity

Heat capacity of a substance is the amount of heat energy required to increase the temperature of a unit mass. It is usually express in $J.kg^{-1}\ K^{-1}$. The heat capacity of water at 1 atm in air-free condition is within 1% of 4186.8 $J.kg^{-1}\ K^{-1}$ (Overman *et al.*, 1939) while the heat capacities of whole and skim milk are 3931.4 and 4052.8 $J.kg^{-1}\ K^{-1}$ respectively (Bertsch, 1982). As expected, the heat capacity of milk is close to that of water because almost 90 wt% of milk is made up of water. The difference in heat capacity between whole and skim milk is partially contributed by the fat content as milk fat has a heat capacity of 2177.1 $J.kg^{-1}\ K^{-1}$ in both solid and liquid state (Yoncoskie, 1969).

Heat capacity of milk, c_p ($J.kg^{-1}\ K^{-1}$), can be calculate by

$$c_p = (0.5\mathrm{m_f} + 0.3\mathrm{m_{snf}} + \mathrm{m_w}) \times 4180 \quad (2.6)$$

where $\mathrm{m_f}$ is the mass fraction of fat, $\mathrm{m_{snf}}$ is the mass fraction of solids-not-fat (snf) and $\mathrm{m_w}$ is the mass fraction of water (Miles *et al.*, 1983).

A refined equation recommended by Kessler (1981a) further differentiate snf into carbohydrate, protein and ash.

$$c_p = 4200\mathrm{m_w} + 1700\mathrm{m_f} + 1400\mathrm{m_c} + 1600\mathrm{m_p} + 1400\mathrm{m_a} \quad (2.7)$$

where $\mathrm{m_c}$ is the mass fraction of carbohydrate, $\mathrm{m_p}$ is the mass fraction of protein and $\mathrm{m_a}$ is the mass fraction of ash (Kessler, 1981a).

Ginzhurg et al (1985) have suggested yet another equation that incorporates temperature as one of the dependence, however individual components are less defined.

$$c_p = 3914 - 19.2X - 1.71F + 5.46T \quad (2.8)$$

where X is the total solids (wt%), F is the percentage fat (wt%) and T is the temperature (°C).

2.2.4 Surface tension

Surface tension is the contracting force per unit length around the perimeter of a surface/interface. From thermodynamic view point, the amount of free energy within the interface is proportional to the interfacial area. Therefore, surface tension also represents the surface free energy per unit increase in surface area. The SI units of surface tension are $N.m^{-1}$ or $J.m^{-2}$. Surface tension measurements on milk have been done by a number of authors (Písecký, 1966; Janál, 1980; Bertsch, 1983). Even though the method used varies among the authors, the variations of surface tension measurements were not significant.

Table 2.4 Surface tension of condensed milk

Milk Type	σ (N m^{-1})	Conditions	Source
Condensed	5.28×10^{-2}	Immediately after production ρ = 1079 $kg.m^{-3}$ μ = 11.78 mPa.s	(Janál, 1980)
	5.34×10^{-2}	After 2 days of storage at 15°C ρ = 1081 $kg.m^{-3}$ μ = 12.9 mPa.s	
	5.57×10^{-2}	After 4 days of storage at 15°C ρ = 1083 $kg.m^{-3}$ μ = 15. mPa.s	
Condensed, sweetened	5.92×10^{-2}	Immediately after production ρ = 1320 $kg.m^{-3}$ μ = 2892 mPa.s	(Janál, 1980)
	6.04×10^{-2}	After 2 days of storage at 15°C ρ = 1325 $kg.m^{-3}$ μ = 2706 mPa.s	
	6.19×10^{-2}	After 4 days of storage at 15°C ρ = 1327 $kg.m^{-3}$ μ = 3900 mPa.s	
Condensed, whole	4.24×10^{-2}	15 min after leaving the evaporator *X* = 55.1 wt% T=55 °C	(Písecký, 1966)
	4.02×10^{-2}	60 min after leaving the evaporator *X* = 55.1 wt% T=55 °C	
	4.78×10^{-2}	120 min after leaving the evaporator *X* = 55.1 wt% T=55 °C	
Condensed, skimmed	4.09×10^{-2}	15 min after leaving the evaporator *X* = 49.92 wt% T=55 °C	(Písecký, 1966)
	4.02×10^{-2}	60 min after leaving the evaporator *X* = 49.92 wt% T=55 °C	
	4.17×10^{-2}	120 min after leaving the evaporator *X* = 49.92 wt% T=55 °C	
	5.20×10^{-2}	180 min after leaving the evaporator *X* = 49.92 wt% T=55 °C	

Following from Table 2.4, surface tension ranges from 4.02×10^{-2} to 6.19×10^{-2} $N.m^{-1}$ for various types of condensed milk and the changes with total solids, time and temperature are relatively small. Work carried out by Bertsch (1983) also shows that there is no significant different in surface tension between whole and skim

milk at similar total solids (12.94 wt% and 8.99 wt% respectively). The change in surface tension of whole and skim with temperature can be represented by the equation:

$$\sigma = 1.8 \times 10^{-4} T^2 - 0.163T + 55.6 \quad (2.9)$$

where σ is the surface tension (mN m-1) and *T* is the temperature (°C) range from 18 to 135°C. At 18 and 55°C, surface tension of 5.27×10^{-2} and 4.72×10^{-2} $N.m^{-1}$ are derived from equation (2.9) respectively. They are well within the range of surface tensions listed in Table 2.4 This has strengthened the theory of the independence of surface tension with varying total solids.

2.2.5 Boiling point elevation

Boiling point elevation, ΔT_b, is a phenomenon where the solution boils at a higher temperature than the pure solvent when compound is added. In a multi-effect evaporator, the boiling temperature of the product is crucial as the vapour produced in one effect is used in a subsequent effect.

As boiling point elevation is governed by the numbers of molecules in the solution and not on the properties (size or mass) of the molecule, it can be derived by the following equation (Berry *et al.*, 1980).

$$\Delta T_b = \frac{-RT_{wb}^2 ln a_w}{\Delta h_v} \quad (2.10)$$

where T_{wb} is the boiling point of water (K), a_w is the water activity, Δh_v is the molar latent heat of vaporisation of water ($J.mol^{-1}$).

Boiling point elevation for milk can be represented by Equation (2.11) where it is a function of total solids.

$$\Delta T_b = \frac{\mathrm{X}}{92 - \mathrm{X}} \times 1.28 - 0.11 \tag{2.11}$$

where X is the total solids (wt%) (Pisecky, 1997b).

2.3 Foams

Foam is the collection of bubbles where the dispersion of gas is enveloped in a thin liquid film. The liquid film between bubbles is known as lamellae and they range in thickness from 10 to 100 nm. The formation of bubbles during evaporation usually involves nucleate boiling where steam bubbles are formed from micro-cavities. The steam bubbles grow to a certain size before they separate from the wall and are carried into the main fluid stream.

2.3.1 Destruction of foam

Prior to foam destruction, foam structure undergoes 3 possible modes of evolution. First of all, the interconnected surfaces between bubbles act as drainage channels which remove liquid under the influence of gravity. The foam structure is then weakened by the thinning of lamellae due to liquid drainage out of the foam.

Secondly, the coalescence of adjacent bubbles resulted from the rupture of liquid film under the influence of random disturbances. This leads to the formation of larger bubble. Similarly, bubbles in the top layer can coalesce with the air above, thus vanishing. Furthermore, the coalescence of bubbles reduces the surface area which results in the lowering of interfacial Gibbs energy. This act as a driving force for the bubbles to coalesce or rupture. This is further discussed in 2.3.2.

Lastly, the effect of Ostwald ripening. Gas from a bubble diffuses through the film into the liquid or adjacent bubble. The solubility of gas is proportional to its pressure. According to Laplace law, the pressure difference between the bubble and its surrounding, Δp (Pa), can be calculated by the following equation

$$\Delta p = \frac{2\gamma}{a} \tag{2.12}$$

where γ is the surface tension (mN m^{-1}) and a is the bubble radius (m).

Smaller bubbles have greater pressure difference, hence dissolving better in a liquid. Therefore, gas from small bubble will diffuse into a larger one, resulting in the disappearance of small bubbles and the growth of larger bubbles. Likewise, the bubble on the top layer of the foam can also disappear since gas diffuses to the air above.

The above 3 modes of foam evolution are concomitant: The thinning of lamellae leads to a higher probability of film rupture, this favours the coalescence of bubbles; similarly, the growth of bubble size through gas diffusion; enhances the chance of coalescence.

2.3.2 Thermodynamic foam stability

Today, there is still no single theory that fully explains the mechanism of foam stability. One of the propose theories of foam stability by introducing surface active solute can be described from a thermodynamic view point as follows. In pure liquids, air entrained only form transitory foams. Air is allowed escape with ease except for what is required for Stokesian rate of rise, which is governed by the bubble size of dispersed air and the viscosity of the liquid. Owning to their high interfacial area (and surface free energy), all foams are thermodynamically unstable. A simplified Helmholtz function demonstrates the instability of foam in a two-component system (pure liquid and a completely insoluble gas)

$$\Delta F = \sigma \Delta A \tag{2.13}$$

where ΔF is the change in the Helmholtz free energy for bubble to coalesce, σ is the surface tension of liquid and ΔA is the change in surface area .

When bubble coalesce, the surface area decreases, which results in the lowering of Helmholtz free energy. This favours the collapse of bubbles, hence the incapability of sustaining stable foam in pure liquid.

However, under the influence of certain solutes that is able to stabilise the thin lamellae of liquid, entrained air remains in the bubbles, even as they rise to the surface of the liquid. An addition negative term needs to be added to Helmholtz function, a term that changes the sign of the expression for ΔF. This can be achieved by surface active solutes which are able to lower the surface or interfacial tension of the solvent. Based on Gibbs adsorption theorem, surface active solute prefers to solutes that are able to be adsorbed positively on the surface or interface. Furthermore, the relocation of solute from the surface to the bulk phase requires energy. Therefore, if the reduction of free energy resulting from the $\sigma\Delta A$ term is less than that gained from the relocation of solutes from the surface into the bulk liquid when bubble coalesce, spontaneous coalescence will not happen, and the foam would be thermodynamically stable.

2.3.3 Ways to stabilise foam

From physical mechanism view point, the ability to retain or restore the thickness of liquid lamellae stabilises the foam structure. This is made possible by several methods, namely the increase in bulk or surface viscosity, adding of surfactants and Gibbs-Maragoni effect.

In general, the rate of drainage may be reduced by increasing the bulk viscosity of the liquid from which the foam is created. This slows down the thinning process of lamellae, hence, retaining the foam structure for a longer period of time.

Similarly, the introduction of high concentration of surfactant on the liquid surface also enhances the structural integrity of foam by creating adhesive or cohesive bonding on the lamellae to hinder the drainage of liquid. For example, milk proteins like whole casein and whey protein give rise to good foamability because the proteins form elastic layers at the air-water interface that hinders the coalescence of bubbles and reduce Oswald ripening.

The Gibbs-Maragoni effect also involved the addition of surface active solute, however, two other criteria have to be satisfied in order for Gibbs-Maragoni effect to operate. Firstly, the surface tension of the solution has to be considerably smaller than the surface tension of the solvent. This surface tension gradient is normally achieved by the adsorbed layer of surface active solute on the liquid surface. Secondly, the diffusion of surface active solute has to be sufficiently slow. (Bikerman, 1973)

When a bubble rises to the surface of the liquid, it forms a new surface. The instantaneous surface tension is large due to insufficient time for the adsorbed layers to form. The surface tension gradient exerts a pulling force on the adjoining areas of lower surface tension. This results in the flow of liquid towards the newly created surface. Therefore, the effects of both gravitational and capillary drainage are counterbalance and the thickness of lamellae is restored. Also, bubbles are prevented from coalescing by the surface elasticity. This is illustrated in Figure 2.3.

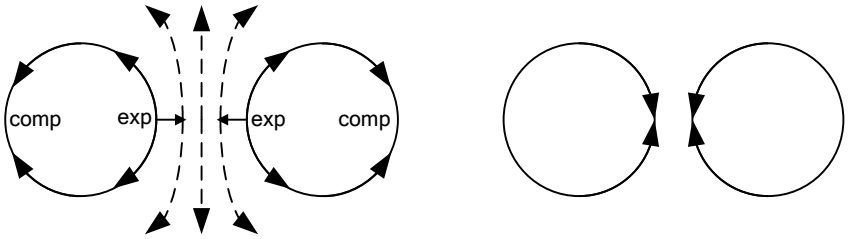

Figure 2.3 Surface tension gradient present at a bubble surface and its stabilising effect against flow of liquid out of the film between two bubbles

As 2 bubbles approach each other, the displacement of medium in between creates an expansion (thinner lamellae) and contraction (thicker lamellae) region on the bubble. Normally, the expansion region will rupture and form a bigger bubble. However, the elasticity of the lamellae resulted from the adsorption of solute forces the liquid back to prevent the expansion region from rupturing (Van Kalsbeck and Prins, 1999).

2.3.4 Foamability and CMC

It has been observed that the maximum foamability happens at a solute concentration equal or close to the critical micelle concentration (CMC). This concentration is similar to that of the saturation point of a solution. To tell them apart, a solution at its CMC forms a colloidal solution where no visible phase separation occur. On the other hand, when crystalline salt solutions reach its solubility limit, visible precipitation can be observed.

To explain the maximum foamability, Gibbs-Maragoni effect plays an important role. At concentration above CMC, Gibbs-Maragoni effect becomes negligible. Any increase in solute concentration no longer causes any changes in the surface tension of the solution. In another words, the surface tension gradient between the solution and solvent remains constant. This is also observed by Adhikari et al on whey protein solutions where surface tension remains unaffected by whey protein concentration beyond 5 wt% (Adhikari *et al.*, 2007).

Therefore, with no further assistance from the surface active solute in lowering of surface tension beyond CMC, maximum Gibbs-Maragoni effect would be expected to occur at concentration just below the CMC. Likewise for the maximum foamability.

2.4 Milk substitutes used in literatures

Fresh milk is seldom being used in experiments due to its availability, shelf-life and cost. In cases like the experiment done by Srichantra et al, where fresh raw milk was obtained for further processing into fresh milk, reconstituted milk and recombined milk, are very rare (Srichantra *et al.*, 2006). Therefore, there are a number of milk substitutes formulated to mimic the physical and chemical properties of real milk by various researchers. Table 2.5 shows some of the physical properties of milk.

Table 2.5 Some physical properties of milk
(Walstra and Jenness, 1984; Sherbon, 1988; Singh *et al.*, 1997)

Osmotic Pressure	~700 kPa
Boiling Point	~100.15 °C
Freezing Point	~0.522 °C (approx.)
Refractive Index, n_D^{20}	1.344 – 1.3485
Specific Reflective Index	~0.2075
Density (20°C)	~1030 $kg.m^{-3}$
Specific Gravity (20°C)	~1.0321
Specific Conductance	~0.0050 $ohm^{-1}cm^{-1}$
Ionic Strength	~0.08 M
Surface Tension (20°C)	~52 $N.m^{-1}$
Coefficient of Viscosity	~2.127 mPa.s
Thermal Conductivity (2.9% fat)	~0.559 $W.m^{-1}K^{-1}$
Thermal Diffusivity (15 -20°C)	~1.25 X 10-7 $m^2.s^{-1}$
Specific Heat	~3.931 $kJ.kg^{-1}K^{-1}$
pH	~6.6

Jebson et al utilised whole and skim milk powder to formulate their milk substitutes (Jebson, 1990; Jebson and Chen, 1996). The specific heat capacity of such milk substitute is comparable to real milk with values of 3.904 $kJ.kg^{-1}K^{-1}$ and 3.931 $kJ.kg^{-1}K^{-1}$ respectively. However, the thermal conductivity and viscosity of Jebson et al's milk substitute are significantly different from real milk with a magnitude of up to 1000 times difference (Jebson and Chen, 1996; Fox and McSweeney, 1998). These differences alter the flow characteristics and the ability to dissipate heat of real milk. Hence, it might not reflect on the true performance of real milk in heat exchangers. Jebson et al also used sugar solution when they were investigating the physical factors of fluid that might affect the heat transfer in falling film evaporators. The reasons for not using milk are as followed. Firstly, the composition varies every day, therefore, the physical properties are not constant. Secondly, the age-thickening characteristic of concentrated milk is unfavourable to

quantify the performance of the evaporator. Lastly, fouling on heating surface requires frequent cleaning. Therefore, tap water and sugar solution were used for a consistent feed composition and convenience (Chen and Jebson, 1997). Another milk substitute fluid, which consists of whey proteins, whole milk, sugar and xanthen gum, was used by Beuf et al. Xanthen gum, a dairy product thickener, was added to alter the viscosity of the fluid to produce a shear thinning behaviour. With the assumption that since the composition is similar to milk, the thermophysical properties (thermal conductivity and specific heat capacity) were calculated based on milk and no actual testing of those properties for verification were mentioned in the literature (Beuf et al., 2007). A similar model were use by Hopper at el and Simmons at el, it is known as whey protein concentrate (WPC). The compositions of WPC powder, WPC solution and milk are shown below.

Table 2.6 Compositions of WPC powder, WPC solution and milk (Paul and Southgate, 1978)

Component	WPC Powder (wt%)	1.5% WPC Solution (wt%)	Typical Milk Composition
Water	4.5	91.86	87.5
Lactose	47.6	4.06	5.0
Lipids	5.6	0.48	3.8
Protein			
Casein	-	-	2.5
β-Lactogloblin	17.6	1.5	0.3
α-Lactoalbumin	7.04	0.6	0.07
Other	10.56	0.9	0.19
Minerals			
Sodium	0.77	0.066	0.05
Potassium	2.65	0.226	0.15
Calcium	1.08	0.092	0.12
Magnesium	0.17	0.014	-
Phosphorous	0.92	0.078	0.1
Chlorine	1.51	0.129	0.1
Other	-	-	0.3

Milk fouling is a function of many variables, both physical and chemical. Physical parameters such as temperature, flow rate and material of construction can be determined by heat exchanger designers whereas the chemistry of milk normally cannot be changed (Bott, 1995; Changani *et al.*, 1997; Beuf *et al.*, 2007). The following section will focus on the physical mechanism of fouling in falling film evaporator due to film breakage.

2.5 Summary

There are many studies on milk compositions and their physical properties. With the understanding of their change in behaviour, both physically and chemically, when the milk is subjected to heat treatment such as sterilisation and evaporation process, their potential impact on the evaporator can be assessed. This information is also essential when building a evaporator model from the fundamental principles of heat and mass transfer. From the literatures, most of the physical properties are sensitive to both concentration and temperature. Furthermore, some of the properties of the milk substitute, such as reconstituted milk, used by various workers vary widely. This question the validity of using those milk substitutes used in evaluation of evaporator performances.

2.6 Nomenclature

a	Bubble radius	m
a_w	Water activity	-
ΔA	Change in surface area	m^2
c_p	Heat capacity	$J.kg^{-1}\ K^{-1}$
F	Mass percentage of fat	wt%
ΔF	Change in Helmholtz free energy for bubbles to coalesce	J
m_a	Mass fraction of carbohydrate	-
m_c	Mass fraction of carbohydrate	-

m_p	Mass fraction of protein	-
m_{snf}	Mass fraction of solids-not-fat	-
m_w	Mass fraction of water	-
m_x	Mass fraction of component x	-
Δp	Pressure difference between bubble and its surrounding	Pa
T	Temperature	˚C or K
ΔT_b	Boiling point elevation	˚C or K
T_{wb}	Boiling point of water	˚C or K
X	Concentration of milk	wt%
η	Viscosity	mPa.s
σ	Surface tension of liquid	dyn cm^{-1} or N m^{-1}
ρ	Liquid density	$kg.m^{-3}$
ρ_x	Apparent density of component x	$kg.m^{-3}$
θ	Measurement temperature	°C

2.7 Reference

Adhikari, B., Howes, T., Shrestha, A. &Bhandari, B. R. (2007). Effect of surface tension and viscosity on the surface stickiness of carbohydrate and protein solutions. *Journal of Food Engineering* 79: 1136-1143.

Berry, R. S., Rice, S. A. &Ross, J. (1980). *Physical Chemistry.* New York: John Wiley & Sons.

Bertsch, A. J. (1982). Specific heat capacity of whole and skim milk between 50 and 140°C. *Le Lait* 62: 265 - 275.

Bertsch, A. J. (1983). Surface tension of whole and skim-milk between 18 and 135°C. *Journal of Dairy Research* 50: 259.

Bertsch, A. J., Bimbenet, J. J. &Cerf, O. (1982). The density of milk and creams from 65°C to 140°C. *Le Lait* 62: 250.

Beuf, M., Rizzo, G., Leuliet, J. C., Muller-Steinhagen, H., Yiantsios, S., Karabelas, A. &Benezech, T. (2007). Fouling and Cleaning of Modified stainless Steel Plate Heat Exchangers Processing Milk Products. *2003 ECI Conference Proceedings*: 99 - 106.

Bikerman, J. J. (1973).Theories of foam stability. In *Foams*New York: Springer-Verlag.

Bitman, J. &Wood, D. L. (1990). Changes in milk phospholipids during lactation. *Journal of Dairy Science* 73: 1208 -1216.

Bott, T. R. (1995). *Fouling of Heat Exchangers.* Amsterdam: Elsevier Science.

Changani, S. D., Belmar-Beiny, M. T. &Fryer, P. J. (1997). Engineering and Chemical Factors Associated With Fouling and Cleaning in Milk Processing. *Experimental thermal and fluid science* 14: 392 - 406.

Chen, H. &Jebson, R. S. (1997). Factors Affecting Heat Transfer in Falling Film Evaporators. *Trans.IChemE* 75(Part C).

De Kruif, C. G. &Roefs, S. P. F. M. (1996). Skim milk acidification at low temperatures: a model for the stability of casein micelles. *Netherlands milk and Dairy Journal* 50: 113-120.

Feely, R. M., Criner, P. E. &Slover, H. T. (1975). Major fatty acids and proximate composition of dairy products. *Journal of the American Dietetic Association* 66: 140 - 146.

Forge, V., Wijesinha, R. T., Balbach, J., Brew, K., Robinson, C. V., Redfield, C. &Dobson, C. M. (1999). Rapid collapse and slow structural reorganisation during the refolding of bovine α-lactalbumin *Journal of Molecular Biology* 288: 673 - 688.

Fox, P. F. (2003).Milk Proteins: General and Historial Aspects. In *Advanced Dairy Chemistry Volume 1: Proteins* (Eds P. F. Fox and P. L. H. McSweeney). New York: Klumer Academic/Plenum Publishers.

Fox, P. F. &McSweeney, P. L. H. (1998). *Dairy Chemistry and Biochemistry.* Springer-Verlag.

Ginzburg, A. S., Gromov, M. A. &Krasovskaya, G. I. (1985). Thermophysical properties of food products (Czech translation). *Prague*.

Hill, R. J. &Wake, R. J. (1969). Amphiphilic nature of κ-casein as the basis for its micelle stabilizing property. *Nature* 221: 635-639.

Holsinger, V. H. (1992).Physical and Chemical Properties of Lactose. In *Advanced Dairy Chemistry Vol.3: Lactose, Water , Salts and Vitamins*(Ed P. F. Fox). London: Chapman & Hall.

Holt, C., Anfinsen, C. B., M., F., T., R. J., Edsall &Eisenberg, D. S. (1992).Structure and Stability of Bovine Casein Micelles. In *Advances in Protein Chemistry*, Vol. Volume 43, 63-151: Academic Press.

Ikeguchi, M., Kuwajima, K. &Sugai, S. (1986). Calcium-induced alteration in the unfolding behaviour of α-lactalbumin *Journal of Biochemistry* 99: 1191 - 1201.

Janál, R. (1980). Physical parameters of condensed milk. *Prum Potravin* 31(8): 453.

Jebson, R. S. (1990). The Performances of Falling Film Evaporators on Whole Milk *Chemeca '90*: 682 - 689.

Jebson, R. S. &Chen, H. (1996). Performances of Falling Film Evaporators on the Whole Milk and a Comparison with performance on Skim Milk. *Journal of Dairy Research* 64: 57-67.

Jenness, R. &Patton, S. (1959). *Princples of Dairy Chemistry.* New York: John Wiley.

Kessler, H. G. (1981). *Food Engineering and Dairy Technology.* Freising, Germany: Verlag A.

Kronman, M. J., Sinha, S. K. &Brew, K. (1981). Charateristics of the binding of Ca^{2+} and other divalent metal ions to bovine alpha-lactalbumin. *Journal of Biological Chemistry* 256: 8582-8587.

Kumwajima, K., Mitani, M. &Sugai, S. (1989). Characterisation of the critical state in protein folding-effects of guanidine hydrochloride and specific Ca^{2+} binding on the folding kinetics of α-lactalbumin

Journal of Biological Chemistry 206: 547 - 561.

McMahon, D. J. &McManus, W. R. (1998). Rethinking casein micelle structure using electron microscopy. *Journal of Dairy Science* 81: 2985-2993.

Miles, C. A., Van Beek, G. &Veerkamp, C. H. (1983). *Physical Properties of Foods.* London: Applied Science Publishers.

Morr, C. V. (1967). Effect of oxalate and urea upon ultracentrifugation properties of raw and heated skimmilk casein micelles. *Journal of Dairy Science* 50: 1744-1751.

Musci, G. &Berliner, L. J. (1985). Physiological roles of zinc and calcium binding to α-lactalbumin in lactose biosynthesis. *Biochemistry* 24: 6945 - 6948.

Nickerson, T. A. (1978). Why use lactose and its derivatives in food? *Food Technology* 32(1): 40 - 46.

Overman, O. R., Garrett, O. F., Wright, K. E. &Sanmann, F. D. (1939). Composition of milk if Brown Swiss cows. *Agricultural Experiment Station Bulletin* 457: 575 - 623.

Papiz, M. Z., Sawyer, L., Eliopoulos, E. E., North, A. C. T., Findlay, J. B. C., Sivaprasadarao, R., Jones, T. A., Newcomer, M. E. &Kraulis, P. J. (1986). The structure of β-lactoglobulin and its similarity to plasma retinol-binding protein. *Nature* 324: 383 - 385.

Paul, A. &Southgate, D. A. T. (1978). *The composition of foods.* Elsevier: North-Holland Biomedical Press.

Payens, T. A. J. (1966). Association of caseins and their possible relation to structure of the casein micelle. *Journal of Dairy Science* 49(1317-1324).

Pisecky, J. (1997). *Hankbook of Milk Powder Maufacture.* Copenhagen, Demark: Niro A/S.

Písecký, J. (1966). Some properties of condensed milk and their effect on the quality of dry milk. *Průmysl potravin* 17(6): 304.

Potter, N. N. (1986).Milk and milk products. In *Food Science*, 349 - 389 Westport: AVI Publishing Co.

Rambke, K. &Konrad, H. (1970). Physikalische Eigenschaften flüssiger Milchprodukten. Dichte von Milch, Rahm und Milchkonzentraten. *Nahrung* 14(2): 137.

Rose, D. &Colvin, J. R. (1966). Internal Structure of Casein Micelles from Bovine Milk. *Journal of Dairy Science* 49: 351-355.

Said, H. M., Ong, D. E. &Shingleton, J. L. (1989). Intestinal uptake of retinol, enhancement by bovine milk β-lactoglobulin *American Journal of Clinical Nutrition* 49: 690 - 694.

Scrimshaw, N. S. &Murray, E. B. (1988a). The acceptablility of milk and milk products in populations with a high prevalence of lactose intolerance: lactose content of milk and milk products. *American Journal of Clinical Nutrition* 48: 1099 - 1104.

Sherbon, J. W. (1988).Physical Properties of Milk. In *Fundamentals of Dairy Chemistry*, 409 - 460 (Eds N. P. Wong, R. Jenness, M. Keeney and E. H. Marth). New York: Van Nostrand Reinhold.

Singh, H., McCarthy, O. J. &Lucey, J. A. (1997).Physico-chemical Properties of Milk. In *Advanced Dairy Chemistry*, Vol. Vol 3: Lactose, Water, Salts and Vitamins(Ed P. F. Fox). London: Chapman & Hall.

Srichantra, A., Newstead, D. F., Mcccarthy, O. J. &Paterson, A. H. J. (2006). Effect of Preheating on Fouling of a Pilot Scale UHT Sterilising Plant by Recombined, Recontituted and Fresh Whole Milks. *Trans IChemE* 84(C4): 279-285.

Van Kalsbeck, H. K. A. I. &Prins, A. (1999).Foam Formation by Food Proteins in Relation to their Dynamic Surface Behaviour

In *Food emulsions and foams - interfaces, interactions and stability*(Eds E. Dickinson and J. M. Rodríguez Patino). Cambridge: The Royal Society of Chemistry.

Visser, H. (1992).A new casein micelle model and its consequences for pH and temperature effects on the properties of milk. In *Protein Interactions*

135-165 (Ed H. Visser). Weinheim: VCH.

Walstra, P. (1990). On the stablility of casein micelles. *Journal of Dairy Science* 73: 1965-1979.

Walstra, P. (1999). Casein Micelles: do they exist? *International Dairy Journal* 9: 189-192.

Walstra, P. &Jenness, R. (1984). *Dairy Chemistry and Physics.* New York: John Wiley & Sons.

Walstra, P., Wouters, J. T. M. &Geurts, T. J. (2006a).Colloidal Particles of Milk. In *Dairy Science and Technology*, 109-157 Boca Raton: CRC Press.

Walstra, P., Wouters, J. T. M. &Geurts, T. J. (2006b).Milk Components. In *Dairy Science and Technology*, 3 - 108 Boca Raton: CRC Press.

Walstra, P., Wouters, J. T. M. &Geurts, T. J. (2006c).Milk: Main Characteristics. In *Dairy Science and Technology*Boca Raton: CRC Press.

Walton, M. (2005). *Energy Use in Dairy Industry.* International Dairy Federation, Bulletin 401/2005.

Wang, Q. W., Alien, J. C. &Swaisgood, H. E. (1997). Binding of vitamin D and cholesterol to β-lactoglobulin *Journal of Dairy Science* 80: 1054 - 1059.

Waugh, D. F., Creamer, L. K., Slattery, C. W. &Dresdner, G. W. (1970). Core polymers of casein micelles. *Biochemistry* 9: 786-795.

Ye, A., Anema, S. G. &Singh, H. (2008). Changes in the surface protein of the fat globules during homogenisation and heat treatment of concentrated milk. *International Dairy Journal* 75: 347 - 353.

Ye, A., Singh, H., Oldfield, D. J. &Anema, S. G. (2004a). Kinetics of heat-induced association of β-lactalbumin with milk fat globule membrane in whole milk. *International Dairy Journal* 14: 389 - 398.

Ye, A., Singh, H., Taylor, M. W. &Anema, S. G. (2004b). Interactions of fat globule surface proteins during concentration of whole milk in a pilot-scale multiple-effect evaporator. *Journal of Dairy Research* 71: 471 - 479.

Yoncoskie, R. A. (1969). The determination of heat capacities of milk fat by differential thermal analysis. *Journal of American Oil Chemists Society* 46: 49 - 55.

CHAPTER THREE: VISCOSITY

3.0 VISCOSITY

Milk viscosity has been extensively studied by a number of authors. The methods used to measure viscosity vary among the authors, from in-line rotating bob viscometer to external cup and bob viscometer. Therefore, the viscosity measured by each author differs as well. Further deviation of viscosity measurements were also affected by other physical factors such as temperature, shearing and the timing. In this chapter the factors that influence viscosity measurement and viscosity models were reviewed. Measurements of milk viscosities were also conducted in order to formulate viscosity models that account for some of the influencing factors.

3.1 Introductions

Falling film evaporation is one of the most important process in milk powder manufacturing. Standard Milks such as skim and whole milk are usually concentrated using multi-effect falling film evaporator(s) to around 50 wt% depending on the type of milk being processed. After which, the concentrate will be sent to the spray dryer to atomize and dry. The fact that the multi-effect falling film evaporator is much more energy efficient than the spray dryer, it is envisaged that removing as much water as possible during the evaporation process would be beneficial in energy saving. However, one of the limitations of doing so is due to the physical property of milk. At high solids concentration (above 45wt%), the viscosity for concentrated milk would increase exponentially and the recommended operating viscosity of the falling film evaporator is usually NOT to exceed 100 mPa.s (100cP) to prevent excessive blocking and likewise for the spray dryer . Therefore, reliable viscosity control is crucial when it comes to the operation of evaporator and deriving an accurate viscosity model will provide an intuitive (even better, quantitative) view of the multi-variable effects upon viscosity. On the other hand, research using fresh concentrate has been hard to come by due to the difficulty in coordination between research organisations and industry and the large cost involved. As such, reconstituted milk has been a popular approach to investigate the general behavior of milk.

In any case, viscosity is quantification of the rate of deformation within a fluid which has been subjected to a shearing force over a surface area, (shear stress). The ratio of shear stress to shear rate is known as the dynamic viscosity. A Newtonian fluid displays a directly proportional relationship between the shear stress and the shear rate while non-Newtonian exhibits a non-linear relationship. For non-Newtonian fluids, dynamic viscosity is also called apparent viscosity. Milks show signs of both Newtonian and non-Newtonian properties which is primarily dependent on solids concentration. Several workers have shown that when the solid content of milk (both skim and whole milk) is lower than 20 wt% behaves like a Newtonian fluid (Chang and Hartel, 1997; Velez-Ruiz and Barbosa-Canovas, 1997). Beyond 20wt%, shear-thinning effect becomes noticeable. Viscosity from this point onwards may still be expressed in the term of apparent viscosity. Therefore it is important to notice the relevant shear rates. In addition to concentration and shear rate, there are a number of other factors that contribute to the accuracy of viscosity measurement, namely temperature, pH, chemical composition, age-thickening and pre-heat treatment, etc.

At low concentration, large portion of milk is water. The influence of non-aqueous components on its flow properties is marginal (Prentice, 1992). However, as milk becomes concentrated, the complex interactions between macromolecules result in greater influence on viscosity. The viscosity of β-lactoglobulin solutions is Newtonian up to 5 wt% and pseudoplastic (shear-thinning) at higher concentration (Pradipasena and Rha, 1977). Eilers (1941) has found out that viscosity can be derived from volume fraction of each disperse particles in milk.

3.1.1 Effect of temperature

The viscosity decreases with increasing temperature. Although water makes up most of the continuous phase, the temperature dependency of milk viscosity is steeper that that of water (Prentice, 1992). Through the use of power-law and Herschel-Bulkley models on viscosity data of milk at concentration up to 48.6 wt%, Velez-Ruiz and Barbosa-Canovas (1998a) described that the consistency index followed the Arrhenius equation temperature dependence. The possible reason

behind this dependence of temperature was explained by Horne (1998). Horne suggested that the hydrophobic interactions causes the casein micelles to tighten up as temperature rises. Consequently, their influence to viscosity diminishes and the further decrease in viscosity by water results in a negative viscosity-temperature relationship. Figure 3.1 illustrates the effect of temperature and protein content has on the milk viscosity.

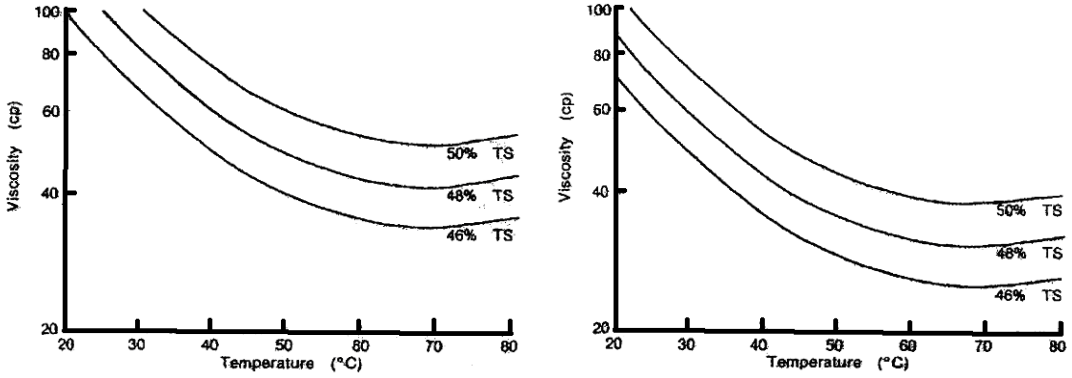

(a) (b)

Figure 3.1 Graphs of concentrate viscosity against temperature for various total solids;

(a) 42% protein (b) 38% protein. (Bloore and Boag, 1981)

Also, Bloore and Boag (1981) have shown that the viscosity of skim milk reaches a minimum at around 70°C at any given concentration. Similar result was also observed by Eilers et al (1947). The reason behind the increase in viscosity beyond 70°C could be due to the denaturation of milk protein β-lactoglobulin at 70°C. β-lactoglobulin begins to unfold, forming string-like structure that extend from the fat globules surface and form complexes with k-casein. At 130°C, sufficient β-lactoglobulin unfolds to cause an increase in voluminosity that changes the viscosity significantly (De Wit, 1981).

3.1.2 Effect of age-thickening

Age-thickening (sometimes also called age-gelation) is defined as the loss of fluidity of the product as a result of changes during storage (Harwalker, 1992).

"Coagulation" and "destabilization" are also sometimes used to describe the instability by many other authors (Tarassuk and Tamsma, 1956; de Koning *et al.*, 1985; Kocak and Zadow, 1985a). In order to investigate the degree to which age-gelation progress, viscometry is used to measure the advancement of the aggregation reaction. Some workers have (Tarassuk and Tamsma, 1956; de Koning *et al.*, 1985; Kocak and Zadow, 1985a) used simplified graphs to show the change in viscosity due to age-gelation. However, such generalization does not reflect on the true nature of milk since more than one type of gel can be formed. Gels ranging from weak and transparent (de Koning et al., 1985) to rennet-like (Snoeren et al., 1979) were reported. Thinning was even observed after age thickening for some evaporated milks (Kocak and Zadow, 1985a; de Koning *et al.*, 1992).

Age-thickening may be due to the structural change in both milk sugar and protein. The association of age-thickening with crystallization of lactose in the concentrate was done by Baucke and Sanderson (1970). They have suggested that the formation of mechanical lattice structure of crystals, or by absorption of serum water as water of crystallization may contribute to the increase in viscosity. The ultimate gelation of their samples was suspected to be the cause of continual growth of lactose crystal at 44˚C. However, in order for crystallization of lactose to occur, the concentration of lactose has to exceed 43 wt% at 44˚C or 22 wt% at 20˚C. Based on the data from Newstead, (1973) the maximum lactose concentration in any native samples was about 25wt%, which is significantly lower than the 43 wt% required to crystallize at 44˚C. Therefore, another mechanism must be responsible for the age-thickening. Buckingham (1978) suggested that the denaturation of protein induces the molecular aggregation of protein and increasing the amount of associated bound water within the aggregates are the cause of age-thickening. Moreover, the reduction in the amount of free water in the concentrate might result in lactose crystallization which further aggravates the situation. Snoeren et al (1982) have observed that with intense agitation, the effect of age-thickening can be reversed, as illustrated in Figure 3.2.

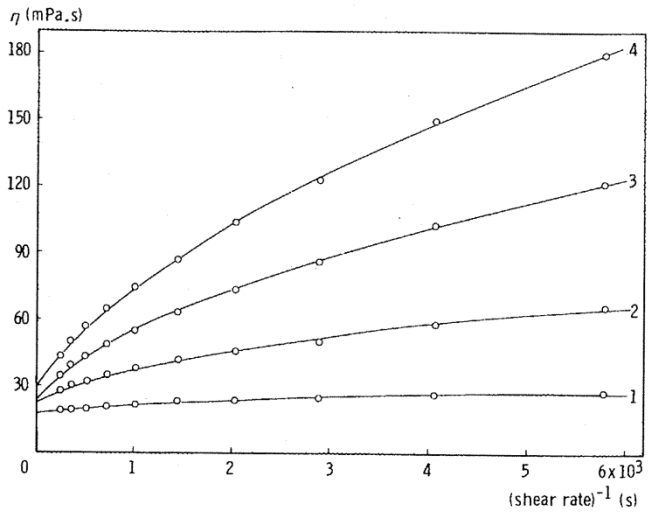

Figure 3.2 Viscosity of various skim-milk concentrates as a function of the reciprocal shear rate (Ø = 0.568). Storage time at 50°C: 1 = 0h, 2 = 2h, 3 = 4h and 4 = 6h. Source: (Snoeren et al., 1982)

3.1.3 Effect of preheat treatments

The purpose of having preheat treatments is usually linked with the product functionalities in its end-use (Carr et al., 2003). Bloore and Boag (1981)have observed that a high temperature, short heating time treatment on skim milk gave a lower concentrate (TS 47.4% and TS 49.1%) viscosity than a low temperature, long heating time treatment when comparing samples of similar Whey Protein Nitrogen Index (WPNI) (Bloore and Boag, 1981). Snoeren et al (1982) have also found that the increase in intensity of the preheat treatment increases the viscosity of skim milk. This is due to the increase in voluminosity by the denatured whey protein during preheat treatment. However, Jeurnink and de Kruif (1995) have concluded that the increase in micelle dimensions alone does not justify the increase in viscosity of skim milk due to heating but were also contributed by temporary clustering of micelles.

3.1.4 Effect of homogenisation

Homogenisation is a process to stabilise the fat emulsion against gravity separation and has long become a standard industrial process (Bylund, 1995). By forcing milk

through a small passage at high velocity, fat globules are disrupted into much smaller globules. However, homogenisation usually results in a rise of apparent viscosity of milk, especially for high fat content milks. This is because the newly formed globules have its original membrane covering them torn off, casein micelles which have highly hydrated shells are attracted to the newly formed surfaces (Dobriyan and Chekulaeva, 1982). They increase the effective volume of the newly formed fat globules in the milk due to the interstitial water trapped within, hence increasing the apparent viscosity. The homogenisation clusters can be dispersed by adding casein micelle-dissolving agents (Walstra *et al.*, 2006b). The viscosity increases linearly with increasing homogenisation pressure (Whitnah et al., 1956) as shown in Table 3.1. The formation of homogenisation clusters is promoted by high fat content, low protein content and high homogenizing pressure.

Another way of disrupting the clusters to large extent (but not completely) is to install a second stage homogeniser. The second stage homogeniser operates at a much lower pressure (around 20% of the pressure for the first stage homogeniser) (Bylund, 1995) and the low turbulent intensity does not disrupt the fat globules but causes the newly formed clusters to break up, hence reducing the viscosity.

Table 3.1 Average increase in viscosity due to increase of homogenisation pressure (Whitnah et al., 1956)

Homogenisation pressure		**Average increase in viscosity of homogenised milk as compared to unhomogenised milk**
kPa	psi	
6900	1000	7.1 %
10300	1500	9.2 %
13800	2000	11.9 %
20700	3000	13.7 %
24100	3500	15 %

3.2 Modelling of viscosity

Milk is generally classified as a suspension due to its discrete randomly distributed particles in a fluid medium (Mewis and Macosko, 1994). The modelling of non-Newtonian fluid is represented by some of the equations in Table 3.2.

Table 3.2 Typical mathematical models for non-Newtonian behaviour of foods (Aguilera and Stanley, 1999)

Model	Equation	Example
Ostwald or power law	$\eta = K\dot{\gamma}^n$	Tomato juice
Bingham plastic	$\eta = \mu_o + K\dot{\gamma}$	Ketchup
Casson	$\eta^{1/2} = K + m\dot{\gamma}^{1/2}$	Molten chocolate
Hershel-Bulkey	$\eta = \mu_o + K\gamma^{\cdot 1/2}$	Meat Batters

Both power law and Hershel-Bulkey models are used to express the rheological behaviour of highly concentrated skim milk, however, Hershel-Bulkey model is less commonly used as it requires yield stress which is not apparent below 40wt% TS (Velez-Ruiz and Barbosa-Canovas, 2000) and the confidence intervals were wide (Chang and Hartel, 1997).

At constant temperature and no age-thickening, the viscosity of dilute suspension solution is dependent on the volume fraction of the dispersed particles within the system and the viscosity of the medium. As the concentration of solid particles in a flowing medium increases, additional energy is required to make the fluid flow, thus rising the viscosity. Einstein has incorporated the interdependence of these factors into a simple equation(Walstra, 2003):

$$\eta = \eta_{ref}(1 + 2.5\phi) \tag{3.1}$$

where η = viscosity of suspension, η_{ref} = viscosity of medium and ϕ = the sum of the volume fractions of all the dispersed particles significantly larger than the

solvent molecules. If the volume fraction becomes greater than 0.01, Equation (3.1) will under-predict the true viscosity of the liquid as ϕ increases.

Another equation was proposed by Eiler and used by a number of other researchers (Eilers, 1941; Van Vliet and Walstra, 1980; Walstra and Jenness, 1984; Fox and McSweeney, 1998) where the viscosity of whole milk, skim milk, cream and some milk concentrate can be predicted as long as they exhibit Newtonian behaviour. The Newtonian coefficient of viscosity is related to the concentration of individual components:

$$\eta = \eta_{ref}\left(1 + \frac{1.25\sum(\phi_i)}{1 - \sum(\phi_i)/\phi_{max}}\right)^2 \tag{3.2}$$

where η_{ref} is the coefficient of viscosity of a reference medium (or the solvent) and ϕ is the volume fraction of all dispersed particles in milk that are at least an order of magnitude greater than water. Volume fraction of any component can be calculated by

$$\phi_i = V_i c_i \tag{3.3}$$

where V_i = voluminosity of component i ($m^3.kg^{-1}$ dry component) and c_i = concentration of the component in the product ($kg.m^{-3}$ product). The typical values of the voluminosity of some key components in milk are given in Table 3.3

Table 3.3 Voluminosity of components in milk
(Walstra and Jenness, 1984; Fox and McSweeney, 1998)

Component	Voluminosity ($m^3.kg^{-1}$)
Fat globules	1.11×10^{-3}
Casein micelles	3.9×10^{-3}
Lactose	1×10^{-3}
Whey protein	1.5×10^{-3}

For milk,

$$\phi \approx \phi_f + \phi_c + \phi_w + \phi_l \tag{3.4}$$

where ϕ_f, ϕ_c, ϕ_w and ϕ_l are the volume fractions of fat, casein, whey proteins and lactose, respectively (Fox and McSweeney, 1998). ϕ_{max}, in a system of spheres with uniform spheres is 0.74, and higher with spheres of different sizes co-exist. Extensive studies on the viscosity of milk were conducted (Snoeren et al., 1982; Snoeren et al., 1984). These include the dependency of volume fraction of macromolecular particles in milk and viscosity of serum on the overall viscosity of the milk. The value for ϕ_{max} was taken as 0.79 by Snoeren et al (1982) based on an extrapolation of gelling time when it is zero. The viscosity of the reference medium, serum is taken as the overall viscosity of a solution consisting of 5 wt% lactose and milk salts. The salts are assumed to contribute 2% increase in water viscosity (Van Vliet and Walstra, 1980).

$$\eta_{ref} = \eta_{water} + (\Delta\eta_s + \Delta\eta_{ls}) \frac{DM_{conc}}{DM_{milk}} \tag{3.5}$$

where $$\Delta\eta_s = \eta_{water+salts} - \eta_{water} = 0.02\eta_{water} \quad (3.6)$$

and $$\Delta\eta_{ls} = \eta_{water+5\%\ lactose} - \eta_{water} \quad (3.7)$$

One of studies by Snoeren et al (1982) focuses on the effects of heat treatment and composition of milk on the viscosity of the concentrate. Volume fractions of caseins, denatured whey proteins and native whey proteins are incorporated into Equation (3.2) as shown below.

$$\eta = \eta_{ref}\left(1 + \frac{1.25(\phi_c + \phi_{nw} + \phi_{dw})}{1 - (\phi_c + \phi_{nw} + \phi_{dw})/\phi_{max}}\right)^2 \quad (3.8)$$

From their result, it is obvious that viscosity of skim milk is better illustrated as a function of volume fraction than that represented by dry matters only, as shown in Figure 3.3 and Figure 3.4.

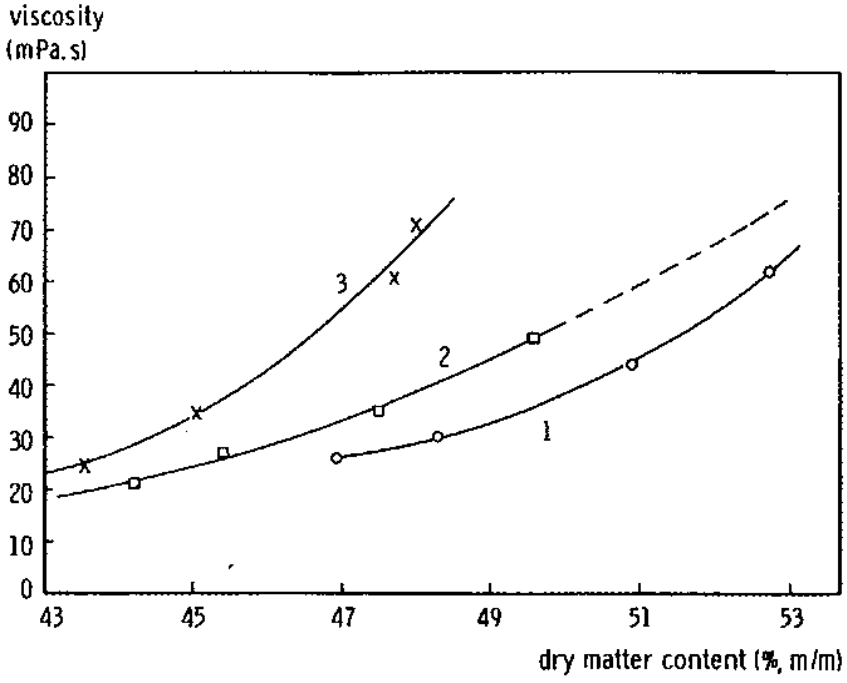

Figure 3.3 Viscosity of skim-milk concentrates as a function of the dry matter content. Preheat treatment of milk: 1 = 10s, 70°C; 2 = 1min, 85°C; 3 = 5min, 95°C. Shear rate = 392 s^{-1}. (Snoeren et al., 1982)

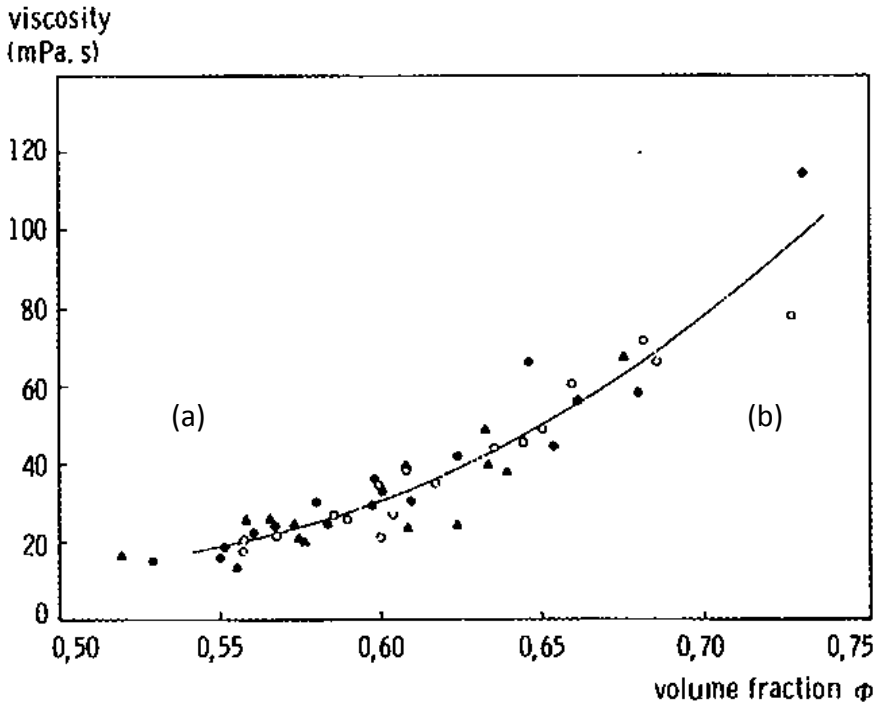

Figure 3.4 Viscosity of skim-milk concentrates as a function of the volume fraction, Φ. Preheat treatment of milk: ▲ = 10s, 70°C; ○ = 1min, 85°C; ● = 5min, 95°C. Shear rate = 392 s^{-1}. (Snoeren et al., 1982)

For suspension of moderate concentration range, extension of Einstein's equation by forming a polynomial in ϕ, such as:

$$\eta = \eta_{ref}(1 + 2.5\phi + b\phi^2 + c\phi^3 + \cdots) \tag{3.9}$$

The values of coefficients are diverse in various theories, ranging from 4.4 to 14.1. (Aguilera and Stanley, 1999; Malkin and Isayev, 2006)

Another commonly used equation is proposed by Mooney (1951), which is an extension of Einstein's equation. This equation has taken first order interaction of particles to account for "crowding" effect.

$$\eta = \eta_{ref}\ exp\left[\frac{2.5\phi}{1-(\frac{\phi}{\phi^*})}\right] \tag{3.10}$$

Mooney's equation has also pointed out an important effect of critical concentration, $\phi^*$where infinite increase in viscosity occurs (Malkin and Isayev, 2006). Critical concentration ranged from 0.63 to 0.74 for low and high shear rates (Macosko, 1994).

The "crowding" effect is also cited in another equation proposed by Ball and Richmond (Barnes et al., 1989).

$$\eta = \eta_{ref}\ (1-K\phi)^{-5/(2K)} \tag{3.11}$$

Equation (3.10) and (3.11) use exponential and power terms respectively to describe the dependence of concentration, essentially volume fraction of each component particles, to determine the viscosity. However, those equations are bounded with assumptions which restrict the ability to reflect the true viscosity of suspension with the following conditions:

- particles of different sizes and shapes
- liquid medium with non-Newtonian properties
- non-spherical particles
- formation of stable surface layers due to physical interaction between solid and liquid particles

- interactions between solid particles

Modification of equations is required in order to account for the unique conditions above. Such modification requires special investigations in the field of multi-component systems.

Many colloidal suspensions display shear-thinning behaviour, where viscosity decreases with increasing shear rate. There are two explanations behind this pseudoplastic behaviour. First of all, it could be due to the realignment of asymmetric dispersed molecules within the shear planes as shear rate increases, thus reducing the frictional resistance (Tung, 1978). Secondly, it could be explained from the perspective of volume fraction. Large effective volume is occupied by aggregates of fat globules and the milk serum trapped in their interstitial spaces owning to their asymmetric shapes. With the increase in shear rate, shear stress acted upon the aggregate increase as well. The increase in shear stress enables the aggregates to disperse and yield smaller or more rounded ones which reduce the interstitial space between the fat globules, as a result reducing the total volume fraction of the fat phase and thus reducing the viscosity. A point to note, when the forces holding the aggregates together is being overcome by the shear force, further increase in shear rate will result in smaller changes in apparent viscosity. Therefore, the fluid will exhibit Newtonian behaviour at high shear rates (Fox and McSweeney, 1998; Walstra, 2003).

A 'cross' equation (Barnes et al., 1989) is usually used to describe the viscosity trend of material displaying Newtonian behaviour at both extreme ends of shear rates.

$$\eta = \eta_{\infty} + \frac{(\eta_o - \eta_{\infty})}{1 + (K\dot{\gamma})^m} \tag{3.12}$$

where *K* and *m* are constants which had to be derived from experimental data.

As shown in Figure 3.5, the typical shear-thinning behaviour at some intermediate region between two Newtonian plateaus (at low and high shear rate).

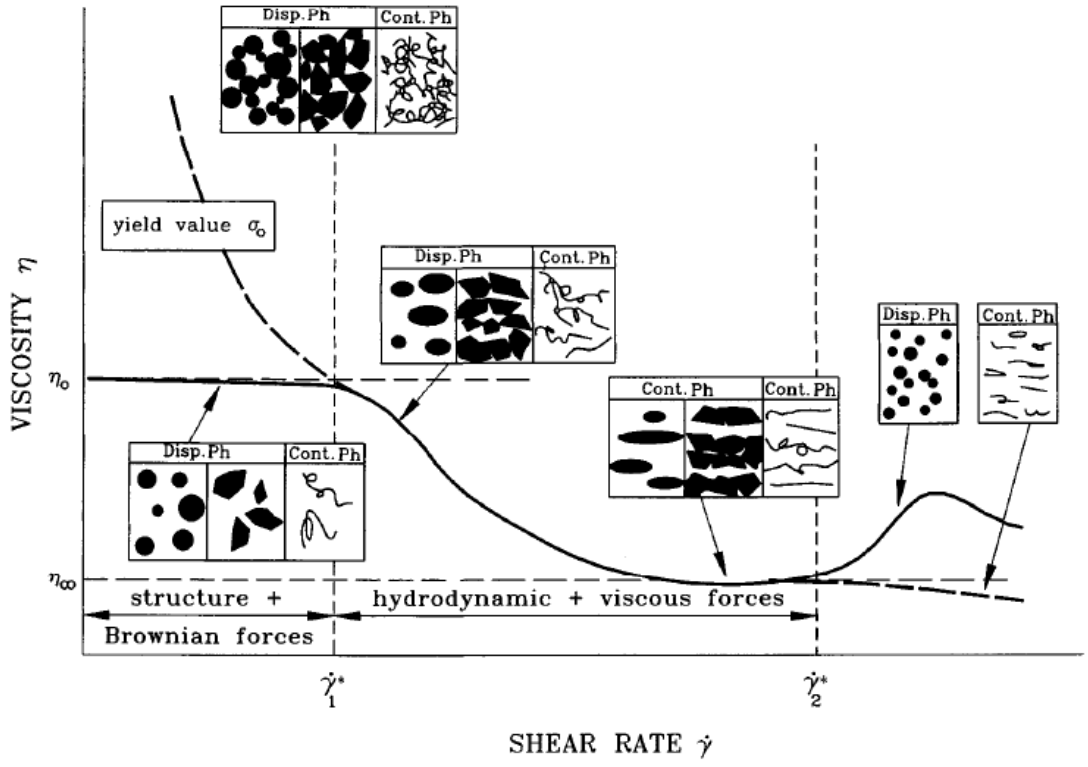

Figure 3.5 Rheological behaviour of a complex suspension and its relation to structure. (Windhab, 1995)

In terms of temperature dependence, Walther (1929) proposed an empirical equation that relates the kinematic viscosity to temperature:

$$\log\log\,(\nu + a) = m\,logT + b \tag{3.13}$$

where ν = kinematic viscosity (centistokes), T = absolute temperature (K), and a, m and b are constants. When constant a was assigned the value 0.8, the equation fits well with the properties of reconstituted skim milk.

When Bucklingham (1978) ploted of log log (v + 0.8) against log θ, the reconstituted skim-milk solution resulted in a family of straight lines.

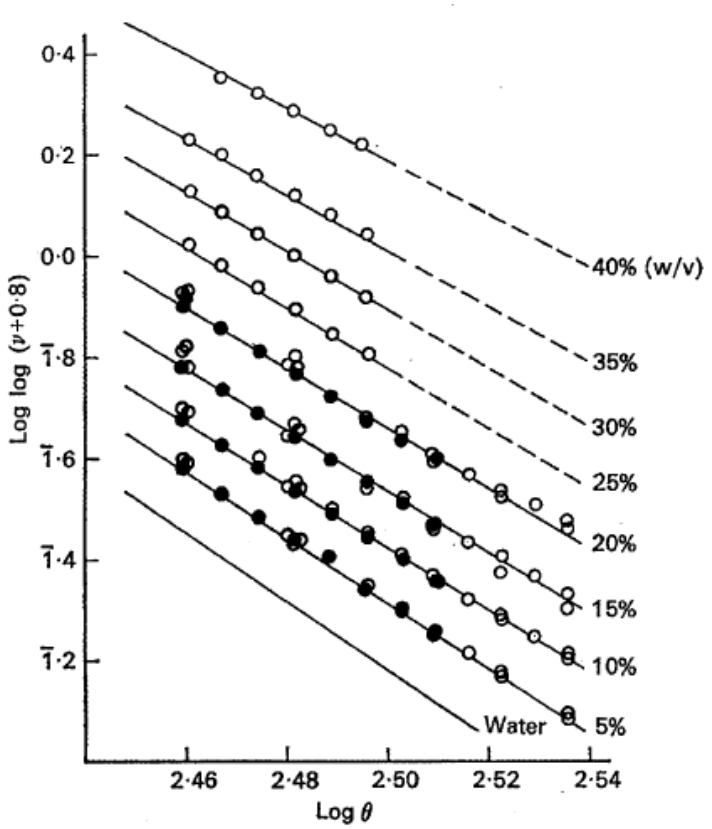

Figure 3.6.Relationship between kinematic viscosity (v) and absolute temperature (θ) for skim milk powder solutions of various solids concentrations. ○, Freshly prepared solutions; ●, solutions aged overnight. (Buckingham, 1978)

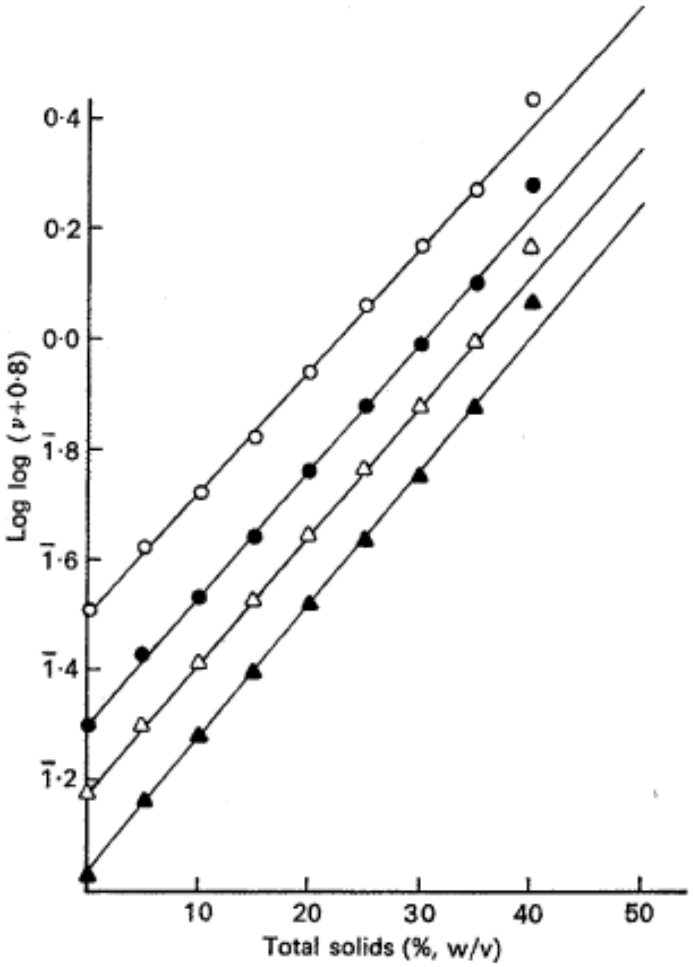

Figure 3.7 Relationship between kinematic viscosity (ν) and %(w/v) total solids for skim milk powder solutions of various temperature. ○, 10˚C; ●, 30˚C; Δ, 44˚C ; ▲, 60˚C. (Buckingham, 1978)

The term " $logT$ " in Equation (3.13) is interchangeable with the percentage of total solid (TS) when correlating viscosity with solid content and produces similar family of straight lines.

The Arrhenius model is also extensively used to describe the effect of temperature on rheological properties of Newtonian and Non-Newtonian food fluid to evaluate the activation energy E_a (Holdsworth, 1971; Rao, 1977; Velez-Ruiz and Barbosa-Canovas, 1998a). Besides viscosity η and apparent viscosity η_a, consistency coefficient K can be correlated with temperature using Arrhenius model as well.

$$\eta, \eta_a, K \sim A_0 e^{\left(\frac{E_a}{RT}\right)} \tag{3.14}$$

where A_0 = constant, R = universal gas constant and T = temperature (K)

Torssell et al (1949) have then modified Equation (3.13) to incorporate total solids X (wt%) and temperature T (K) as the dependencies of viscosity

$$loglog(v + 0.8) = A \cdot X + B - (C \cdot X + D) log \frac{T}{313} \tag{3.15}$$

where A,B,C and D are model constants.

Another polynomial expression with the same functionalities as Equation (3.15) was used by both Fernandez-Martin (1972) who experimented with ten different types of milks and Bloore and Boag (1981) who investigated on skim milk, as shown below:

$$\begin{aligned} log\eta = {} & A_0 + A_1 T + A_2 T^2 + (B_0 + B_1 T + B_2 T^2) X \\ & + (C_0 + C_1 T + C_2 T^2) X^2 \end{aligned} \tag{3.16}$$

where A_i, B_i and C_i were calculated by the least square method, T is temperature (K) and X is total solids (wt%).

Reddy and Datta (1994) have proposed a set of equations for non-Newtonian fluids, which correlates concentration and temperature with viscosity. The approach they made was to employ a linear relationship to fit the flow behaviour index, n, dependent on total solids, X (wt%) (Equation (3.17)) and an exponential term to describe the reliance of consistency coefficient, K on temperature, T and total solids (Equation (3.18))

$$n = mX + b \tag{3.17}$$

$$K = B_1 \exp\left(\frac{C_2}{T}\right) 1.25^X \tag{3.18}$$

By fitting Equation (3.17) and (3.18) to a power law model, the apparent viscosity can be expressed as:

$$\eta_a = B_1 \exp\left(\frac{C_2}{T}\right) 1.25^X (\dot{\gamma})^{mX+b} \tag{3.19}$$

From all the models that are stated above, most of the authors focused on milk at low concentration (<40 wt%) and reconstitution of milk powder, except for Bloore and Boag's study, were commonly used. Therefore, experiments were carried out on viscosity measurements at high concentrations (30 to 55 wt%) on reconstituted skim milk with the aim of comparing the models fitted to the viscosity profiles. In addition, the fundamental models (Equation 3.1, 3.2, 3.8. 3.9, 3.10 and 3.11) reported so far require accurate knowledge about the concentration dependent voluminosity function which are in general of unknown properties, hence may not give guidance that easily direct practical operation in terms of predictive power.

Table 3.4 Summarised Table of Viscosity Equations

Model Equations	Author(s)	Equation
Concentration Dependent Model		
$\eta = \eta_{ref}(1 + 2.5\phi)$	Einstein (3.1)	(3.1)
$\eta = \eta_{ref}\left(1 + \frac{1.25\sum(\phi_i)}{1 - \sum(\phi_i)/\phi_{max}}\right)^2$	Eiler	(3.2)
$\eta = \eta_{ref}\left(1 + \frac{1.25(\phi_c + \phi_{nw} + \phi_{dw})}{1 - (\phi_c + \phi_{nw} + \phi_{dw})/\phi_{max}}\right)^2$	Snoeren et al	(3.8)
$\eta = \eta_{ref}(1 + 2.5\phi + b\phi^2 + c\phi^3 + \cdots)$	Einstein	(3.9)
$\eta = \eta_s \ exp\left[\frac{2.5\phi}{1 - (\frac{\phi}{\phi^*})}\right]$	Mooney	(3.10)
$\eta = \eta_{ref}\,(1 - K\phi)^{-5/(2K)}$	Ball and Richmond	(3.11)
$\eta = \eta_\infty + \frac{(\eta_o - \eta_\infty)}{[1 + (K\dot{\gamma})^m}$	Barnes et al	(3.12)
Temperature Dependent Model		
$\log\log\,(\nu + a) = m\,logT + b$	Walther	(3.13)
$\eta, \eta_a, K = A_0 e^{\left(\frac{E_a}{RT}\right)}$	Arrhenius model	(3.14)
Concentration and Temperature Dependent Model		
$loglog(\nu + 0.8) = A \cdot X + B - (C \cdot X + D)log\frac{T}{313}$	Torssell et al	(3.15)
$log\eta = A_0 + A_1T + A_2T^2 + (B_0 + B_1T + B_2T^2)X + (C_0 + C_1T + C_2T^2)X^2$	Fernandez-Martin	(3.16)
$\eta_a = B_1 \exp\left(\frac{C_2}{T}\right) 1.25^X (\dot{\gamma})^{mX+b}$	Reddy and Datta	(3.19)

3.3 Viscometry and Density Measurement

3.3.1 Concentric cylinder measuring system

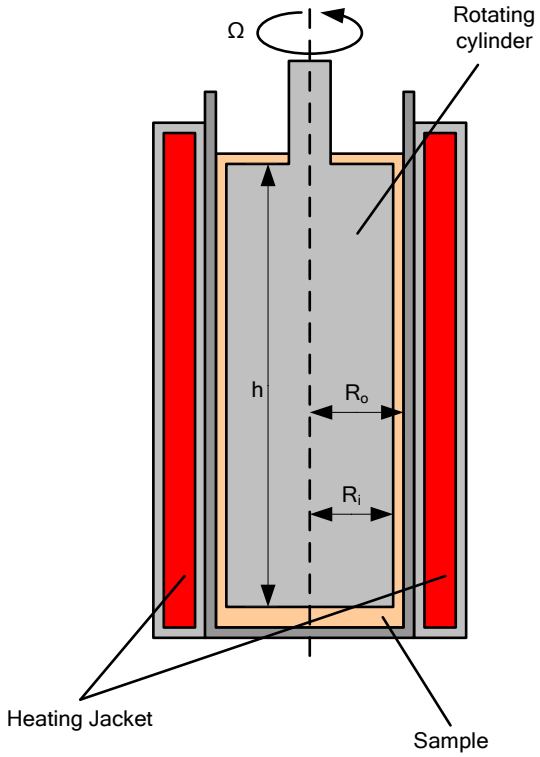

Figure 3.8 Schematic representation of viscometer consisting of two coaxial cylinders.

A schematic diagram of a cylinder-cylinder type rotational viscometer with a heating jacket is shown in Figure 3.8. The viscometer consists of a hollow outer cylinder, a solid inner cylinder with radius of R_o and R_i respectively and a heating jacket that surrounds the outer cylinder. Both cylinders share a common axis and Ω (rad.s^{-1}) is the rotational speed of the inner cylinder while taking viscosity measurements. The height of the inner cylinder is given as h (m). Liquid sample is filled into the outer cylinder until the entire height of the inner cylinder submerges in the sample.

For Newtonian fluid, the shear stress, σ (Pa), experienced by the fluid can be formulated in a standard form as:

$$\sigma = \eta\dot{\gamma} \tag{3.20}$$

where $\dot{\gamma}$ is the shear rate (s^{-1}) and η is the constant coefficient of proportionality, also known as viscosity (Pa.s).

The torque, τ (Nm), located at distance r from the axis of the cylinder is expressed as

$$\tau = 2\pi r^2 h\sigma \tag{3.21}$$

When a rotational viscometer has both its inner and outer cylinder rotates, the velocity distribution, *u(r)*, in between the inner and outer cylinder can be calculated by the following equation:

$$u(r) = \frac{(\Omega_o R_o^2 - \Omega_i R_i^2)r^2 - (\Omega_o - \Omega_i)R_i^2 R_o^2}{(R_o^2 - R_i^2)r} \tag{3.22}$$

where Ω_o is the angular frequency of the outer cylinder and Ω_i is the angular frequency of the inner cylinder.

For viscometer where the inner cylinder rotates while the outer cylinder remains stationary ($\Omega_i \neq 0$ and $\Omega_o = 0$) and vice versa,

$$u(r) = \frac{\Omega R_i^2(R_o^2 - r^2)}{(R_o^2 - R_i^2)r} \tag{3.23}$$

The distribution of shear rate, $\dot{\gamma}(r)$, in between the cylinders can be written as:

$$\dot{\gamma}(r) = r\frac{\partial\omega}{\partial r} = 2\Omega\frac{R_i^2 R_o^2}{R_o^2 - R_i^2}\frac{1}{r^2} \tag{3.24}$$

The viscosity, η (Pa.s), can be expressd in the following equation:

$$\eta = \frac{\tau}{\Omega} \frac{R_o^2 - R_i^2}{4\pi R_i^2 R_o^2 h} \tag{3.25}$$

For non-Newtonian liquid, the calculating of shear rate in Equation (3.24) can be simplified if the gap between the cylinders, Δ, is small compared to the radii of the inner cylinder.

$$\frac{\Delta}{R_i} = \frac{R_o - R_i}{R_i} \ll 1 \tag{3.26}$$

If the above criterion is satisfied, the shear rate for non-Newtonian liquid can be calculated by

$$\dot{\gamma} = \Omega \frac{R_i + R_o}{2(R_o - R_i)} \approx \frac{\Omega R}{\Delta} \tag{3.27}$$

where R can be either R_i or R_o.

3.3.2 Coriolis measurement technique

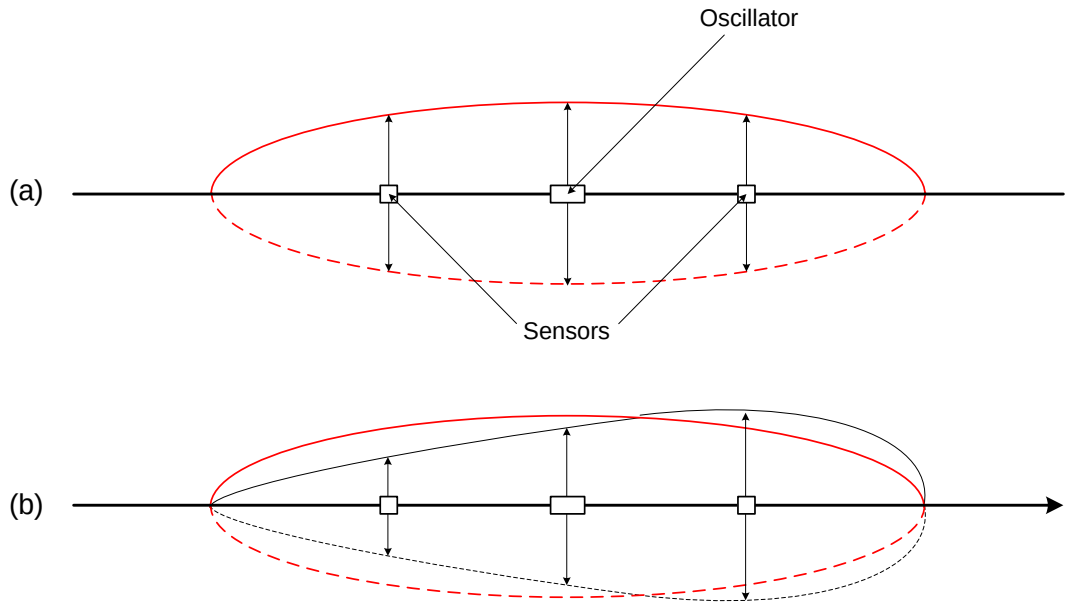

Figure 3.9 An exaggerated illustration of Coriolis Effect (a) Flow velocity = 0, (b) Flow velocity ≠ 0

The coriolis measurement technique utilises the twisting motion induced by the fluid travelling through a osillating tube to measure the flow properties such as density, flow rate, viscosity, etc. Within the mass flow meter, an oscillator located on center of the measuring tube vibrates, causing the tube to oscillate. If there is no flow through the tube, it will oscillate uniformly as shown in Figure 3.9(a). Sensors are located at the inlet and outlet of the measuring tube registers the oscillation precisely. However, as soon as the fluid begins to flow through the measuring tube, additional twisting is imposed on the oscillation as a result of the fluid's inertia. This is illustrated in Figure 3.9(b). The coriolis effect cause the inlet and outlet section of the tube to oscillate in different direction at the same time. The highly sensitive sensors pick up the change in oscillation pattern in terms of time and space, also known as the phase shift. The amount of gas or liquid flowing through the tube can be measured directly base on this phase shift. The higher the flow velocity (mass flow rate), the greater the deflection of the oscillating tube.

Besides the measurement of flow velocity, density of the fluid can also be measured by analysing the frequency of the oscillation. The resonant frequency of a tube filled with liquid, ω (rad s^{-1}), is derived from the following equation:

$$\omega = 2\pi f = \sqrt{\frac{K}{M}} \tag{3.28}$$

where f is the frequency of oscillation (Hz), K is the spring constant and M is the mass.

The mass consists of 2 components, the measuring tube and the liquid.

$$M = M_{tube} + M_{liquid} \tag{3.29}$$

The mass of the liquid is expressed as

$$M_{liquid} = \rho_L V \tag{3.30}$$

The period of frequency, t (s), is the inverse of frequency of oscillation.

$$t = \frac{1}{f} \tag{3.31}$$

By substituting Equation (3.29),(3.30) and (3.31) into (3.28) and solving for ρ

$$\rho = \frac{Kt^2}{4\pi^2 V} - \frac{M_{tube}}{V} \tag{3.32}$$

where V is the volume of fluid in the tube

Since π, M_{tube} and V are constants, Equation (3.32) can be simplified to the following equation.

$$\rho = K_1 t^2 - K_2 \quad \textbf{(3.33)}$$

where K_1 and K_2 are the sensor-dependent calibration constants. These are derived from the calibration performed with two different density fluids (Kalotay, 1999).

The dampening effect of a denser fluid lowers the oscillation frequency more than that of a lighter fluid. Both the flow velocity and density can be measured simultaneously but independently via the tube oscillation.

To measure the viscosity in the same flow meter, an additional pendulum is attached to the middle of the oscillating measuring tube. The pendulum will induce a torsional oscillation onto the measuring tube as illustrated in Figure 3.10. The velocity profile shown in Figure 3.11 varies with viscosity. The shear forces created by the velocity gradient in the velocity profile dampen the measuring tube. This dampening effect can be measured via the excitation current that maintains the tube oscillation. Therefore, the viscosity can be determined by measuring the excitation current. The coriolis measurement technique is employed by Endress+Hauser Promass 83I mass flow meter that is shared between steam- and electric-heated pilot evaporator.

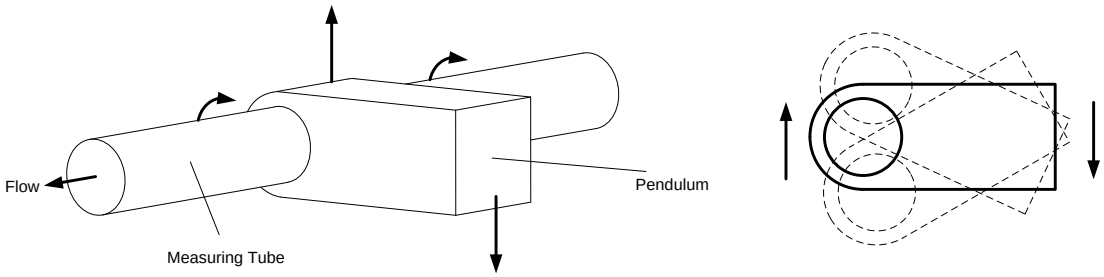

Figure 3.10 Torsional oscillation on the measuring tube

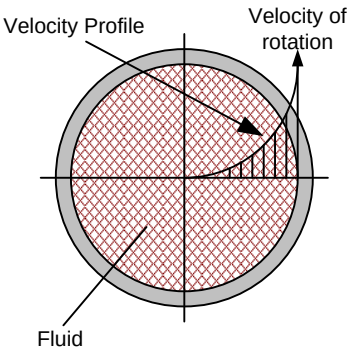

Figure 3.11 Cross-sectional view of the measuring tube and velocity profile of the fluid inside the measuring tube (Drahm and BjØnnes, 2003)

3.4 Materials and Methods

The study of the effect of rheology on the operation of falling film evaporator is complex because the measurement of instantaneous viscosity of milk during the evaporation process, in most cases, is not reliable. The measurement of milk viscosity can be influenced by many factors as mentioned in Section 3.1.

From previous literatures, many authors worked with milks of low solids content (<40 wt%). Within this range, the viscosity is less than 10 cP. From the view point of milk viscosity profile, this is regarded as the bottom of the spectrum as viscosity increases exponentially between total solids of 40 to 60 wt% at the same temperature

Therefore, the main focus of this work is on the measurement of viscosity on at higher solids content (> 40wt%) of skim milk at various conditions, e.g. temperature, total solids and shear rate and the performance of the falling film evaporator with changing milk rheological properties.

In the evaporation process of milk where some of the structural changes may be irreversible, such as age-thickening and disposition of protein in terms of fouling within the system, repeatable measurements has proven to be a difficult task. In order to remove most of the variables to give repeatable results, emphasis were put on the measurement of process parameters, like steam temperatures, temperature profile along the evaporator, operating pressure, etc, when designing the evaporators.

The ideal experiment would consist of the ability to extract large number of measurements at each total solids level at any given time. The viscosities of all the samples have to be measured simultaneously, covering a desirable range of shear rates and temperatures (e.g. 0 – 1000s^{-1} and 20 – 70 °C) on identical viscometers. Measurement has to be taken immediately after the samples has been extracted to minimise the age-thickening effect (Section 3.1.2), especially at total solids over 50 wt%. Clearly, such idealised experiment is not practical yet, if not possible at all.

Therefore, the first task is to develop a viscosity measurement protocol that is both robust and feasible. Some of the main criteria for viscosity measurement are:

1. Measurement should be taken at various shear rate
2. Temperature is controlled
3. With minimum delay in viscosity measurement after sample extraction
4. Sample volume should not be too large.

The next task was to design evaporation systems that are able to mimic the operation conditions similar to those used in dairy industries and meeting the requirements in the viscosity measurement protocol. Some of the operation conditions include evaporation in a -80 kPa vacuum environment, the ability to control the temperature of the heat source between 60 to 70 °C and the capability to pump viscous fluid.

Once the viscosity measurement protocol and evaporators were in place, experiments were carried out to analyse the difference in milk viscosity profile in various type of milk and the influences of total solids, temperature and shear rate have on viscosity. Heat transfer during the evaporation process was also examined in some of the evaporators. Data collected from the experiment were thoroughly analysed to ensure only the correct information was extracted and no artifacts were included. Truncation and correction of the raw data was carried out where applicable.

3.4.1 Viscosity measurement

Viscosities of samples were measured using a rotational viscometer (Visco Basic Plus with Low Viscosity Adaptor (LVA), Fungilab, Barcelona) of cylinder-cylinder type with flow jacket for temperature control which has a precision of ±1% of full scale. This viscometer is capable of measuring viscosity as low as 1 cP and only require a sample volume of 20ml. The viscometer is calibrated with Cannon silicone viscosity standard RT10 for rotational viscometer (2003). Other auxiliary equipments includes a hot water bath (Thermoline Scientific TWD – 22D), a

peristaltic pump (Masterflex L/S Ecomomy Digital Console Pump System) and a temperature logger (Picolog TC-08 thermocouple data logger)

3.4.1.1 Viscosity measurement protocol

The hot water bath was preheated to the desired temperature prior to any measurement. The hot water was pumped into the flow jacket around the LVA by a peristaltic pump at around 800ml/min. Usually, the set point of the water hot water bath is 2-5 °C higher (depending on the temperature difference between the ambient temperature and desired water temperature) than the desired measurement temperature as the water cools down while it is pumped into the flow jacket. Two thermocouples inserted at the inlet and outlet of the flow jacket to monitor the water temperature entering and leaving the jacket. The two temperatures should be within ± 0.5 °C from the desired measurement temperature. For preheating purposes, the sampling cylinder was kept in the heated LVA while the spindle was submerged in the hot water bath prior to every measurement.

When a sample is collected from the evaporator, 20ml of the sample was injected into the preheated sampling cylinder with a syringe. The spindle was then removed from the hot water bath and dried before inserted into the sampling cylinder. After which, the sampling cylinder containing the sample and spindle was inserted into the LVA. The samples were allowed to rest in the LVA for one minute for it to reach the designed temperature before viscosity measurements were taken.

Consecutive measurements of viscosities at rotational speeds of 100, 60, 50, 30, 20, 12 rpm respectively were recorded. Those rotational speeds correspond to shear rates of 104.7, 62.8, 52.3, 31.4, 20.9, 12.6, 10.5 s^{-1} respectively. The viscosity measurement of one sample should take less than 5 min to complete.

Figure 3.12 Hot water bath and Visco Basic Plus with Low Viscosity Adaptor

In Figure 3.12, it shows the viscometer setup with the sampling cylinder and spindle inserted into the LVA.

3.4.1.2 Reproducibility of viscosity measurement

The reproducibility of the viscosity measurements was tested to show the robustness of the viscosity measurement protocol mentioned in Section 3.4.1.1. In this repeatability test, fresh medium heat-treated skim milk from MG, Koroit was evaporated using the steam-heated falling film evaporator. Viscosities of concentrated milks were measured at 60°C with shear rates ranged from 10.5 to 104.8 s^{-1}. Viscosity measurements were taken during the evaporation process to capture the viscosity profile at different solids contents. Three repetitive runs were conducted using the same type of milk and evaporation conditions. From Figure 3.13, the viscosity profiles from the three runs were matched closely with each other and this suggested that the viscosity measurement protocol is reproducible.

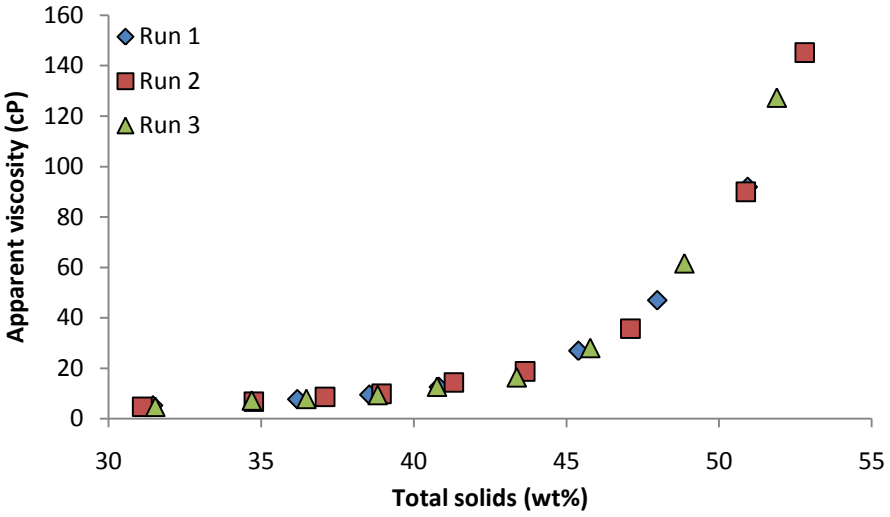

Figure 3.13 Repeatability of viscosity measurement on 3 separate runs

A further analysis on the deviation between the three runs was conducted using models fitted to the three viscosity profiles. The deviation among the three models was plotted in Figure 3.14. This shows that as the solids content increases, the deviation becomes greater.

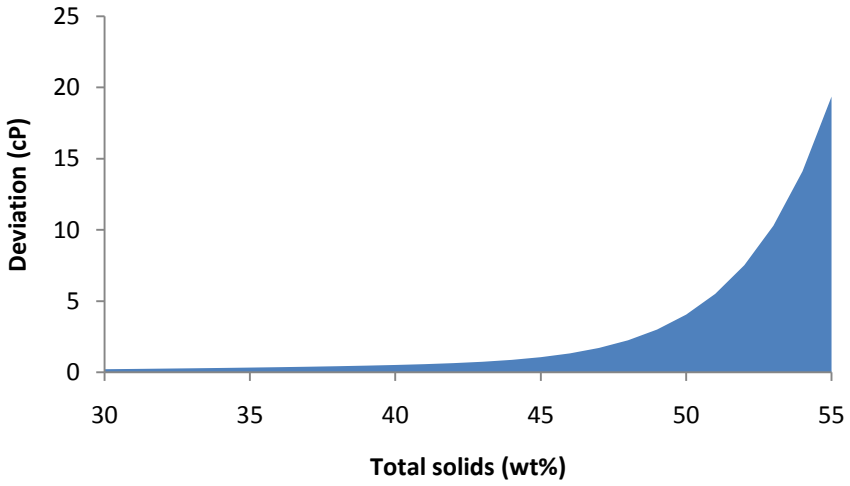

Figure 3.14 Deviation of viscosity measurements at 31.4s^{-1}

However, when the deviation was compared to the viscosity measured between the three runs, the percentage deviation stayed nearly constant, hovering between 5 to 6.5%, throughout the entire range of solids content tested, as illustrated in Figure 3.15. This means that a 300cP measurement at 55wt% has a deviation of merely 20cP.

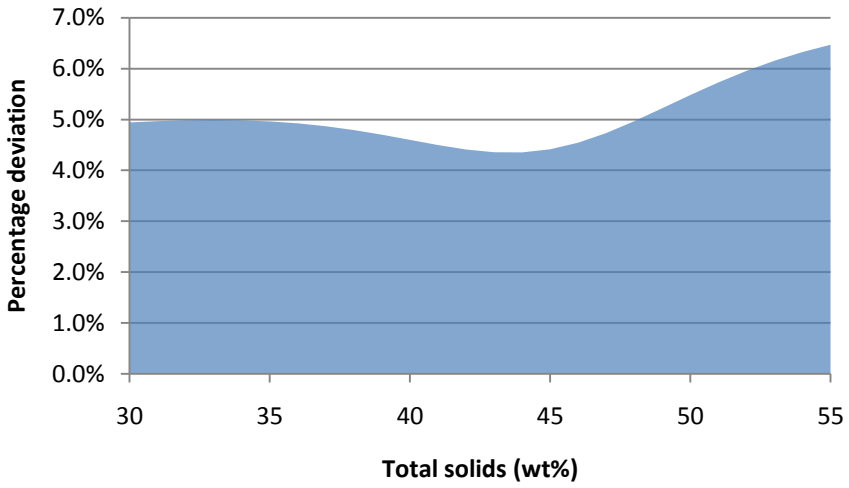

Figure 3.15 Percentage deviation of viscosity measurement at 31.4s^{-1}

To date, the viscosity measurement of non-Newtonian liquid with high precision and accuracy has been a difficult task. Therefore, a 6.5% deviation at 300cP is an acceptable degree of error. Similar deviation results were produced by viscosity measurements at other shear rates as well.

3.4.1.3 Viscosity measurement after 24 hours of storage

On some occasions where the supply of milk concentrate (around 30wt%) from the factory had to be delivered to Monash University, the delivery and storage time could last up to 24 hours before viscosity measurements and pilot scale evaporation could commence at the university. During the delivery and storage process, the milk was kept in a 4°C or lower environment. However, there were concerns regarding the reliability of the viscosity measured from the stored milk concentrate as age-thickening could potentially alter the viscosity measurement. Even though Snoeren et al (1982) have observed that with intense agitation, the effect of age-thickening can be reversed and the repeated pumping action during the evaporation process might provide the necessary agitation, a test was carried out to verify the reliability of the viscosity measured from the stored milk concentrate.

The verification test was conducted in Warrnambool Cheese and Butter Factory (WCBF) and it consists of two sections. Firstly, skim milk concentrate was evaporated immediately after it was collected from the commercial evaporator by

the steam-heated pilot evaporator. Viscosities of the milk concentrate were measured during the evaporation process to capture the viscosity profile within a range of solid content levels. Secondly, an identical evaporation and viscosity measurement process as the first section was performed on a batch of skim milk concentrate subjected to 24 hours of cold storage. Same batch of skim milk concentrate at around 30wt% was used in both sections of the verification test. The viscosity profiles were then compared and analysed to find out if there is any differences between the viscosity measurements of fresh and stored milk.

In Figure 3.16, both viscosity profiles seems to be aligned with each other and show no observable differences between the profiles when the skim milk concentrate was stored at 30wt%.

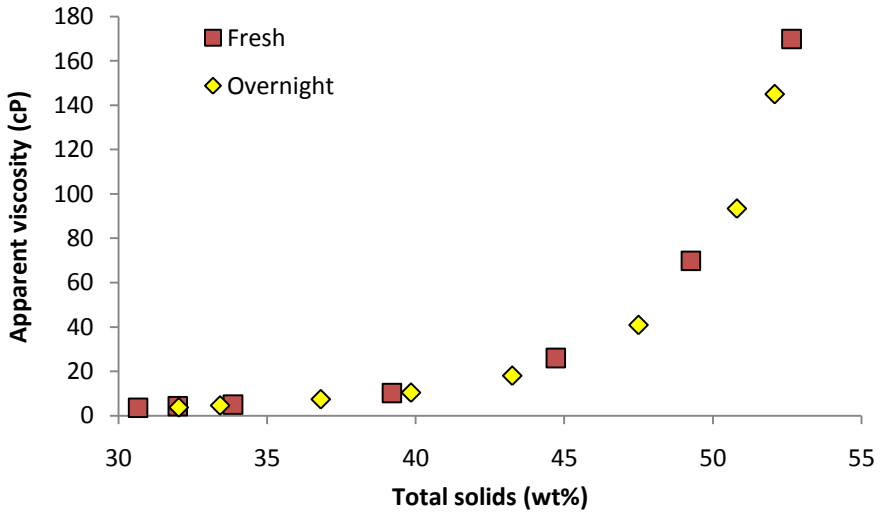

Figure 3.16 Comparison of viscosity profile of fresh and overnight skim milk concentrate (30wt%, 34% DB protein measured at 31.4 s^{-1})

The verification test has proven that there is no effect of 24 hours cold storage at 30wt% on the viscosity measurement.

A second set of verification tests was conducted on 41wt% skim milk at WBCF and the results are presented in Figure 3.17. An obvious distinction between the two viscosity profiles was observed right from the beginning of the viscosity profiles. The overnight milk concentrate has consistently produced a higher viscosity than the fresh counterpart that ranged from 12cP at 43wt% to over 100 cP at 51wt%.

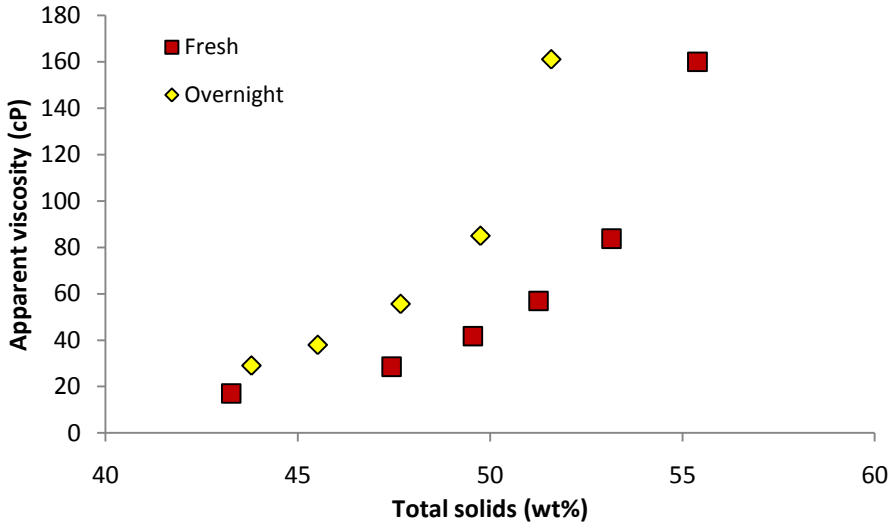

Figure 3.17 Comparison of viscosity profile of fresh and overnight skim milk concentrate (41wt%, 36% DB Protein at 31.4 s^{-1})

With the two sets of verification tests, it might indicate that the reversibility of the age-thickening effect is influenced by the solids content to which it was stored in. In other words, at or below 30wt% in cold storage over 24 hours, skim milk tested showed little sign of age-thickening which was initially expected to happen.

3.4.2 Total solids measurements

In dairy industries, the total solids (TS) of milk concentrate has an important role in the operation of the evaporator system. The rheological properties of milk is reflected directly on the TS of milk concentrate although the extent of rheological influence by the TS varies among the different type of dairy products. At high concentrations (above 45wt%), the viscosity of concentrated milk increases exponentially and the recommended operating viscosity of the falling film evaporator should not exceed 100 cP to prevent excessive fouling. Usually, the TS monitored by the evaporator system is a conversion of density measured inline that is pre-configured into the control system. Therefore, it is crucial to establish the relationships between the total solids, density and viscosity.

Before the relationships can be established, focus was placed on the method of TS measurement. The most commonly used method is the oven drying method, which has been regarded as an exact reference method.

3.4.2.1 Total solids measurement procedure

Initially, the total solids measurement method used was adopted from the International Dairy Federation (IDF) standard 21B: 1987 for milk, cream and evaporated milk described in Section 3.4.2.2 (IDF, 1987). However, the IDF standard was then found to be inacurrate in representing the TS at high solids level. The results from IDF method were suspected to be higher than the true TS level and two separate studies were conducted in the current work to verify the hypothesis. Firstly, an independent investigation of the IDF standard was carried out with control solution to find out if the drying time affects the TS measurement. The second study was to introduce another method, Australian standard AS2300.1.1 (Australia, 1988) described in Section 3.4.2.3, to compare the 2 methods. The results of both studies are presented in Section 3.4.3, 3.4.4 and 3.4.5.

3.4.2.2 IDF Standard 21B:1987

A clean flat bottom dish was weighed on a electronic balance to the nearest 1mg (m_0). 2.5 – 3 g of sample was then spread evenly on the dish. The dish with the sample was reweighed to the nearest 1mg (m_1) again before it is placed in the oven (102˚C) for 2 hours. After which, the dish with dried sample was covered and left to cool at room temperature for 10 minutes before weighing (m_2) commences.

The total solids content, expressed as a percentage by mass, can be calculated by (Steiger and Martens, 1986):

$$TS\ (wt\%) = \frac{m_2 - m_0}{m_1 - m_0} \times 100 \tag{3.34}$$

where m_0 = mass of the dish (g), m_1 = mass of the dish with test portion (grams) and m_2 = mass of dish with dried test portion (g).

3.4.2.3 Australia Standard AS 2300.1.1

The preparation procedure of the Australian standard includes the drying of a dish containing about 25g of prepared sand and its corresponding lid and glass stirring rod in an oven at 102 ±2°C for at least an hour. The lid with the rod and the dish were then placed in a desiccator for cooling until they were within 1°C of the balance room temperature before they were weigh to the nearest 0.1mg (m_0). Once the sample was available, approximately 1.5g of sample and 5g of water was added to the dish and they were weigh (m_1) again together with the lid and the rod. Thereafter, the mixing and drying of diluted sample with sand was carried out with the rod on a steam bath for 30min. The mixing process was performed with caution to ensure the dried sample was well aerated. From then on, the dish was placed in the oven at 102 ±2°C for 1.5 hr with its lid alongside and the glass rod lying flat in the dish. After the initial drying period, the dish, covered with the lid, returns to the desiccator for cooling as before and reweigh. The drying process was repeated with heating period of 1 hr until successive weighings does not exceed 0.5 mg (m_2). The calculation of total solids content uses the same equation (Equation (3.34)) as the IDF standard.

3.4.3 Total Solids Measurement at Different Drying Duration

The objective of this experiment is to determine the differences in total solids measurement resulted from varying drying time using the IDF standard. The skim milk concentrations tested were 28.87 wt%, 42.91 wt%, 45.48 wt% and 55.52 wt% with drying duration of 2, 3, 4, 5, 6 and 24 hours.

3.4.3.1 Reconstituting control solution

Medium heat skim milk powder (34% Protein (dry basis) and 1.1% fat) from Warrnambool Cheese and Butter Factory (WCBF) was used to reconstitute the control solutions. The mass of an empty 600ml beaker was measured (± 0.01 g) before a known amount of powder (± 0.01 g) was added into the beaker. Hot water

at about 80°C was then poured into the beaker to mix with powder. The initial dissolution of powder was carried out using a spatula and any powder that was sticking on the beaker wall was scrapped off into the solution. With the spatula kept in the beaker, Wisemix Homogenizer HG15D is lowered into the solution to homogenise the solution at 800rpm for 5 min. During homogenisation, any stagnant region within the solution was stirred up using the spatula to ensure good mixing. Once homogenisation was finished, any residue on the homogeniser and the spatula were flushed back into the solution with distilled water. The final mass of the beaker and the solution were recorded (± 0.01 g). A sample of 30ml was extracted with a syringe to minimise evaporation during the preparation of TS measurement.

3.4.3.2 Calculation of total solids in the control solution

$$TS\ (wt\%) = \frac{\left(\frac{(100 - MC)}{100}\right) \cdot m_p}{m_s} \tag{3.35}$$

where MC is the moisture content within the powder (wt%), m_p is the mass of powder added (g) and m_s is the final mass of the solution (g).

3.4.3.3 Determination of moisture content in powder

This method of moisture content, MC, measurement for milk powder follows the procedures from GEA Process Engineering Pty Ltd. A clean flat bottom petri dish was weighed on a electronic balance to the nearest 0.1 mg. Approximately 10 g of sample was then spread evenly on the dish. The dish with the sample was reweighed to the nearest 0.1 mg again before it was placed in the oven (102˚C) for 3 hours. After which, the dish with dried sample was covered and left to cool at room temperature for 10 minutes before weighing commences.

$$MC\ (wt\%) = \left(\frac{m_P - m_{DP}}{m_P}\right) \cdot 100 \tag{3.36}$$

where m_P= mass of powder (g) and m_{DP} = mass of dried powders (g).

3.4.3.4 Total solids content measurement

A clean flat bottom petri dish was weighed on a electronic balance to the nearest 0.1 mg. 2.5 – 3 g of sample was then spread evenly on the dish. The dish with the sample was reweighed to the nearest 0.1 mg again before it is placed in the oven (102˚C) for 2, 3, 4, 5, 6 and 24 hours. After which, the dish with dried sample is covered and left to cool at room temperature for 10 minutes before weighing commences.

The total solids content, expressed as a percentage by mass, can by calculated by Equation (3.4).

3.4.3.5 Moisture content of powder

Three samples of the same batch of milk powder were tested for their moisture content based on the method mentioned in Section 3.4.3.3. The results tabulated in Table 3.5 shows that the moisture content of the milk powder is subjected to the drying time it has undergone. According to the GEA's measuring procedure of 3 hours drying time, the moisture content of medium heat skim milk powder from Warrnambool Cheese and Butter Factory during the reconstitution process was 4.4 wt%.

Table 3.5 Moisture content measurement on the milk powder at varying drying time

Sample	Drying time (hr)			
	2 hours	3 hours	4 hours	24 hours
1	4.3247	4.4071	4.4328	5.0118
2	4.3724	4.4701	4.5418	5.0372
3	4.3856	4.4297	4.4626	5.0130
Std Dev	0.032	0.032	0.056	0.014
1.96 σ	0.063	0.063	0.110	0.028
Average	4.361	4.436	4.479	5.021

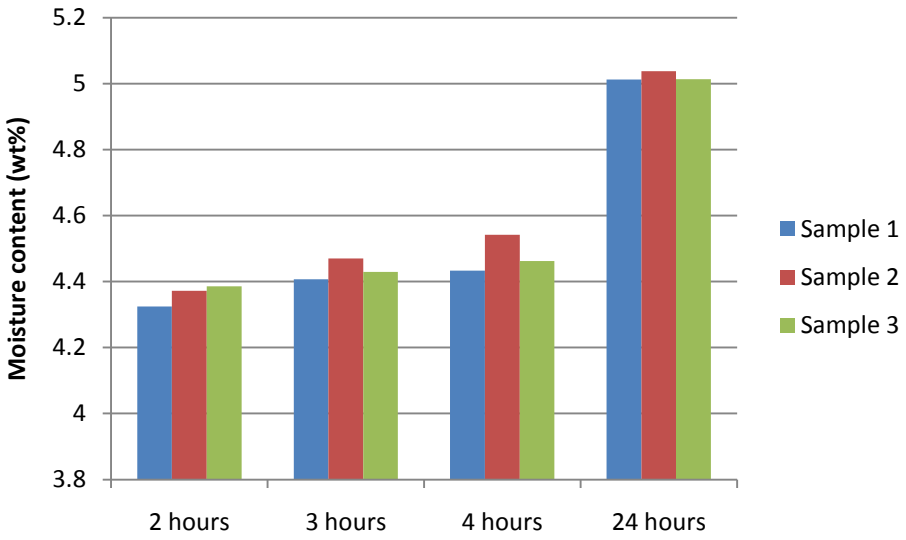

Figure 3.18 Moisture content measurement on the milk powder at varying drying times

3.4.3.6 Total solids measurement at 28.87wt%

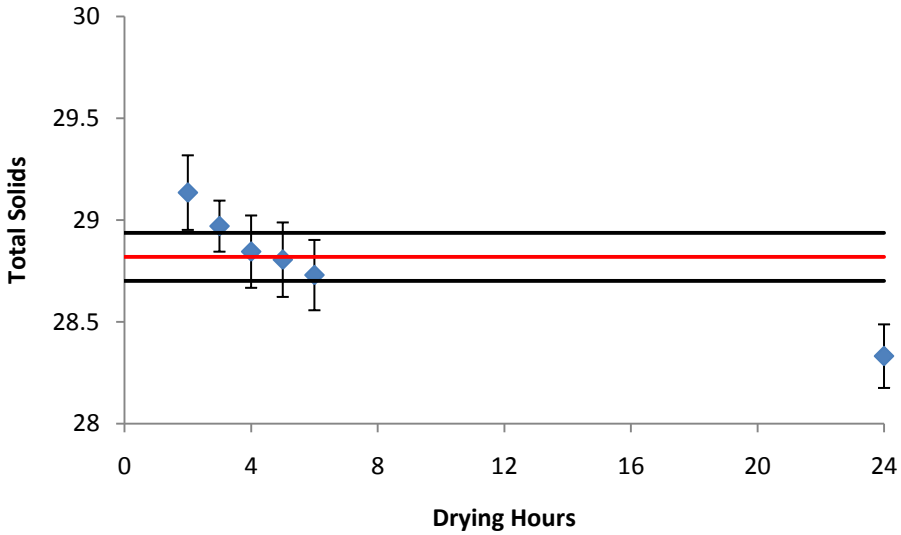

Figure 3.19 Total solids measurement against drying time at milk concentration of 28.82wt%

Figure 3.19 illustrates the reduction of TS measurements with drying time. The red line is the TS of the control solution based on the amount of powder reconstituted and the black lines are the systematic errors involved during the measurement process. With longer drying time, more moisture is able to evaporate from the sample, hence reducing the apparent TS measurement. The normal practice in Monash University uses 2 hrs of drying time and that correspond to 0.3wt% higher than the control solution. It seems the ideal drying time was around 4 hours where the TS from the oven match the control solution. However, further drying will result in TS measurement lower than that of the control solution. This could be due to the compilation of errors from the weigh measurements during TS measurement and reconstitution. With 24 hours of drying, the excessive drying duration could potentially evaporate that the "bonded" water within the structure, hence resulting in further lowering of TS. Similarly, the same principal may be applied to the measurement of moisture content in powder.

3.4.3.7 Total solids measurement at 42.91wt% and 45.48wt%

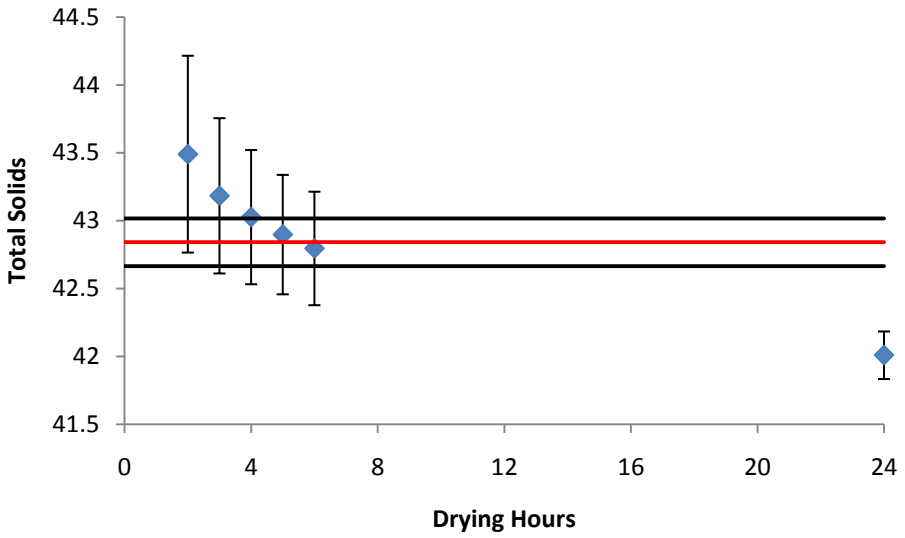

Figure 3.20 Total solids measurement with drying time at 42.91wt%

Similarly, in Figure 3.20 and Figure 3.21 display the same trend where TS reduces with drying time. With 2 hours of drying time, the TS measurement is about 0.7 wt% and 0.6 wt% higher than control solution respectively. The ideal drying time is around 5-6 hours.

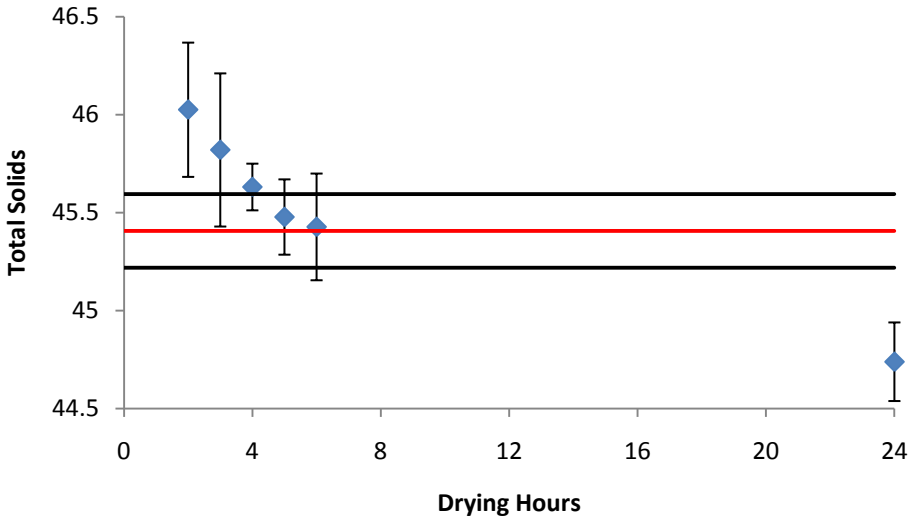

Figure 3.21 Total solids measurement with drying time at 45.48wt%

3.4.3.8 Total solids measurement at 55.52wt%

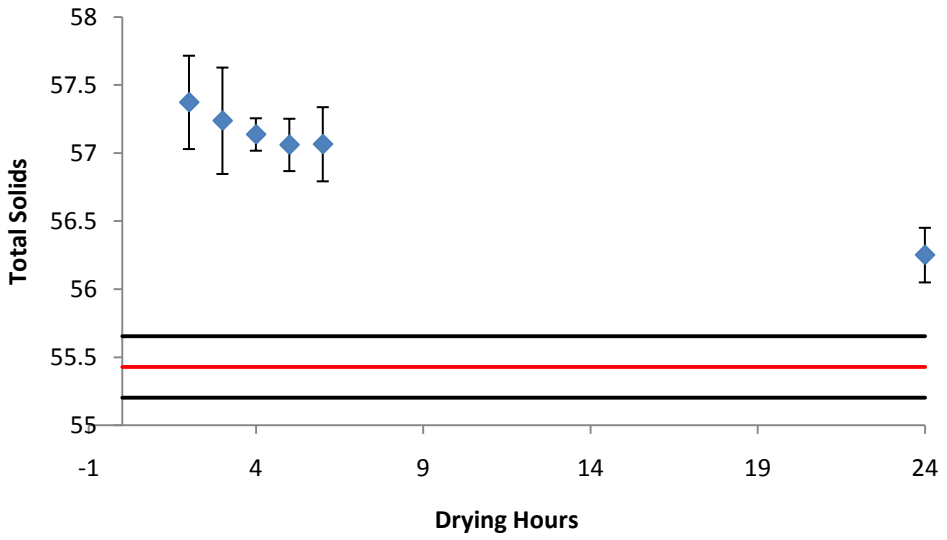

Figure 3.22 Total solids measurement with drying time at 55.52wt%

At 55.52wt%, the TS measurement never reached the TS of the control solution, even after 24 hours. This could be due to the crust form on the surface of the sample and trapped the moisture trap within. With 2 hours of drying time, the TS measurement is close to 2.0 wt% higher than control solution.

3.4.3.9 Conclusions

The amount of drying time to achieve an accurate measurement of total solid varies with the milk concentration. Longer drying time is required for sample with higher concentration. For high TS (>40wt%), the IDF standard of TS measurement may not be suitable to obtain a accurate measurement.

3.4.4 Relationship between the TS measurement methods

The comparison of the IDF and Australian standard for determining total solids content was conducted using both low and medium heat treated skim milk (34% protein (dry basis) and 1.1% fat) from Warrnambool Cheese and Butter Factory (WCBF). The skim milk at 40 wt% was further concentrated using the steam heated

pilot evaporator (Section 3.7.1). Samples of concentrated skim milk were extracted from the evaporator at random timing during the evaporation process. A total of 9 samples from 2 occasions were tested. For each sample, duplicate testing were carried out on both standards.

Table 3.6 Comparison of the IDF and Australian standard for determining TS.

Density ($g\ cm^{-3}$)	IDF (wt%)	Deviation ±	Australian (wt%)	Deviation ±	Milk Type
1.1449	38.97	0.11	38.97	0.05	Low Heat
1.1692	43.33	0.21	43.15	0.00	Low Heat
1.1704	43.98	0.05	43.54	0.02	Med Heat
1.1924	49.33	0.05	48.13	0.13	Med Heat
1.2034	50.84	0.09	50.12	0.13	Low Heat
1.2106	53.69	0.83	51.89	0.11	Med Heat
1.2321	57.62	0.53	55.83	0.17	Med Heat
1.2374	59.39	0.25	56.79	0.21	Low Heat
1.2501	63.38	0.09	59.25	0.10	Low Heat

Initially, at lower concentration level (around 40 wt%), there show no significant distinction, if any, between both IDF and Australian standards. However, as the total solids level rises, the deviation between the two standards becoming increasing apparent. The IDF standard had consistently produced higher total solids measurement than the Australian standard and the difference can be as much as 4 wt% on the densest sample collected. The deviation became more obvious in Figure 3.23.

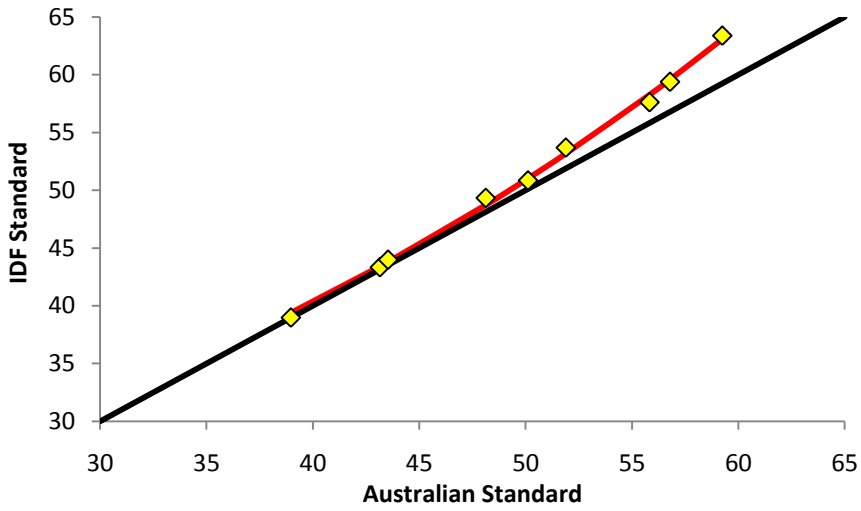

Figure 3.23 Comparison of the IDF and Australian standard for determining TS.

The black line corresponds to the perfect equality line where both standards produce identical results. When the data from Table 3.6 were plotted against the perfect equality line, it shows an exponential deviation between the two standard that can be represented by the Equation(3.37).

$$IDF_s = 15.92e^{0.02324A_s} \tag{3.37}$$

where IDF_s is the total solids measured by the IDF standard and A_s is the total solids measured by the Australian standard.

It was concluded that both IDF and Australian standards were able to produce the same results when the TS content (based on the Australian Standard) is lower than 40wt%. Beyond 40 wt%, the IDF standard would consistently produce higher TS measurement than the Australian standard.

3.4.5 Verifying the standards for determining TS

To verify if the Australian Standard produces a more accurate result than the IDFS, the IDFS – AS correlation (Equation (3.37)) was applied to the drying time study. The TS measurements of 2 hours drying time in Section 3.4.3 (same duration as

those tested in Section 3.4.4) were used for the conversions. The results are tabulated in Table 3.7.

Table 3.7 Comparison of IDFS (2 hr) and IDFS – AS correlation with control solution

TS after 2 hours of drying (IDFS) (wt%)	Deviation from control (wt%)	Converted TS (IDFS – AS) (wt%)	Deviation from control (wt%)	Control Solution (wt%)
29.135	+ 0.315	26.005	- 2.815	28.82
43.490	+ 0.650	43.243	+ 0.403	42.84
46.025	+ 0.6190	45.680	+ 0.274	45.41
57.373	+ 1.940	55.163	- 0.267	55.43

When the correlation was applied to the 28.82 wt% control solution, the result after the conversion was almost 3 wt% lower. This was expected as the valid range for the correlation is 40 wt% < TS < 60wt%. Once the conversion were carried out in the valid TS range, marked improvements were observed. The deviation of the converted TS was less than 0.5 wt% from the control solution. When the systematic errors (about ± 0.2 wt%) were taken into account, the difference between the converted TS and control solution becomes much smaller. In contrast, the TS measurements by the IDFS produced error as high as 1.94 wt%. More comparison were plotted in Figure 3.24.

Therefore, the Australian Standard proved to be a more accurate method of determining the TS of concentrated milk, especially milk with TS above 40 wt%.

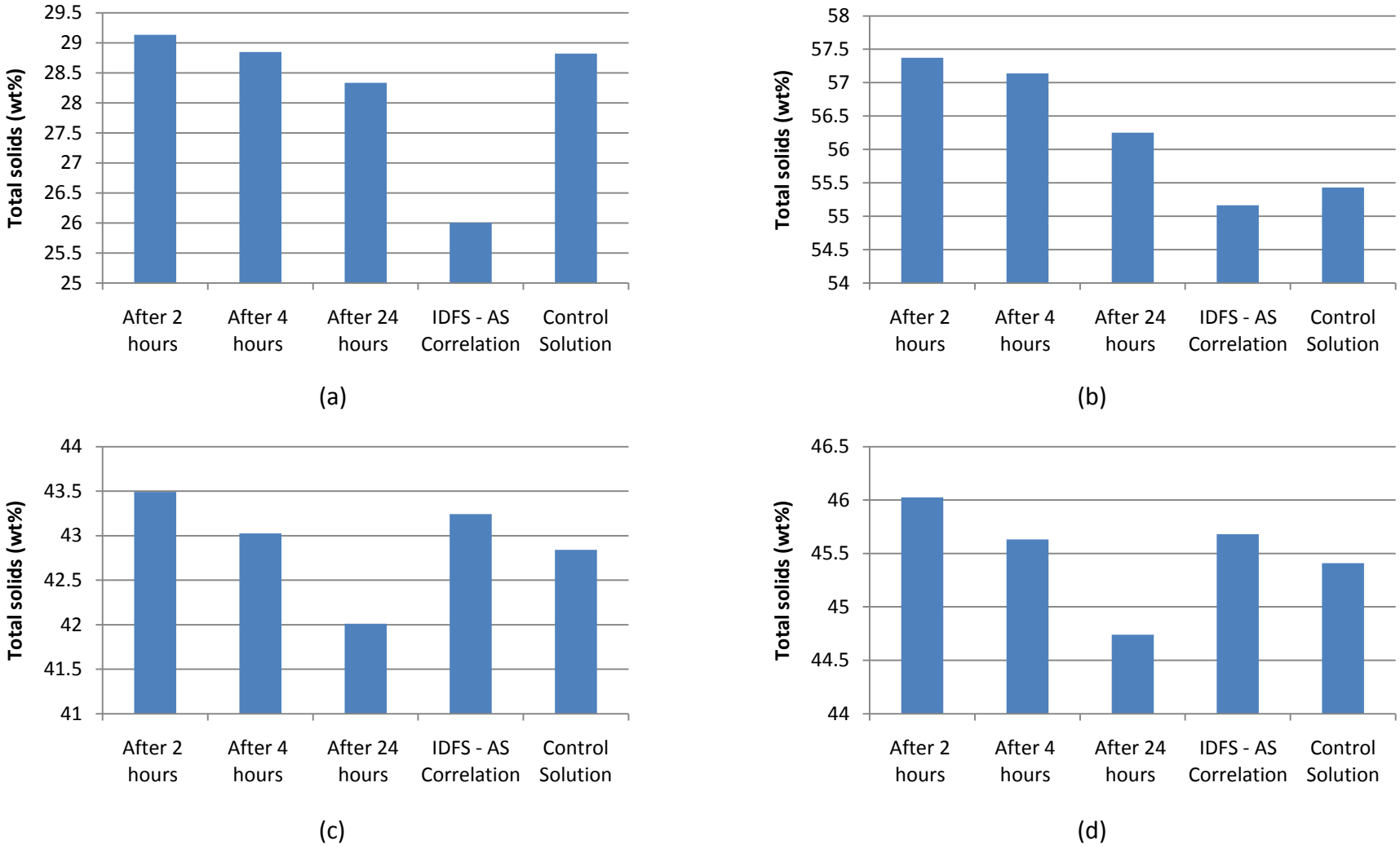

Figure 3.24 Comparing IDF drying time and IDFS – AS Correlation at different TS. (a) 28.82 wt%, (b) 42.84wt%, (c) 45.41wt% and (d) 55.43 wt%

3.5 Reconstitution of Milk Powder

To establish a repeatable and reliable rheological characteristic of a time-dependent system such as reconstituted milk, it was essential to standardise the reconstitution procedure of milk powder. This would minimise the number of variables that could potentially affect the out come of the characterisation process.

3.5.1 Procedure of reconstituting milk powder

The powder to distilled water ratio was weighed accordingly to achieve an estimation of total solids content desired. The 4.5wt% moisture in the skim milk powder was taken into account and the calculation for the milk powder requirement is shown below:

$$TS\ (wt\%) = \frac{m_p \times 0.955}{(m_p \times 0.955) + m_w} \tag{3.38}$$

where m_p is the mass of powder (g) and m_w is the mass of distilled water is used (g).

The mixture was then homogenized with Wisemix Homogenizer HG15D for 15 minutes. Milk concentrate was pre-mixed to around 30wt% and kept over night in the refrigerator at 4 °C. Total solids contents were verified again at the end of the experiments using the total solids content measurement method mentioned in Section 3.4.2.2.

3.6 Thermocouple Calibration

3.6.1 Type of thermocouple used

Type K thermocouple from Omega Engineering, Inc. were used. The thermocouples were insulated with PFA or Neoflon with an insulation range of -267°C to 260°C. Two sizes of thermocouples were used in the experiments. They were TT-K-36-SLE-

500 with diameter of 0.13mm and TT-K-30-SLE-500 with diameter of 0.25mm. Both types of thermocouples had a tolerance value of 1.1°C or 0.4%.

3.6.2 Welding of thermocouple

All the thermocouples were welded with Omega Engineering, Inc. thermocouple welder (TL-weld). Each of the welding was examined under the microscope to ensure optimum contact between the wires before they were installed in to the electric-heated pilot evaporator.

3.6.3 Calibration of thermocouple

All the thermocouples were calibrated with the Brannan BS 593 thermometer (England) with division of 0.2°C using a hot water bath and a aluminium block as shown in Figure 3.25. A hole of Ø 8mm × 65mm was drilled on the top of a 50 × 50 × 95 mm aluminium block. The thermometer and thermocouples were lowered into the aluminium block and were fully submerged in the hot water bath. The calibrations were based on four temperatures (40, 53, 66 and 80 °C) and were conducted using a Picolog TC-08 Data logger. Each thermocouple is assigned to a specific channel on the data logger to minimise any calibration errors. Once the temperature in the water bath has stabilised, temperature on the thermometer was recorded every 30 seconds for 2 minutes and the every 5 seconds for 2 minutes for the thermocouples. A magnifying glass were used to read the temperature on the thermometer and was held as perpendicular to the scale as possible. The average was taken from the recordings and the calibration was established

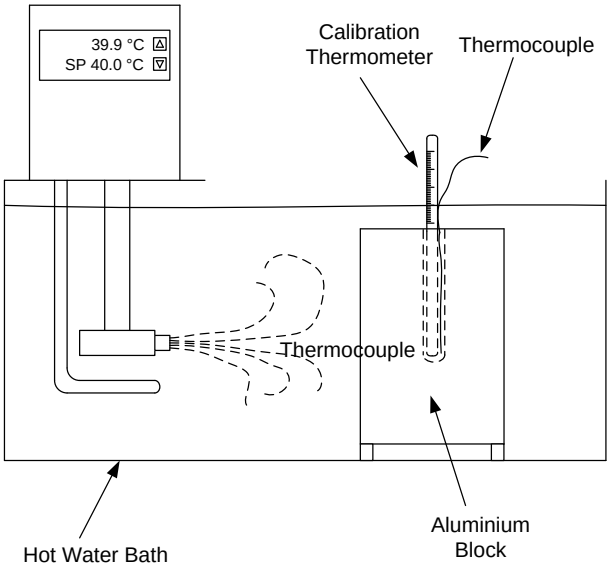

Figure 3.25 Thermocouple calibration diagram

3.7 Design of Experimental Rig

The main aim of the evaporator rig design was to establish the viscosity profile of milk and the performance of the evaporator under different operation conditions. The four main criteria to consider when it comes to the design an evaporator. They are the heat source (e.g. steam or electric heating), the heat transfer surface (e.g. static or dynamic), evaporation environment (e.g. pressurised or vacuum) and the type of process operation (e.g. batch or continuous). A mixture of the criteria stated above were employed (also illustrated in Figure 3.26), however a batch design philosophy was applied to all evaporator designs due to material and space constraint.

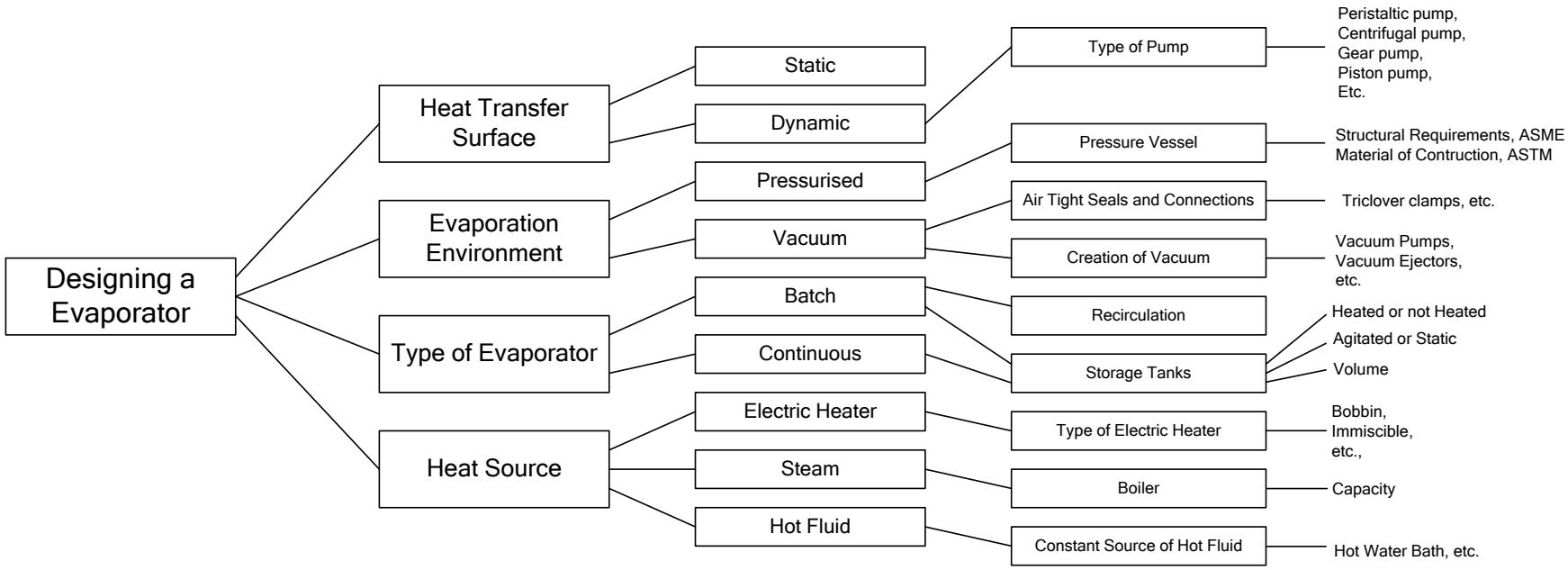

Figure 3.26 Design philosophy for evaporator

3.7.1 "Pot" evaporator

The preliminary investigation of milk viscosity focuses on viscosity measurement at varies total solids while the milk is evaporated close to industrial operating temperatures. This leads to the first task of designing a simple evaporation system where samples of milk concentrate can be extracted from the system at any given time during evaporation and can be setup in a relatively short period of time.

The creation of a vacuum environment for evaporation was solved by modifying a pressure pot. The air tight seal and sturdy built pot structure had made the pressure pot an ideal vessel to maintain a vacuum environment. Therefore, minimal modification was required. Only 2 holes were drilled on the lid for the thermocouples insertion and air extraction. The rubber seal on the lid was also carefully glued onto the lid by silicone adhesive (Dow Corning, Silastic 732 Silicone RTV adhesive/sealant) to prevent any air leakage into the pot while maintaining the air tight seal.

The vacuum was created using the vacuum ejector (SMC, ZH13BS-08-02). A pressure regulator with filter and pressure gauge (SMC, AW20-02H-C and G40-K10-1) was installed prior to the vacuum ejector so as to control the compressed air going into the ejector, hence regulating the vacuum. The filter flask between the pot and the ejector act as a condenser where steam generated in the pot would be condensed and collected in the flask while air escapes through the ejector. A vacuum gauge (Ambit Instruments Pty Ltd, Model 308-16) was placed some distance away from the pot to prevent potential bubble formation during evaporation from entering the gauge, hence influencing the pressure measurement (see Figure 3.27).

A hot water bath (Thermoline Scientific, TWB-22) was used as the heat source for the evaporation process because of the ease to control and maintain the temperature within the hot water bath. Temperature of milk and water temperatures were monitored by 3 type K thermocouples (Omega Engineering, Inc. TT-K-30-SLE-500) as illustrated in Figure 3.27 (also see Figure 3.28).

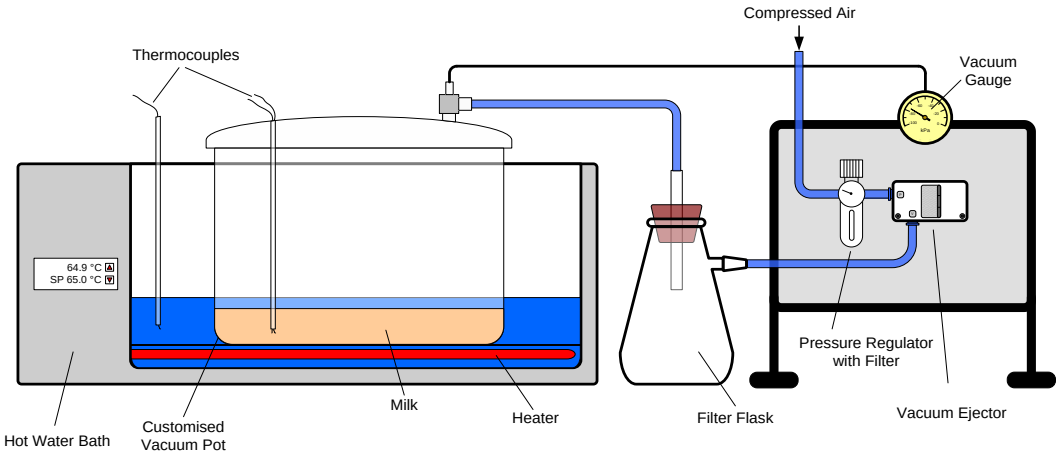

Figure 3.27 Layout of the "pot" evaporator

Figure 3.28 "Pot' Evaporator setup

3.7.1.1 Operation of "pot" evaporator

First, the hot water bath was preheated to the desired temperature (around 65°C). Thereafter, a batch of milk (2-4 kg, normally cold) was poured into the pot and the lid was securely fastened. While the milk got heated up, the vacuum ejector was also turned on to -80 kPa to deaerate the milk. This would help to reduce the foam formation while the milk boiled. Once the temperature of the milk reached around 60 °C, boiling began and condensate should start to gather in the filter flash. The condensation capability of the filter flash was not ideal, therefore, some condensate would start to form at the exit of the vacuum ejector. However, the condensate formed in the vacuum ejector did not affect its performance.

To extract sample out of the evaporator, the vacuum ejector had to be turned off before the lid could be released. The sample was then taken out with a syringe. The evaporation process was continued by replacing the lid back and turning on the vacuum ejector.

Some of the benefits of the "pot" evaporator include:

1. **Relatively short fabrication and commission time**

   Most of the equipments in this evaporator were readily installed. The only modifications required were to drill 2 holes on the lid and to glue the rubber seal on the lid. No major custom-made part was required.

2. **Easy to operate**

   Once the hot water bath and vacuum ejector were adjusted in the beginning of the experiment, constant attention on the evaporator was not required.

3. **No problems with transporting viscous fluid**

   Milk stayed in the pot throughout the entire evaporation process, therefore, no special pumping requirement needed.

4. **Vacuum condition was easily maintained**

   There were not many connectors present in this evaporator setup, as long as the lid is air tight, the chance of air leakage was minimal.

Some of the drawbacks of the "pot" evaporator include:

1. **No tap to extract samples while evaporator was still operating**

   The vacuum ejector had to be turned off completely in order to release the lid from the evaporator for sample extraction.

2. **Slow evaporation rate**

   The evaporator was not well insulated and the heat transfer area was restricted to the surface area in contact with the hot water. The evaporation rate was about 3-5g of water per minute.

3. **Formation of foam during evaporation gets into the filter flask**

The formation of foam during evaporation was almost inevitable, especially at the beginning of the evaporation process. Sometimes, the loss of milk from the pot through foam getting into the filter flask was substantial.

4. **The formation of "skin" on the surface of the milk**

When the lid was opened for sample extraction, the surface of the milk comes in contact with the cooler ambient air. This results in the formation of skin on the milk surface, particularly the more concentrated milk. As a result, caution had to be exercised when extracting any sample from the pot.

5. **The density of the milk could not be monitored during evaporation**

Density is an good indicator for total solids content in the milk. Without such indicator, the extraction of samples of different total solids content could only be done at random time intervals during the evaporation process.

6. **Small processing quantity**

Only 2-4 kg of milk can be processed at one time. The initial total solids content determines the number and amount of samples could be taken, e.g. If the initial mass was 4kg at 10 wt%, in order to get to 50wt%, about 3kg of water has to be evaporated. The amount left for testing was merely 1kg and this has not taken into account the samples extracted during the evaporation process.

3.7.1 Steam-heated Pilot Evaporator

To this point, the design of the previous evaporator ("pot" evaporators) was restricted to lab scale dimensions. The quantity to which they could process was no more than 5 L and the evaporation rates were slow (3-5g of water / min). The long processing time, sometimes up to 7 hours, by the lab scale evaporators would definitely affect the viscosity measurement, particularly at high total solids content (above 50 wt%) where age-thickening effect becomes prominent. Thus, a pilot scale evaporator that is able to process substantial volume of milk to high total solids (> 55wt%) in a relatively short period of time was desirable.

Most of the design ideas for the steam-heated pilot scale evaporator came from the commercial falling film evaporators. The main components of a falling film evaporation system include a storage tank, a preheater, a evaporation column, a separator, and a condenser. The preliminary design of the steam-heated pilot evaporator was based on the assembly of the main components as illustrated in Figure 3.29. A detail version can be found in Figure 3.31.

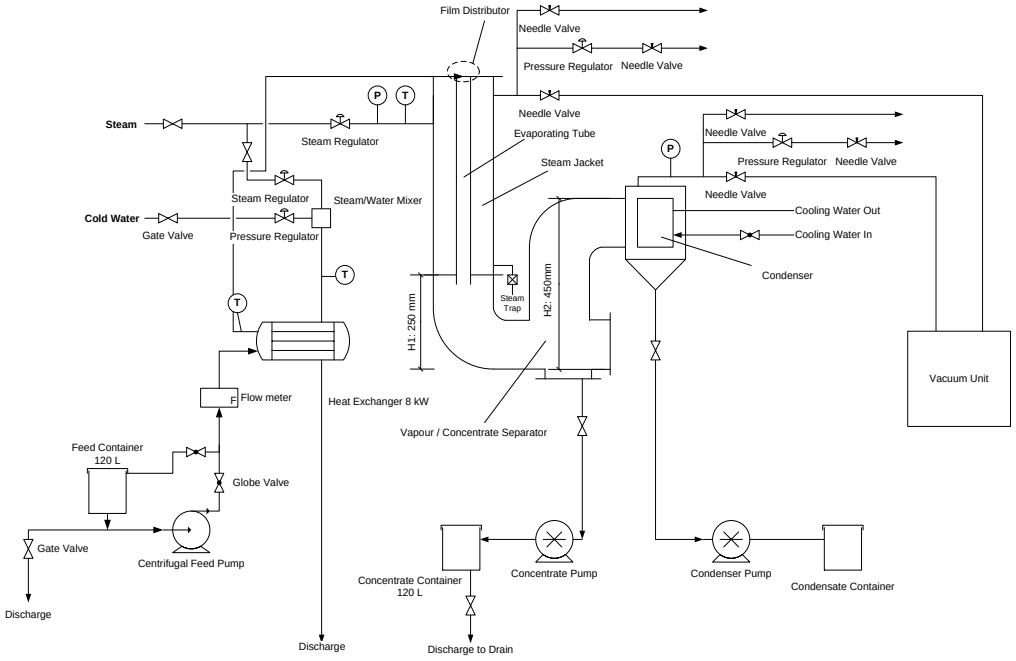

Figure 3.29 Preliminary design of steam heated pilot falling film evaporator

The preliminary design was passed over to Stainless Design, in Hamilton New Zealand, who was in-charge of the fabrication of the steam-heated pilot evaporator Several revisions were made on the preliminary design by the engineers in Stainless Design and the CAD drawing for the final design was shown in Figure 3.30.

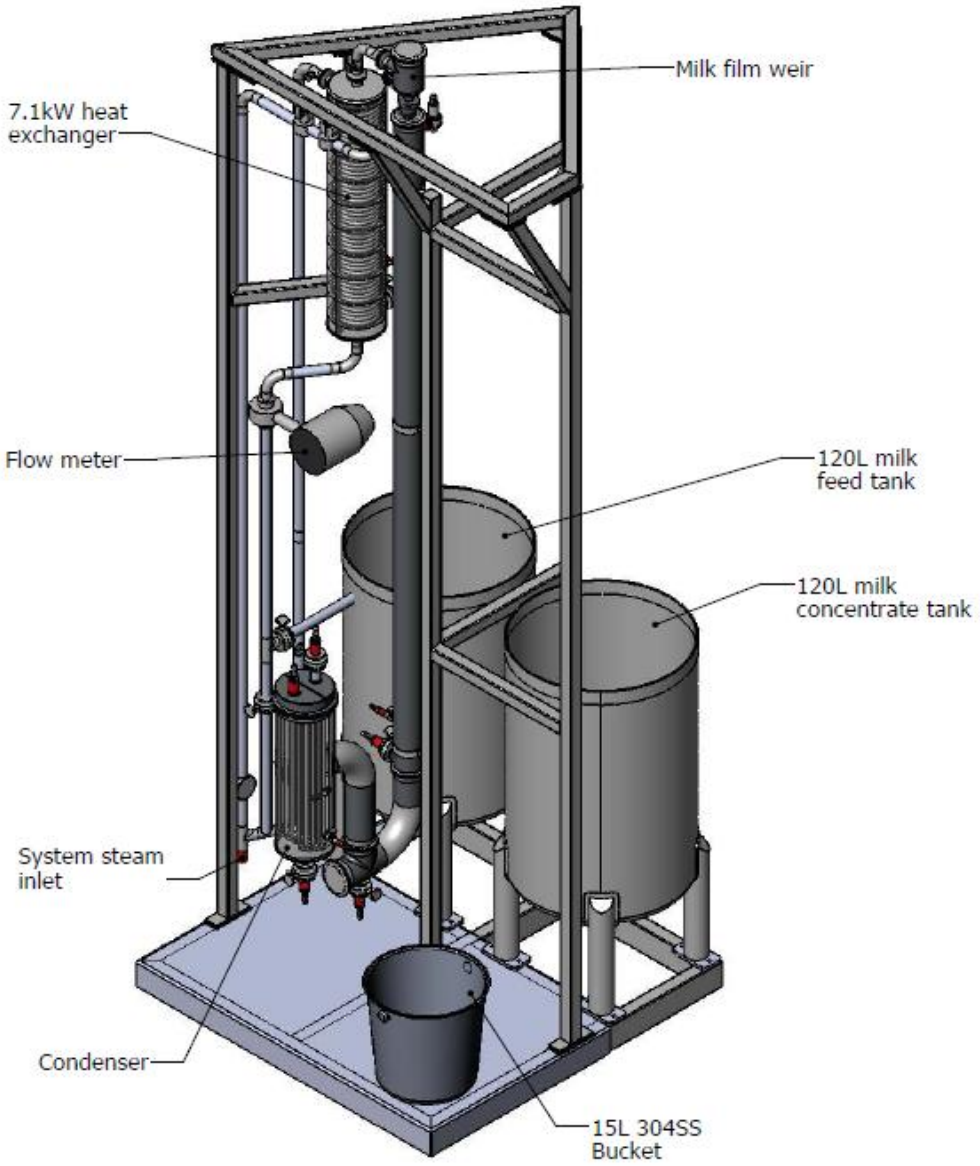

Figure 3.30 CAD drawing of the steam-heated pilot evaporator

In the CAD drawing (Figure 3.30), it shows the skeleton of the 2m tall steam-heated pilot evaporator. Auxiliary components such as the boiler, pumps, vacuum ejectors, vacuum gauges, temperature probes, temperature control valves, etc. were not illustrated. A clearer diagram of the evaporation system with all the auxiliary components can be found in Figure 3.31

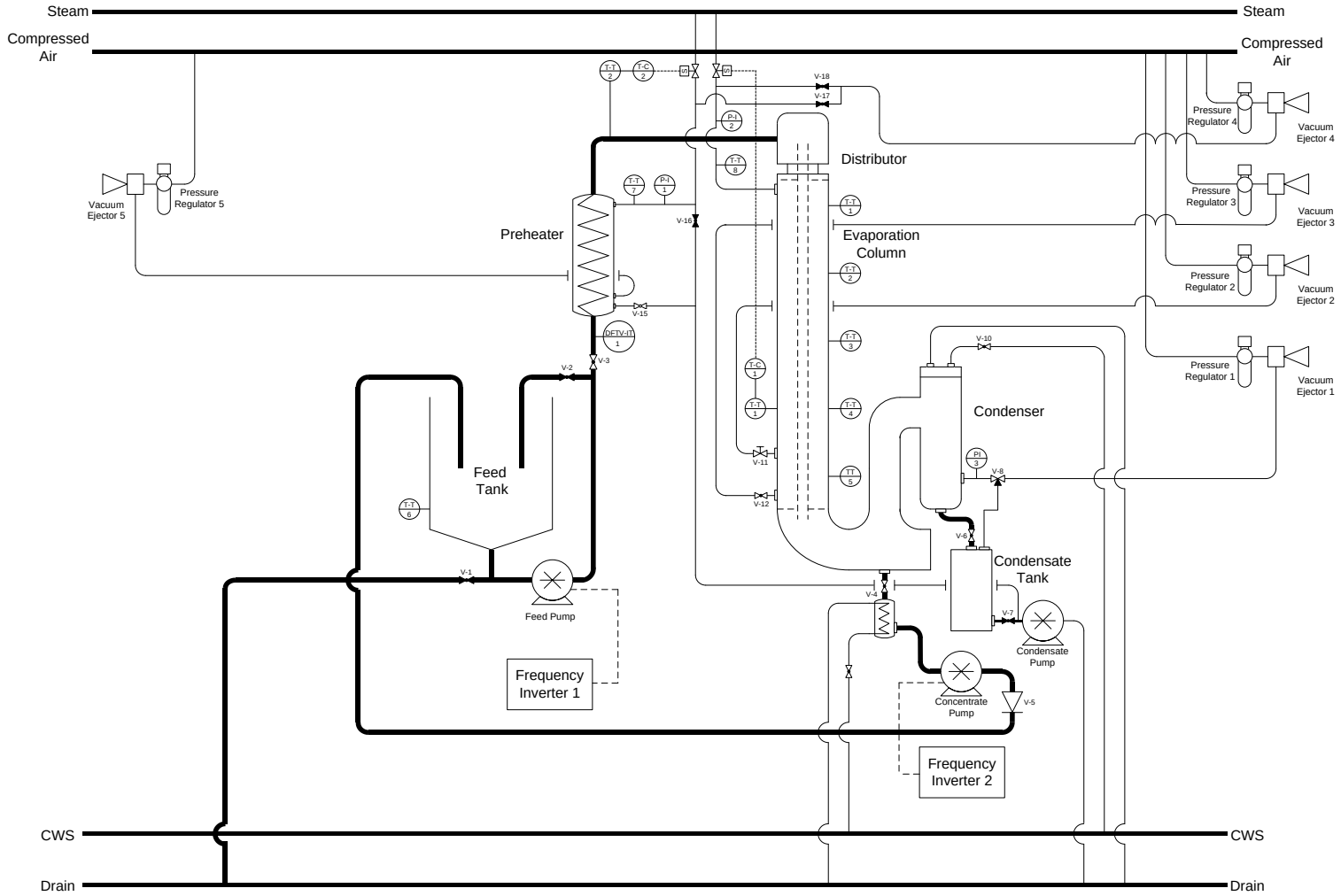

Figure 3.31 Schematic layout of steam-heated pilot evaporator

3.7.1.1 Design specifications

Figure 3.32 Steam-heated pilot evaporator

In Figure 3.32, it shows the setup up of the steam-heated pilot evaporator (centre), the boiler (left) and the viscometer (right), The photo was taken at factory site where the evaporator was once located to produce viscosity data for the company of concern.

Feed tank

The feed tank was made of 304 stainless steel with inner diameter of 480mm and 700mm tall. The bottom of the tank was slightly tapered to enhance the flow to the centrifugal feed pump (Lowara, CEA 70/3) (this pump was replaced afterwards, see Section 3.7.1.7) attached next to it. Heat loss was minimised by insulating the evaporation column and steam tube to the preheater and evaporation column (not shown in Figure 3.33). Through the centrifugal pump, the feed was pumped to the preheater.

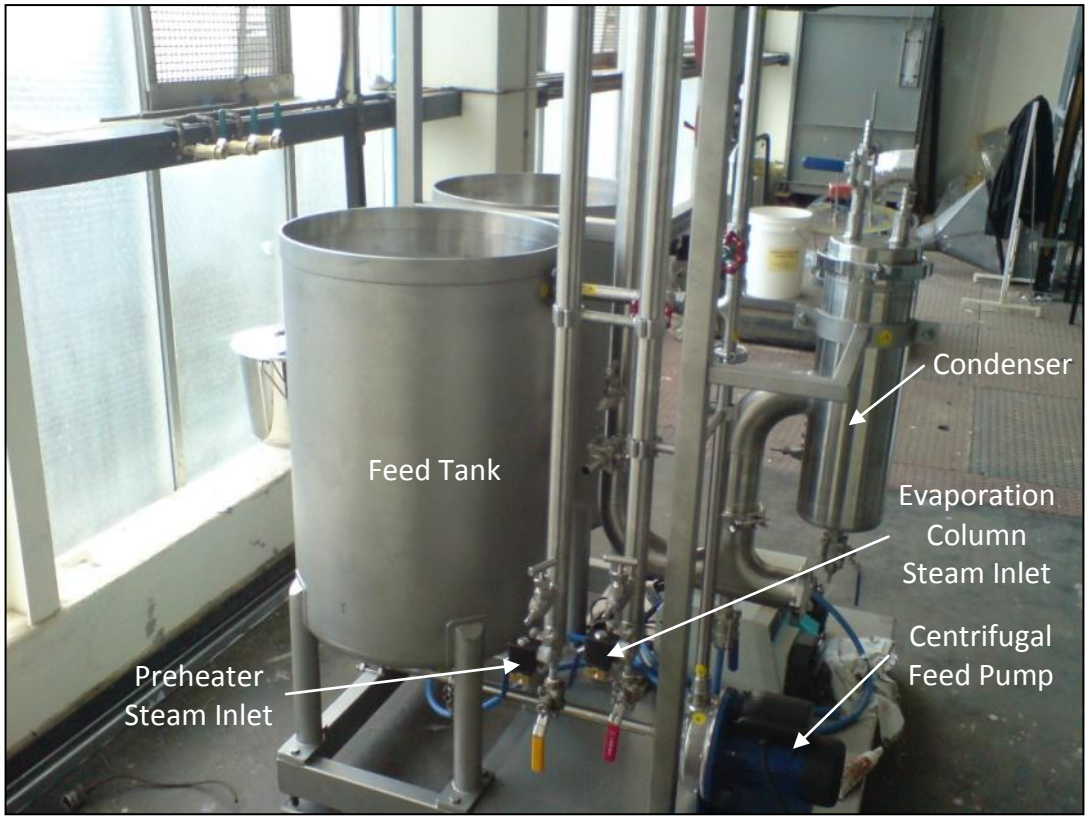

Figure 3.33 Side view of the steam-heated pilot evaporator

Preheater

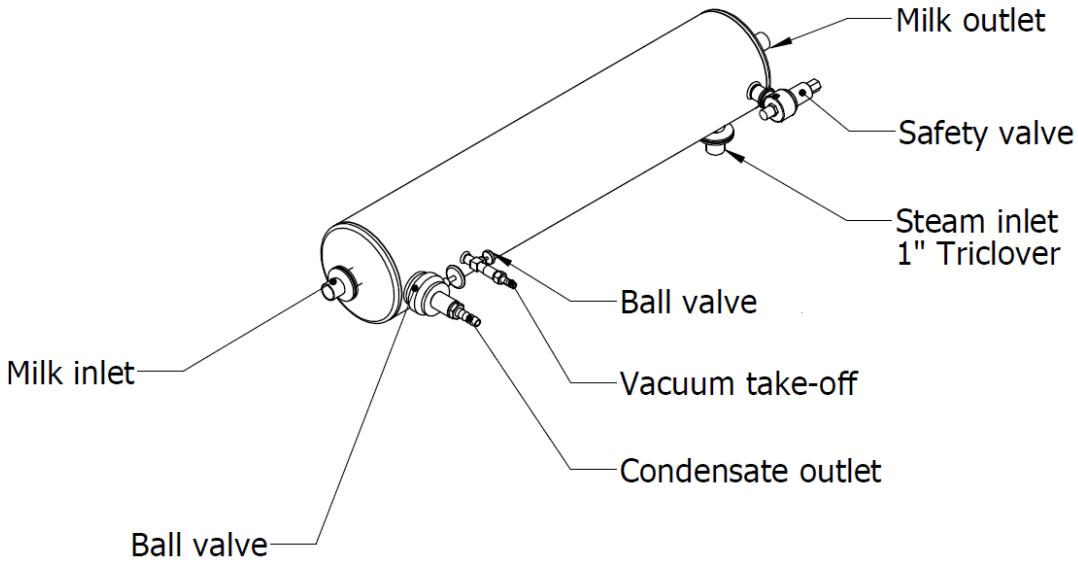

Figure 3.34 Schematic drawing of the preheater

The tube side of the preheater consists of a spiral 17m long 304 stainless steel tube with outer and inner diameter of 7.4mm and 5.6mm respectively. The milk inlet and outlet of the tube were connected by a 1" triclover. The shell of the preheater was made of a 6" stainless steel tube capped on both sides. The steam inlet was also connected by a 1" triclover. Ball valves were installed at both the vacuum take-off point and the condensate outlet

Condenser

There are 15 cooling tubes (Ø 6.35 × 1.5mm) within the condenser with an expose length of 903mm each. Steam generated during the evaporation process enters the condenser by the side and the condensate exit from the base. The vacuum port is located close to the bottom of the condenser.

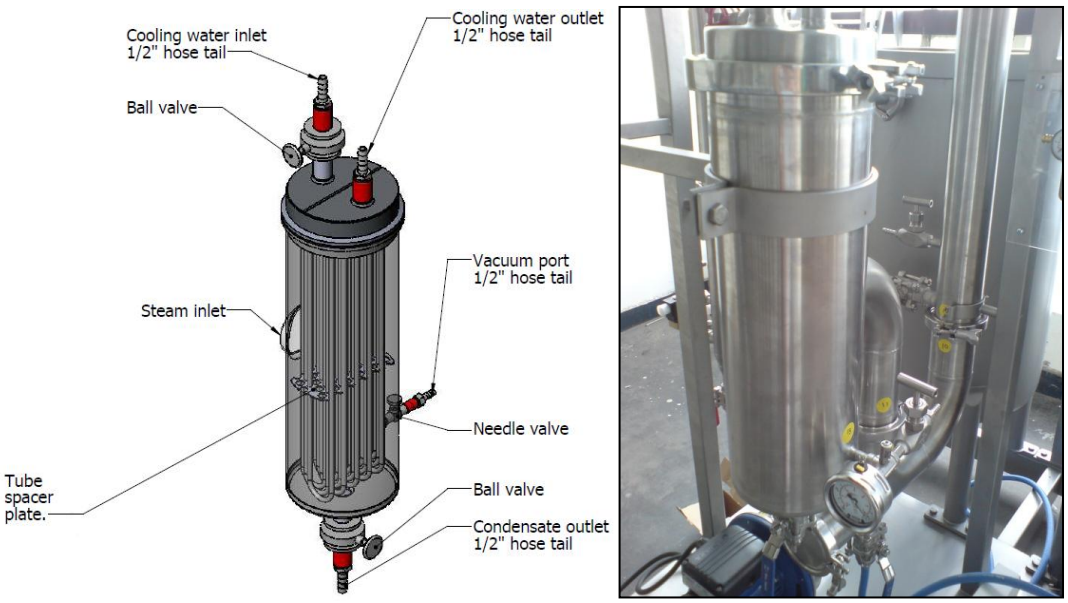

Figure 3.35 Condenser

Evaporation column

There were 3 major parts in the evaporation column; they were of a distributer (detail A in Figure 3.36), the 2m long evaporation tube and the separator at the bottom (detail B in Figure 3.36). The distributer utilised the overflow principle to spread a layer of milk film on the inner surface of the evaporation tube. The milk

film falls along the evaporation tube and was being heated by the steam on the shell side.

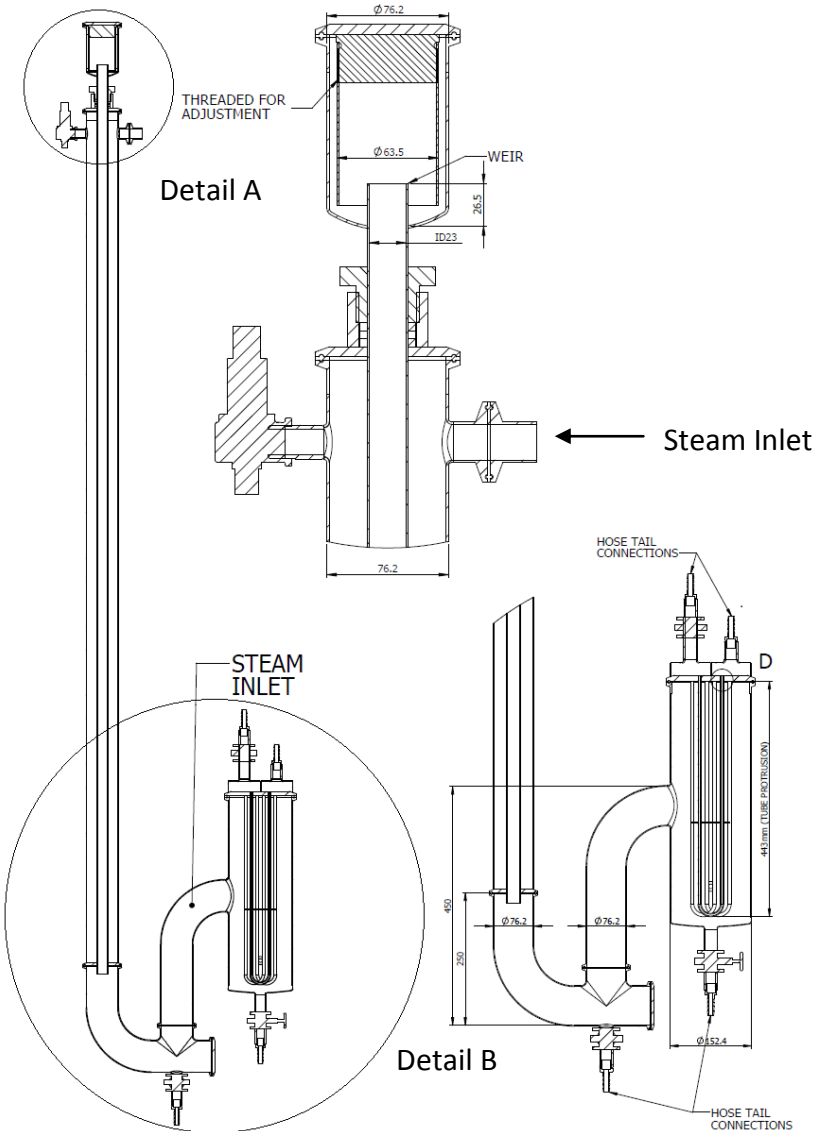

Figure 3.36 Cross-section of the evaporation column

The mixture of concentrated milk and steam generated along the evaporation tube became separated. The steam entered the condenser while the concentrated milk exited the bottom of the separator.

3.7.1.2 Temperature measurements

There were 10 thermocouples (Type K) installed in the pilot evaporator. 8 thermocouples were merely used for monitoring purposes while the other 2 thermocouples act as feedbacks for the temperature controllers of the preheater and evaporation column. In Table 3.8, it shows the locations of the thermocouples installed and where they were connected to (refer to Figure 3.31 for the locations on the steam-heated pilot evaporator).

Table 3.8 List of thermocouples installed in steam-heated pilot evaporator

Thermocouple	Location	Connect to	Purpose
T-T 1*	About 330 mm from the top of the evaporation column	Picolog TC-08 Data Logger	Monitor
T-T 2*	About 660 mm from the top of the evaporation column	Picolog TC-08 Data Logger	Monitor
T-T 3*	About 990 mm from the top of the evaporation column	Picolog TC-08 Data Logger	Monitor
T-T 4*	About 1320 mm from the top of the evaporation column	Picolog TC-08 Data Logger	Monitor
T-T 5*	About 1650 mm from the top of the evaporation column	Picolog TC-08 Data Logger	Monitor
T-T 6	Feed tank	Picolog TC-08 Data Logger	Monitor
T-T 7	Preheater steam temperature	Picolog TC-08 Data Logger	Monitor
T-T 8	Evaporation column steam temperature	Picolog TC-08 Data Logger	Monitor
T-T 9*	About 1320 mm from the top of the evaporation column	PID Temperature Controller	Temperature Control
T-T 10	Feed inlet to the evaporation column	PID Temperature Controller	Temperature Control

*Note: Thermocouples 1 – 5 and 9 were attached to the shell of the evaporation column.

Thermocouple 9 and 10 were feedback temperature measurements for the Proportional-Integral-Derivative (PID) temperature controllers (Eurotherm, Model 2132) to regulate the amount of steam entering the preheater and evaporation column respectively.

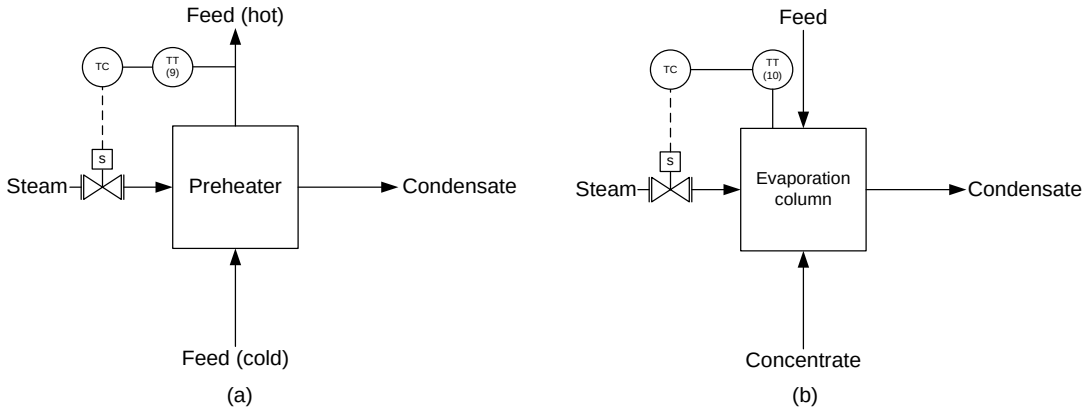

Figure 3.37 Process control flow diagram. (a) Preheater, (b) Evaporation column

The process control flow diagrams of preheater and evaporation column are illustrated in Figure 3.37. In Figure 3.37a, the temperature of the feed is controlled by varying the amount of steam entering the preheater. Similarly, the steam temperature in the evaporation column is regulated by varying the amount of steam entering the evaporation column, as shown in Figure 3.37b.

3.7.1.3 Boiler and steam control

In this pilot evaporator, a boiler (Simon Boiler Co., VS 150-24) was used to generate the steam required for the heating. There were 2 components in the evaporator system that needed steam heating, they were the preheater and the evaporation column. To control the temperature of both components, solenoid valves (Bürkert Compact Solenoid Valve, Type 6013) (see Figure 3.33) were installed at the steam inlets to regulate the steam. 2 separate PID temperature controllers (feedback signal from thermocouple 9 and 10) instruct the valves to open or close.

A point to note, the feedback signals to the PID controllers were just reference temperatures, they do not suggest a uniform temperature distribution on the steam side of the component or the temperature of the steam at all. For instance, in the case of controlling the amount of steam entering the preheater, the feedback signal for the PID controller was based on the feed temperature leaving the preheater and not the steam temperature within the preheater. To achieve the setpoint temperature for the exiting feed, the PID controller would regulate the amount of steam entering the preheater but it does not control the temperature of

the steam. The steam entering the preheater could be still in excess of 100°C. At this temperature, denaturation of protein in milk could occur and potentially alter the outcome of the rheological characteristics. According to thermodynamics, the steam temperature reduces with pressure (Figure 3.38). Therefore, the regulation of the steam temperatures for the preheater and evaporation column were attained by vacuum ejectors.

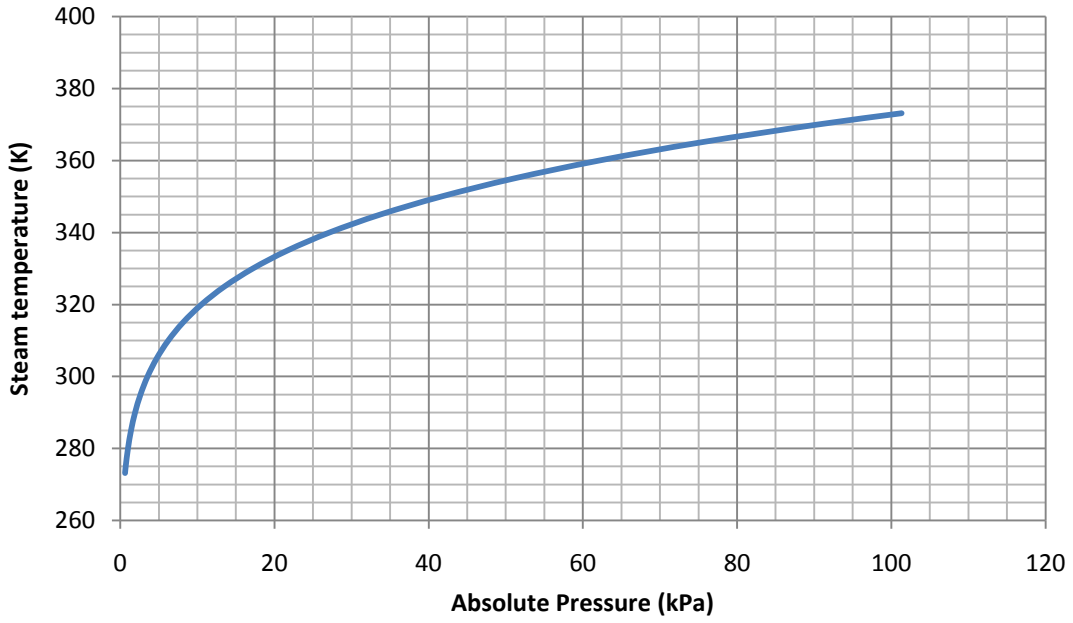

Figure 3.38 Variation of steam temperature with pressure (Incropera and DeWitt, 2002b)

Depending on the process requirement, the pressure within each component was adjusted accordingly to reach the desired steam temperature. Actual steam temperatures of the preheater and evaporation column were also monitored by thermocouple 7 and 8.

3.7.1.4 Pressure measurements

There were 3 pressure sensitive sections within the evaporation system; the shell side of preheater and evaporation column and the tube side of the evaporation column. Each section was fitted with a pressure gauge (Ambit Instruments, Model-300-16) that had a measuring range of 0 to -100 kPa and an accuracy of ± 3% in compliance with AS1349-1986.

3.7.1.5 Removal of condensate

Steam injected or generated during the evaporation process would be condensed in the system eventually. The removal of the condensate was crucial as the condensate might flood the system. However, the entire evaporation system operates under vacuum conditions ranging from -70 to -80kPa (gauge). The pumps had to compete with the vacuum environment within the evaporator system in order to remove the condensate. This issue was overcome by installing a vacuum ejector or a peristaltic pump at the condensate outlet.

3.7.1.6 Flow measurements

A mass flow meter (Endress+Hauser, Promass 83I) was installed vertically in between the feed pump and preheater to prevent any accumulation of air bubbles that could potentially affect the measurements. Promass 83I was capable to measure density, mass flow rate, volume flow rate, temperature and viscosity of the feed. The measurement principle of Promass 83I was based on the coriolis effect (Section 3.3.2).

Figure 3.39 Endress+Hauser Promass 83I

The specification of Promass 83I were listed be in Table 3.9

Table 3.9 Specification of Endress+Hauser Promass 83I

Parameter	Accuracy	Repeatability
Mass and Volume Flow	± 0.10% of reading	± 0.05% of reading
Density	±0.0005 kg/L	±0.00025 kg/L
Temperature	± 0.5 °C	± 0.25 °C
Viscosity	± 5% of reading	-

All measured parameters could be exported realtime to a computer via a Modbus RS485 connection.

Connecting Endress+Hauser Promass 83I

Data signals from the Endress+Hauser (E+H) Promass 83I was transmitted in the form of RS485. To get the signal to a computer, a convertor (Advantech, Adam 4521) was used to convert the signal from RS 485 to RS232. From the convertor, the RS 232 signal was connected to the computer serial port using a serial cable. Next, a Object Linking and Embedding for Process Control (OPC) server program (Advantech Modbus OPC Server 1.0) was required to be installed into the computer in order to decipher the signal of the realtime measurements into useful data such as density, temperature, viscosity, mass flow rate, etc.

The OPC server was configured to extract signals from the serial port by the following settings shown in Figure 3.40. These configurations let the server know the location (in this case, the serial port) and the type signal that it was receiving.

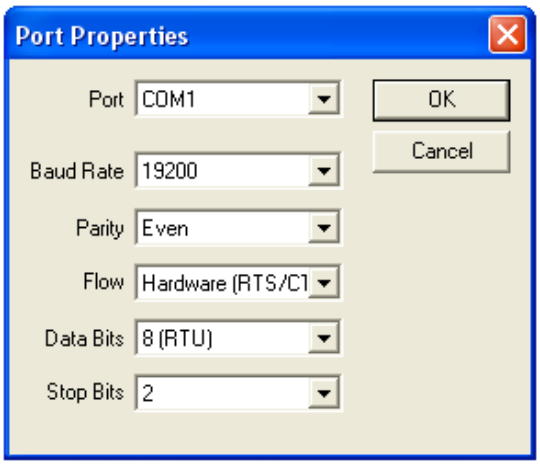

Figure 3.40 Configuration for received signal

The signal settings could also be found and changed in E+H Promass 83I transmitter. Once the OPC server knew the location and the type of signal that it was receiving, the device (E+H Promass 83I) had to be added into the server. The device type and the unique address for the E+H Promass 83I was Modbus and 247 respectively as shown in Figure 3.41.

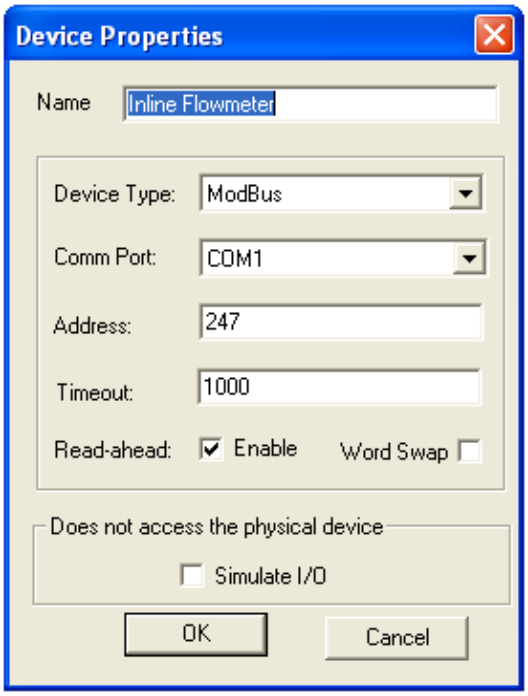

Figure 3.41 Configuration for device

Tags, representing an individual parameter measured by E+H Promass 83I, were then added to the device. Each individual parameter had an unique address as well. The setup of the tag (e.g. the density) should look like Figure 3.42.

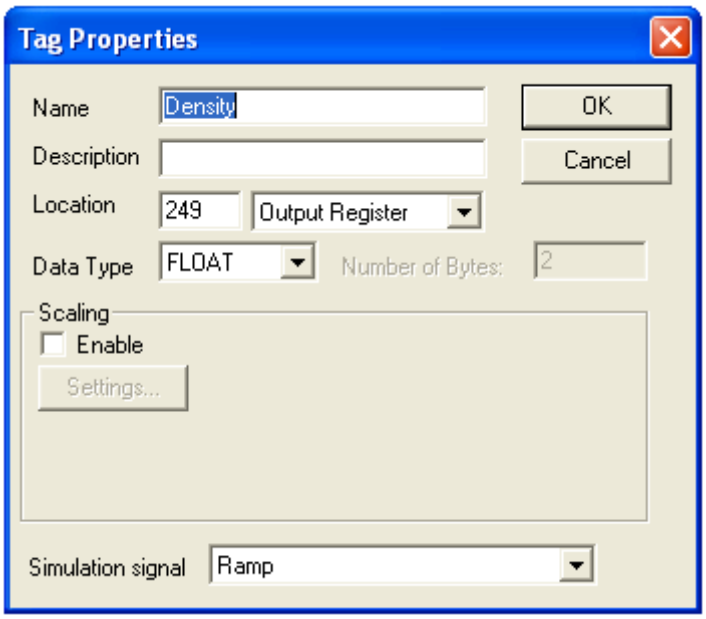

Figure 3.42 Configuration of tag

Below is a list of addresses for the parameters.

Table 3.10 List of address for measured parameters in by E+H Promass 83I

Parameter	Address
Mass Flow	247
Volume Flow	253
Density	249
Temperature	251
Pressure	257
Dynamic Viscosity	2019
Kinematic Viscosity	2083

When all the tags were properly setup, the realtime measurements of the parameters specified should be displayed on the OPC server.

Recording the data from OPC server

To record the data received by the OPC server, another logging program (L.H. Controls, OPC Data Logger) was installed. Search for the server that was receiving the signal and add the tags (represent each measured parameter) accordingly.

Adjust the time interval between each recording and the location where the file would be saved to. Once the signal starts to stream in (realtime measurements of each parameter should be displayed in the logger as well), the recording could commence.

3.7.1.7 Commissioning

The main reason for performing the commissioning process of the evaporation system was to identify the problems with the design and to make the necessary amendments afterwards. The commissioning process was separated into 4 phases of testing, these include the testing of the vacuum ejectors, pump, heating capability and the overall system operation test.

Vacuum test

The first task was to identify if there was any major air leaks in the system that would affect the creation of a vacuum environment within the evaporator. All valves were closed to isolate the evaporator system and the vacuum ejectors were turned on. Tests to maintain a vacuum pressure of -85 kPa (gauge) were conducted in all sections (shell side of preheater, shell and tube side of the evaporation column) of the evaporator. Once all the air leakages were sealed, the next phase was to test the pumps.

Pump test

Water was pumped into the evaporation system to ensure the both the feed and concentrate pumps met the flow requirement. Under atmospheric pressure, both pumps worked flawlessly. However, when the vacuum ejector on the tube side of the evaporation column was turned on (-85 kPa gauge), problems emerged. The concentrate pump (a peristaltic pump) that was not able to pump the fluid out of the evaporator fast enough to keep up with the feed going in and the inability to control the flow rate of the feed pump indicates that flooding in the evaporator was inevitable. The problems were rectified by replacing the peristaltic pump with a magnetic driven gear pump (Micropump, GD series) and frequency inverters

(Sew-Eurodrive, Movitrac LTE A) were installed to both feed and concentrate pump to regulate the flow rate.

Heating test

The next phase of the commissioning process was to check the heating system for the preheater and the evaporation column. Water was circulated in the system during the testing and the vacuum for the tube side of the evaporation column was turned on to -80 kPa (gauge). Maintaining the steam temperature (± 2°C) was relatively straight forward as long as the pressure within the preheater and the evaporation column was adjusted correctly and the condensate could be drained smoothly.

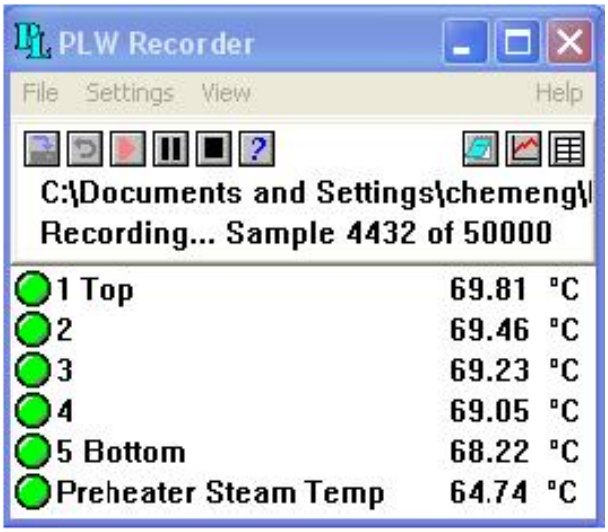

Figure 3.43 Temperature profile of the evaporation column and the preheater steam temperature

In Figure 3.43, it shows the uniform steam temperature profile of the evaporation column (target temperature was 70°C) and the temperature of the steam entering the preheater (target temperature was 65°C) during the commissioning process. A point to note, the reason that thermocouple 5 (the bottom most thermocouple) displayed a slightly lower temperature was because of a slight accumulation of condensate at the bottom of the shell side of the evaporation column.

Overall system operation test

The overall system operation test was conducted using reconstituted medium heat skim milk. The objective was to concentrate the milk to 50 wt% (at least) and estimate of the evaporation time. A 20L batch of reconstituted skim milk at 30 wt% was used in this test.

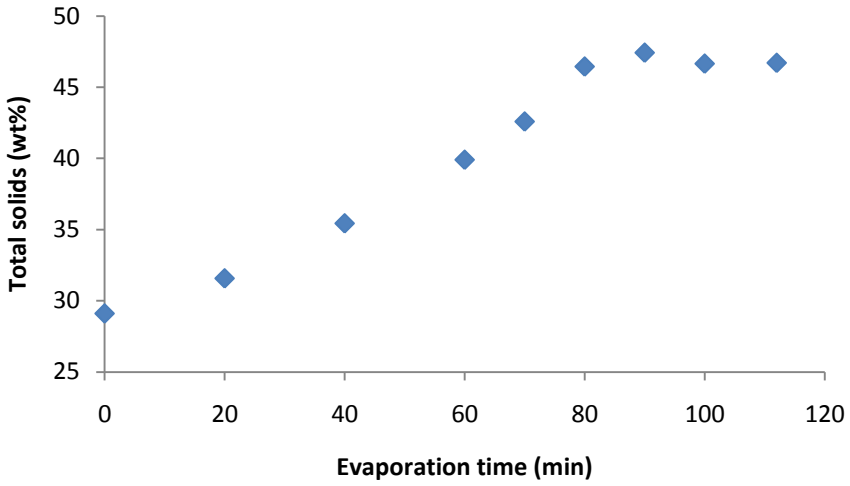

Figure 3.44 The progression of total solids with evaporation time during the commissioning process using a centrifugal feed pump

In Figure 3.44, it clearly showed that the total solids of the milk concentrate plateaus at around 47 wt% after 80 min of evaporation and had failed to reach the minimum desired solids content of 50 wt%. The reason was obvious. The feed pump (a centrifugal pump) was not able to deliver the adequate amount of feed into the evaporator at high viscosity when the milk becomes concentrated. Therefore the amount of water evaporated from the milk concentrate reduced significantly resulting in the plateau of the constant solids content. After a magnetic driven gear pump (similar to the concentrate pump) replaced the centrifugal pump, the performance of the evaporator improved noticeably (Figure 3.45). Although the flow rate for the gear pump still decreased with increasing but its performance was sufficient for the evaporator to reach the desired solids content.

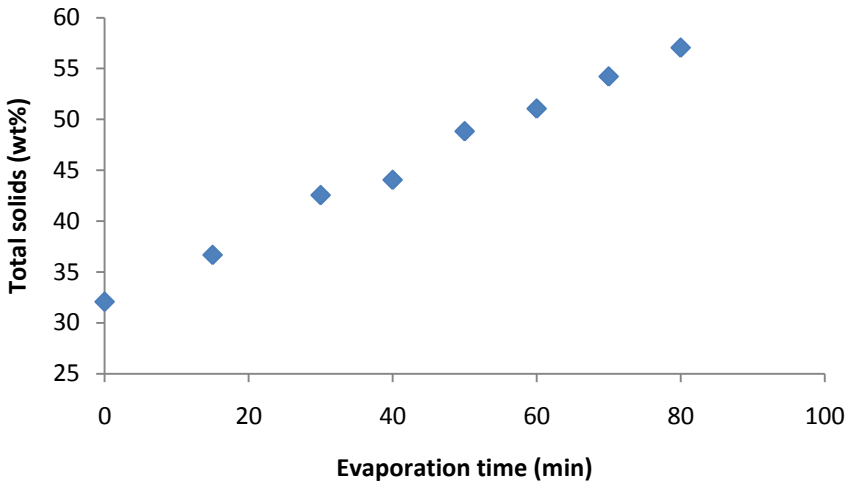

Figure 3.45 The progression of total solids with evaporation time during the commissioning process using a gear feed pump

Note that the slightly faster evaporation rate in Figure 3.45 (although not very obvious) than the prior was because of a smaller batch (15L) of reconstituted skim milk was used. During the testing, a vessel with cooling coil was also installed at the bottom of the evaporation column. The purpose was to cool down the milk concentrate slightly so that bubbles formed during the evaporation process would not flood the system.

3.7.1.8 Operation of steam-heated pilot evaporator

The operation of the steam-heated pilot evaporator could be separated into 3 phases: start-up, operating and shutdown procedures. Most of the process parameters (steam temperatures, vacuum pressure, flow rates, etc.) were adjusted manually via regulators, valves and frequency inverters (except for the 2 solenoid valves regulating the steam input for the preheater and the evaporation column). Therefore, special attention was essential on the gauges and the temperature readings on the evaporator. Once the start-up process was initiated correctly, only minimal adjustment would be required during the evaporation process.

Start-up procedures

The general guideline to start-up the evaporator follows 3 basic sequential steps; turn on the flow, followed by the vacuum and then the heat. The detail of the start-up procedures are as follow.

1. Turn on the boiler and close the steam isolation valve.
2. Adjust the temperature controllers for the feed and evaporation column. (e.g. 62°C for the feed and 70°C for the evaporation column)
3. Pour the milk of specific volume and total solids content into the feed tank.
4. Turn on the feed pump via the frequency inverter 1 and adjust the flow rate to at least 2 L min^{-1}.

Note: Take note of the liquid level in the evaporator through the observation window at the bottom of the evaporation column.

5. Turn on the concentrate pump via another frequency inverter 2 when the liquid level can be seen on the observation window.
6. Match the flow rate of the feed and concentrate pump by adjusting both frequency inverters.
7. Turn on the vacuum ejectors 1 to 5 with the settings in Table 3.11.

Table 3.11 Vacuum ejector setting during start up

Vacuum Ejector	Description	Settings
1	Evaporator column tube side pressure	Adjust the pressure regulator 1 accordingly by referring to pressure gauge 1
2	Evaporator column shell side pressure	Adjust the pressure regulator 2 accordingly by referring to pressure gauge 2
3	Evaporator column shell side condensate removal	3.5 to 4 bars on the pressure regulator 3
4	Periodical condensate removal	3.5 to 4 bars on the pressure regulator 4
5	Preheater shell side pressure	Adjust the pressure regulator 5 accordingly by referring to pressure gauge 5

Note: Pressure displayed on gauge 1, 2 and 5 corresponds to the boiling or steam temperature within each section. Refer to Figure 3.38 for the operating temperature and its corresponding pressure. (E.g. if the operating temperature on the shell side of the preheater was 70°C (or 343 K), adjust

pressure regulator 5 until pressure gauge 5 reached approximately -67.8 kPa)

8. Readjust the frequency inverters as the vacuum environment created in the tube side of the evaporator would enhance the feed rate and hinder the concentrate removal rate.
9. Turn on the condenser cooling water valve (V-10).
10. Open the steam isolation valve once the boiler reaches its design pressure.
11. Adjust the pressure reducing valve (Spirax Sarco, BRV 2) to 10 to 15 psi g.

Operating procedures

After the start-up procedures have been properly executed, the operating procedures are relatively straight forward.

1. Take note of the fluid level in the evaporator and adjust the frequency inverter accordingly

Note: The feed rate would reduce throughout the entire evaporation process, especially beyond 50wt%, as the viscosity of the milk increases. The minimum feed rate should not fall below 1.7 L min^{-1}. Follow the shut down procedure if the feed rate should get close to 1.7 L min^{-1}.

2. Make appropriate adjustment to the pressure regulators for the vacuum ejectors to maintain the right vacuum pressure.
3. Occasionally, turn on V-17 and V-18 to drain off the condensate in the steam column leading to the preheater and the evaporation column.

As long as the vacuum pressure and the steam supply are maintained correctly, the temperature within each section should not fluctuate more than 2 °C from the desired temperature set point.

Shut down procedures

The shut down procedures follows the reverse order of the general guideline for the start-up procedures. At the end of evaporation process, it is essential to follow

the shut down procedures to minimise the chance of extensive fouling and potential blockage within the preheater and the evaporation column.

1. Pour 5 L of water (preferably warm water) into feed tank to dilute the concentrate.

Note: Do not turn off the vacuum at this stage to prevent any blockage within the preheater.

2. Close the steam isolation valve.
3. Once the feed rate returns back to the original value, turn off all the vacuum ejectors
4. Turn off the feed pump and pump out as much residual liquid from the evaporator before turning off the concentrate pump.

To this stage, the evaporation system is still contaminated with milk or even fouling cakes. Therefore, a thorough cleaning process needs to done prior to the complete shutdown of the evaporator.

3.7.2 Potential design improvements

Although the current evaporator configuration of the steam-heated pilot evaporator was able to operate smoothly and process the milk concentrate to the required solids content, there were still some improvements could be done. The 3 main areas that had the potential for improvement were the vacuum system, the preheater and the synchronisation of the feed and concentrate pump.

3.7.2.1 Vacuum system

The vacuum system can be separated in 3 sections within the evaporator; preheater, shell and tube side of the evaporator. In each section, the vacuum requirements are different, e.g. in the shell and tube side of the evaporator, the pressure on each side depends on the evaporation temperature of the process fluid and the temperature difference desired. Presently, the temperature within each section is regulated via pressure and the pressure is determined by manually

adjusting the amount of compressed air supplied to the vacuum ejectors. Constant attention is required on the pressure gauges to maintain the desired pressure within each section. This can be eliminated by installing a PID controller that regulates a pneumatically-actuated valve on the compressed air supply to the vacuum ejectors based on the temperature in the target section.

3.7.2.2 Preheater

At this stage, the main reason for terminating the experiment at around 60wt% was the high pressure drop across the preheater, especially at high solids content. With internal diameter of 5.6 mm and 17m long, the pressure drop across the preheater was 1200 kPa when 50wt% skim milk flows through the spiral tube at 0.000045 m^3 s^{-1}. Although the vacuum in the evaporation tube was able to contribute positively to the delivery of feed through the preheater, but it is not sufficient to avoid significant decrease in pump performance. Calculations had shown that by increasing the diameter of the spiral tube within the preheater, the pressure drop would decrease drastically (see Figure 3.46), even at high solids content. The formula used for the calculation can be found in Appendix A.3.

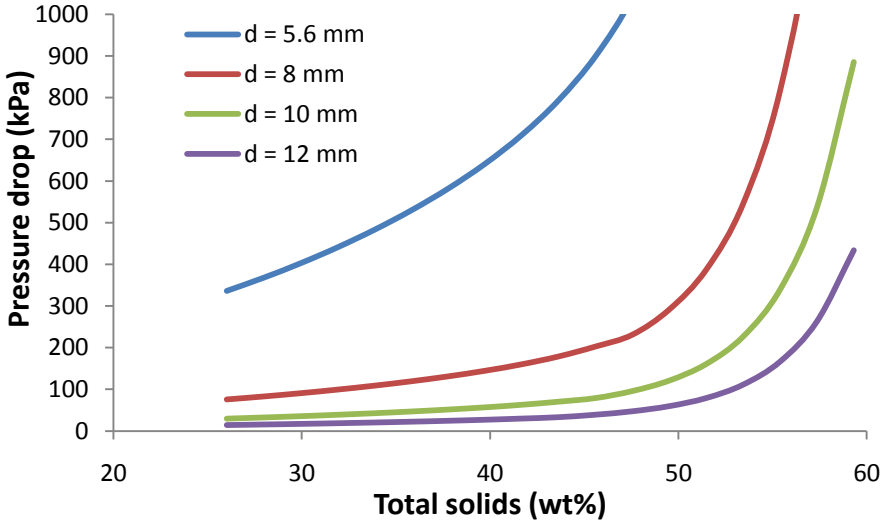

Figure 3.46 Pressure drop across the preheater using different tube size when skim milk at various solids content is pumped through at 0.000045 m^3 s^{-1}

However, with the increase in tube diameter, the volume to heat transfer area ratio would reduce as well. This led to the reduction in heat transfer performance by the preheater. Therefore, the design of the preheater had to be re-evaluated to find

the optimum tube size and length that met the heat transfer requirements and had low pressure drop across it.

3.7.2.3 Level control for concentrate outlet

With the reduction in performance by the feed pump as the solids content rises, the concentrate pump has to be manually adjusted via the frequency inverter to maintain the liquid level in the evaporation column. This task can be automated by installing a level control that monitors the concentrate level at the bottom of the evaporator and regulate the frequency inverter to throttle the pump speed accordingly to maintain the liquid level.

3.8 Results

3.8.1 Preliminary study of viscosity

The preliminary study of viscosity was conducted using the "pot" evaporator (Section 3.7.1) on four different samples and they include reconstituted skim milk, UHT skim milk, market skim milk and skim milk samples from factory. Viscosities were measured at 60°C and at shear rate of 10.5 to 104.7s^{-1}. The general trend of all test samples shows an exponential increase in viscosity as total solids content increases. The increase in viscosity becomes more prominent once the solids content goes beyond 45 wt%. Such trend agrees with many other authors. (Fernandez-Martin, 1972; Snoeren *et al.*, 1982; Chang and Hartel, 1997; Trinh *et al.*, 2007; Velez-Ruiz and Barbosa-Canovas, 1998a). In Figure 3.47, it shows the typical exponential increase in viscosity as solids content gets higher. There is no significant difference between each type of skim milks up to 40wt%. Further investigation was conducted focusing on high solids content (> 40 wt%) and a model (Equation (3.39)) was fitted to each type of skim milk.

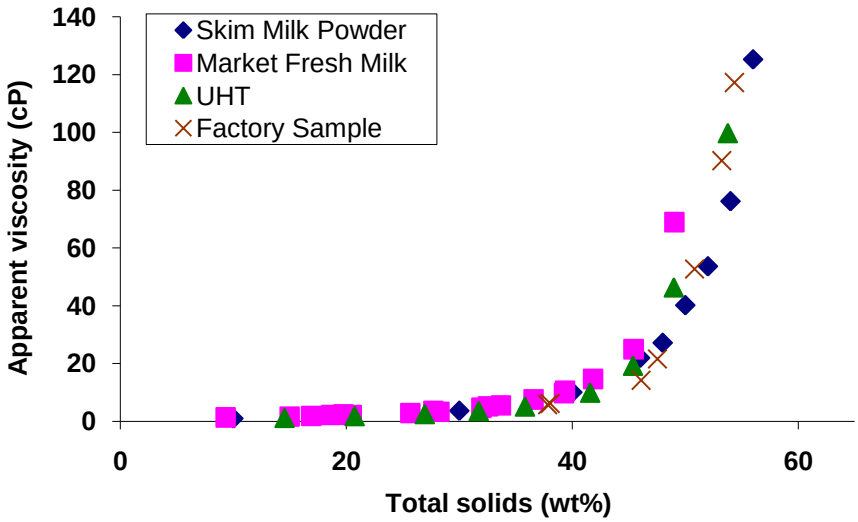

Figure 3.47 Viscosity measurements of different type of milk at various solids content (60°C, 31.4s^{-1})

In order to have a fair comparison between samples of different concentrations, shear rate has been standardised. A lower shear rate of 31.4s^{-1} was chosen to ensure that the viscometer produces more accurate measurements at high viscosity.

At the same temperature, model was found to fit the viscosity profile of high solids content well with high degree of accuracy ($R^2 > 0.99$). Below in Figure 3.48 shows the fitting of model to each type of skim milk.

$$\mu = a + (b \exp(cX)) \tag{3.39}$$

where *X* is the total solids (wt%) and *a, b* and *c* are fitting constants

Table 3.12. Parameters in the exponential model relating the apparent viscosity to the solids content

	Reconstituted skim milk	Market fresh skim milk	UHT skim milk	Factory skim milk
a	9.9536	8.6212	-9.4636	2.6955
b	1.7989E-4	1.7675E-06	3.8260E-02	1.3759E-04
c	2.3848E-01	3.5360E-01	1.4801E-01	2.5088E-01
R^2	0.9958	0.9990	0.9972	0.9980

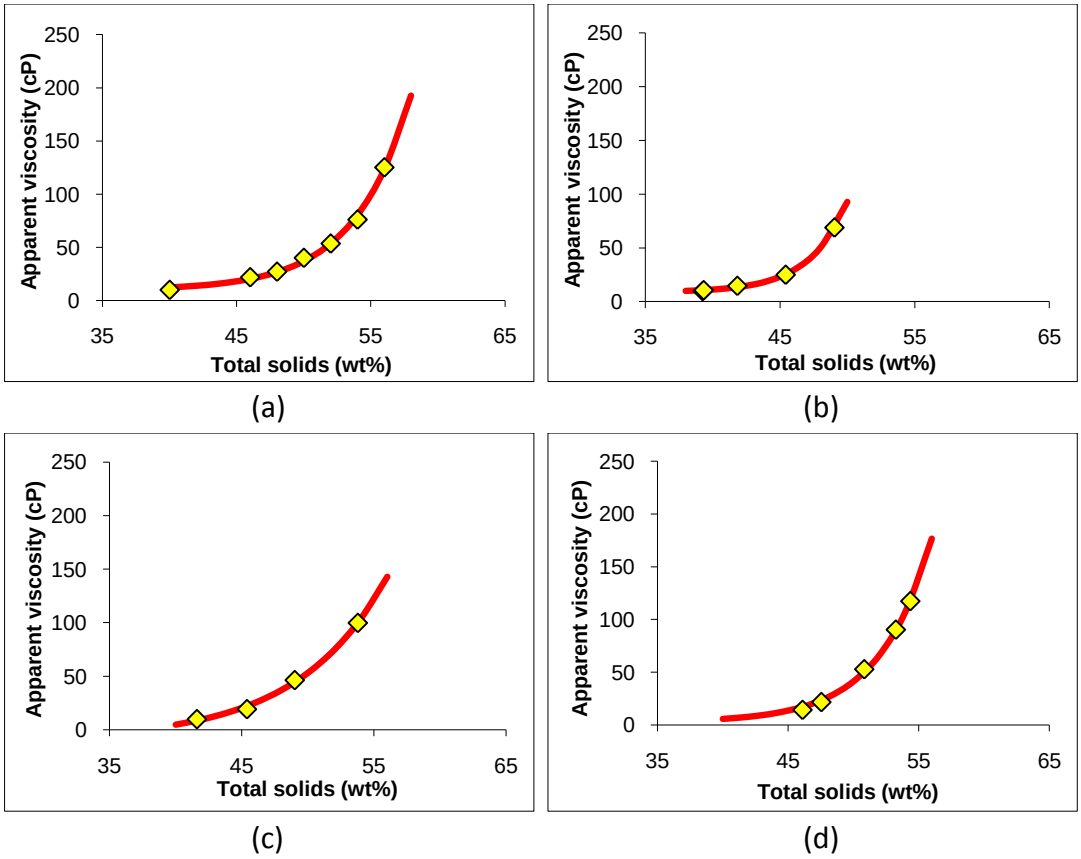

Figure 3.48. Viscosity profiles and the models fitted in various types of skim milk.

(a) Reconstituted skim milk (b) Market Fresh skim milk

(c) UHT skim milk (d) Factory skim milk

At first glance, it is noticed that UHT milk has a gentler curve as compared to the rest of the samples. This means that the increase in apparent viscosity is more gradual as the total solids content increases. It is noted that the harsh heat treatment it has undergone comparing with others.

Plotting all the viscosity models up in a single graph as shown in Figure 3.49, there is a distinctive difference in viscosity trend for fresh skim milk compared with the others. The onset of the rise in viscosity appears to be earlier than the others. At 50wt %, the viscosity for market fresh skim milk can be up to twice of factory skim milk.

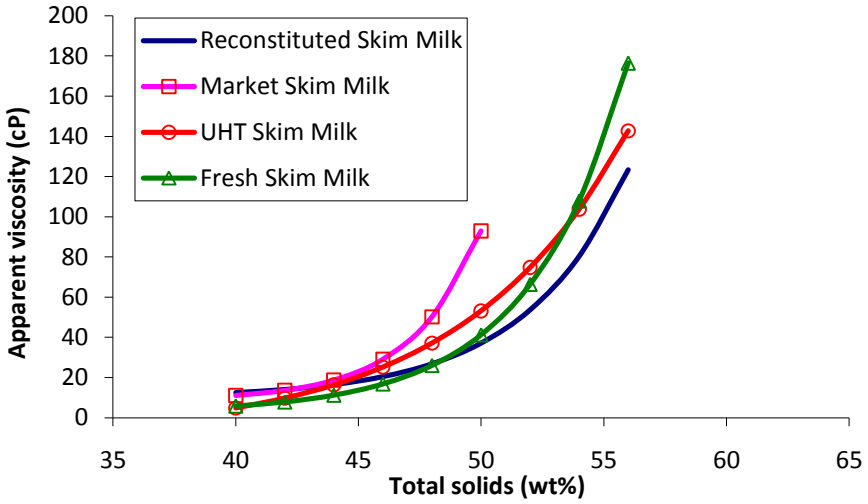

Figure 3.49 Comparing viscosity curves of various types of skim milk.

The reason behind the drastic difference between the market fresh skim milk with the rest of the skim milk is unknown. It could be due to the additives that were introduced into the milk that might have enhanced the rise in viscosity upon heating.

3.8.2 Factors influencing viscosity measurement

3.8.2.1 Concentration

The rheology properties of milk are comparable to a suspension where discrete randomly distributed particles (e.g. proteins) are suspended in a fluid medium mainly consist of water. During the evaporation process, water is removed from the suspension and the particles within the fluid medium become more compacted. The compaction of particles is directly reflected on the viscosity of the milk as more force is required to overcome the shear resistance within the fluid. A typical viscosity profile of milk with varying solids content is represented by Figure 3.50. The viscosity profile exhibits an exponential behaviour with increasing solids content. Prior to 30wt%, the viscosity is not sensitive to the change in solids content, with viscosity of less than 10cP. In between 30 to 45wt%, viscosity doubles to around 20cP. Beyond 45wt%, a steep rise in viscosity initiates, with the doubling of viscosity in every 5wt% increase in solids content. A point to note, the general statements above were based on the viscosity measurements conducted with

equipments and conditions specified in Section 3.4.1, these statements may vary with the equipments used and conditions tested.

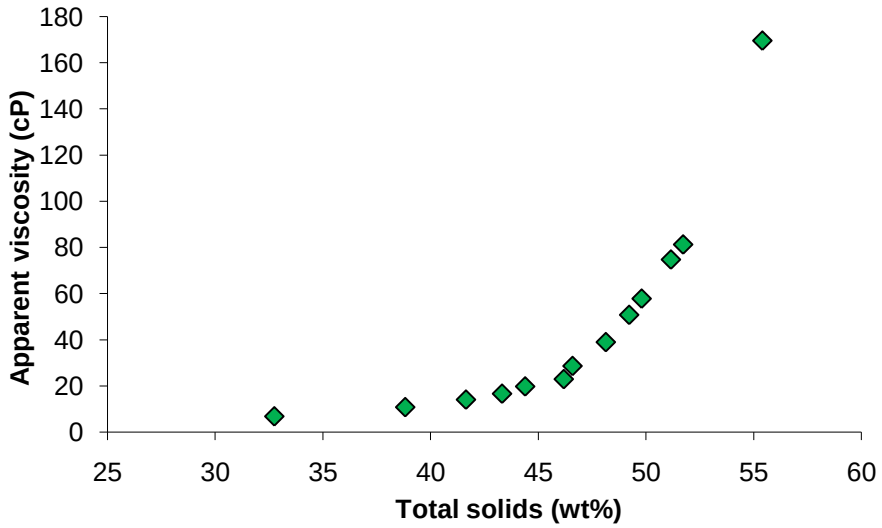

Figure 3.50 Viscosity measurement of reconstituted medium heat treated skim milk at various solids contents (50°C, 31.4s^{-1})

3.8.2.2 Temperature

In general, the viscosity of milk decreases with increasing temperature. This holds true until the temperature reaches beyond 70°C, where the possible denaturation of β-lactoglobulin could increase the viscosity with elevated temperature (Section 2.1.1).

For illustration purposes, data in Figure 3.51 were taken from the viscosity measurements of reconstituted skim milk. All the other types of milk display comparable viscosity trends as Figure 3.51 as they were subjected to similar measurement conditions.

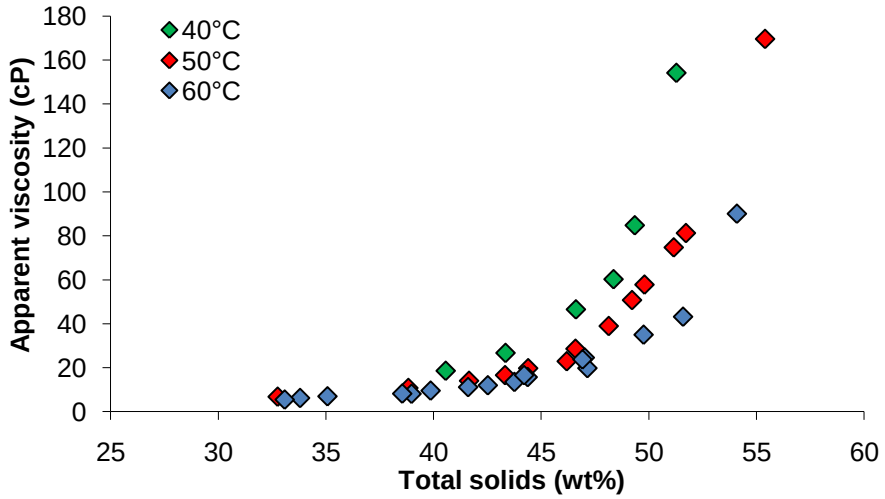

Figure 3.51 Viscosity measurement of reconstituted medium heat skim milk concentrates at various solids contents and temperatures (31.4 s^{-1})

In Figure 3.51, the deviation in viscosity profiles across the 3 temperatures measured were not evident until the solids content reaches 40 wt%. Beyond 40 wt%, the viscosity profile measured at 40°C begins to rise at a faster rate than the other 2 profiles. Similar phenomenon also occurred to the viscosity profile measured at 50°C beyond 47.5 wt%.

On first glance, the 3 viscosity profiles look identical in shape. This hypothesis was verified by attempting to shift the viscosity profiles measured at 40 and 50°C to the right, with the intention of matching the viscosity profiles measured at 60°C. This attempt was plotted in Figure 3.52 and the result has proven the hypothesis is correct to a certain degree, if not, completely.

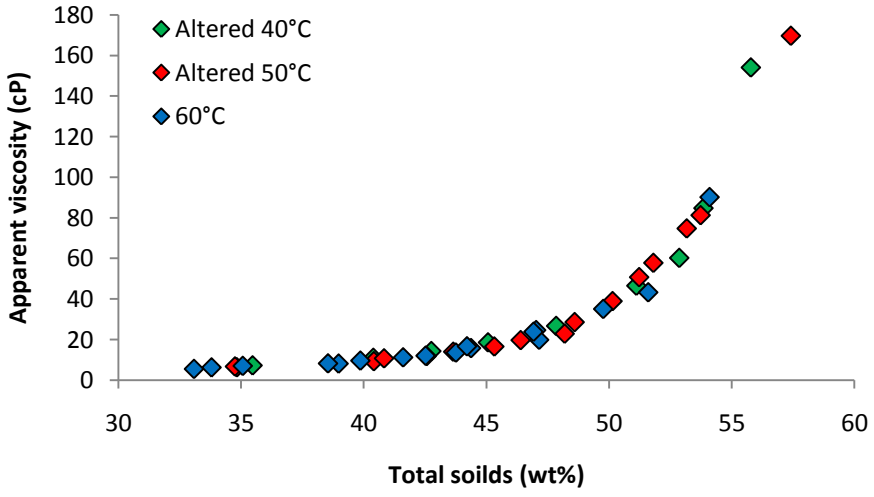

Figure 3.52 Viscosity profiles of reconstituted medium-heated skim milk concentrate with altered positions (31.4 s^{-1})

Similar attempts of matching viscosity profiles at different temperatures were also conducted on fresh medium and low heat treated skim milk from WCBF. Although the magnitude of shifting the viscosity profiles varies among each type of milk, the final results were comparable. This shows that the viscosity profiles share the same shape for all temperatures but their position slightly differ each other. With this information, the integration of temperature into the viscosity model of skim milk (see Section 3.8.3) becomes slightly easier.

3.8.2.3 Shear rate

The shear-thinning effect on milk viscosity measurement has been a widely known phenomenon where the viscosities appear to be lower at higher shear rates. Literatures has shown that milk behaves as a non-newtonian fluid only beyond 20wt% (Trinh et al., 2007; Velez-Ruiz and Barbosa-Canovas, 1997). The effect of shear-thinning becomes very obvious as concentration gets higher (>40 wt%). At 50 wt%, the viscosity decreases as much as 5 folds due to increasing shear rate. However, the reduction in viscosity is reversible once that sample is relieved from the shear stress (Bienvenue *et al.*, 2003a). Tung (1978) had explained the shear-thinning effect is caused by the realignment of dispersed molecule along the shear plane and this reduces the shear resistance, thus reducing the viscosity. However, a different hypothesis was given by Fox and McSweeney (1998). They believe that the shear force breaks down of fat globule aggregates and results in reduction of effective volume of the suspension. Consequently, it reduces the viscosity. The measurement of milk viscosities at various shear rates was also done by several workers (Kyazze and Starov, 2004; Bienvenue *et al.*, 2003b; Velez-Ruiz and Barbosa-Canovas, 1998b).

The viscosity measurements presented in Figure 3.53 were extracted from the preliminary investigation of milk viscosity from the “pot” evaporator experiments. Fresh medium heated skim milk delivered from Murray Goulburn Co-operative, Koroit was used to illustrate the effect of shearing on viscosity measurement.

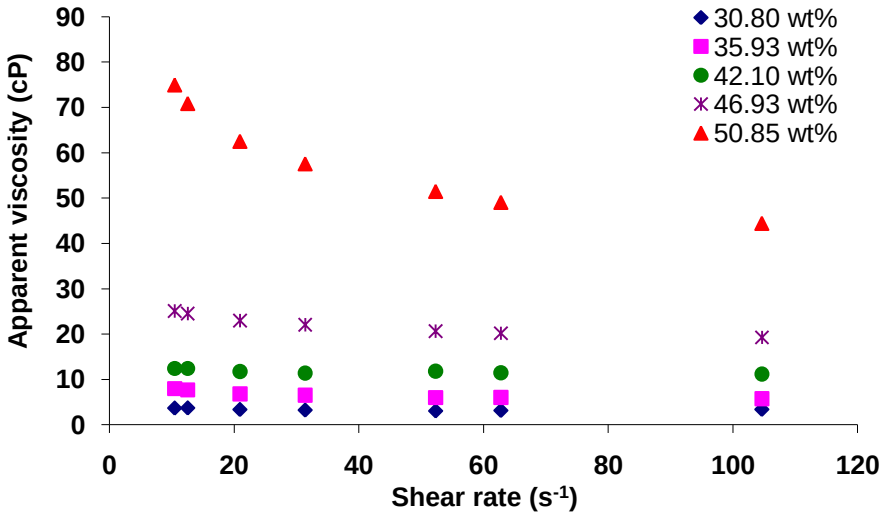

Figure 3.53 Viscosity measurement of fresh medium heat skim milk concentrates at various solids content and shear rate (60°C)

Viscosity was measured at various shear rates ranged from 10.5 to 104.7 s^{-1}. The viscosity measurements remain virtually unaffected by the shear rate to which it was measured in until approximately 47 wt%. The early sign of shear thinning could be observed at 46.93 wt% where the apparent viscosity decreases by 5.8 cP within the shear rates tested. At 50.85 wt%, the deviation in apparent viscosity decrease further to 30.6 cP. An exponential increase in apparent viscosity with decreasing shear rate was also observed. This means that the apparent viscosity of skim milk at specific solids content and conditions would reach a steady value ultimately when the induced shear rate is high enough. This is known as the infinite-shear viscosity.

Similarly, when the apparent viscosity was plotted against total solids in Figure 3.54, distinct viscosity profiles could be observed at each shear rate they were measured. The same attempt to match the viscosity profiles at different shear rates, like in Section 3.8.2.2 for the temperatures, was also carried out in Figure 3.55. Surprisingly, the shape of the viscosity profiles at different shear rate matches each other when they were shifted accordingly.

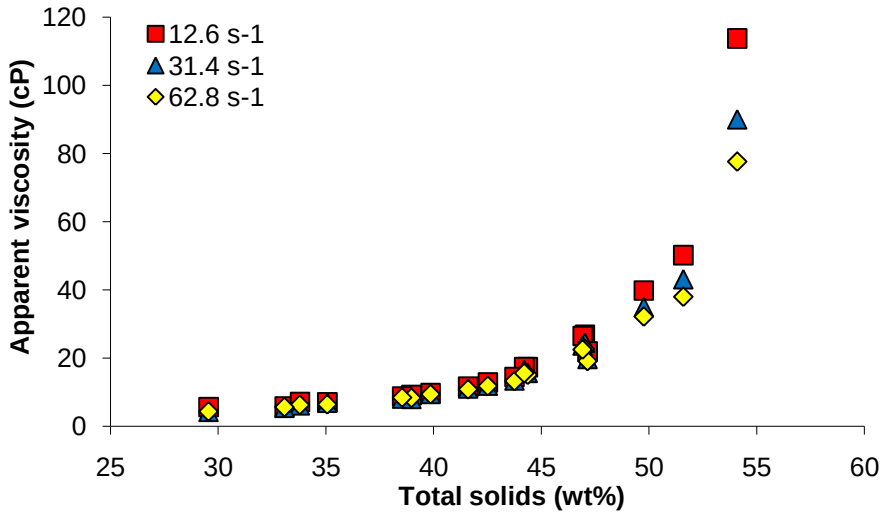

Figure 3.54 Viscosity profiles of reconstituted medium-heated skim milk concentrate at various solids content and shear rates (60°C)

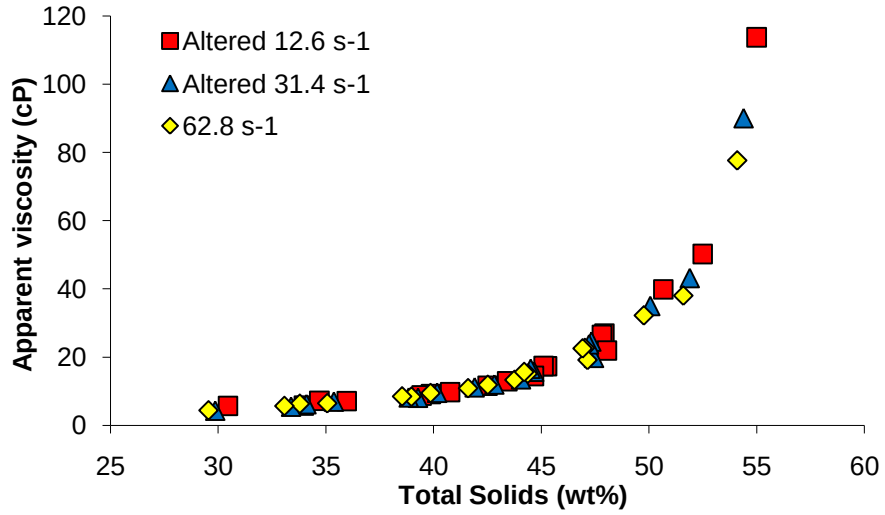

Figure 3.55 Viscosity profiles of reconstituted medium-heated skim milk concentrate at with altered positions (60°C)

3.8.3 Modelling of skim milk viscosity

In this section, attempts were made to model skim milk viscosity revolved around 3 main factors, total solids, temperature and shear rate to which the viscosity was measured in. In order to incorporate all the 3 factors into a model, the behaviour of the individual factor had to be characterised. In Section 3.8.2, the main 3 factors influencing the viscosity behaviour of skim milk indicate that the shape of the viscosity profiles is almost identical. This shows that as long as the curve of a viscosity profile can be accurately modelled, the correction of the viscosity profile for the temperature and shear rate can be integrated.

Such a comprehensive and hopefully simple model begins with a basic formulation where only total solids effect can be expressed by the following double-exponential equation, for constant temperature and no age-thickening present:

$$\mu = a \cdot e^{bX} + c \cdot e^{dX} \tag{3.40}$$

where *X* is the total solids (wt%) and *a, b, c* and *d* are constants.

The ability to match the viscosity profiles of different temperatures by adjusting the total solids in Section 3.8.2.2 indicates that the temperature dependency of milk viscosity can be characterised by Arrhenius model. The application of Arrhenius model in characterising food rheology is not unusual and it has been widely used to describe the influence of temperature on viscosity of various types of fluid (Simuang *et al.*, 2004; Herceg and Lelas, 2005; Yanniotis *et al.*, 2006).

$$\mu = \mu_o exp\left(\frac{E_a}{RT}\right) \tag{3.41}$$

where μ is the apparent viscosity (cP), μ_o a reference viscosity (cP), E_a the activation energy (J/mol), R the gas constant (8.315 J/mol.K) and T the temperature (K).

In this model, the reference viscosity chosen is water and in order to establish the 'additional' effect of temperature on water viscosity within concentrate on 'top' of that inserted by water, two separate Arrhenius equations were used as shown below:

$$\mu = A \cdot \exp\left(\frac{\Delta E}{RT}\right) \cdot B \cdot \exp\left(\frac{E_w}{RT}\right) \cdot \tag{3.42}$$

where E_w is the activation energy for pure water (J/mol) while ΔE is the 'additional' or 'correctional' activation energy for concentrate (J/mol). A and B are the correlation constants for skim milk concentrate and water respectively.

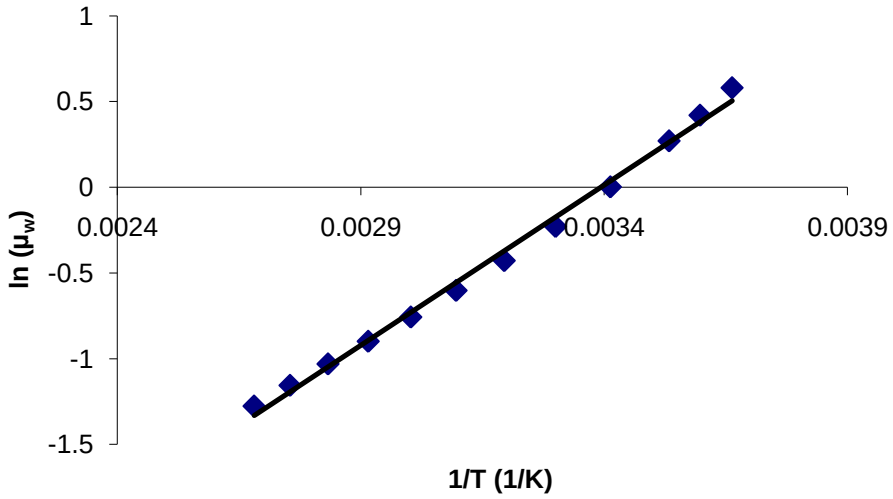

Figure 3.56. ln (μ_w) as a function of the reciprocal temperature (1/K) to showing the temperature dependence of water viscosity in terms of the Arrhenius equation, giving ln (μ_w) = 1870.2 (1/T)-6.3452

For water, from the relationship in Figure 3.56, B and E_w were derived to be 1.755×10^{-3} and 155.48×10^{3}J/mol respectively.

An appropriate ΔE was found to be able to collapse the three data sets (in Figure 3.57) obtained at different temperatures together.

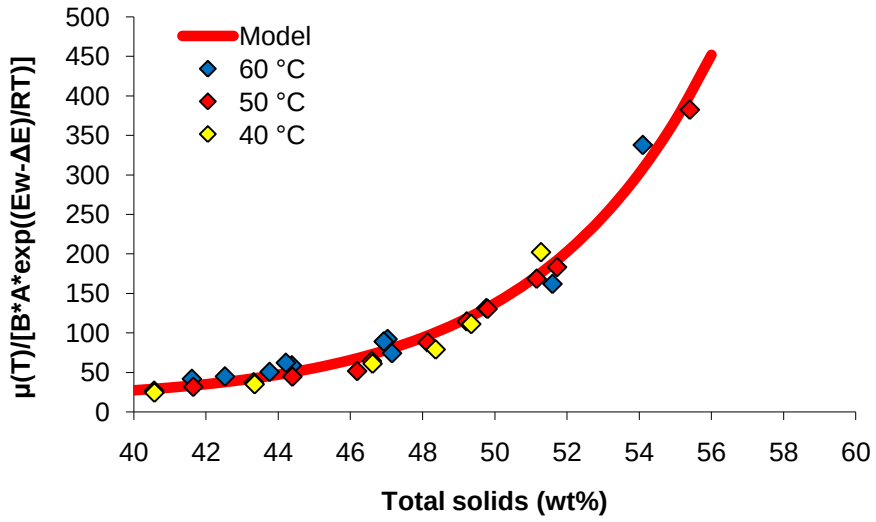

Figure 3.57. The collapse of the data sets of μ/[A*B*exp((Ew+ΔE)/RT)] vs. total solids (wt%) at 40, 50 and 60 °C respectively into a single function (data shown here were obtained at a single shear rate of 31.4 s^{-1}, a modified version of Figure 3.51)

A double-exponential model to Equation (3.42) was then fitted to the curve in Figure 3.57. Therefore the apparent viscosity can then be expressed as:

$$\mu(X,T) = A \cdot B \cdot exp\left(\frac{E_w + \Delta E}{RT}\right) \cdot [a \cdot exp(b \cdot X) + c \cdot exp(d \cdot X)] \quad (3.43)$$

where *X* is the total solids (wt%) and *a,b,c* and *d* are constants.

Also, the influence of shear rate at different temperatures on viscosity is found to behave in a similar manner where apparent viscosity decreases with increasing shear rate. Therefore, the shear rate dependence can also be expressed using an Arrhenius type equation as well:

$$\mu(X,T) = K \cdot exp\left(\frac{C}{\dot{\gamma}}\right) \cdot exp\left(\frac{E_w + \Delta E}{RT}\right) \cdot [a \cdot exp(b \cdot X) + c \cdot exp(d \cdot X)] \quad (3.44)$$

where C is the constant accounting for the shearing effect (s^{-1}) and $\dot{\gamma}$ is the shear rate (s^{-1}) at which the viscosity measurement was taken. The correlation constants for skim milk concentrate and water, *A* and *B*, are combined to form K in Equation (3.44).

Identical viscosity models were applied to all skim milk subjects tested and their fitting constants were listed in Table 3.13.

Table 3.13 Fitting constants of various type of milk

Constants	Recon. MHSM*	Fresh MHSM	Fresh LHSM**
a	7.234	1.587	0.2928
b	0.01735	0.06628	0.1063
c	6.683E-04	1.152E-06	2.641E-08
d	0.237	0.334	0.396
K	1.9089E-08	2.81419E-05	2.81419E-05
C	5.41256	4.33005	5.05172
E_w	15548.84	15548.84	15548.84
ΔE	30000	10000	10000
R	8.314	8.314	8.314

*MHSM = medium heat treated skim milk

** LHSM = low heat treated skim milk

From Table 3.13, the activation energy of pure water, E_w, in reconstituted medium-heat treated skim milk accounts only for one third of the total activation energy. This shows that the influence of temperature on milk viscosity lies greater on the solids composition than the water. This echoes the conclusion of Siedler and Elke (1949). However, with the fresh medium-heat and low-heat treated skim milk, there is a reduction in 'additional' or 'correctional' activation energy of concentrate, ΔE, of 66% when compared with the reconstituted skim milk concentrate. This means that the viscosity of reconstituted skim milk concentrate is more resilient to temperature changes than the fresh skim milk concentrate.

The viscosity models were fitted to the raw data of reconstituted medium heat-treated skim milk, fresh medium and low heat-treated skim milk in Section 3.8.4 and their correlation coefficient, r^2, were listed in Table 3.14, Table 3.15 and Table 3.16 respectively

Table 3.14 Correlation coefficient r^2 of recon. MHSM

r^2	**12.6 s^{-1}**	**31.4 s^{-1}**	**62.8 s^{-1}**
40 °C	0.983	0.974	0.989
50 °C	0.989	0.995	0.996
60 °C	0.976	0.978	0.976

Table 3.15 Correlation coefficient r^2 of fresh MHSM

r^2	**12.6 s^{-1}**	**31.4 s^{-1}**	**62.8 s^{-1}**
40 °C	0.999	0.999	0.998
50 °C	0.999	0.999	0.997
60 °C	0.999	0.999	0.997

Table 3.16 Correlation coefficient r^2 of fresh LHSM

r^2	12.6 s^{-1}	31.4 s^{-1}	62.8 s^{-1}
40 °C	0.999	0.999	0.999
50 °C	0.999	0.999	0.997
60 °C	0.998	0.999	0.999

The correlation coefficients indicate that the model (Equation (3.44)) fits the actual viscosity measurements at various conditions very well, with r^2 no less than 0.97 for any viscosity profile fitted.

3.8.4 3-D viscosity models and fitting of model

The viscosity models created in Section 3.8.3 enable the construction of three dimensional models of skim milk viscosity for easier illustration. The three dimensional models permits the integration of two influential factors (e.g. temperature and total solids) into a plot, thus providing a better visualisation of the effect of total solids, temperature and shear rate have on the viscosity of skim milk.

The analysis was divided into 2 sections. Firstly, a general overview of the skim milk viscosity on a three dimensional plot where the X- and Z-axis were the influencing factors of viscosity. Thereafter, the three dimensional plot was separated into 2 side views (from the X and Z directions) for detail study. Each plot was also painted with colour gradient to enhance the visualisation.

The range and grid division of each factor were as follow:

Table 3.17 Range and division on 3-D viscosity model

Influencing factor	Range	Division
Total solids	35wt% to 55wt% for Recon. MHSM 40wt% to 60wt% for Fresh MHSM and LHSM	1 wt%
Temperature	40°C to 60°C	1 °C

Shear rate	$12.6s^{-1}$ to $62.8s^{-1}$	$1.255s^{-1}$

3.8.4.1 Reconstituted medium heat-treated skim milk

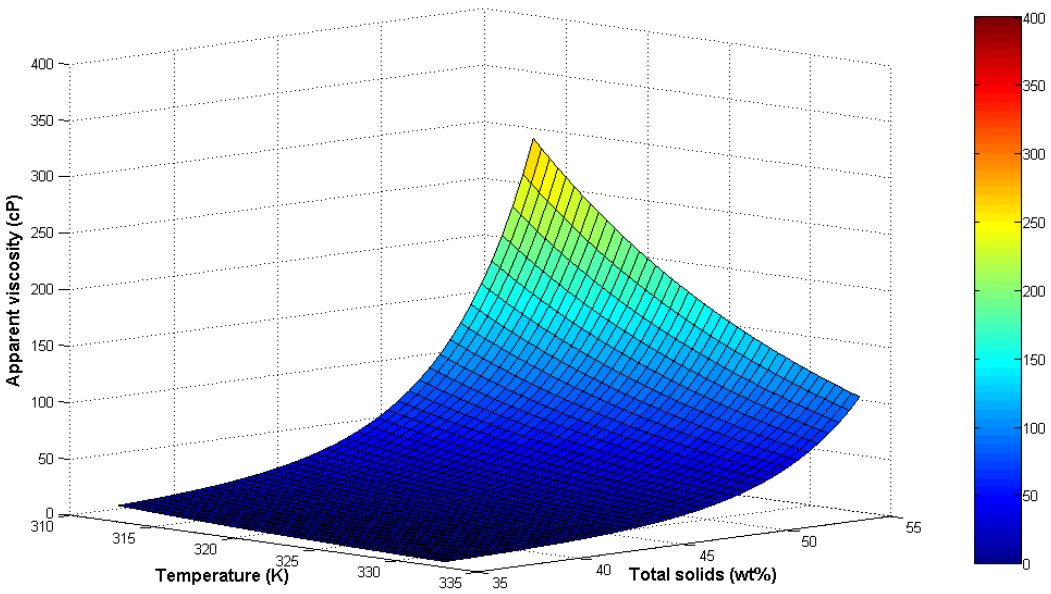

Figure 3.58 3D viscosity profile of reconstituted medium heat-treated skim milk with varying temperature and total solids (31.4s^{-1}).

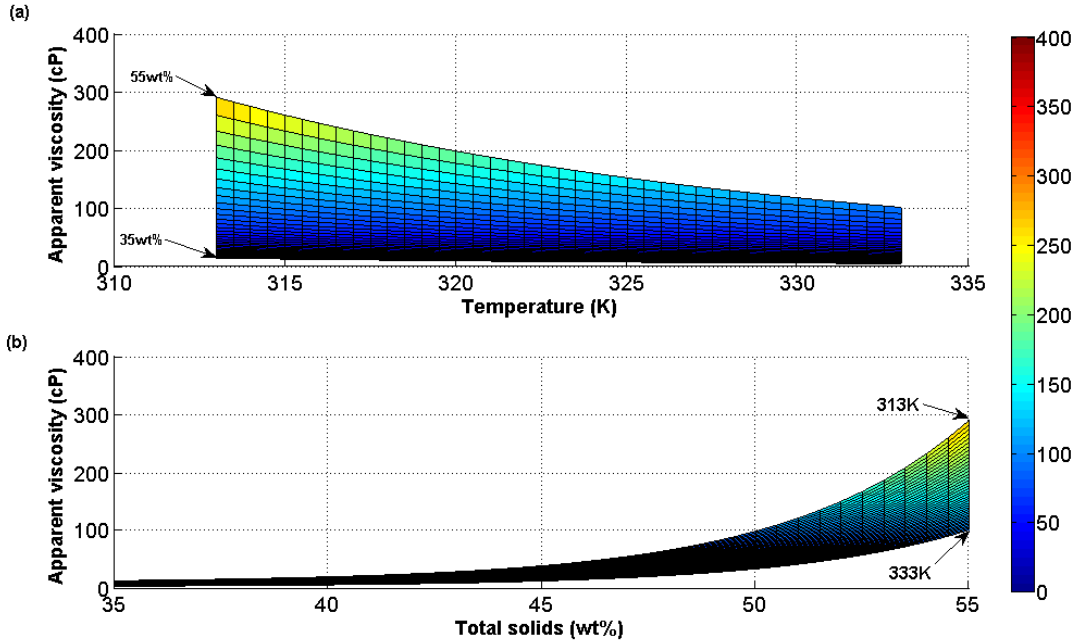

3.59(a) Temperature dependency on apparent viscosity of reconstituted medium heat-treated skim milk at various total solids. (31.4 s^{-1}), (b) Solids content dependency on apparent viscosity of Figure reconstituted medium-heat treated skim milk at various temperatures (31.4 s^{-1}).

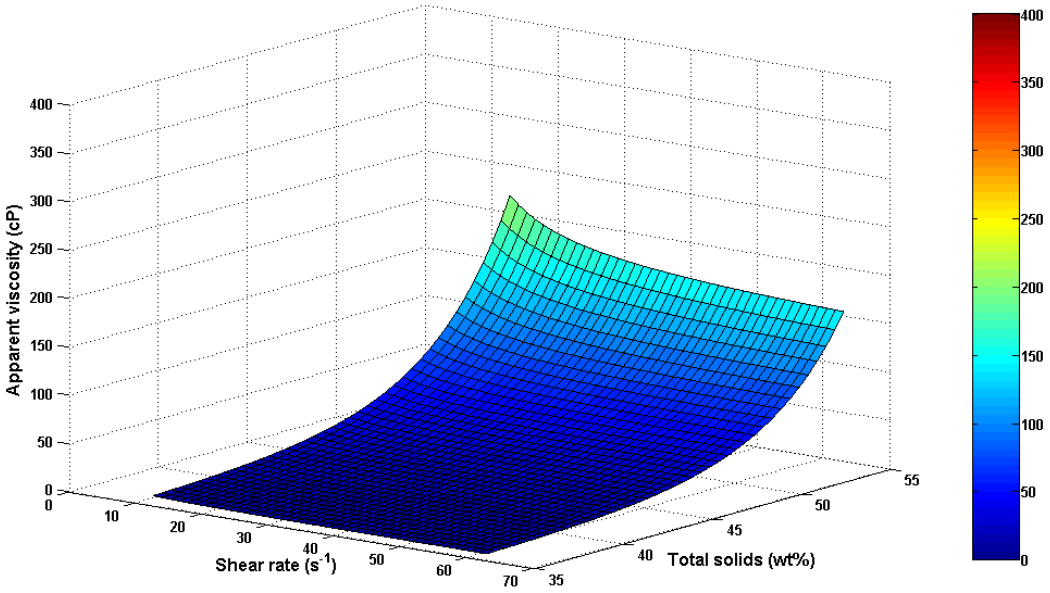

Figure 3.60 3D viscosity profile of reconstituted medium heat-treated skim milk with varying shear rate and total solids (50°C) .

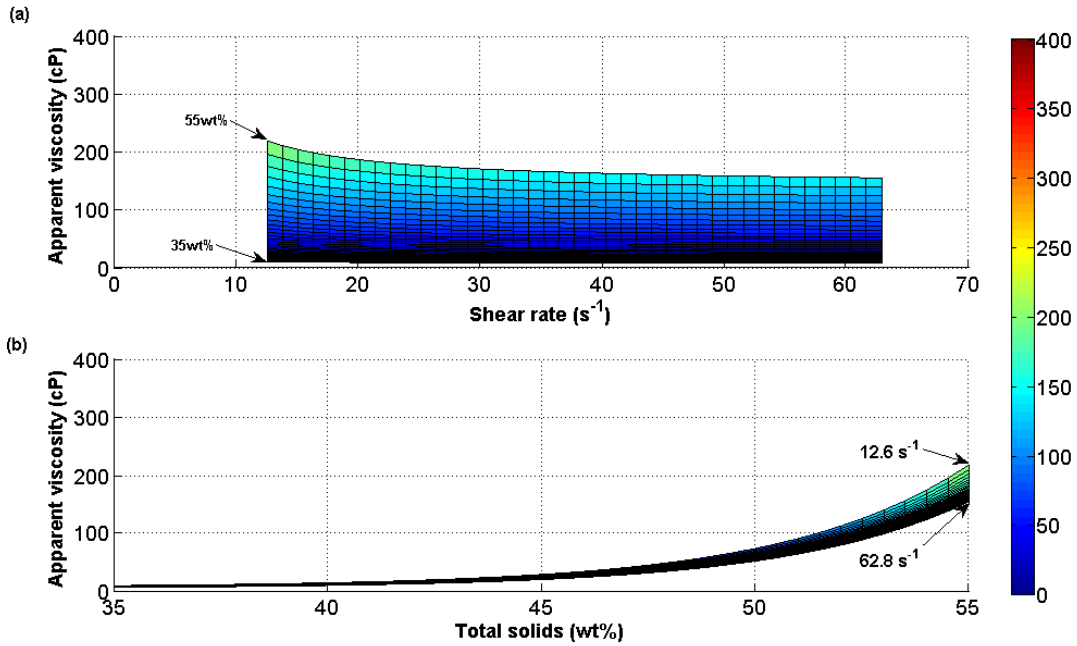

Figure 3.61(a) Shear rate dependency on apparent viscosity of reconstituted medium heat-treated skim milk at various total solids (50°C), (b) Solids content dependency on apparent viscosity of reconstituted medium-heat treated skim milk at various shear rates (50°C).

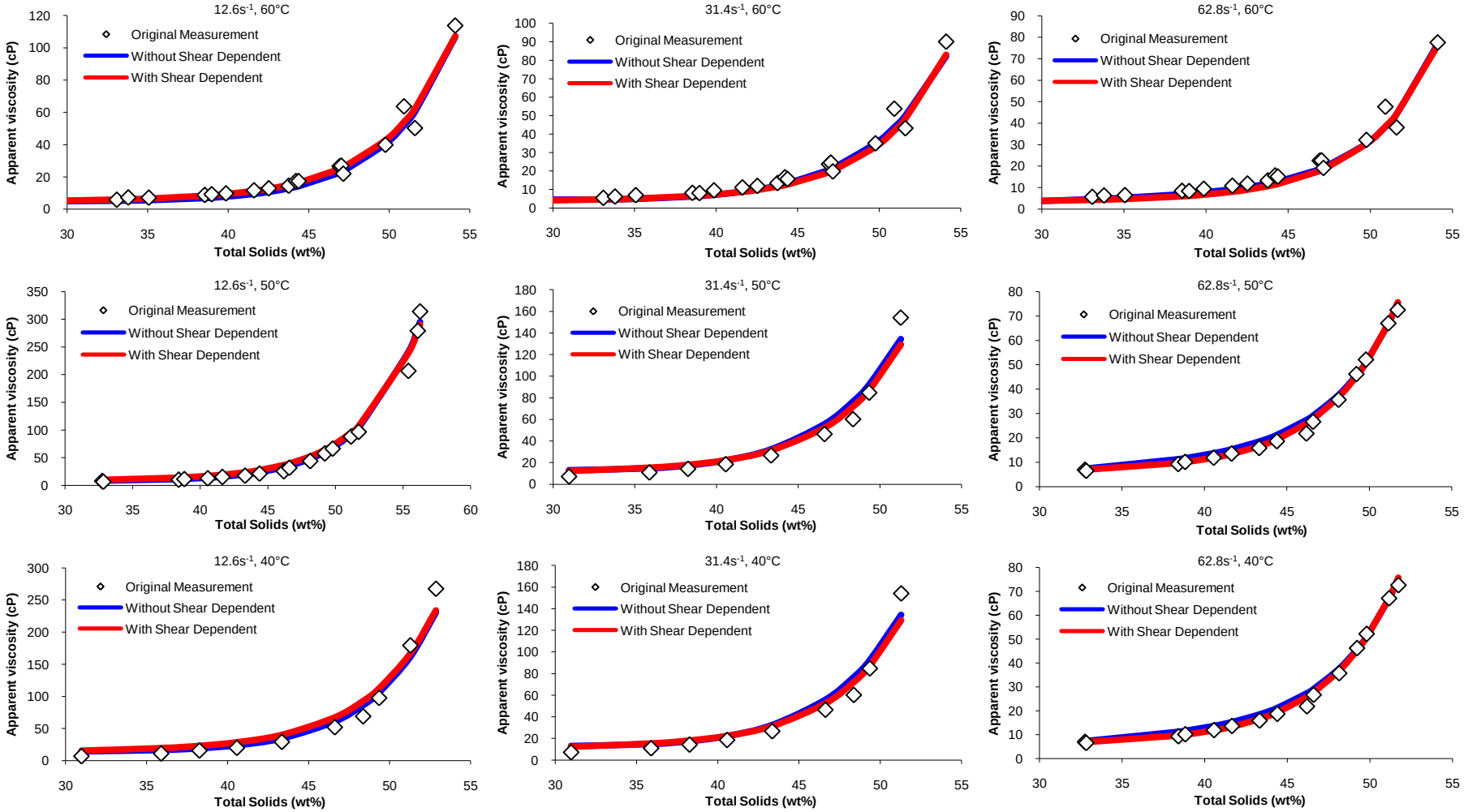

Figure 3.62 Fitting of reconstituted medium heat-treated skim milk viscosity model to raw data

3.8.4.2 Fresh medium heat-treated skim milk

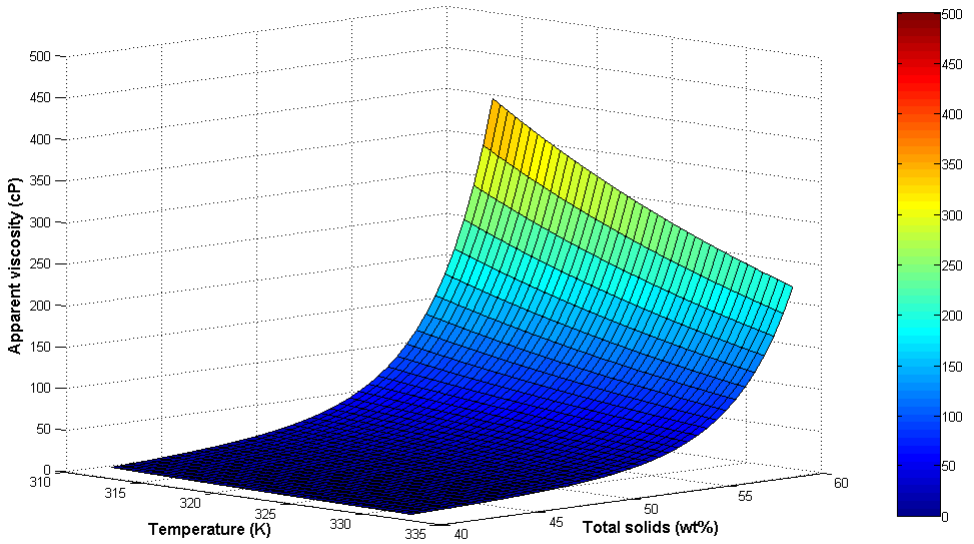

Figure 3.63 3D viscosity profile of medium-heat treated skim milk with varying temperature and total solids (31.4s^{-1}).

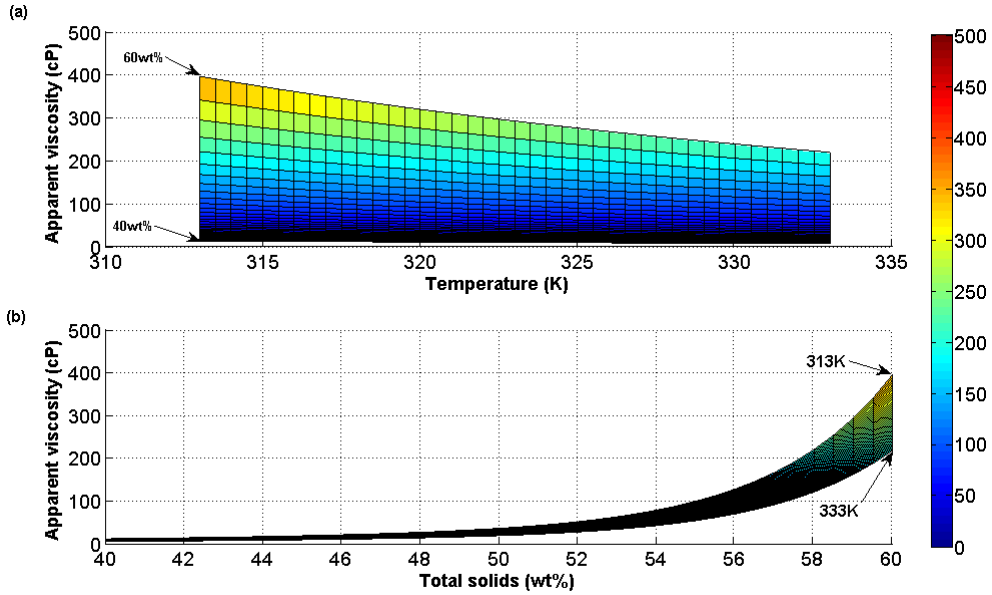

Figure 3.64(a) Temperature dependency on apparent viscosity of medium-heat treated skim milk at various total solids (31.4 s^{-1}), (b) Solids content dependency on apparent viscosity of medium-heat treated heat skim milk at various temperatures (31.4 s^{-1}).

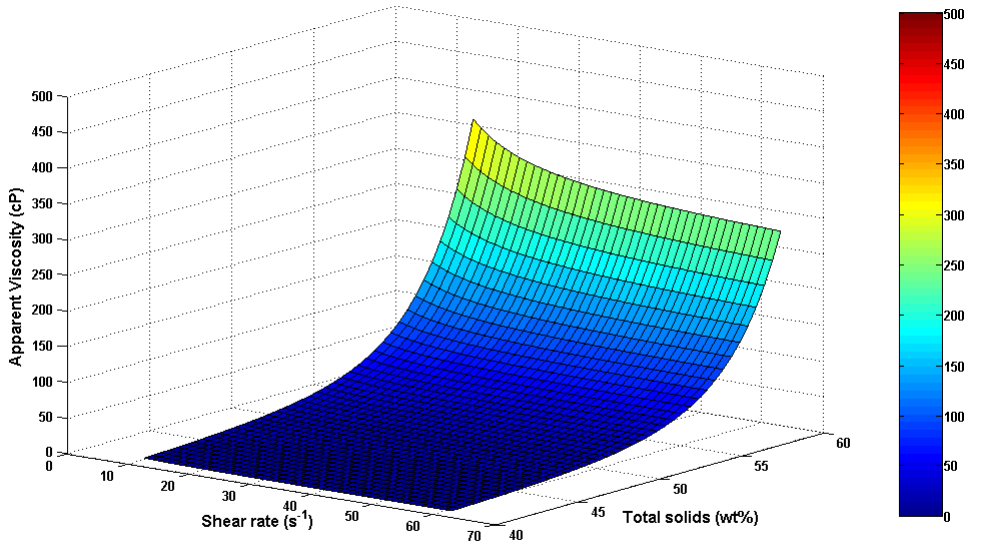

Figure 3.65 3D viscosity profile of medium-heat treated skim milk with varying shear rate and total solids (50°C).

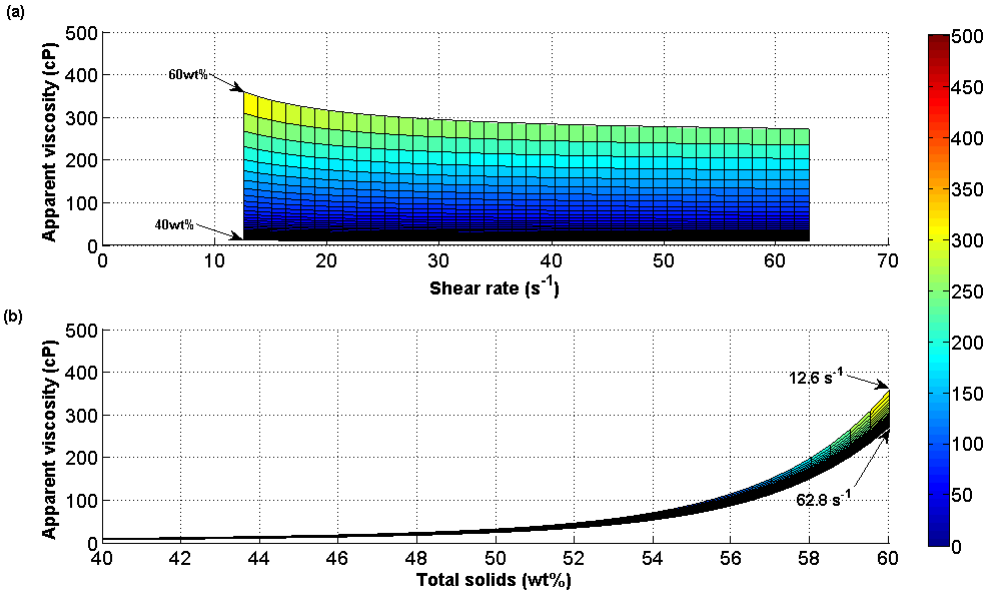

Figure 3.66(a) Shear rate dependency on apparent viscosity of medium-heat treated skim milk at various total solids (50°C), (b) Solids content dependency on apparent viscosity of medium-heat treated skim milk at various shear rates (50°C).

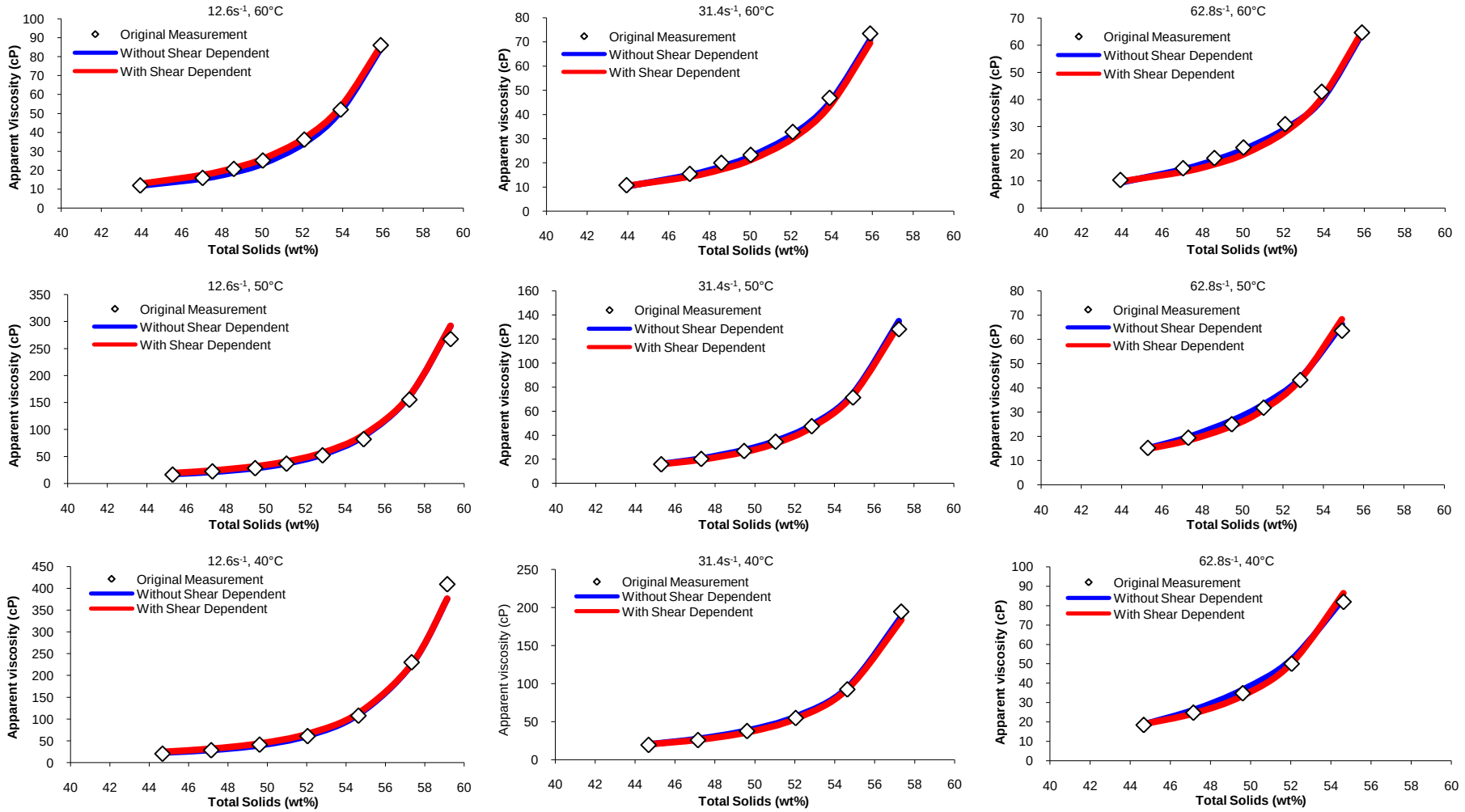

Figure 3.67 Fitting of fresh medium heat-treated skim milk viscosity model to raw data

3.8.4.3 Fresh low heat-treated skim milk

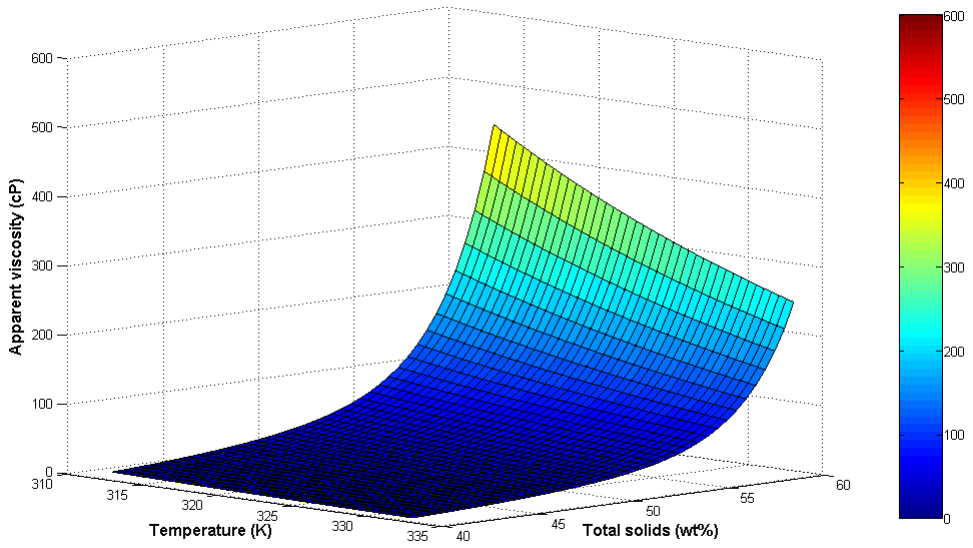

Figure 3.68 3D viscosity profile of low-heat treated skim milk with varying temperature and total solids (31.4s^{-1}).

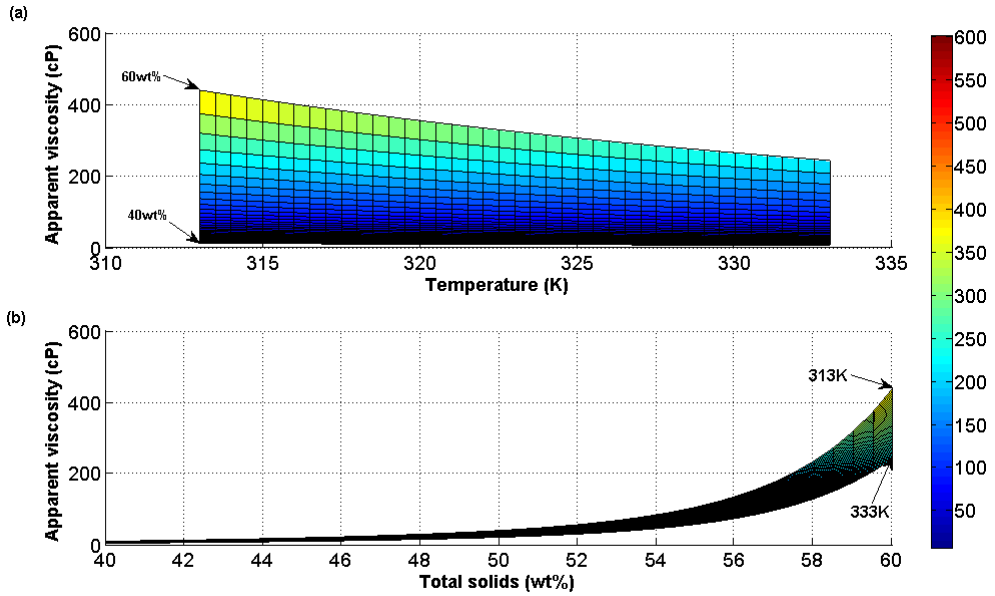

Figure 3.69(a) Temperature dependency on apparent viscosity of low-heat treated skim milk at various total solids (31.4 s^{-1}), (b) Solids content dependency on apparent viscosity of low-heat treated skim milk at various temperatures (31.4 s^{-1}).

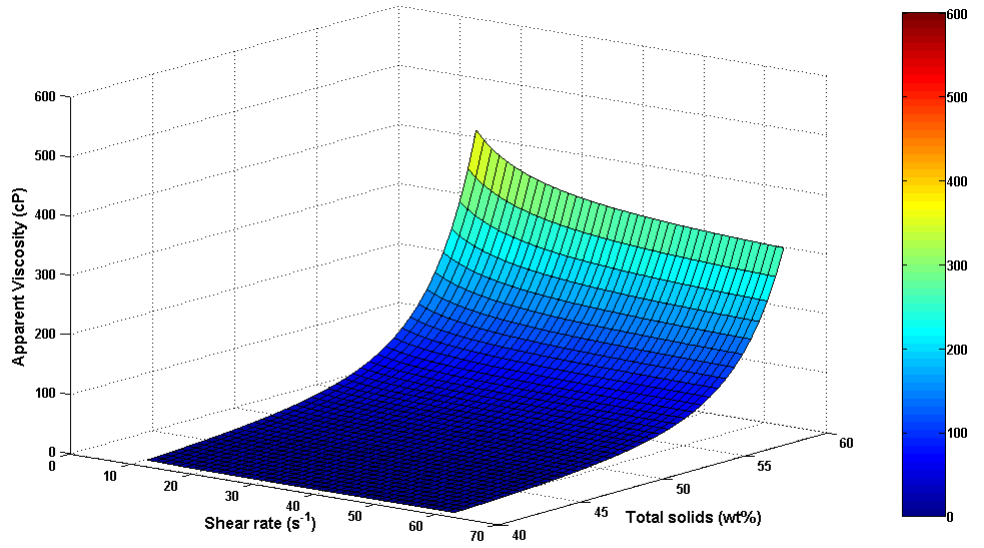

Figure 3.70 3D viscosity profile of low heat skim milk with varying shear rate and total solids (50°C).

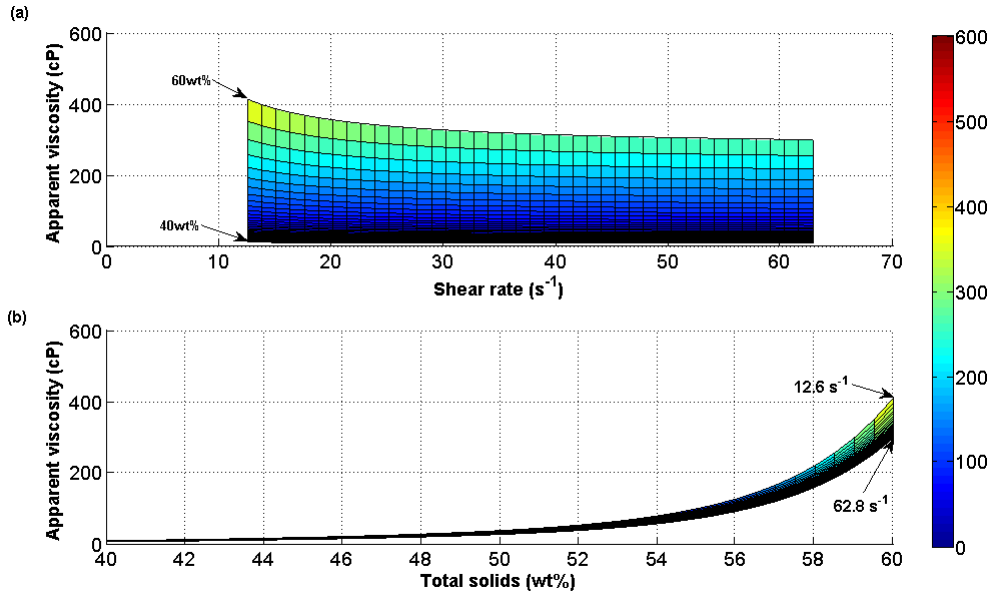

Figure 3.71(a) Shear rate dependency on apparent viscosity of low-heat treated skim milk at various total solids (50°C), (b) Solids content dependency on apparent viscosity of low-heat treated skim milk at various Shear rates (50°C).

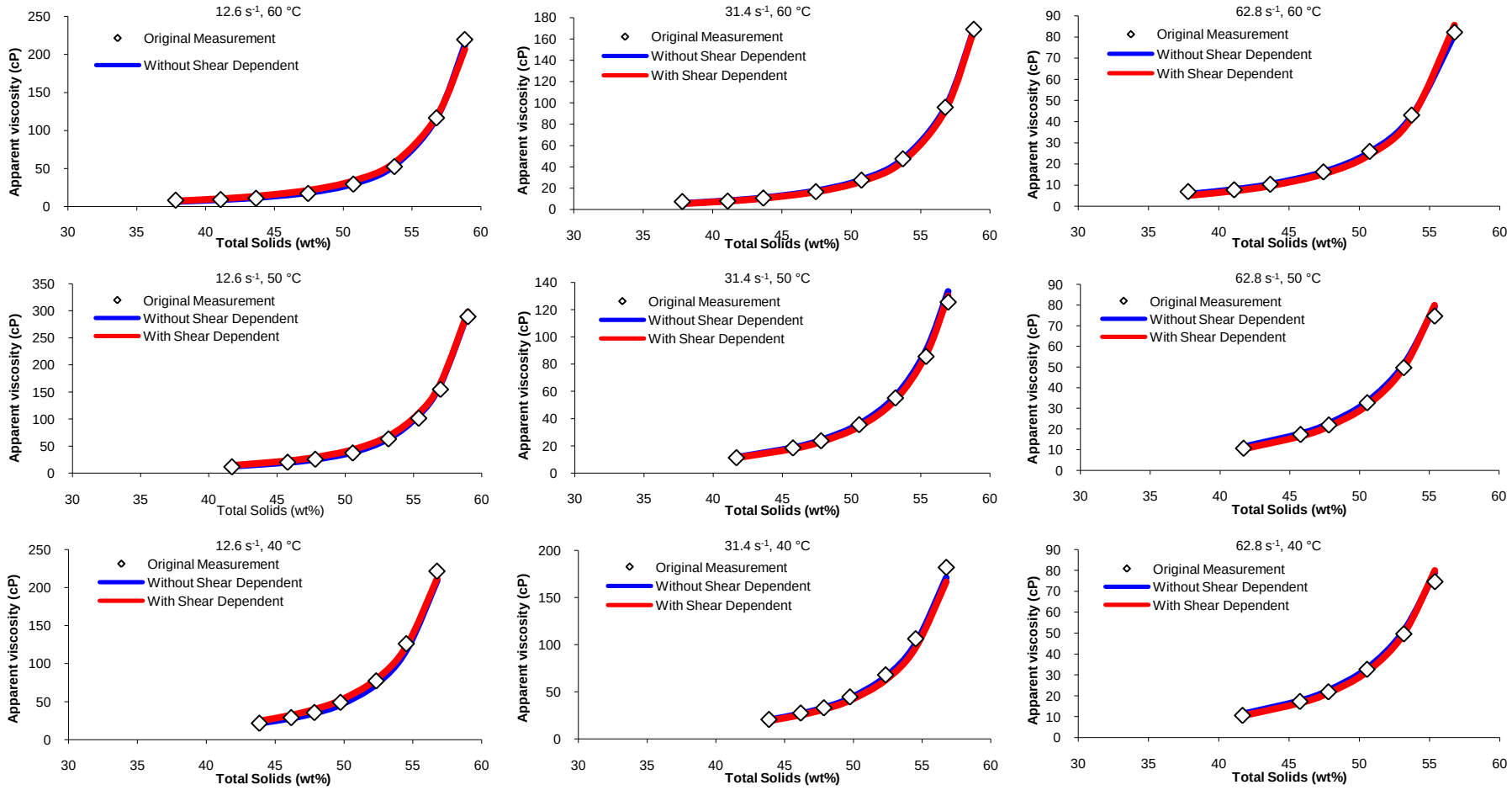

Figure 3.72 Fitting of fresh low heat-treated skim milk viscosity model to raw data

3.8.5 Comparison of milk viscosity

In this section, the comparisons of the viscosities of the different skim milk types were based on the model described in Section 3.8.3. The purposes are to find out if there is any significant differences between reconstituted and fresh skim milk and the influence of the following factors: total solids, temperature and shear rate of viscosity measurement.

In Figure 3.73, the differences between the viscosity profiles of reconstituted and fresh skim milk are apparent. Up to 43wt%, both reconstituted and fresh skim milk exhibits almost the same viscosity profile. However, beyond 43wt%, the viscosity profile of reconstituted skim milk begins to deviate from the fresh skim milk and rose rapidly.

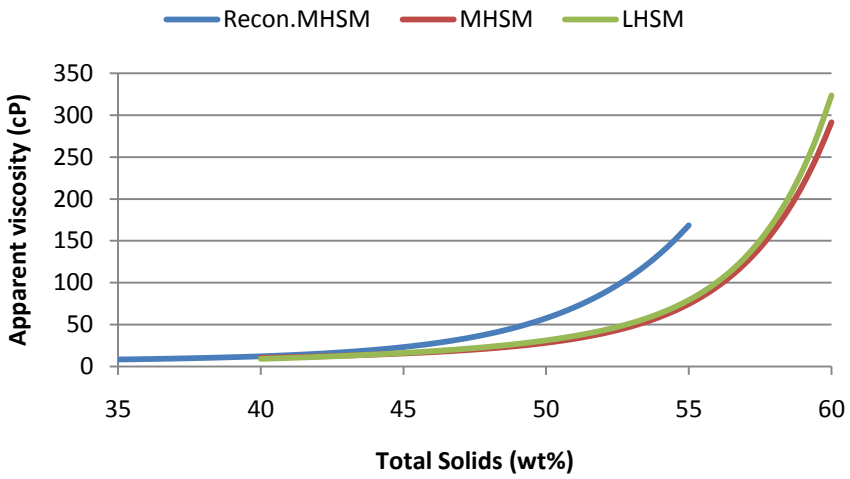

Figure 3.73 Viscosity profile at various total solids (50°C, 31.4s^{-1})

At 45wt%, the viscosity of reconstituted skim milk was almost 1.5 times of fresh skim milk (both medium and low heat-treated), with a viscosity measurement of just over 23cP. When the solids content reached 50wt%, the viscosities of all milks have doubled. This widens the viscosity gap between the reconstituted and fresh skim milk even further. The viscosity of all milk almost tripled when the solid content increased from 50 to 55wt%. On the other hand, there is no significant difference in viscosity between medium and low heat-treated skim milk as their ratio remains close to 1:1 throughout the evaporation process.

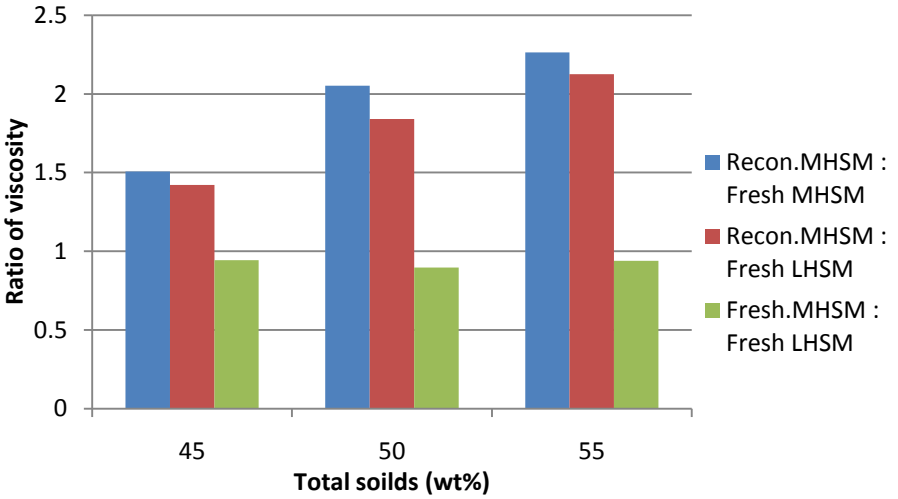

Figure 3.74 Comparison of viscosity at various solids content (50°C, 31.4s^{-1})

Although the reconstituted skim milk has higher viscosity compared with fresh skim milk, its viscosity is also more sensitive to temperature changes as shown in Figure 3.75.

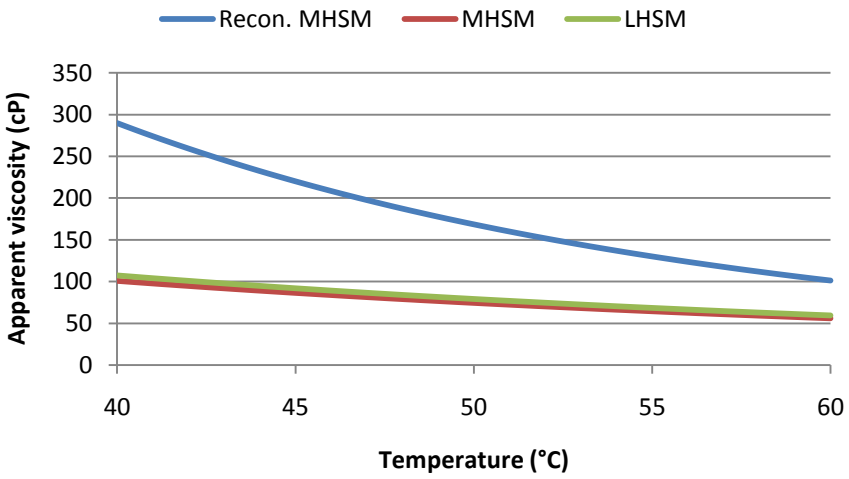

Figure 3.75 Viscosity profile at various temperature (55wt%, 31.4s^{-1})

On average, the viscosity of reconstituted skim milk reduces by 22-24% for every 5 °C rise within the temperature range tested. Conversely, the viscosity of fresh skim milks only reduces by 14% for every 5 °C rise.

Besides being more sensitive to temperature changes, reconstituted skim milk is also more responsive to the shear rate used for viscosity measurement. Within the range of shear rate tested, the viscosity of reconstituted skim reduced by 60 cP whereas fresh skim milk by 20-25 cP.

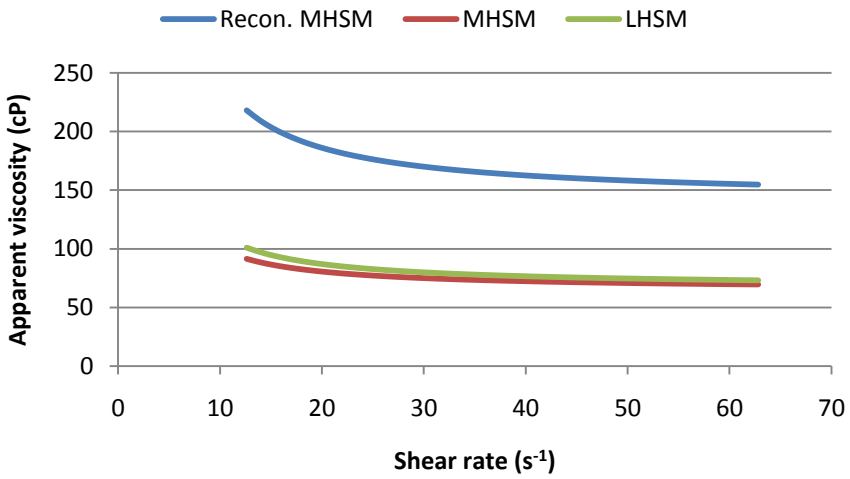

Figure 3.76 Viscosity profile at various shear rate (55wt%, 50°C)

Also, the influence of shear rate on viscosity reduction becomes more gradual as the shear rate increase as shown in Figure 3.77. There would be a point where any raise in shear rate would not further reduce the viscosity and this is known as infinite shear viscosity as mentioned in Section 3.8.2.3.

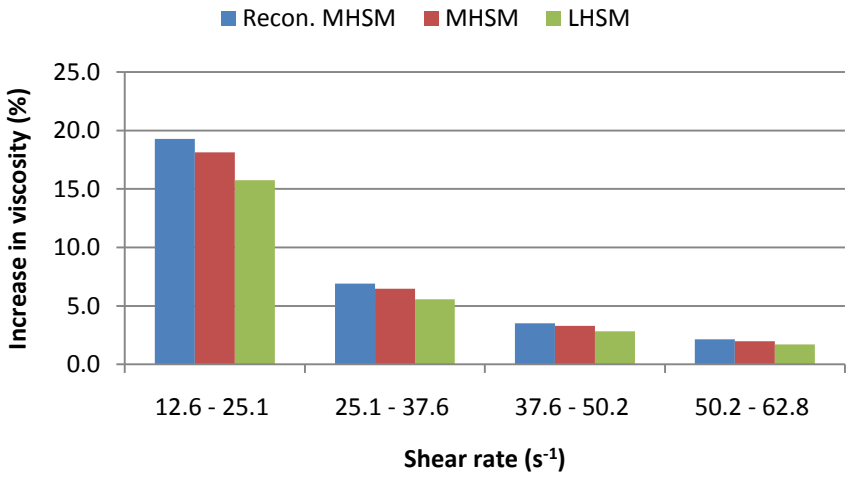

Figure 3.77 Percentage increase in viscosity with shear rate (55wt%, 50°C)

Note that the comparisons given above were based on three most important factors i.e. total solids, temperature and shear rate. Similar trend can also be observed with other condition but the degree of influence would be different.

3.9 Conclusions

In this chapter, the focus was on the establishment of a robust and practical viscosity models for skim milk in relation to solids content, temperature and shear rate. A steam-heated pilot evaporator was designed and fabricated with the purpose of generating industrially relevance dairy concentrates for viscosity studies. The design considerations and engineering requirements for the pilot evaporator were also described in detail in this chapter. The design of steam-heated pilot evaporator was more straightforward, compared to the commercial evaporators due to it is a single effect, single tube pilot evaporator. This simple design has yielded a highly effective pilot tool to produce milk concentrate with consistent viscosity profiles. Furthermore, this pilot evaporator operates in batch, yet, the time taken to concentrate a substantial amount of milk to high solids content (55 wt%) was still possible, e.g. to increase the total solids content of a batch of 15L of 30wt% milk concentrate at 60°C to 55wt% took about 1.5 hours.

The accuracy of the measurement of total solids (TS) has been investigated thoroughly by comparing the two different methods and the influence of the drying duration was tested. The viscosity measurement protocol was also proven to be highly repeatable. Generally, the Australia Standard AS 2300.1.1 method produces a more accurate total solids measurement, especially with solids content beyond 40 wt%.

Preliminary experimental results on the viscosity profiles of different types of milks were presented in this chapter. Milk viscosities measured from 40 – 55wt% total solids were compared and the general trend of all test subjects is an exponential increase in viscosity as total solids content increases. A model was fitted to all type of milk with good accuracy ($R^2 > 0.99$).

$$\mu(X,T) = K \cdot exp\left(\frac{C}{\dot{\gamma}}\right) \cdot exp\left(\frac{E_w + \Delta E}{RT}\right) \cdot [a \cdot exp(b \cdot X) + c \cdot exp(d \cdot X)]$$

It was observed that there is no significant difference in viscosity profiles at 60°C among the types of milk tested except for market fresh skim milk. At 50wt %, the

viscosity for market fresh skim milk can be up to twice as much as the rest of the milk samples.

A general mathematical viscosity models of skim milk, formulated from detail measurement of skim milk viscosities at various solids contents, temperatures and shear rates, was found to fit the experimental data well ($R^2 > 0.97$). Moreover, the influence of the above variables and the differences in viscosity profile between the reconstituted and fresh skim milk was also illustrated using the model calculations. In general, the viscosity of reconstituted skim milk remains similar to the fresh milk up to about 43wt%. After that, the viscosity of reconstituted skim milk reaches twice as high as fresh skim milk. The influences of temperature and shear rate become increasingly significant on the viscosity measurement with rising solids content.

3.10 Nomenclature

$A, Ai, B, Bi, C, Ci, D, K$ a, b, c, n, m	Model constants	-
$A_i and\ A_0$	Inner and outer surface area of the tube	m^2
A_s	Total solids measured by Australian standard	wt%
c_i	Volume concentration of the components in the product	m^3kg^{-1}
DM_{conc}	Dry matter content (concentrate)	wt%
DM_{milk}	Dry matter content (milk)	wt%
E_a	Activation energy	$J.mol^{-1}$
f	Frequency of oscillation	Hz
h	Height of viscosity measurement cylinder	m
IDF_s	Total solids measured by the IDF standard	wt%
M_{liquid}	Mass of liquid	kg
M_{tube}	Mass of tube	kg
MC	Moisture content of powder	wt%
m_0	Mass of the dish	g

m_1	Mass of the dish with test portion	g
m_2	Mass of dish with dried test portion	g
$\mathrm{m_w}$	Mass of distilled water	g
$\mathrm{m_p}$	Mass of powder	g
R	Molar gas constant	$J.mol^{-1}\ K^{-1}$
R_i	Radius of viscosity measurement inner cylinder	m
R_0	Radius of viscosity measurement outer cylinder	m
r	Radius	m
$\mathrm{m_s}$	Final mass of solution	g
TS	Total Solids	wt%
t	Period of frequency	s
V	Volume of liquid in tube	m^3
V_i	Voluminosity of component i	$m^3.kg^{-1}$
X, s	Total solids of milk	wt%
$\dot{\gamma}$	Shear rate	s^{-1}
η	Viscosity	Pa.s
η_a	Apparent viscosity	Pa.s
η_{ref}	Viscosity of reference medium	Pa.s
η_{water}	Viscosity of water	Pa.s
$\eta_{water+salts}$	Viscosity of water and milk salt solution	Pa.s
$\eta_{water+5\%lacto}$	Viscosity of water and 5% lactose solution	Pa.s
η_0	Viscosity at low shear rate	Pa.s
η_∞	Viscosity at high shear rate	Pa.s
ρ_L	Liquid density	$kg.m^{-3}$
ϕ	Sum of the volume fractions of all dispersed particles	-
ϕ_c	Volume fraction of casein	-
ϕ_{dw}	Volume fraction of denatured whey protein	-
ϕ_f	Volume fraction of fat	-

ϕ_l	Volume fraction of lactose	-
ϕ_{max}	Maximum sum of volume fractions of all dispersed particles	-
ϕ_{nw}	Volume fraction of native whey protein	-
ϕ_w	Volume fraction of whey protein	-
ϕ^*	Volume fraction of all component at critical concentration	-
τ	Torque	Nm
ν	Kinematic viscosity	10^{-6} m^2 s^{-1}
ω_i	Angular frequency of inner cylinder	Rad.s^{-1}
ω_0	Angular frequency of outer cylinder	Rad.s^{-1}
Δ	Gap between the cylinders	m

3.11 References

(2003).Cannon viscosity & flash point standards. 6 State College, Pennsylvania: Cannon Instrument Company.

Aguilera, J. M. &Stanley, D. W. (1999).Fundatmentals of Structing: Polyme, Colloid, and Materials Science. In *Microstructural Principles of Food Processing and Engineering*, 93-154 Gaithersburg, Maryland: An Aspen Publishers, Inc.

Australia, S. (1988).General methods and principles - Determination of total solids and moisture. Vol. AS 2300.1.1Australia: Standards Association of Australia.

Barnes, H. A., Hutton, J. F. &Walters, K. (1989). *Introduction to Rheology.* Amsterdam: Elsevier.

Baucke, A. G. &Sanderson, W. B. (1970).New Zealand Dairy Research Institute Annual Report. 44.

Bienvenue, A., Jimenez-Flores, R. &Singh, H. (2003a). Rheological Properties of Concentrated Skim Milk: Importance of Soluble Minerals in the Changes in Viscosity During Storage. *J. Dairy Sci.* 86: 3813 - 3821.

Bienvenue, A., Jimenez-Flores, R. &Singh, H. (2003b). Rheological properties of concentrated skim milk: Influence of heat treatment and genetic variants on the changes in viscosity during storage. *J. Agric. Food Chem* 51: 7.

Bloore, C. G. &Boag, J. F. (1981). Some Factors affecting the viscosity of concentrated skim milk. *New Zealand Journal of Dairy Science and Technology* 16(12): 143.

Buckingham, J. H. (1978). Kinematic viscosities of New Zealand skim milk. *J. Dairy Res.* 45: 25-35.

Bylund, G. (1995). *Dairy Processing Handbook.* Lund: Tetra Pak Processing Systems AB.

Carr, A. J., Southward, C. R. &Creamer, L. K. (2003).Protein Hydration and Viscosity of Dairy Fluid. In *Advanced Dairy Chemistry*, Vol. 1 Part B, 1289 (Eds P. F. Fox and P. L. McSweeney). New York: Kluwer Academic/Plenum Publishers.

Chang, Y. &Hartel, R. W. (1997). Flow properties of freeze-concentrated skim milk. *Journal of Food Engineering* 31: 375-386.

de Koning, P. J., de Wit, J. N. &Drisessen, F. M. (1992). Process conditions affecting age-thickening and gelation of sterilised canned evaporated milk. *Neth. Milk Dairy J.* 46: 3-18.

de Koning, P. J., Kaper, J., Rollema, H. S. &Drisessen, F. M. (1985). Age-thinning and gelation in concentrated and unconcentrated UHT-sterilised skim milk. *Neth. Milk Dairy J.* 39: 71-87.

De Wit, J. N. (1981). Structure and functional behaviour of whey protein. *Netherlands Milk and Dairy Journal* 35: 47-64.

Dobriyan, E. I. &Chekulaeva, L. V. (1982). *Izv. Vyssh. Ucheb. Zaved. Pishch. Tekhnol.* 6: 39.

Drahm, W. &BjØnnes, H. (2003). A Coriolis mass flowmeter with direct viscosity measurement. *IEE Computing & Control Engineering* 14(4): 42 - 43.

Eilers, H. (1941). Die Viskositat von Emulsionen hochviskoser Stoffe als Funktion der Konzentration. *Kolloid-Z* 97: 313.

Eilers, H., Saal, R. N. J. &van der Waaden, M. (1947). *Chemical and Physical Investigation on Dairy Products.* Amsterdam: Elsevier.

Fernandez-Martin, F. (1972). Influence of temperature and composition on some physical properties of milk and milk concentrates. II. Viscosity. *J. Dairy Res.* 39: 75.

Fox, P. F. &McSweeney, P. L. H. (1998). *Dairy Chemistry and Biochemistry.* Springer-Verlag.

Harwalker, V. R. (1992).Age gelation of sterilised milks. In *Advanced Dairy Chemistry -1: Proteins*, 691-734 (Ed P. F. Fox). London: Elsevier Applied Science Publishers.

Herceg, Z. &Lelas, V. (2005). The influence of temperature and solid matter content on the viscosity of whey protein concentrates and skim milk powder before and after tribomechanical treatment. *Journal of Food Engineering* 66(4): 433-438.

Holdsworth, S. D. (1971). Applicability of rheological models to the interpretation of flow and processing behaviour of fluid food products. *Journal of Texture Studies* 2: 393-418.

Horne, D. S. (1998). Casein Interactions: Casting Light on the Black Boxes, the Structure in Dairy Products. *International Dairy Journal* 8(3): 171-177.

IDF (1987).Milk, cream and evaporated milk. In *Determination of total solids content*Brussels, Belgium: IDF.

Incropera, F. P. &DeWitt, D. P. (Eds) (2002). *Fundamentals of heat and mass transfer.* Hoboken, NJ: John Wiley & Sons, Inc.

Jeurnink, T. J. M. &de Kruif, K. G. (1995). Calcium concentration in milk in relation to heat stability and fouling. *Netherlands Milk and Dairy Journal* 49: 151-165.

Kalotay, P. (1999). Density and viscosity monitoring systems using Coriolis flow meters. *ISA Transactions* 38: 303 - 310.

Kocak, H. R. &Zadow, J. G. (1985a). Age gelation of UHT whole milk as influenced by storage temperature. *Aust. J. Dairy Technol.* 40: 14-21.

Kyazze, G. &Starov, V. (2004). Viscosity of milk: Influence of Cluster Formation. *Colliod Journal* 66(3): 6.

Macosko, C. W. (1994). *Rheology:Priniciples, measurements and applications.* New York: VCH Publishers.

Malkin, A. Y. &Isayev, A. I. (2006).Liquids. In *Rheology: Concepts, Methods, & Applications*, 123-208 Toronto: ChemTec Publishing.

Mewis, J. &Macosko, C. W. (1994).Suspension rheology. In *Rheology: Principles, Measurements and Applications*, 425-474 (Ed C. W. Macosko). USA: Wiley-VCH, Inc.

Mooney, M. (1951). The viscosity of a concentrated suspension of spherical particles. *J.Colloid Sci.* 6: 162-170.

Newstead, D. F. (1973).Summary of Proceedings, Symposium on Spray Dried Milk Powders. 5 New Zealand Dairy Research Institute.

Pradipasena, P. &Rha, C. K. (1977). Pseudoplastic and rheopectic properties of glubular protein (β-lactoglobulin) solution. *Journal of Texture Studies* 8: 311-325.

Prentice, J. H. (1992). *Dairy Rheology: A Concise Guide.* VCH Publishers, Inc.

Rao, M. A. (1977). Rheology of Liquid Food - A Review. *Journal of Texture Studies* 8: 135-168.

Reddy, C. S. &Datta, A. K. (1994). Thermophysical Properties of Concentrated Reconstituted Milk during Processing. *J. Food Eng.* 21: 31-40.

Siedler, L. &Elke, M. (1949). *Milchwissenschaft* 4: 105.

Simuang, J., Chiewchan, N. &Tansakul, A. (2004). Effects of fat content and temperature on the apparent viscosity of coconut milk. *Journal of Food Engineering* 64(2): 193-197.

Snoeren, T. H. M., Damman, A. J. &Klok, H. J. (1982). The viscosity of skim-milk concentrates. *Neth. Milk Dairy J.* 36: 305-316.

Snoeren, T. H. M., Damman, A. J. &Klok, H. J. (1984).Effect of droplat size on the properties of spray-dried whole milk. In *Kyoto Int. Conf.*Kyoto.

Snoeren, T. H. M., van Riel, J. A. M. &Both, P. (1979). Proteolysis during the storage of UHT-sterilised whole milk. 1. Experiments with milk heated by the direct system for 4 seconds at 142˚C. *Neth. Milk Dairy J.* 33: 31-39.

Steiger, G. &Martens, R. (1986). Bulletin of IDF. (No 207): 10 - 40.

Tarassuk, N. P. &Tamsma, A. F. (1956). Milk Sterilisation: Control of gelation in evaporated milk. *J.Agr.Food Chem.* 4: 1033-1035.

Torssell, H., Sandberg, U. &Thureson, L. E. (1949).In *12th International Dairy Congress*, Vol. 2, 246 Stockholm.

Trinh, B., Trinh, K. T. &Haisman, D. (2007). Effect of total solids content and temperature on the rheological behaviour of reconstituted whole milk concentrates. *Journal of Dairy Research* 74(01): 116-123.

Tung, M. A. (1978). Rheology of protein dispersions. *Journal of Texture Studies* 9: 3 - 31.

Van Vliet, T. &Walstra, P. (1980). Relationship between viscosity and fat content of milk and cream. *Journal of Texture Studies* 11: 65-68.

Velez-Ruiz, J. F. &Barbosa-Canovas, G. V. (1997). Effects of concentration and temperature on the rheology of concentrated milk. *Transactions of the ASAE* 40(4): 1113-1118.

Velez-Ruiz, J. F. &Barbosa-Canovas, G. V. (1998a). Rheological properties of concentrated milk as a function of concentration, temperature and storage time *J. Food Eng.* 35: 177-190.

Velez-Ruiz, J. F. &Barbosa-Canovas, G. V. (1998b). Rheological Properties of Concentrated Milk as a Function of Concentration, Temperature and Storage Time. *Journal of Food Engineering* 35: 14.

Velez-Ruiz, J. F. &Barbosa-Canovas, G. V. (2000). Flow and Structural Characteristics of Concentrated Milk. *Journal of Texture Studies* 31: 315-333.

Walstra, P. (2003).Transport Phenomena. In *Physical Chemistry of Foods*(Ed P. Walstra). New York: Marcel Dekker, Inc.

Walstra, P. &Jenness, R. (1984). *Dairy Chemistry and Physics.* New York: John Wiley & Sons.

Walstra, P., Wouters, J. T. M. &Geurts, T. J. (2006).Concentrating Processes. In *Dairy Science and Technology*, 297 Boca Raton: CRC Press.

Walther, C. (1929). Erdol und Teers. No. 34.

Whitnah, C. H., Rutz, W. D. &Fryer, H. C. (1956). Some Physical Properties of Milk-Part III. Effects of Homogenisation Pressure on the Viscosity of Whole Milk. *Journal of Dairy Science* 39(11): 1500 - 1505.

Windhab, E. J. (1995).Rheology in Fodd Processing. In *Physiochemical Aspects of Food Processing*, 86 (Ed S. T. Beckett). Aspen Publishers, Inc.

Yanniotis, S., Skaltsi, S. &Karaburnioti, S. (2006). Effect of moisture content on the viscosity of honey at different temperatures. *Journal of Food Engineering* 72: 372-377.

CHAPTER FOUR:
HEAT AND MASS TRANSFER

4.0 HEAT AND MASS TRANSFER

In food processing industries, concentrating of fluid food products by evaporation has long been common. Even though there are many other means of concentrating liquids, evaporation is still the dominant technique used in food processing (Hartel, 1992). One of the reasons for its domination is the high thermal efficiency of evaporators, e.g. 90% in evaporators compared with 60% in dryers, thus, saving energy. Multi-effect evaporation, thermal vapour recompression and mechanical vapour recompression are some of the energy saving techniques employed today (Morison and Hartel, 2007). Evaporation is able to remove most of the water from liquid food, leaving behind concentrated products which can be used as they are or further processed, e.g. drying to form powders. (Saravacos and Kostaropoulos, 2002) The principle behind evaporation is relatively straight forward. Solvent in fluid food, water in most cases, is brought to its boiling point by external heating. Water is then evaporated and vapour escapes from the surface of the liquid (Pisecky, 1997a).

Some of the guidelines in optimising the evaporation process are as follow (Standiford, 1963):

- *Sufficient heat transfer*. The rate of heat transfer will govern the amount of time required by the evaporator to concentrate product to its desired concentration. Factors that affect the heat transfer are the size of heat transfer area, the design of evaporator and the physical properties of the food being concentrated.

- *Efficient vapour-liquid separation*. An evaporator saturated by the vapour it evaporates will not perform well due to the high vapour pressure within, thus hindering the evaporation process. Therefore the separation of vapour from the liquid is important to an efficient evaporator design.

- *Efficient energy use*. Heat and energy sources have to be fully utilised in all possible ways, especially when sustainability is part of an important practice

today. Over the years, several methods of using energy efficiently were invented. For instance, a multi-effect evaporator uses the vapour generated from one stage to heat another stage (see Section 4.1.4).

Most of the fluid food is susceptible, to some degree, to thermally induced changes during processing. Some of the negative effects include denaturation of protein, which induces precipitation and fouling of evaporators, chemical reactions such as vitamin degradation and browning of dairy products (Hartel, 1992).

Gray (1984) has developed ways of minimising the negative thermal reactions and they can be classified into three categories. Firstly, evaporation is conducted at low pressure, low temperature conditions. The reduced pressure will cause water to boil at lower temperature, thus resulting in less thermal destruction. Evaporation temperature of most of the fluid food products is usually kept below 70°C. The second design principle involves the reduction of high temperature exposure by fluid food. The purpose is to minimise the amount of time spent under conditions of high reaction rate (Thijssen, 1970). Last but not least, the maximum temperature experienced by the product has to be reduced and this can be done by minimising the overall temperature driving force. In common practice, low thermal driving forces (2-3 °C) are used in evaporating heat sensitive foods.

Due to the heat sensitive nature of milk, mainly the fear of proteins denaturation, evaporation of milk is always carried out in reduced pressure. Figure 4.1 shows the relationship between pressure and boiling temperature of pure water.

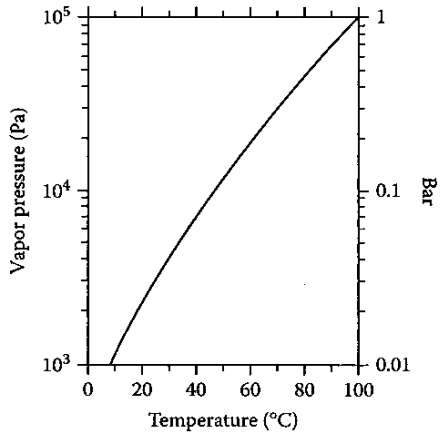

Figure 4.1 Vapour pressure of water as a function of temperature

Vapour pressure of solution can be altered by the solute molecules it contains, therefore affecting the equilibrium boiling point, known as boiling-point elevation. Boiling point elevation due to dissolved substances is not taken into account in Figure 4.1. Nevertheless, the elevation is rather small: for milk, 0.17°C and for evaporated skim milk, around 2°C (see Section 2.2.5) (Walstra *et al.*, 2006a). The normal evaporation temperature does not go beyond 67°C to prevent the denaturation of protein, especially β-lactoglobulin, which will induce fouling within the evaporators and the final product may not be fit for consumption.(Westergaard, 1994).

In this chapter, the main focus was on the energy transfer within a falling film evaporator, its process mechanisms and performance.

4.1.1 Basic principles of evaporators

There are several types of evaporator used in the food processing industries today. All of the evaporator works on the same basic principle as mentioned in above. However, when it comes down to individual design of each type of evaporator, they provide specific functionalities which suit the thermal requirements of different food processing operations. An evaporator normally consists of the following components:

1. *Preheater*. There are 4 main purposes of a preheater. Firstly, the milk is preheated to temperature in excess to the boiling point of the milk before it

enters the evaporator. This ensures the heat transfer surfaces within the evaporator is fully utilised and reduce energy wasted in the evaporator. Secondly, the preheat treatment also act as a pasteurisation process to control the bacteriological quality of the powder. Thirdly, temperature elevation altered some of the feed properties, such as the viscosity, that is beneficial to the operation of the evaporator. Lastly, with the right combination of preheated milk temperature and holding time, the desired degree of protein denaturation can be attained (Gray, 1981).

2. *Feed Distributor*. In industrial applications, it is rare to see an evaporator which consists of only one evaporation tube. Therefore, a feed distribution system is normally located just before the evaporation tubes. This will ensure the feed is fed equally between the tubes.

3. *Energy Source*. Along the tubes, there will be a energy source that provides the enthalpy of vaporisation to the product stream to remove solvent from the product. Usually steam or electricity is supplied.

4. *A method of heat transfer to boiling liquid*. The method of heat transfer is normally governed by the product requirements. A specific method of heat transfer gives unique characteristics such as short residence time, better heat transfer and capability to handle viscous fluids.

5. *Vapour/liquid Separator*. After the evaporation process, the vapour and the liquid stream has to be separated with minimal liquid carryover.

6. *Vacuum system*. With heat sensitive products, the lowering of boiling point by reducing the pressure during evaporation is usually favourable.

7. *Condenser*. The condenser helps to remove the energy from the vapour steam and is usually used as an energy source for another application. Also, the vacuum system operates better with the vapour condensed.

4.1.2 Falling film evaporator

Today, majority of the evaporator used in the dairy industries are falling film evaporator. Long tube falling film evaporator is one of the most popular evaporator used in concentrating heat sensitive products owning to its high heat transfer rate, short residence time and low pressure drop. This type of evaporator consists of a bundle of vertical tubes where food fluid flows along the inner tube walls while steam heats it up from outside. The diameter of the tube ranged from 25-60mm and 4-18m long. Fluid is pumped through a preheater before reaching the distributor (Figure 4.2) where the fluid is distributed evenly, forming a film of fluid inside each tube. The water from the falling film within each tube will be heated up by the condensing steam outside the tubes and evaporates away. The concentrate is drained or pumped away based on it viscosity and the vapour is then separated in a condenser at the bottom of the evaporator (see 4.1.2.1).

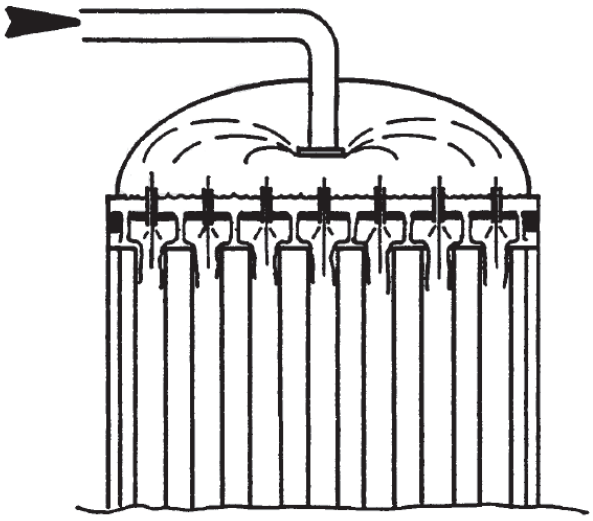

Figure 4.2 Fluid distributor (Westergaard)

4.1.2.1 Single effect evaporator

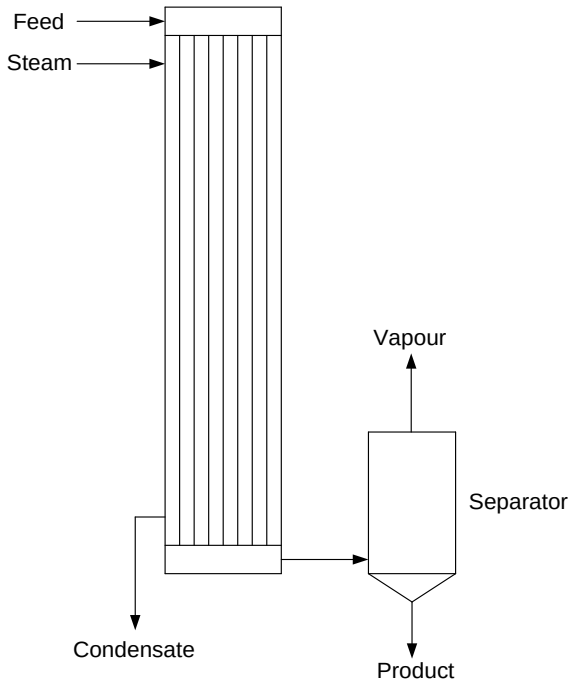

Figure 4.3 Single effect falling film evaporator

A schematic diagram of a simple single effect-effect evaporator is shown in Figure 4.3. The feed stream enters the evaporator from the top of the column into the distributor at close to the boiling point of the liquid dictated by the evaporator pressure. The liquid is concentrated to some extent before leaving the evaporator from the bottom of the separator and the vapour escapes from the top of the separator. Steam at reduced pressure (depending on the desired vapour temperature required) enters the steam chest and condenses along the tube as heat energy is transferred to the tube and ultimately to the fluid film within. The condensate is then removed from the bottom of the steam chest.

The overall and component mass balance,, for a single effect evaporator is relatively straight forward as shown below, respectively.

$$F = V + P \tag{4.1}$$

$$x_F F = x_p P \tag{4.2}$$

where *F*, *V* and *P* are the mass flowrate of feed, vapour and product respectively; x_F and x_P are the solid mass fraction in the feed and product respectively. The enthalpy balance for the evaporator can be written as:

$$Fh_f + SH_s = VH_v + Ph_p + Ch_c \tag{4.3}$$

where h_f, H_s, H_v, h_p and h_c represent the enthalpies of feed, steam, vapours, product and condensate, respectively. S and C are the mass flow rate of steam and condensate. The efficiency of the evaporation process is commonly quantified by steam economy (SE) which can be calculated by the following equation:

$$SE = \frac{m_{evap}}{m_{steam}} \tag{4.4}$$

where m_{evap} is mass of water evaporated and m_{steam} is mass of steam utilised

Table 4.1 Steam economy comparison among different evaporator configurations (Kessler, 1986; Chen and Hernandez, 1997)

Evaporation System	SE, kg water / kg steam
Single Effect	0.90 – 0.98
Double Effect	1.70 – 2.00
Triple Effect	2.40 – 2.80
Six Effect	4.60 – 4.90
Triple Effect with Thermocompressor	4.00 – 8.00
Mechanical Vapour Recompression	10 - 30

Above all**,** the most important principle for any heat exchange equipment is the rate of heat transfer it is capable of transferring to the product and it is given by a general equation.

$$q = UA\Delta T \tag{4.5}$$

where *U* = overall heat transfer coefficient (W $m^{-2}K^{-1}$), *A* = area of heating surface (m^2) and *ΔT* = temperature difference between the heating medium and the boiling medium (°C or K).

Heat transfer coefficient (HTC) has been an important factor evaporator designer has to keep firmly in mind. The overall heat transfer coefficient of an evaporator is determined by the design of the evaporator, the material of construction, operation conditions (e.g. flow rate, temperature, etc.), heating source and the product being processed. Experiments carried out by Jebson and Chen (1996) have reported a number of heat transfer coefficient for skim milk, where the solids content is unknown, ranged from 190 to 3200 $W.m^{-2}K^{-1}$ from a falling film evaporator.

The overall heat transfer coefficient can be calculated on a theoretical basis; however, such calculations only provide rough estimates as the fouling resistance on the heating surface cannot be measured accurately. Nonetheless, the analysis of thermal resistances within an evaporation system is still important, as reduction in any of the thermal resistances enhances the overall heat transfer coefficient as shown in Equation (4.6) (Saravacos and Kostaropoulos, 2002).

$$\frac{1}{U} = \frac{1}{h_s} + \frac{x}{k_w} + \frac{1}{h_i} + r_f \tag{4.6}$$

where h_s = heat transfer coefficient at the heating (steam) side (W $m^{-2}K^{-1}$), h_i = heat transfer coefficient of evaporation side (W $m^{-2}K^{-1}$), x = thickness of wall (m), k_w = thermal conductivity of wall (W $m^{-2}K^{-1}$) and r_f= resistance due to fouling on

the heat transfer surface. Fouling resistance can be assumed to be contributed by only the evaporation side since clean steam and clean metallic surfaces are used in food evaporators. For evaporators with small diameter tubes (e.g. less than 50mm), correction of the thermal resistances of the wall and the evaporation side have to be made by the ratio of outside to inside diameter. Therefore, Equation (4.7) can be rewritten as (Hartel, 1992):

$$\frac{1}{U} = \frac{1}{h_s} + \frac{xA_0}{k_w A_m} + \frac{A_o}{h_i A_i} + r_f \qquad (4.7)$$

where A_i and A_o are the inner and outer surface area of the tube and A_m = log mean area for heat transfer.

4.1.3 Heat transfer

4.1.3.1 Heating medium

In most of the evaporators, the common heating medium used has been steam. There are two main types of condensation, film-type condensation and dropwise condensation.

In film-type condensation, vapour condenses on a surface like a vertical tube whose surface temperature is lower than the saturation temperature. Film of condensate is formed on the surface and flows over the surface by gravity force. A resistance of heat transfer is then created by the film of liquid between the vapour and the surface. Equations of heat transfer coefficient on the condensation side of the tube are empirical in nature. The flow of condensate is assumed to be laminar and the thickness of the film is zero on the top of the wall or tube with increasing thickness as the flow proceeds downward due to condensation. The coefficient changes as the quantity of condensate flowing down the tube increases, hence average value are often used. Nusselt assumed that the heat transfer from the condensing vapour (T_{sat} K) passes through the liquid film and the wall (T_w K) by conduction (Holman, 1976; Welty *et al.*, 1984). Based on the assumptions mentioned above, an

expression can be obtained for the average heat-transfer coefficient over the entire heat transfer surface on the steam side.

$$h_o = 0.943\left[\frac{\rho_l(\rho_l-\rho_v)gh_{fg}L^3}{\eta_L L(T_{sat}-T_w)}\right]^{1/4} \tag{4.8}$$

However, experimental data show that the heat transfer coefficient of laminar film condensation is 20% above Equation (4.8). Therefore, the final recommended expression is (McAdams, 1954)

$$Nu = \frac{h_o L}{k_L} = 1.13\left[\frac{\rho_l(\rho_l-\rho_v)gh_{fg}L^3}{\eta_L k_L(T_{sat}-T_w)}\right]^{1/4} \tag{4.9}$$

where ρ_l= liquid density (kg m^{-3}), ρ_v= vapour density (kg m^{-3}), g = 9.8066m.s^{-2}, L = length of tube (m), η_L= Liquid viscosity (Pa.s), μ_v= vapour viscosity (Pa.s), k_L= liquid thermal conductivity (W m^{-1} K^{-1}) and h_{fg} =Latent heat (J kg^{-1})

There is another equation proposed by Chen et. al.(1987) which calculates the average film coefficient on a vertical tube in a stagnant environment

$$h = k_l\left(\frac{\rho_l^2 g}{\mu_l^2}\right)^{1/3}\left[Re_L^{-0.44} + 5.82\times10^{-6}Re_L^{0.8}Pr_l^{1/3}\right]^{1/2} \tag{4.10}$$

Subscript lower case l is the condensate properties, while upper case L is the total condensation at the base of the tube.

The Reynolds number, Re and the Prandtl number, Pr for film heat transfer is defined as

$$Re = \frac{4\Gamma}{\mu} \tag{4.11}$$

$$Pr = \frac{C_p \mu}{k} \tag{4.12}$$

where Γ is the tube wetting rate (kg $m^{-1}s^{-1}$), μ is viscosity (Pa.s), C_p is the heat capacity (J $kg^{-1}K^{-1}$), k is thermal conductivity (W $m^{-1}K^{-1}$).

The tube wetting rate, Γ is the flow rate divided by the appropriate circumference which can be calculated from the evaporation flow rate from the calandria.

$$\Gamma = \frac{\dot{m}_{\text{feed}}}{\pi D_i n_{tubes}} \tag{4.13}$$

where $\dot{m}_{\text{feed}}$is mass flow rate of feed, D_i is the inner diameter of the evaporation tube (m) and n_{tubes} is the number of evaporation tubes.

A typical value of outside film coefficient for food evaporator is found to range from 7000 to 8000 $Wm^{-2}K^{-1}$.

In dropwise condensation, small drops of condensate form on the surface, they grow and coalesce and the liquid flows from the surface. In this type of condensation, large areas of the tube are in direct contact with the vapour which results in very high heat transfer rates at the bare areas. The average heat transfer coefficient from a dropwise condensation can be as high as 110 000 $Wm^{-2}K^{-1}$, which is 5 – 10 times higher than that of film condensation. In heat exchanger applications where dropwise condensation is promoted, the resistance for condensation is significantly lower than that of other thermal resistances; hence, there is no need for a reliable correlation for this kind of condensation. For steam condensation on well promoted copper surfaces, heat transfer coefficient of dropwise condensation can be derived from the following equations (Incropera and DeWitt, 2002a).

$$\bar{h}_{dc} = 51104 + 2044T_{sat} \qquad (\text{W m}^{-2}\text{K}^{-1}) \tag{4.14}$$

for T_{sat} (˚C) is between 22˚C and 100˚C

$$\bar{h}_{dc} = 255{,}510 \qquad (\text{W m}^{-2}\text{K}^{-1}) \tag{4.15}$$

for T_{sat} (˚C) is greater than 100˚C

4.1.3.2 Heating surface

Resistance created by the heating surface material poses the second part of the overall resistance as shown in Equation (4.6). Given that the surface is normally made of metal like stainless steel, which has known physical properties and thickness, computing the wall resistance is relatively straightforward. For instance, the thermal conductivity of 316 stainless steel is 16.3 $\text{Wm}^{-1}\text{K}^{-1}$ and the wall thickness is at around 1mm. With the thickness, thermal conductivity and diameter of the tube known, the wall resistance can be calculated using

$$R_{wall} = \frac{xA_0}{k_w A_m} \tag{4.16}$$

where x is wall thickness (m), A_0 is the outer surface area of tube, A_m is the mean surface area of tube (m) and k_w is the thermal conductivity of tube wall ($\text{W m}^{-1}\text{K}^{-1}$)

4.1.3.3 Product

The flowing product film within the tube possibly poses the most complex resistance to heat transfer and the convective heat transfer coefficient is difficult to determine. To great extent, the rate of heat transfer relies on the product flow conditions within the tubes of a falling film evaporator. Several other factors such as the rate and type of boiling taking place, the film thickness, the velocity of fluid flow along the wall and the product physical properties also contribute to the

determination the overall heat transfer coefficient. During the course of evaporation, many of these factors changes. For instance, as the product concentrates along the length of the tube, the viscosity of the product fluid changes. At high concentration, milk or milk products become so viscous that they have trouble flowing within the tubes, thus the tubes tend to foul or block more easily. Ultimately, heat transfer coefficients will be affected.

The common equation used for predicting product side convective coefficients, h_i, has been given as (Schwartzberg, 1989)

$$h_i = C \cdot Re^n \cdot Pr^m \qquad (\text{W.m}^{-2}\text{K}^{-1}) \tag{4.17}$$

For laminar flow (Re < 2100), Angelletti and Moresi (Angelletti and Moresi, 1983) proposed that C = 1.1, n = -0.333 and m = 0 while Chun and Seban (Chun and Seban, 1971) suggested that C = 0.606, n = -0.22 and m = 0. . For turbulent flow (Re > 2100), Chun and Seban (Chun and Seban, 1971) proposed that C = 0.0038, n = 0.4 and m = 0.65.

For film heat transfer, some modification has to be done on Equation (4.17) by incorporating the average film thickness into the equation as shown below. (Chun and Seban, 1971)

$$h_i = C \cdot k \left(\frac{\rho^2 g}{\mu^2}\right)^{1/3} Re^n \cdot Pr^m \qquad (\text{W.m}^{-2}\text{K}^{-1}) \tag{4.18}$$

On the other hand, product side convection correlations vary widely among each industry. Therefore, film coefficient correlation of each product has to be determined empirically. The following correlation is given by Hall and Hedrick (1971) for dairy products.

$$Nu = \frac{h_i L}{k_L} = 0.11(Re^a)^{0.686} Pr^{0.4} \tag{4.19}$$

where a = 0.961 for whole milk and 0.964 for skim milk, h_i is the heat transfer coefficient of evaporative side (W $m^{-2}K^{-1}$), L is the characteristic length (m) and k_L is the thermal conductivity of liquid (W $m^{-1}K^{-1}$).

4.1.3.4 Overall heat transfer

For overall heat transfer coefficient in a falling film evaporator, Bouman et al. (Bouman *et al.*, 1993) has derived the equations for whole and skim milk.

For whole milk,

$$h_i = 6.05 \cdot q''^{0.47} \cdot \Gamma^{0.26} \cdot \mu^{-0.44} \qquad (\text{W.m}^{-2}\text{K}^{-1}) \tag{4.20}$$

For skim milk,

$$h_i = 0.77 \cdot q^{0.69} \cdot \mu^{-0.41} \qquad (\text{W.m}^{-2}\text{K}^{-1}) \tag{4.21}$$

where q" is the heat flux (W.m^{-2}), Γ is the wetting rate (kg.m^{-1} s^{-1}) and μ is the viscosity (kg.m^{-1} s^{-1}). However, Equation (4.20) and (4.21) gives prediction of up to five times other estimates. Hence, measurements needs to be done on the evaporator (e.g. measuring the condensate produced) to obtain a reasonable accurate overall heat transfer coefficient.

4.1.4 Multi-effect evaporation

Multi-effect evaporators are widely used in food processing industries due to its efficient use to of energy (steam). A multi-effect evaporator system is somewhat

similar to a few single effect evaporators combining together in series.

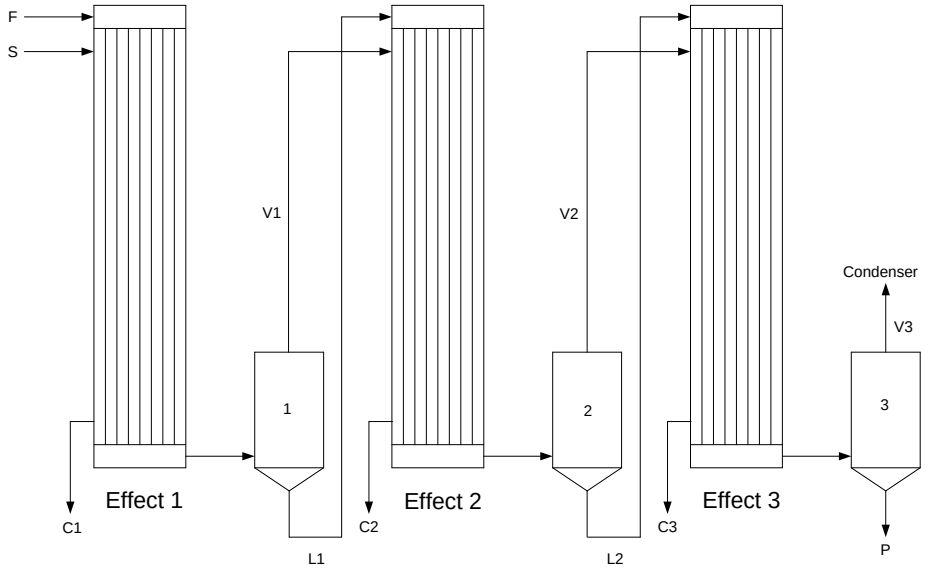

Figure 4.4 Schematic diagram of a three-effect, forward-feed evaporator. F, feed; L, liquid; V, vapour; P, product; S, steam; C, condensate

The principle to which multi-effect evaporators operate on is mainly based on the fact that boiling temperature decreases with pressure. The vapour generated from one effect can be utilised to heat the next one as long as the next effect is operating at lower pressure than the previous one. Therefore, the operational pressure of subsequent evaporator effects must be reduced accordingly. The steam economy of various combinations of multi-effect evaporator is shown in Table 4.2**.** The temperature for the first effect should not be higher than 100˚C when concentrating heat sensitive food fluid (e.g. <70˚C for milk) and the last effect should not be lower than 40˚C in order to use water at room temperature in the condenser to cool the vapour. Generally, the last effects have the lowest rate of heat transfer owning to the fact that heat transfer rate reduces with temperature. Therefore, by increasing the resistance of these effects, temperature difference across effects can be lifted, resulting in increasing temperature and heat transfer rates in all prior effects (Minton, 1986a). Besides the limitation by the cooling water temperature in the condenser, the sharp increase in viscosity at lower temperature by concentrated fluid food poses a major constraint on the operating temperature of the last effect. At high viscosity, the evaporator is susceptible to fouling (see

Section 4.2) and lowers the heat transfer coefficient on the evaporation side (see Section 4.1.3) (Saravacos and Kostaropoulos, 2002).

As a guideline, the maximum numbers of effects (*N*) can be calculated by the following equation.(Saravacos and Kostaropoulos, 2002)

$$N = \frac{60}{\Delta T} \tag{4.22}$$

where ΔT = temperature difference in each effect (K).

Table 4.2 Heat of vapourisation of water and examples of energy requirement in some processes to remove water (Walstra *et al.*, 2006a)

	Energy required to evaporate 1kg of water (kJ)
Heat of vaporisation of water at 100˚C	2255
Heat of vaporisation of water at 40˚C	2405
Triple Effect Evaporation	~800
Six Effect Evaporation with TVR	~230
Single Effect Evaporation with MVR	~115
Rolling Drying	~2500
Spray Drying	~4500

4.1.5 Evaporation using vapour recompression

Steam economy of an evaporation system can be further improved by using thermocompressor to recompress vapours from evaporation unit which is then reused as a heating medium. Vapour recompression can be accomplished by one of the following two ways, thermal or mechanical compressors (Minton, 1986d; Saravacos and Kostaropoulos, 2002).

4.1.5.1 Thermal vapour (TVR)

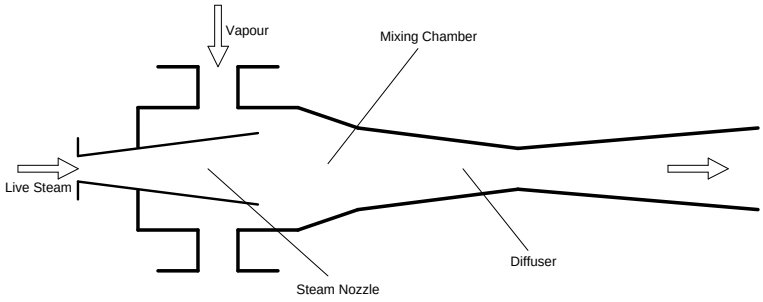

Figure 4.5 Thermocompressor (Pisecky, 1997a)

The principle to which a thermal compressor based upon is very similar to that of steam ejectors used for producing vacuum. A thermal compressor consists of three main parts: nozzle, mixing chamber and diffuser as shown in Figure 4.5. High pressure steam (about 7 bars) enters the nozzle section and creates suction when it expands in the mixing chamber. Vapour from the evaporator is sucked into the mixing chamber and both the vapour and live steam gets compressed along the diffuser before being discharged against the back pressure. The back pressure is determined by the operating pressure in the steam chest of the evaporator. The discharge from a thermocompressor carries vapour at higher temperature compared to the entering vapour and it is used as a heating medium for other effects. Steam economy of 4 to 8 can be achieved. As a general guideline, the temperature difference across the thermocompressor should be less than 15˚C. Thermal compressor is cheaper than the mechanical vapour compressor counterpart. Other advantages are their low maintenance costs, reliability, simplicity and occupy little space. The main disadvantages are their inflexibility to change the operating conditions and the need to have high pressure steam readily available. In processes where more than seven effects are used, mechanical vapour compression systems offer a better alternative than thermal compression evaporators and it is discussed below (Minton, 1986d; Hartel, 1992; Geankoplis, 1993; Saravacos and Kostaropoulos, 2002).

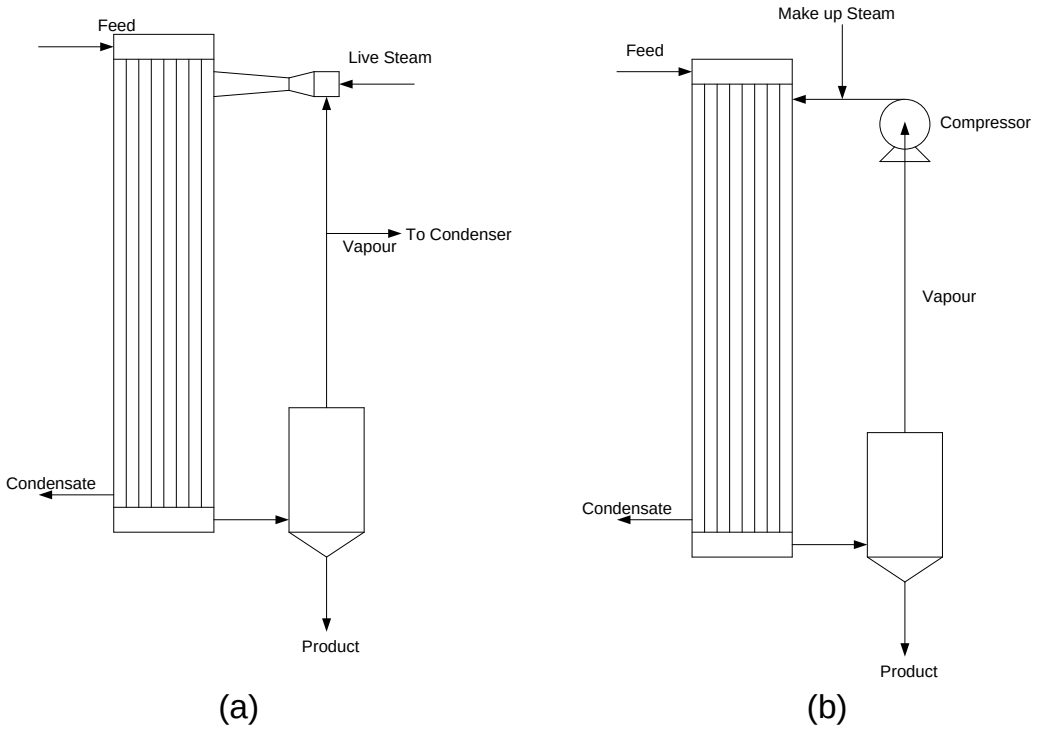

Figure 4.6 Vapour recompression evaporators. (a) Thermal; (b) Mechanical compressor (Saravacos and Kostaropoulos, 2002)

4.1.5.2 Mechanical vapour recompression (MVR)

In an evaporator working with a mechanical vapour recompression (MVR) system, the vapour from the steam channel of the evaporator does not enter a condenser but either a centrifugal or positive displacement compressor driven by an electric motor or steam as shown in Figure 4.6. However, MVR system requires a vacuum system to remove the non-condensable gases in order to establish and maintain the vacuum. Vapour is compressed mechanically to lift its saturation temperature above the boiling temperature of the solution to the desired net temperature difference. Small amount of heating steam is added to make up the condensate formed during vapour compression. The compressed vapour is then sent back to the steam chest and the cycle repeats. The low temperature difference (5 to 10˚C) to which vapour compression unit normally operates on requires large heat transfer areas. Therefore, the initial capital costs involved in these units are usually higher than multi-effect units due to the larger area and the relatively expensive compressor and drive unit. However, the high initial capital cost can be justified by

the lower energy costs in long run. MVR evaporators are more commonly used than TVR evaporators because of their high steam economy (greater than 10) and the lower operating cost, particularly when cheap electrical power is available (Zimmer, 1980; Minton, 1986c; Geankoplis, 1993; Saravacos and Kostaropoulos, 2002). MVR systems are well suited for falling film evaporators because of the low temperature difference the evaporators operate on and have very little entrained liquid which can pose major problems to the compressor (Meili and Stuecheli, 1987).

In milk powder manufacturing, it is desirable to remove as much water in the evaporation process as possible due to the superior energy efficiency compared to spray dryers. (Knipschildt and Andersen, 1994) In modern plants, skim milk and whole milk are concentrated to 48wt% and 52wt% respectively before they are sent to the spray dryer for further processing. (Bylund, 1995) However, the extent of evaporation by falling film evaporators is generally limited by the high viscosity of the concentrate. High viscosity retards the flow of the concentrate on the heating surface which results in higher minimum flow rate, Γ_{min}. (see Section 4.2.4) In a falling film evaporator, the viscosity of the concentrate should not exceed 100 mPa.s but at low temperature, highly concentrated milk (both whole and skim milk) would go beyond this limit. To counter this problem, the order to which the milk concentrate flow in the last two effects is reversed, milk at its highest concentration is being evaporated at a higher temperature (second to last effect), which results in lower viscosity. This is only possible when vapour recompression system is installed (Walstra *et al.*, 2006a). Besides the falling film evaporator, the operation of spray dryer is also influence by the viscosity of the concentrate. The average size of droplets from the atomizer within the dryer decreases with viscosity. The reduction in size enhances the heat transfer to the droplets and this enables the lowering of drying air temperature without compromising the specific moisture content of the powder. With gentler drying, the powder quality improves, especially the solubility (Knipschildt and Andersen, 1994). The viscosity of the concentrate is therefore an important parameter not restricted in the evaporating process but the subsequent drying processes as well.

4.2 Review of fouling within evaporator

One of the major ongoing problems which all of the thermal processing industries are facing is fouling. Heat exchanger fouling is a inevitable process where undesired deposit accumulates on the heat transfer surfaces (Bott, 1995). The formation of fouling deposits can have a number of effects such as increasing thermal resistance, impeding fluid flow (raising pressure drop), impairing safe operation of equipment and assisting or initiating corrosion (Melo *et al.*, 1987). Besides the wastage in energy consumption, fouling, in some cases, is also a potential source of biological contamination to products especially in food related industries (Palen, 1986; Melo *et al.*, 1987). The cost of fouling can be categorised into two sections, capital cost and operating cost. Capital cost includes over-sizing of heat exchanger to compensate for the loss of thermal efficiency and the usage of exotic and expensive materials of construction to minimise fouling. Operating cost comprises of increasing energy input to balance the escalating pressure drop across the heat exchanger, the loss of production and cleaning of exchangers (Garett *et al.*, 1985; Melo *et al.*, 1987; Bott, 1995). It is estimated that fouling is responsible for US$20 – 30 million per annum of extra cost to run a refinery processing half a million barrels of cruel oil per day (Van Nostrand *et al.*, 1981).

In dairy processing industry, fouling poses a more severe problem as compared with the other industries. For instance, heat exchangers in petrochemical refineries are usually cleaned annually whereas cleaning them every 5-10 hours is a common practice in dairy industry (Georgiadis *et al.*, 1998). It has been estimated that the operating cost of fouling in the U.S. fluid milk industry (pasteurised milk production alone) is accountable for $140 millions per year (Sandu and Singh, 1991). Therefore, in order to reduce cost of cleaning and plant downtime while meeting the legal requirements for food safety and hygiene, minimising fouling rates and optimising cleaning efficiency is of key importance (Pelligreno *et al.*, 1995). However, the mechanism of fouling by milk needs to be understood thoroughly before prevention measures and optimisation of cleaning techniques can be done.

4.2.1 Fouling mechanisms

Fouling can be classified into 6 different categories; they are precipitation fouling, particulate fouling, chemical reaction fouling, corrosion fouling, biological fouling and solidification fouling (Minton, 1986a). Milk fouling can be loosely classified as chemical reaction fouling where chemical reaction takes place under the influence of temperatures present in heat exchanger. In normal circumstances, the heat transfer surface does not take part in the reaction but in some exceptional cases where metal surface may act as a catalyst or inhibitor to the potential chemical reaction (Bott, 1995). Fouling is a transient process, where the exchanger starts off clean and becomes fouled. A general model of fouling may include an induction or initiation period where no significant changes occur to the heat transfer or flow conditions, followed by a fouling period. More often than not, the initiation period is extremely difficult or impossible to predict even with the benefit of experience, therefore, it is commonly ignored in most mathematical models (Bott, 1995; Changani *et al.*, 1997).

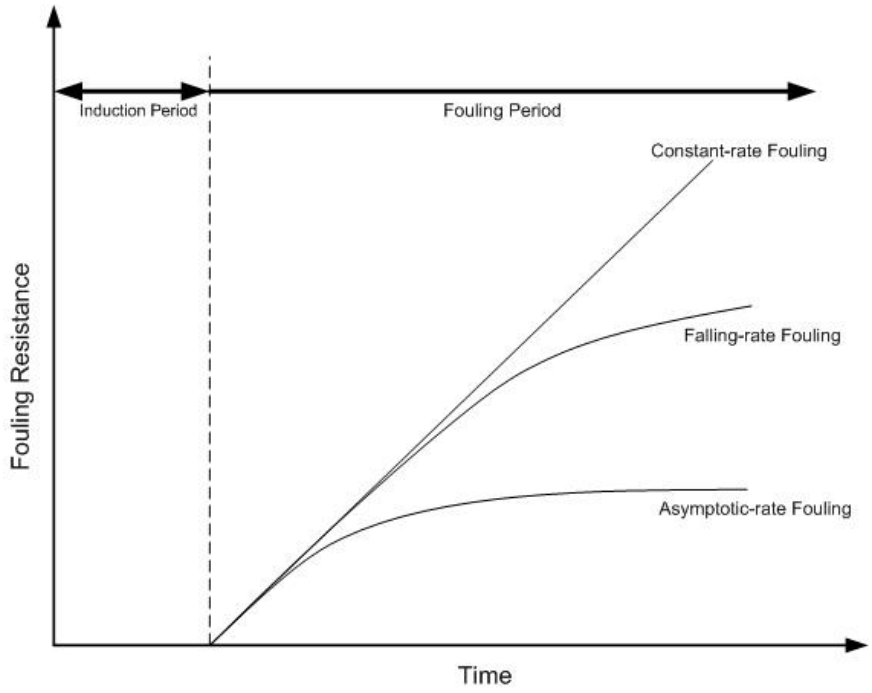

Figure 4.7 Fouling model (Bott, 1995)

Milk fouling is a function of many variables, both physical and chemical. Physical parameters such as temperature, flow rate and material of construction can be

determined by heat exchanger designers whereas the chemistry of milk normally cannot be changed (Bott, 1995; Changani *et al.*, 1997; Beuf *et al.*, 2007). "Heat Stability" refers to the relative resistance of milk to coagulation when it is heated at sterilization temperature (Fox and Morrissey, 1977).

4.2.1.1 Effect of composition on fouling

The amount of the various main constituents of milks can vary considerably between cows of different breed and between individual cows of the same breed (Bylund, 1995; Boland, 2003). The variation of main constituents in milk is shown in Table 4.3

Table 4.3 Quantitative composition of milk (Bylund, 1995)

Main Constituent	Range of Variation (%)	Mean Value (%)
Water	85.5 – 89.5	87.5
Total Solids	10.5 – 14.5	13.0
Fat	2.5 – 6.0	3.9
Proteins	2.9 – 5.0	3.4
Lactose	3.6 – 5.5	4.8
Minerals	0.6 – 0.9	0.8

The degree of fouling is affected by the concentration and the composition in the milk. A positive relationship between total amount of whey protein deposit and protein concentration was established by Fryer et al (Fryer *et al.*, 1992). Jeunink found that the increase in concentration of serum protein promotes fouling together with calcium deposition (Jeurnink, 1995b). Also reported by Jeunink, reconstituted milk exhibit much less fouling than fresh milk. The cause for this is unknown. However, with the knowledge that 25% of β-lactoglobulin is denatured during evaporation and drying in reconstituted milk production and the reduction of calcium concentration (9%) and ion activity (11%), some of these factors, if not all, could result in reduction of fouling (Jeurnink, 1995a).

It is also known that by holding milk for 24 hours at 4°C prior to processing, deposition can be reduced considerably (Burton, 1968), even though longer-term aging promotes fouling (Burton, 1968; Jeurnink, 1991).

The ability for urea to improve heat stability of milk is well-known (Muir and Sweetsur, 1976; Robertson and Dixon, 1969; Pyne, 1958; Holt *et al.*, 1978). Although the addition of urea at low concentration (< 7mM) does not affect the heat stability significantly, however with higher concentration, the heat stability of milk can be improved throughout the pH range 6.4 – 7.3 (Muir *et al.*, 1978). Sweetsur and Muir explained this stabilization effect in terms of the formation of cyanate-casein complex, possibly via ε-amino groups of lysine residues (Sweetsur and Muir, 1981). On the other hand, urea does not improve the heat stability of concentrated milks (Muir and Sweetsur, 1977). The addition of capric acid, a fatty acid, enhances the stability of casein micelle, therefore reducing deposit formation. Conversely, other fatty acids do not have the desired effect (Al-Roubaie and Burton, 1979). Although the heat stability of milk can be improved by additives but in most of the countries, such additives are not permitted (Lyster, 1970; Skudder *et al.*, 1981a; Changani *et al.*, 1997)

The effect of pH on deposit formation has been widely investigated but the mechanism behind is not well understood (Changani *et al.*, 1997; Bansal and Chen, 2006). Normal milk is slightly acidic with a pH ranging from 6.5 to 6.7 (Bylund, 1995). According to Skudder et al, at acidic pH, fouling increased noticeably while alkali pH has no effect (Skudder *et al.*, 1986). Such effect was explained by Hegg et al and Hege and Kessler, in terms of increased β-lactoglobulin adsorption towards its isoelectric point (Hegg *et al.*, 1985; Hege and Kessler, 1986). Increasing of ionic calcium concentration is also observed with decreasing pH. This could be due to the dissolution of calcium phosphate from casein micelle and its increased solubility (Lewis and Heppell, 2000).

4.2.1.2 Effects of processing parameters on fouling

Processing parameters such as temperature, flow rates and air contents can be easily altered through the use of equipments like heater, pumps and air or steam injector.

According to Gynning et al, air content of milk is proportional to the severity of fouling and this theory is backed-up by several other researchers (Gynning *et al.*, 1958; Burton, 1968; de Jong, 1997; de Jong *et al.*, 1998). The formation of bubbles on the heat-transfer surface significantly enhance fouling by creating a nuclei for deposition (Burton, 1968; Fryer, 1986; de Jong, 1997). Such fouling will result in a change in protein deposit composition from serum proteins to casein (Jeurnink, 1995a). Therefore, maintaining high pressure in process plant is desirable, but not always feasible, to impede bubble formation.

The presence of turbulence in fluid flow has shown to help in reducing deposition (Belmar-Beiny *et al.*, 1993; Santos *et al.*, 2003). An inversely proportional relationship has also been established between both the rate and amount of fouling and flow rates in a tubular heat exchanger (Gordon *et al.*, 1968; Fryer, 1986; Gotham, 1990). The explanation can be easily related to the escalating fluid shear-stresses by the increasing flow rate which encourages deposit removal (Rakes *et al.*, 1986).

Temperature is certainly the single most important factor governing fouling. The dependence of fouling on temperature is further discussed below.

4.2.2 Deposit composition

Dairy fluid fouling can be classified into two types. Type A deposit consist of 50-70% protein, 30-40% minerals and 4-8% fat. The deposit is white and spongy and its formation initials above 75°C, is greatest in the range 95-110°C. The main constituents are whey proteins and immunoglobulins. At the lower end of the temperature range, the deposit mainly consists of β-lactoglobulin whereas casein predominates at the higher temperatures. This type of fouling is commonly found

in both pasteurizer and sterilizer. With processing time over an hour, two layers of type A deposit can be found: a calcium- and phosphate-rich layer on the heat exchange surface and a outer layer rich in protein. The formation of the sublayer can be explained by the diffusion and successive crystallisation of insoluble calcium phosphate. Type B deposit, however, only consist of 15-20% protein (entirely consist of casein), 70-80% minerals and 4-8% fat. This type of deposit is hard, granular and brittle. It takes place at temperature above 110°C and is usually found in sterilizer. In contrast with type A deposit, type B shows no distinct layers. According to Foster and Green, protein together with calcium and phosphate were concentrated near the outside of the deposit while magnesium gathers near the heat exchange surface (Foster *et al.*, 1989).

Table 4.4 Concentration of proteins in milk (Bylund, 1995)

	Conc. in milk (g/kg)	% of total protein (w/w)
Caseins		
α_{s1}-casein	10.0	30.6
α_{s2}-casein	2.6	8.0
β-casein	10.1	30.8
κ-casein	3.3	10.1
Total Casein	26	79.5
Whey Proteins		
α-lactalbumin	1.2	3.7
β-lactoglobumin	3.2	9.8
Blood Serium Albumin	0.4	1.2
Immunoglobulins	0.7	2.1
Miscellaneous	0.8	2.4
Total Why Proteins	32.7	19.3
Fat Globule Membrane Proteins	0.4	1.2

Total Protein	32.7	100

4.2.3 Heat-induced changes in milk proteins

Between the two main types of proteins found in milk, caseins are very resistant to temperatures used in processing milk. However, severe heating (e.g. 140°C for prolonged period), triggers simultaneous dissociation and aggregation of the micelles and ultimately coagulation (Hui, 2006). Furthermore, they do precipitate upon acidification (Fox, 1989; Visser and Jeurnink, 1997). On the other hand, whey proteins are relatively vulnerable to changes on heating, especially β-lactoglobulin where thermal denaturation is dependent on factors like ionic strength, pH and protein concentration (McKenzie, 1971; Sawyer, 2003)**.** Upon denaturation, β-lactoglobulin exposes the hydrophobic molecular core together with highly reactive disulfide and sulphydryl group. Reaction occurs between denatured β-lactoglobulin and other proteins, for instance κ-casein a micelle-stabilising protein which is concentrated on the surface of casein micelles, via sulphydryl-disulphide interchange reactions (Sawyer, 1968)**.** The aggregation of such complexes can be found either at the surface of micelles or in the serum phase, depending on the pH. These complexes may be responsible for fouling, but the processes are not yet understood (Jeurnink, 1991; Jeurnink, 1995b). There are a few different theories suggested by a number of researchers regarding the relationship of fouling with aggregation. According to Changani et al, only when aggregation occurs next to the heated surfaces, fouling will take place (Changani *et al.*, 1997). Delplace et al believe that aggregation reaction of protein governs fouling, however van Asselt et al think otherwise (Deplace *et al.*, 1997; van Asselt *et al.*, 2005).

Remedies to prevent fouling by aggregation were suggested in a number of articles. By adding potassium iodate to milk before pasteurization, fouling can be reduce considerably as this oxidises the sulfhydryl groups exposed during β-lactoglobulin denaturation, impeding aggregation (Skudder et al., 1981b). Hydrogen peroxide has proved to be effective in decreasing aggregation and fouling by blocking disulfide exchange reactions (Marshall, 1986). Study from Burdett has shown that UHT

fouling can be reduced significantly by adding sodium pyrophosphate and he suggested that it was due to the enhanced casein micelle stability and inhibition of calcium phosphate precipitation (Burdett, 1974).

4.2.4 Minimum flow rate

Fouling can have adverse effects on the overall heat transfer coefficient. In falling film evaporator, dry patches are formed when film breaks within the tube due to insufficient wetting. The stability of the dry patch will determine whether fouling will take place (Schwartzberg, 1989). If the dry patch is re-wetted quickly, then severe fouling is unlikely to occur. Therefore, maintaining a minimum product flow condition to wet the heat transfer surface is crucial for the operation of falling film evaporator. (Hartley and Murgatroyd, 1964; Kessler, 1981b)

Hartley and Murgatroyd (Hartley and Murgatroyd, 1964) proposed an equation to calculate the minimum flow rate, Γ_{min} (kg.m^{-1}s^{-1}) which has to be maintained to prevent dry patch formation.

$$\Gamma_{min} = 1.69\left(\frac{\mu\rho}{g}\right)^2 (\sigma(1-\cos\theta))^{0.6} \quad (4.23)$$

where μ is viscosity (Pa.s), ρ is liquid density (kg.m^{-3}), σ is surface tension of the liquid (N.m^{-1}) and θ = advancing contact angle.

Minton (1986b) has also suggested another way of calculating the minimum flow rate without taking the advancing contact angle into account.

$$\Gamma_{min} = 0.008(\eta s\sigma^3)^{1/5} \quad \text{(kg.m}^{-1}\text{s}^{-1}\text{)} \quad (4.24)$$

where η is viscosity (mPa.s), s is specific gravity related to water, and σ is surface tension of the liquid (N.m^{-1}).

Once the falling film is formed, the film will be maintained even at reduced flow rates. The terminal flow rate, Γ_T (kg.m^{-1}s^{-1}), can be found as (Minton, 1986b)

$$\Gamma_T = 0.001(\eta s \sigma^3)^{1/5} \qquad \text{(kg.m}^{-1}\text{s}^{-1}\text{)} \tag{4.25}$$

When the flow rate is below Γ_T, the film will break and dry patches will form. The evaporator becomes susceptible to fouling which further reduces the heat transfer.

In both Equation 4.24 and 4.25, viscosity of the flowing liquid has played an important role in determining the minimum flow rate. The lower the viscosity, the smaller the minimum flow rate needs to be to maintain the film. With lower flow rate, the film thickness is reduced and heat transfer may improve. However, the reduction in flow rate also means the fall in production rate which might be undesirable. The equations also show that viscosity has significant influence on the fouling. If fouling due to film breakage can be prevented or minimised, the overall heat transfer coefficient of the evaporator can be improved.

4.3 Materials and Methods

The measurement of heat transfer coefficient (HTC) of a commerical evaporator is a difficult task, where the access to certain components or measurements are not possible or available. Therefore, the advantage of a pilot evaporator is the ability to integrate HTC measurement capability, usually, with manageable modifications.

In Chapter 2, a steam-heated pilot evaporator was constructed mainly to satisfy the need for concentrating milk to at least 55wt% in a relatively short time and the ability to extract samples during the evaporation process for viscosity measurements. Direct measurement of temperatures on the heat transfer surface (wall between steam and process fluid) within the evaporator was not possible due to the nature of the construction for the steam-heated pilot evaporator. However, an in-direct and simple approach was employed by measuring the amount of condensate produced during the evaporation process. The condensate from the

condenser was redirected to a vacuum tight filter flask that was resting on an electronic balance. The rate of condensate production was measured at random time intervals for 2 min during the evaporation process. At the same time, a sample of milk concentrate was also collected for total solids measurements. With the rate of condensation, the effective heat transfer coefficient of the steam heated pilot evaporator can be estimated using the latent heat of vaporisation of water at specific pressure.

Although the modification of the steam-heated pilot evaporator was able to give a good indication of the heat transfer of the evaporator but in order to get an accurate measurement of the HTC, temperature has to be measured directly on heat transfer surface. Initially, a bench top evaporator has been designed and built. However, it was not sufficient in gaining the level of details we want. (Nevertheless, we have included it in the Appendix A.4). Therefore, a new custom built electric-heated evaporator has to be constructed. A detail description of the new design can be found in section 4.3.1. With the new evaporator, different operation conditions (e.g. energy input and fluid composition) can be tested.

4.3.1 Electric-heated Pilot Evaporator

The design of the electric-heated pilot evaporator was similar to the scaled up version of the bench top evaporator. Many ideas such as the external falling film and the complete isolated vacuum evaporation system design were adopted from the trial and errors exercises undertaken on the bench top evaporator (see Appendix A.4). When this evaporation system was designed, one of design criteria was to use electric heaters to meet all heating requirements within this system instead of steam. Major deficiencies of the bench top evaporator were rectified during the design and testing of the bench top and steam-heated pilot evaporator. Therefore, the fabrication of this evaporator was almost free from complications.

The main objective for building the electric-heated pilot evaporator was to investigate the heat transfer within an evaporator at different operation conditions

and flow pattern during evaporation process. In order to understand the phenomena behind, the film was observed and pictures were taken.

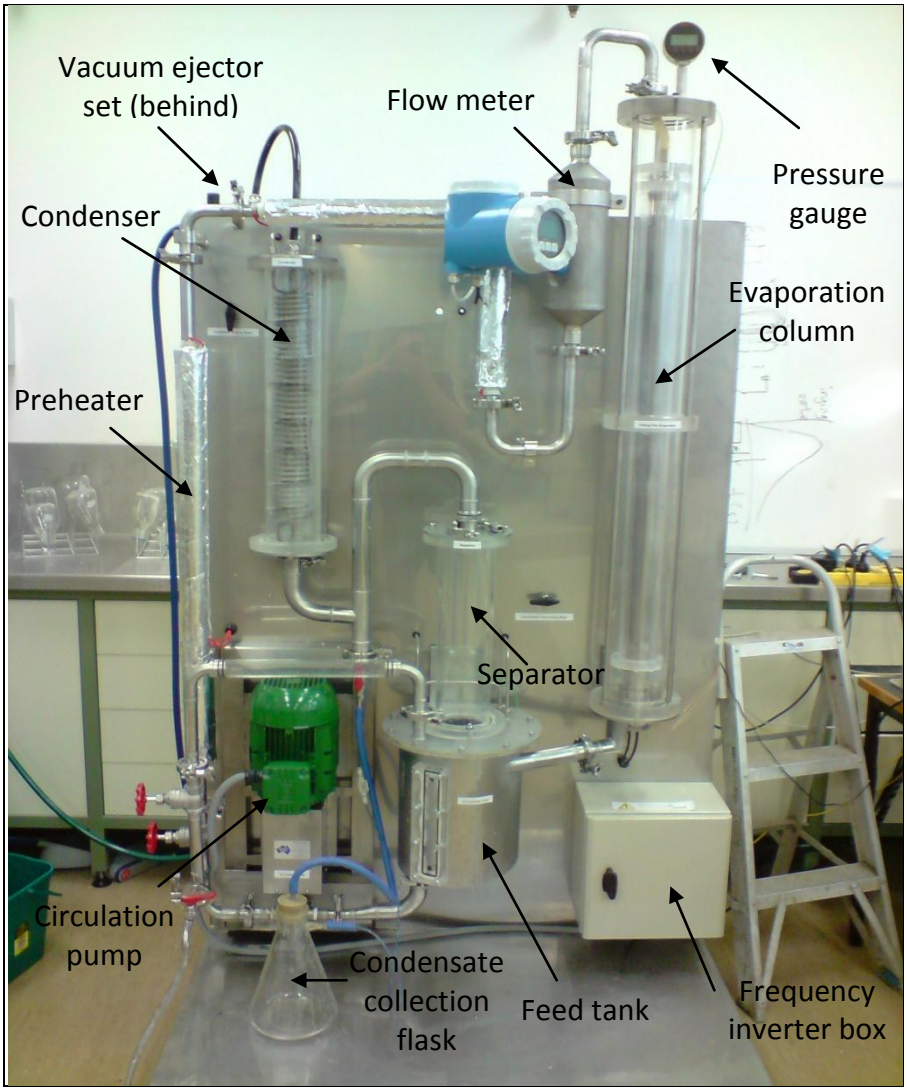

Figure 4.8 Electric heated pilot evaporator

4.3.1.1 Design specifications

The main components of the electric-heated pilot evaporator were the same as the steam-heated pilot evaporator. They consisted of a storage tank, a preheater, a evaporation column, a separator and a condenser. Majority of the connections were 1" stainless steel pipe with triclover connectors.

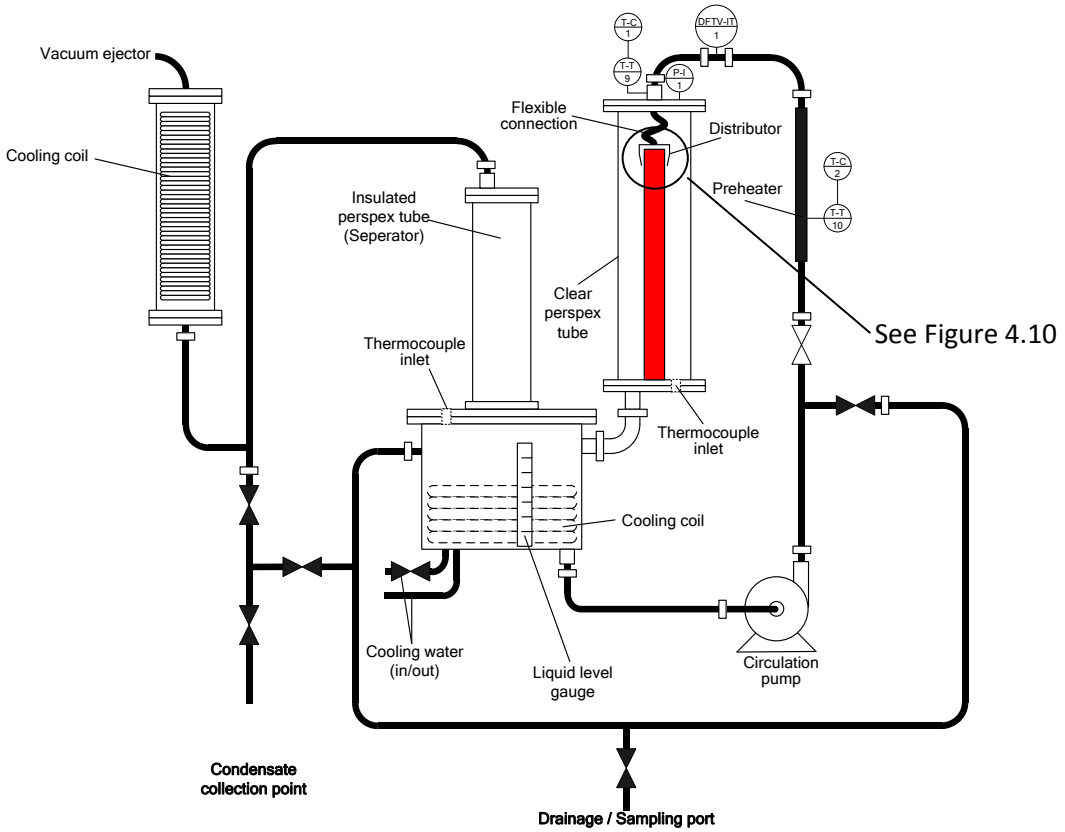

Figure 4.9 Schematic layout of the electric-heated pilot evaporator

Feed tank

The feed tank had a capacity of 20L and is made of stainless steel. The bottom of the feed tank is slightly tapered to the drainage port leading to the circulation pump. A vertical window is created on the wall to observe the liquid level within the feed tank. A cooling coil is installed inside the feed tank to cool the liquid within. The cooling coil is proven to be essential during the testing of the bench top evaporator. The vapor bubbles formed during the evaporation process created a layer stable bubbles on the surface of the milk in the feed tank. This layer of bubbles would multiply and flood the entire system with bubbles if the milk within the feed tank is not cooled down.

Preheater

The heating requirement of the preheater (see Figure 4.9) is met through the use of silicone rubber heating cable (Argus Heating Ltd, HS0002R) which has a heat rating of 40W m^{-1}. A section of the stainless steel piping between the circulation pump

and the flow meter is used as the preheater. It took about 25.7m long silicone rubber heating cable to wrap a meter of the 1" OD pipe. Silicone adhesive/sealant (Dow Corning, Silastic 732 RTV) was applied on the heating cable to secure the cable onto the pipe and the insulation around the cable. The preheater regulates the feed temperature entering the evaporation column. Over heat protection was installed onto the preheater, details can be found in Section 4.3.1.3.

Evaporation Column

The major components in the evaporation column in the electric-heated pilot evaporator are similar to the bench top counterpart. They consist of a liquid distributor at the top of the heater, a electric heater situated in the centre and the a casing surrounding the heater. However, the distributor no longer uses the overflow principle to create the liquid film on the heat transfer surface found in the bench top and steam-heated pilot evaporator. A distributor cap was placed on top of the electric heater with a small gap (1-2 mm) in between. Liquid was fed into the distributor cap from the hose-tail connector on top and the liquid was force into the small gap between the cap and the electric heater. This formed a liquid film around the electric heater (stainless steel tube) effectively.

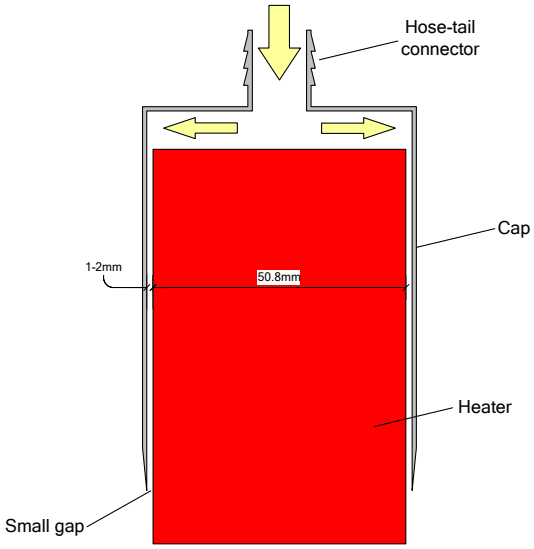

Figure 4.10Cross-section of the distributor on the electric heater

The heating requirement in the evaporation column was supplied by a Φ 2" × 1m bobbin electric heater (Helios Electroheat Pty Ltd, BEW 24) with wattage of 2400W.

The 2” BSP thread on the heater coated with thread sealant (Loctite 592) was screwed into the base disc of the evaporation column.

The casing of the evaporation column is made of two Φ OD 170mm × 0.6m acrylic tubes (5mm thick) jointed in the middle by an acrylic ring. Flanges were built on both ends on the tube for the top and base disc. O-rings were fitted in between the flanges and disc to ensure the evaporation column was air tight.

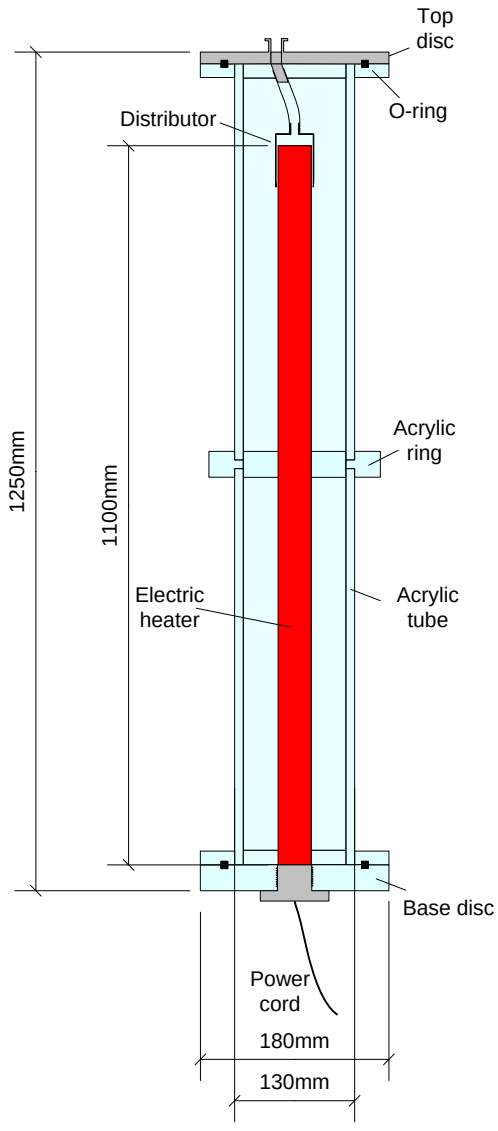

Figure 4.11 Cross-section of the electric-heated evaporation column

Separator

A separator was incorporated on top of the feed tank. Steam generated during the evaporation process rose through the separator and left the concentrate back in the feed tank. The separator (see Figure 4.9) was made of another acrylic tube similar those found on the casing of the evaporation column. On top of the tube, a steel disc seals the separator and the opening on the disc was connected to the condenser via 2" stainless steel pipe.

Condenser

A 6 m steel cooling coil was installed into the condenser that was constructed in the similar way as the evaporation column and separator. A vacuum ejector located at the top of the condenser enhanced the steam flow towards the condenser and the condensate could be either collected in a filter flask at the bottom of the condenser or return back to the system.

4.3.1.2 Temperature measurements

Temperature measurement within the electric-heated pilot evaporator was an important task as they would be used to calculate the temperature difference, ΔT, between the heater wall and the boiling fluid temperature. In addition to the calibration stated in Section 3.6.3, the location of the thermocouples also played a vital role in obtaining accurate temperature measurements.

In total, there were 10 thermocouples (Type K) installed in the pilot evaporator. Among them, 5 × Φ 0.13mm thermocouples were placed on the heater wall and 3 × Φ 0.25mm thermocouples measured the fluid and vapour temperatures within evaporation column. To regulate and maintain the feed temperature, 1 × Φ 0.25mm thermocouple situated at the entrance of the evaporation column acted as a feedback for the temperature controllers of the preheater and 1 × Φ 0.25mm thermocouple glued to the surface of the heating cable on the preheater served as a feedback for the temperature limiter. In Table 4.5, it shows the locations of the thermocouples installed and where they were connected to. All measurements from thermocouple 1-8 were recorded during the entire evaporation process.

Table 4.5 List of thermocouples installed in electric-heated pilot evaporator

Thermocouple	Location	Connect to	Purpose
T-T 1*	Middle of the electric heater	Picolog TC-08 Data Logger	Monitor/ Record
T-T 2*	Middle of the electric heater	Picolog TC-08 Data Logger	Monitor/ Record
T-T 3*	Middle of the electric heater	Picolog TC-08 Data Logger	Monitor/ Record
T-T 4*	Middle of the electric heater	Picolog TC-08 Data Logger	Monitor/ Record
T-T 5*	Middle of the electric heater	Picolog TC-08 Data Logger	Monitor/ Record
T-T 6	Bulk liquid	Picolog TC-08 Data Logger	Monitor/ Record
T-T 7	Vapour temperature	Picolog TC-08 Data Logger	Monitor/ Record
T-T 8	Vapour temperature	Picolog TC-08 Data Logger	Monitor/ Record
T-T 9	Feed temperature	PID Temperature Controller	Temperature Control (T-C 1)
T-T 10	Temperature of heating cable for preheater	PID Temperature Controller	Temperature Control (T-C 2)

*Note: Refer to Figure 4.12 for the exact position of thermocouple 1-5 on the electric heater

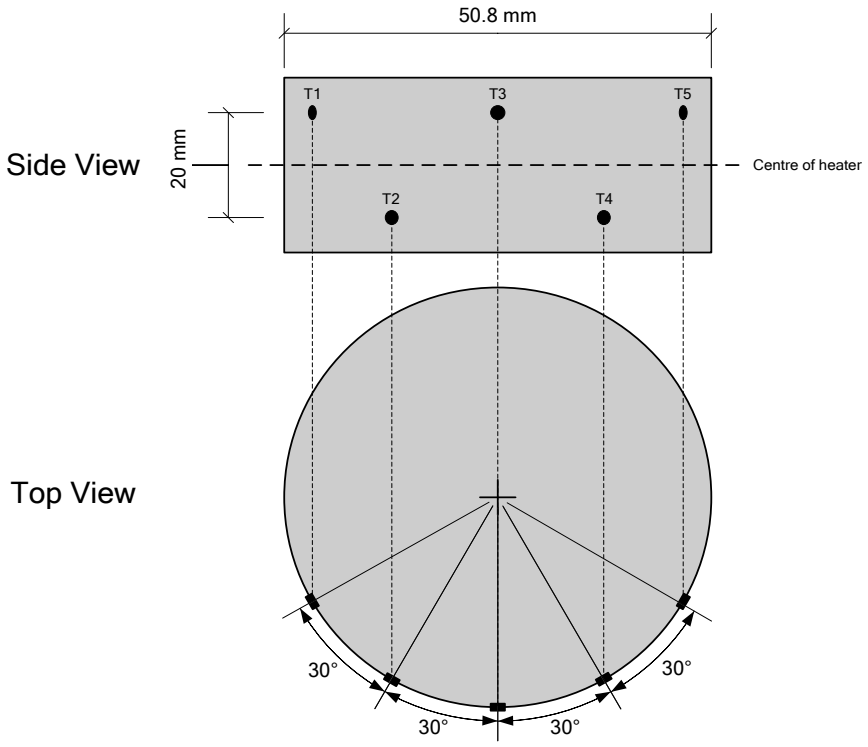

Figure 4.12 Thermocouple positions on the electric heater

4.3.1.3 Heating protection for preheater

The silicone rubber heating cable wrapped around the preheater is capable of heating up to temperature of 150 °C. At such high temperature, potential fouling might occur within the stainless steel pipe. Therefore, as an operation precaution, a temperature limiter is installed on the surface of the heater wire along with the feed temperature controller. In Figure 4.13, the top controller (T-C 1) was the PID temperature controller for the feed entering the evaporation column while the bottom controller (T-C 2) is the temperature limiter for the preheater.

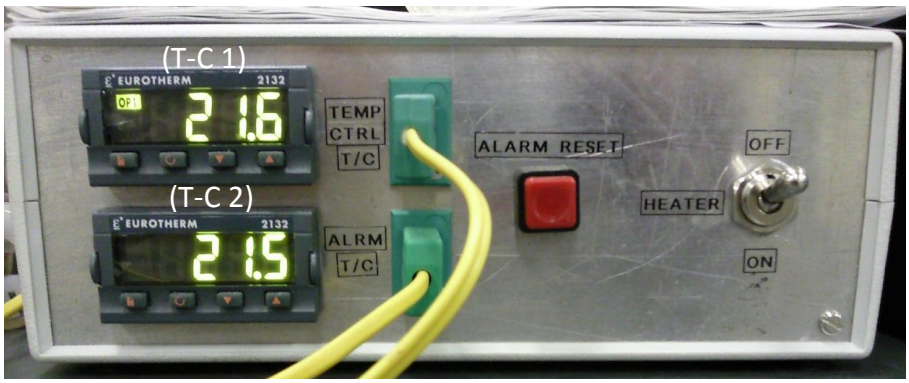

Figure 4.13 Feed temperature controller with over heat protection

T-C 1 regulated the feed temperature (T-T 9) by controlling the amount of power entering the heating cable and the PID controller settings could be found in Table 4.6.

Table 4.6 PID controller settings

Control variables	Setting
Proportional Band	2.3 units
Integral Time	127 s
Derivative Time	21 s
Low Output Power Limit	0%
High Output Power Limit	100%

To prevent the silicone rubber heating cable from overheating, T-C 2 is connected to T-C 1 as shown in Figure 4.14. When the surface temperature of the heating cable (T-T 10) reach the set point temperature (80°C), T-C 2 would send a signal to

T-C 1 to cut off the power of the preheater until T-T 10 fall below the set point temperature.

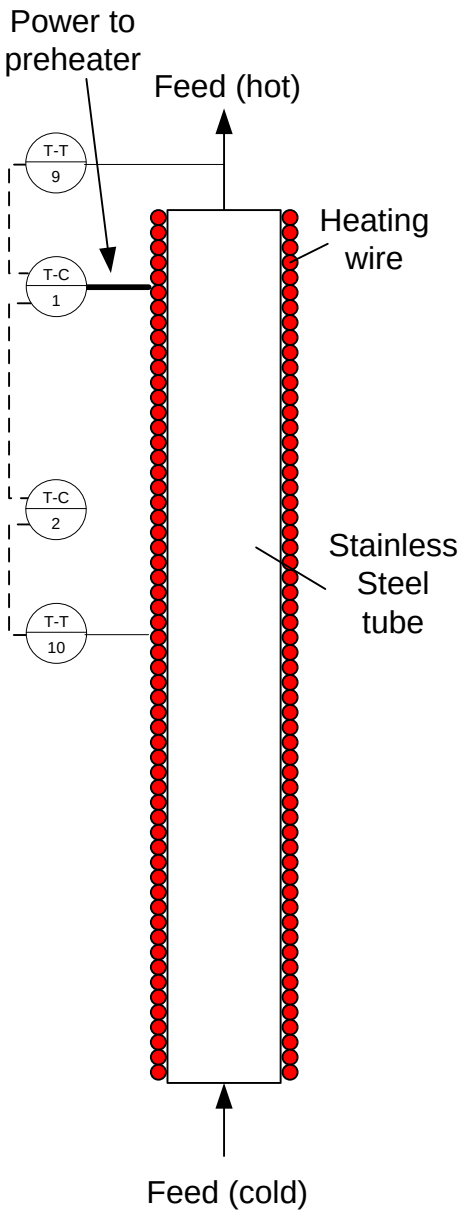

Figure 4.14 Process control flow diagram for electric-heated pilot evaporator

4.3.1.4 Power management and measurement

The amount of power going into the bobbin heater in the evaporation column could be adjusted using a variac transformer (Carroll & Meynell, CMV10E-1) shown in Figure 4.15. The variac transformer was able alters the voltage that was going

into the heater, hence varying the power input to the heater according to Equation (4.26) .

$$P = V \times I \tag{4.26}$$

where P is power (W), V is voltage (V) and I is current (A)

Figure 4.15 Variac transformer

Although the variac transformer gives a good indication of the voltage transmitted to the heater, exact amount of power going into heater could not be determined without a power meter. The digital power meter used to measure the current and voltage entering the heater is WT210 (Figure 4.16) manufactured by Yokogawa (Australia). The power meter was capable of measuring voltage, current and power with an accuracy of 0.1% of reading.

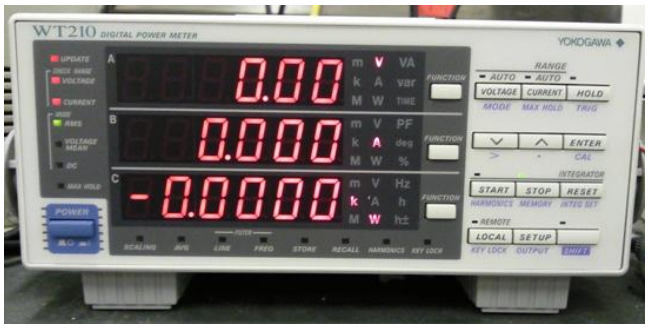

Figure 4.16 Digital power meter

4.3.1.5 Pressure measurements

The pressure within the evaporator was measured by a digital pressure gauge (Dwyer, DPG-100) located at the top of the evaporation column. The pressure gauge had a pressure range of -14.7 to 0 psi and an accuracy of 0.25% of full range.

4.3.1.6 Flow measurements

The flow meter used in the electric-heated pilot evaporator is the same as the one used in steam-heated pilot evaporator. Refer to Section 3.7.1.6 for details.

4.3.1.7 Commissioning

The commissioning process for the electric-heated pilot evaporator was similar to the steam-heated counterpart. The commissioning process began with the 3 preliminary tests: vacuum, pump and heating tests. Ultimately, the overall system test was conducted to ensure the evaporator works smoothly.

Vacuum test

Most of the connections on the evaporator were connected by tri-clover fittings and they were known to seal very well under vacuum conditions. Therefore, attention was focused on the seals found on the custom made components such as the evaporation column, feed tank/separator and condenser. The empty evaporator was subjected to vacuum up to -85 kPa (gauge) and was held at that pressure for 5 min. Stress creaks were normally the first sign prior to structural failure and was carefully listened for during the test. Once the entire evaporator was deemed to be air-tight, the pump test were commenced.

Pump test

The idea of pumping liquid in a vacuum environment was proven to be feasible during the testing of the bench top evaporator as long as there were no major air leaks within the evaporation system. Since, air-leaks were checked for in the prior test, no complication had emerged during the testing of the pump.

Heating test

The heating test could be separated into 2 sections. The first test was to find out if the overheat protection for the preheater was functioning properly. The second test was to examine the structural integrity of the evaporator subjected to high temperature by turning on the bobbin electric heater in the evaporation column to its maximum power (2400W). Water was circulated in the system during both test and the vacuum was turned on to -80 kPa (gauge). The overheat protection worked flawlessly and the heater wall temperature never exceeded 70 °C throughout the entire commissioning process as shown in Figure 4.17.

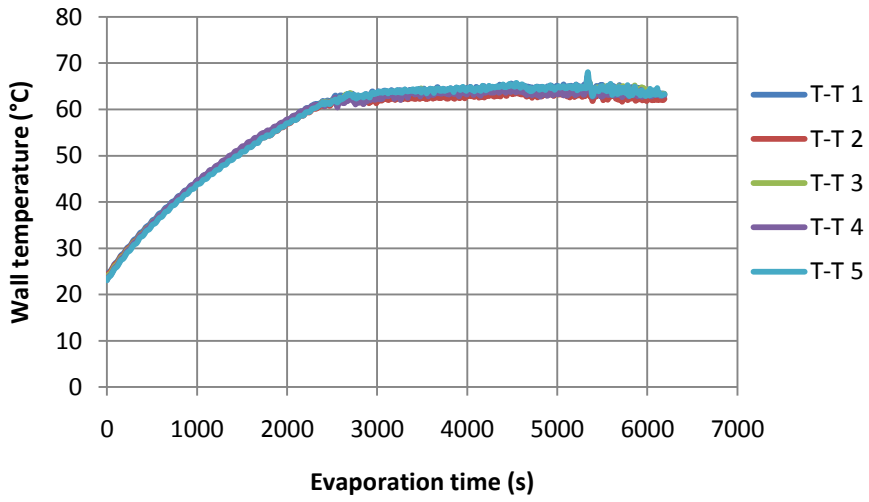

Figure 4.17 Typical heater wall temperature profile during heating test

Overall system operation test

The overall system operation test was conducted using reconstituted medium heat skim milk. The objective was the same as the steam heated pilot evaporator, to concentrate the milk to 50 wt% (at least) and estimate of the evaporation time. A 7L batch of reconstituted skim milk at about 32 wt% was used in this test.

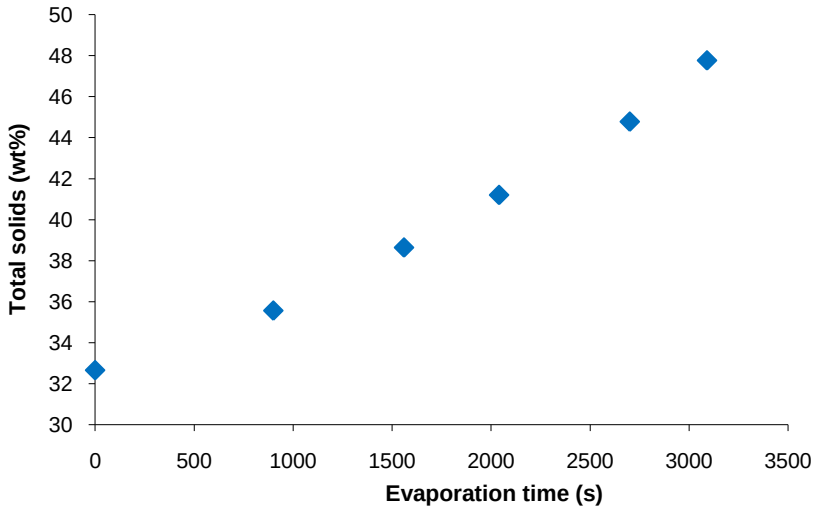

Figure 4.18 The progression of total solids with evaporation time during the commissioning process

In Figure 4.18, it shows that the total solids of the milk concentrate reached close to 49 wt%. However, the experiment had to be stopped at that stage because dry patches began to form around the heater and the temperature on the wall began to rise. As shown in Figure 4.19. Note that the time difference between the Figure 4.18 and Figure 4.19 was due to the way they were recorded. The evaporation time in Figure 4.18 started from the first sample that was collected while in Figure 4.19, temperatures were recorded throughout the preheating and evaporation period. The powers of the heaters were turned off immediately and water was added into the feed tank to cool off the heater.

During the evaporation process, it was observed that the bubbles generated by the boiling milk tend to spread outwards to the casing of the evaporation column. The bubbles act as bridges for the milk concentrate that was travelling along the heater wall to stray outwards and left the heater wall dry. A restriction tube (ID 70mm) was then installed into the evaporation column as illustrated in Figure 4.20.

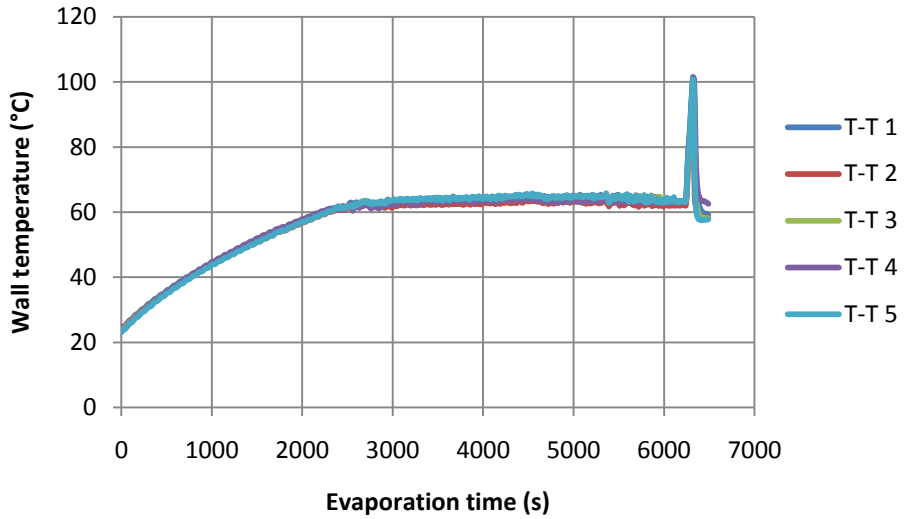

Figure 4.19 Heater wall temperature profile during overall operation system test

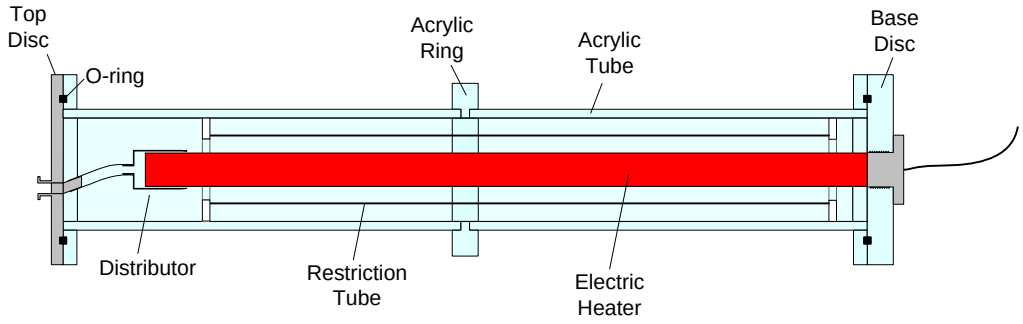

Figure 4.20 Cross-section of the electric-heated evaporation column with restriction tube

With the restriction tube installed, the total solids could get up to 52 wt% but beyond that, problems with the dry patches and rising wall temperature emerged again. The problem was not further rectify due to time constraint.

4.3.1.8 Operation of steam-heated pilot evaporator

The operation of the electric-heated pilot evaporator was simpler than the steam heated pilot evaporation and the process could also be divided into 3 phases. They were start-up, operating and shutdown procedures. Most of the process parameters (temperatures, flow rates, density, etc.) were displayed onto the computer monitor (except for the pressure gauge on top of the evaporation

column). Thus, any spike in temperature within the evaporation system could be identified with ease.

Start-up procedures

The start-up of the evaporator follows the same general guideline; turn on the flow, followed by the vacuum and then the heat. Note that the start-up procedure assumed that the evaporation system was well cleaned from the previous sessions. The detailed of the start-up procedures are as follow.

1. Turn on the computer and ensure all programs are working correctly
2. Pour the test liquid into the feed tank
3. Ensure all connector and openings are tightly sealed
4. Turn on the feed pump via the frequency inverter and adjust the flow rate to at least 5 L min^{-1}
5. Test the preheater overheat protection
6. Turn on the vacuum ejector and adjust the pressure regulator until P-I 1 display 0.8barg
7. Specify the temperature set point of the feed via T-C 1.
8. Turn on the bobbin heater to the desire voltage via the variac

Operating procedures

After the start-up procedures have been properly executed, the operating procedures are relatively straight forward.

1. Take note of the pressure in the evaporator and adjust the pressure regulator accordingly to maintain the right vacuum pressure.

Note: The feed rate would reduce throughout the entire evaporation process, especially beyond 50wt%, as the viscosity of the milk increases. The minimum feed rate should not fall below 4.5 L min^{-1}. Follow the shut down procedure if the feed rate should get close to 4.5 L min^{-1}.

2. Occasionally, drain off the condensate from the filter flask (unless the condensate was fed back to the system).

As long as the vacuum pressure and the falling film on the heater are maintained correctly, the temperature on the heater wall should not rise beyond 75°C. If one of the 5 thermocouples on the wall does increase beyond 75°C, shut down both the heater immediately and add in cold water into the feed tank.

Shut down procedures

At the end of evaporation process, it is critical to follow the shut down procedures to minimise the chance of extensive fouling in the preheater and on the bobbin heater.

1. Add in at least 5L of water into the feed tank
2. Turn off the power for both the preheater and the bobbin heater
3. Gradually increase the pressure within the system by reducing the pressure to the vacuum ejector
4. Keep the fluid circulation within the system on and wait until the heater wall cools down to 40°C
5. Discharge as much residual liquid from the evaporator before turning off the feed pump

To this stage, the evaporation system is still contaminated with milk or even fouling cakes. Therefore, a thorough cleaning process needs to done prior to the complete shutdown of the evaporator.

4.3.2 Heat transfer coefficient calculation

4.3.2.1 Steam-heated pilot evaporator

The overall heat transfer coefficient (OHTC) of the steam-heated pilot evaporator was determined experimentally by collecting and weighing the condensate from the condenser. During the evaporation process, condensate was collect for 2 min at intervals. With the collected condensate, the average heat flux, $\bar{q}''$ (W m^{-2}), along

the evaporation tube at a specific time interval was calculated by the following equation.

$$\bar{q}^{"} = (\dot{m}_c \cdot h_v)/A_e \tag{4.27}$$

where $\dot{m}_c$ is condensation rate (kg s^{-1}), h_v is the latent heat of vapourisation (J kg^{-1}) and A_e is the heat transfer area in the evaporator (m^2).

Thus, the overall heat transfer coefficient (W $m^{-2}K^{-1}$), U,

$$U = \frac{q^{"}}{\Delta T} \tag{4.28}$$

where ΔT is the overall temperature difference between steam and process liquid (°C)

Measuring overall temperature difference, ΔT

To measure the average steam temperature, $\bar{T}_s$, along the evaporator, 5 thermocouples were placed along the shell of the evaporator before insulation was installed (Section 4.3.1.2). From Figure 4.21, it shows a typical steam temperature profile along the evaporator (for 1 being the top of the evaporator and 5 is at the bottom). Throughout the evaporation process, the steam temperature along the evaporator hovered around 70.3 °C with ± 0.5 °C of fluctuation.

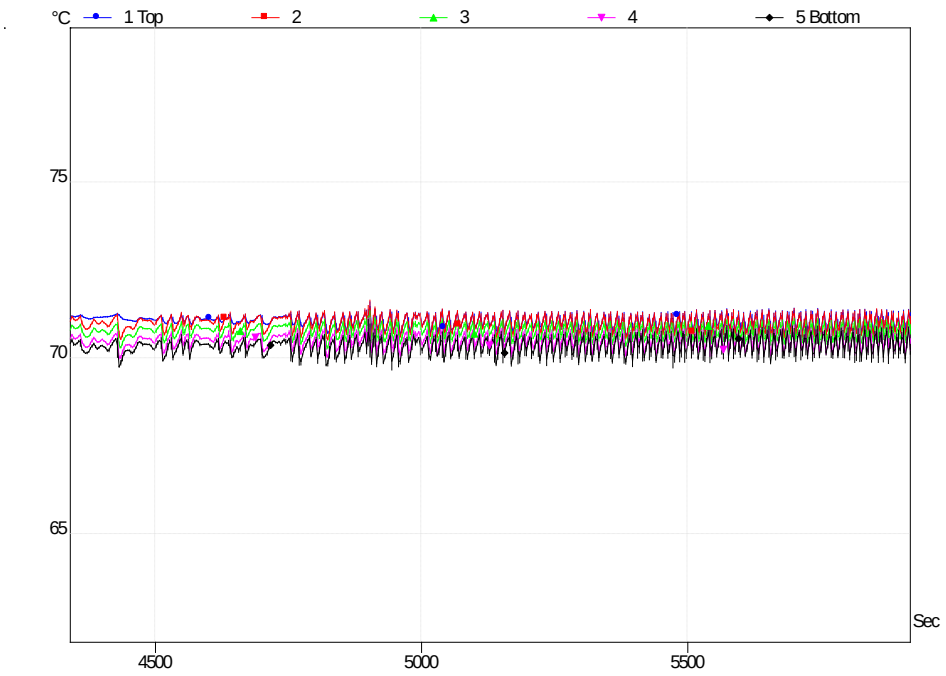

Figure 4.21 Temperature profile along the evaporator during evaporation (17/12/2009) MHSMP

The temperature of the process milk, T_p , was calculated based on the operating pressure in the evaporation tube and temperature elevation, ΔT_e (Section 2.2.5) due to difference in total solids level. At -80 kPa, the corresponding boiling temperature of pure water is 60.3 °C and the temperature elevation at certain total solids was calculated using Equation (2.11).

$$T_p = 60.3 + \Delta T_e \tag{4.29}$$

Hence,

$$\Delta T = \bar{T}_s - T_p \tag{4.30}$$

4.3.2.2 Electric-heated pilot evaporator

The calculation of heat transfer coefficient, U, of the electric heated pilot evaporator was based upon a simple energy balance:

$$U = \frac{q}{A\Delta T} \tag{4.5}$$

where q is the amount of power transferred (W), A is the heat transfer area (m^2) and ΔT is the temperature difference between the heater wall and boiling liquid.

The average amount of energy transmitted to the electric heater within a 2 min time frame was obtained from the power meter. During the 2 min time frame, the temperature on the heater wall (T 1-5) and fluid (T 6) were also recorded. The average wall temperature and fluid temperature during the 2 min time frame were used to calculate the temperature difference, ΔT.

4.4 Results

4.4.1 Heat transfer in steam-heated pilot evaporator

The heat transfer measurement of the steam-heated pilot evaporator was conducted using fresh medium heat treated skim milk from Murray Goulburn Co-operative, Koroit, Victoria, Australia. The condensation rates, which effectively the evaporation rate within the tube, were measured at random points in the evaporation process. With the rate of condensation, the rate of energy transfer can be calculated based on latent heat of vapourisation of water at 20kPa (absolute).

In Figure 4.22, when the condensation rate from the steam-heated evaporator was plotted against the mass flow rate of the milk flowing through the evaporator, they display a dependent relationship where the condensation rate is proportional to the mass flow rate. This indicates that the heat transfer rate was almost constant for most of the evaporation process.

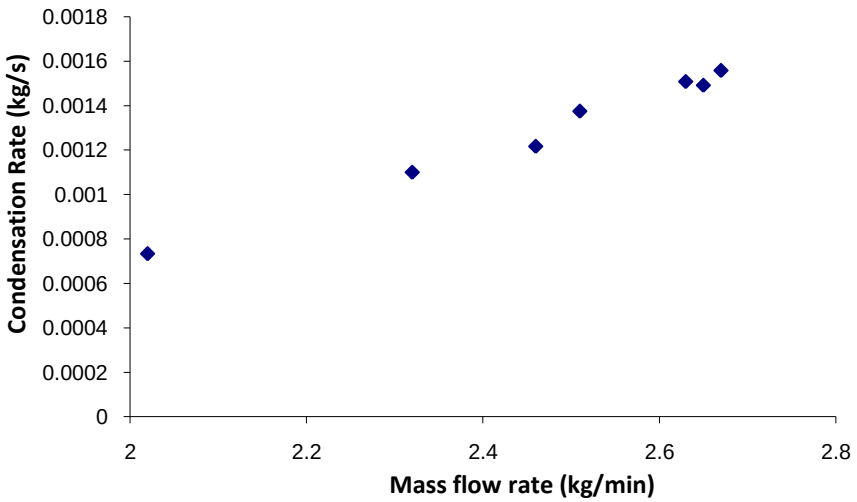

Figure 4.22 Condensation rate with increasing mass flow rate of milk

The reason behind the decrease in mass flow rate, even though the pump setting was kept constant, was due to the increase in viscosity of milk concentrate as the solids level increase. The mass flow rate and viscosity exhibit a negative and almost linear relationship as shown in Figure 4.23. At 50wt% (where most of the commercial evaporator would process to), the pump was able to deliver 2.5 kg min^{-1} of milk concentrate to the evaporator. However, once the total solids reaches

57wt%, the pump displays a 20% reduction in pumping capacity to 2 kg min^{-1}. This poses a potential problem to the operation of falling-film evaporator at high total solids level, especially for long duration. Note that the viscosity of milk was measured by the E+H Promass 83I and the measurement uses Coriolis effect as described in section 3.3.2.

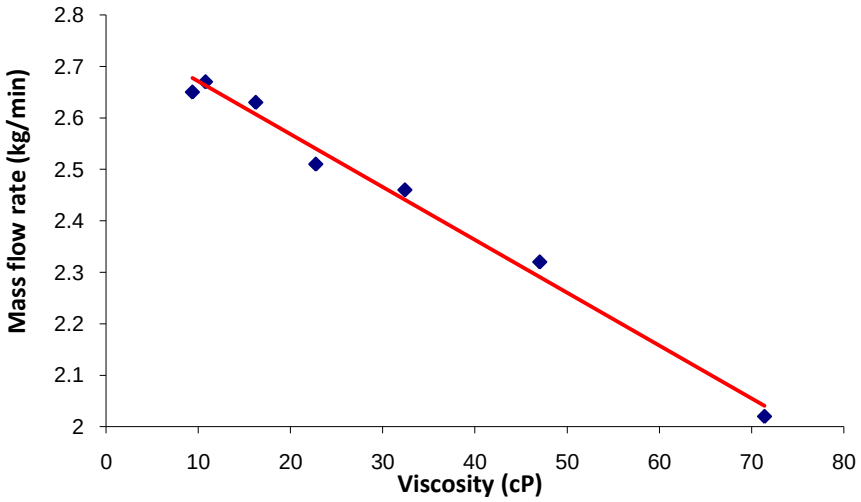

Figure 4.23 Influence of viscosity on mass flow rate

With the varying flow rate, viscosity and density, the overall heat transfer coefficient (HTC) for the steam-heated pilot evaporator was characterised with the Reynolds number, Re, as illustrated in Figure 4.24. During the entire evaporation process, the overall heat transfer coefficient ranged from 1.3 to 2.5 kW $m^{-2}K^{-1}$. This range of HTC agrees with Jebson and Chen (1996). For Re greater than 130, the overall heat transfer of the evaporator remains constant at around 2.5 kW $m^{-2}K^{-1}$. Below Re of 130, the overall heat transfer coefficient decreases rapidly with deceasing Re.

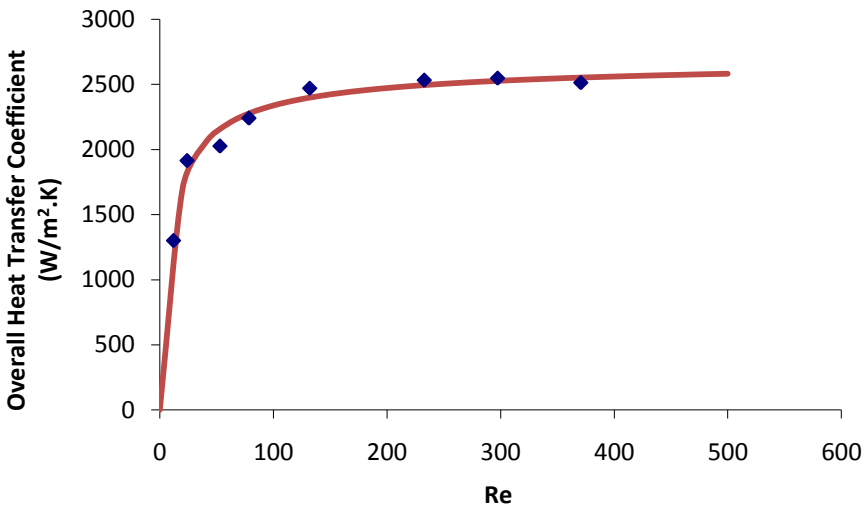

Figure 4.24 Overall heat transfer coefficient of steam-heated pilot evaporator

A point to note, the boiling point of the concentrated milk increases slightly with solids content, therefore, the temperature difference between the heat transfer surface and the process milk has taken boiling point elevation of milk into account. A model was fitted to the OHTC graph as a function of Re for pilot evaporator modelling purposes in Section 5.2

$$\mathrm{U} = \mathrm{a} \cdot \mathrm{Re}^{\mathrm{b}} + \mathrm{c} \tag{4.31}$$

where a, b and c are constants listed below.

Table 4.7 Constants for overall heat transfer coefficient with Reynolds number (for Equation (4.31))

Contants	**Values**
a	-6223
b	-0.5993
c	2732

4.4.2 Heat transfer in electric-heated pilot evaporator

The approach of measuring the heat transfer coefficient of the electric-heated pilot evaporator was totally different from the steam-heated counterpart. The design of the electric-heated pilot evaporator was revolved around the ability to measure accurate temperature measurements on the heat transfer surface (wall temperature). Five thermocouples were located at the center of the electric heater (see Section 4.3.1.2) to ensure that sufficient distance was given to the falling film to reach its equilibrium state before the wall temperatures were taken. The HTC calculated in the electric-heated pilot evaporator is derived from the direct measurement of temperature difference between the heat transfer surface and boiling fluid temperature. Heat loss through the evaporator is not taken into account at this stage.

Two types of skim milk were used for the experiments; reconstituted medium heat-treated skim milk and fresh medium heat-treated skim milk from Murray Goulburn Co-operative, Koroit. Each type of milk was evaporated from around 30 to 50wt% and the temperatures on the heat transfer surface and of the process fluid were monitored and recorded throughout the entire evaporation process. The evaporation process took place at various amount of power transmitted to the electric heater so as to study the effect of heat flux (5.092, 7.638 and 10.185 $kW.m^{-2}$ respectively) and flow characteristics (Re) on the performance of the falling film evaporator. Table 4.8 is the list of experimental trials conducted with electric heated pilot evaporator. During the evaporation process, the volumetric flow was kept constant (around 0.0057 $m^3\ min^{-1}$) in order to have a fair comparison. The maximum error range is ± 10 $W.m^{-2}k^{-1}$

Table 4.8 Tests conditions for HTC measurements

Milk type	Power (W)	Heat flux ($kW.m^{-2}$)	Maximum concentrated solids content (wt%)	Absolute pressure (kPa)
Reconstituted medium heat-treated skim milk	800	5.092	49.55	20
	1200	7.638	48.38	20
	1600	10.185	51.01	20
Fresh medium heat-treated skim milk	800	5.092	50.52	20
	1200	7.638	50.05	20
	1600	10.185	51.01	20

4.4.2.1 Reconstituted medium heat-treated skim milk

The heat transfer coefficient measured by the reconstituted medium heat-treated skim milk fluctuate around 3.75 $kW.m^{-2}k^{-1}$ regardless of the amount of power transmitted to the electric heater or the flow characteristic of the milk concentrate as shown in Figure 4.25.

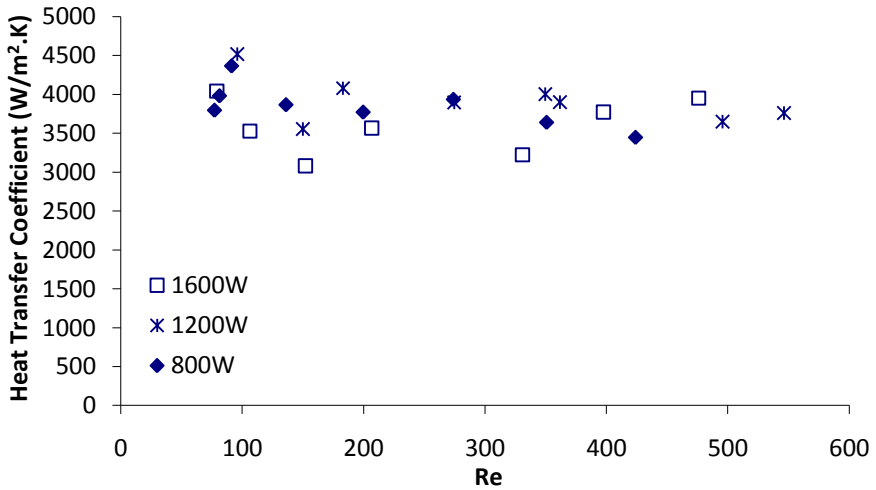

Figure 4.25 Heat transfer coefficient of electric-heated pilot evaporator with reconstituted medium heat-treated skim milk

This is unusual as the rates of evaporation do vary with different power input. Therefore, this indicates that the temperature difference between the heat transfer

surface and the process fluid increases with heat fluxes but maintains close to constant with Re as illustrated in Figure 4.26.

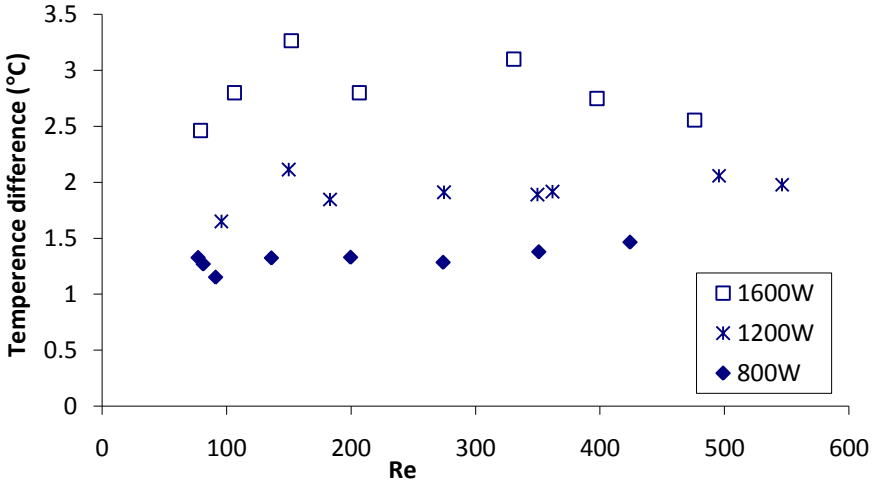

Figure 4.26 Temperature difference of electric-heated pilot evaporator with reconstituted medium heat-treated skim milk

The HTC calculated from the electric heated pilot evaporator is considerably higher than the steam-heated counterpart as it is purely based on the heat transfer from the heated wall to the process fluid oppose to the overall HTC for the entire system like that in the steam case.

However, such trend ceases to exist when the experiment were repeated with fresh medium heat-treated skim milk in section 4.4.2.2.

4.4.2.2 Fresh medium heat-treated skim milk

Similar to reconstituted medium heat-treated skim milk, the fresh medium heat-treated skim milk exhibit no significant differentiation of HTC of the evaporator at various power inputs, however, it does show a positive relationship with Re. Again, a closer look at the temperature difference was conducted as plotted in Figure 4.28. There is an obvious reduction in temperature difference with increasing Re for all power inputs tested.

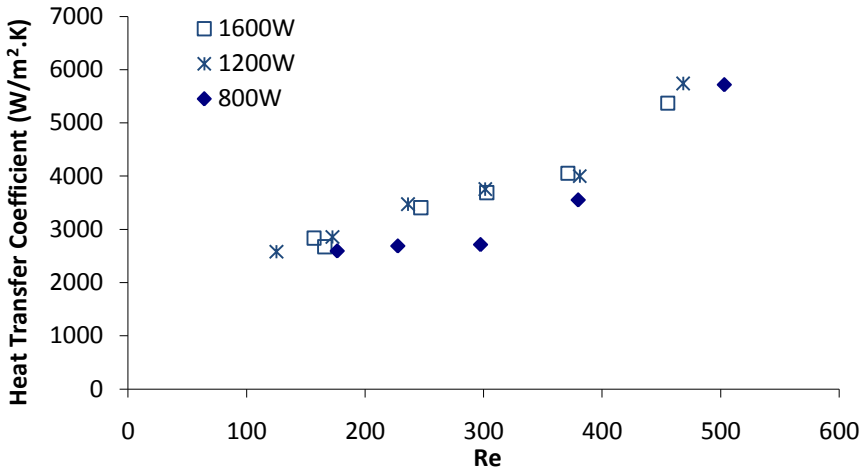

Figure 4.27 Heat transfer coefficient of electric-heated pilot evaporator with fresh medium heat-treated skim milk

The differentiation of temperature difference among the power inputs was not as distinct as the reconstituted skim milk counterpart, with a slight overlapping between 800 and 1200W at Re=300. The difference in trend of HTC between the reconstituted and fresh medium heat-treated skim milk was not expected and the exact reason is still unknown.

There was speculation that the difference might be caused by the difference in number and size of particles (predominately protein clusters) in the two types of milk. If assumption that the reconstitution processes could not break the particle in reconstituted milk back to the natural size is valid, particles in reconstituted milk would be bigger than those in fresh milk. Therefore, considering milk of the same solid content, there would be more particles in dilute fresh milk than dilute reconstituted milk.

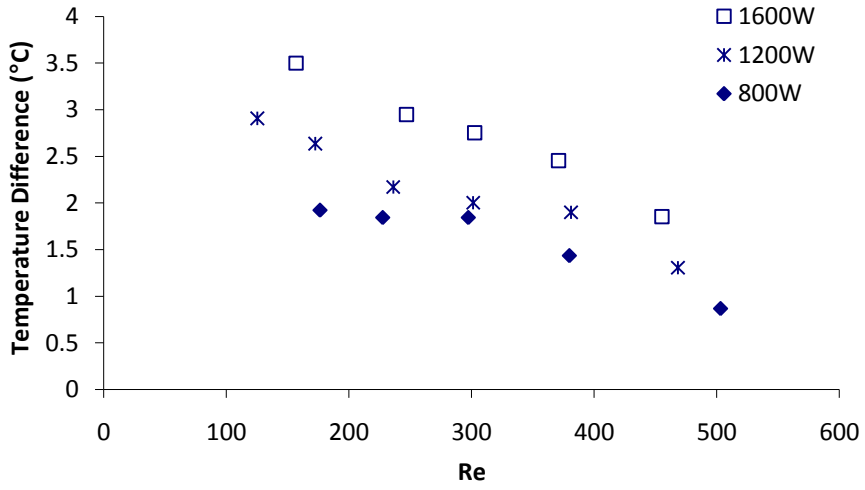

Figure 4.28 Temperature difference of electric-heated pilot evaporator with fresh medium heat-treated skim milk

During the evaporation process, given that the heat flux is high enough to promote nucleation boiling, bubbles formed during the boiling of milk enhances the heat transfer by creating turbulence. The number of bubbles formed depends on the number of micro voids on the heat transfer surface and the number of particles in the fluid which acted as nucleation sites. Assuming the size of particles in reconstituted milk remain relatively stable throughout the concentration process while the particles agglomerate in fresh milk, the number and rate of bubbles formed should decrease in fresh milk while remaining relatively constant in reconstituted milk when they were being concentrated.

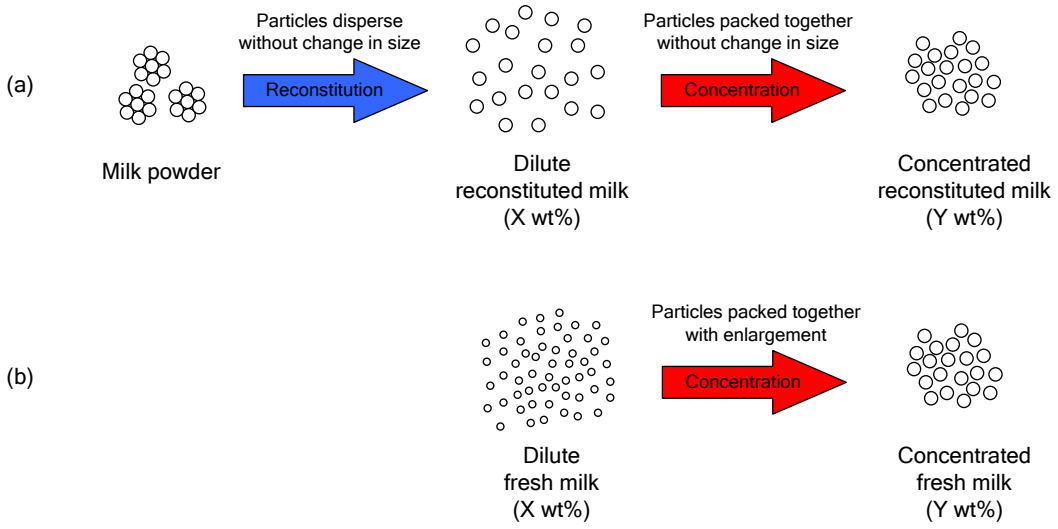

Figure 4.29 (a) Assumption of the reconstitution and concentration process of milk from milk powder, (b) Assumption of concentration process of fresh milk

In turn, these would result in the constant HTC regardless of Re for reconstituted milk and a rise in HTC with increasing Re for fresh milk. This is only one of the possible hypotheses to the phenomenon.

4.4.3 Influence of protein content, flow rate and heat flux on HTC

In this section, the effect of protein content, flow rate and heat flux on the performance of the evaporator, in terms of heat transfer coefficient, was evaluated. Sucrose solution was used as the base solution for the experiment and different amount of milk protein concentrate, MPC, (NatraPro MPC85) was added into the sucrose solution to vary the protein content. The concentration of the sucrose-protein solution was kept constant by connecting the condenser back into the feed stream to kept any loss of vapour to the minimum. The viscosity of the sucrose-protein solution was kept within 14 to 18 cP (measured by Endress+Hauser Promass 83I), which is equivalent to skim milk concentrate with total solids of 45wt%. To mimic the operation conditions in a dairy evaporator, pressure was kept at 20kPa (absolute) throughout the entire experiment. Detail photographs were taken at time of measurement. Table 4.9 is the list of conditions tested on the electric heated pilot evaporator using sucrose-protein solutions.

Table 4.9 Test conditions for HTC measurements using sucrose-protein solutions

Conditions	Test Range
Protein Content (wt%)	0, 0.1, 0.3, 0.6, 0.9, 2.0
Heat Flux ($kW\ m^{-2}$)	3.75, 6.25, 8.75, 11.25
Flow rate ($L\ min^{-1}$)	4, 7, 10

4.4.3.1 Influence of protein content

When the sucrose-protein solution was subjected to 6.25 kW m^{-2} of heat flux during evaporation as shown in Figure 4.30, the HTC rises steeply from 1.4 to 2.5 kW $m^{-2}K^{-1}$ between 0 to 0.3wt% of protein content. Thereafter, the rate of increase in HTC begins to slow down and eventually plateau at 2.0wt% protein with HTC of almost 3.0 kW $m^{-2}K^{-1}$. Similar trend was observed throughout all flow rates and the other heat fluxes.

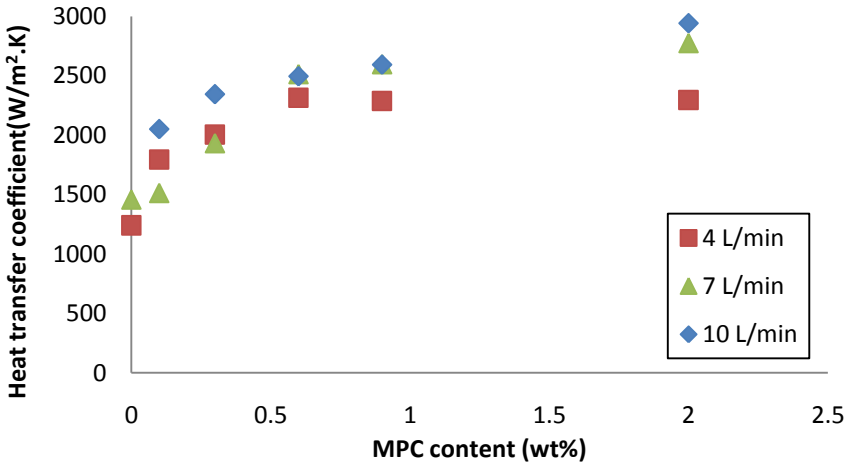

Figure 4.30 Heat transfer coefficient of electric-heated pilot evaporator with heat flux of 6.25kW m^{-2}

When the photographs were reviewed, a trend was observed on the number of bubbles formed during the evaporation process. For all heat fluxes and flow rates tested, the number of bubbles formed increases consistently with increasing protein content in the solution. A sample of the trend were displayed Figure 4.31.

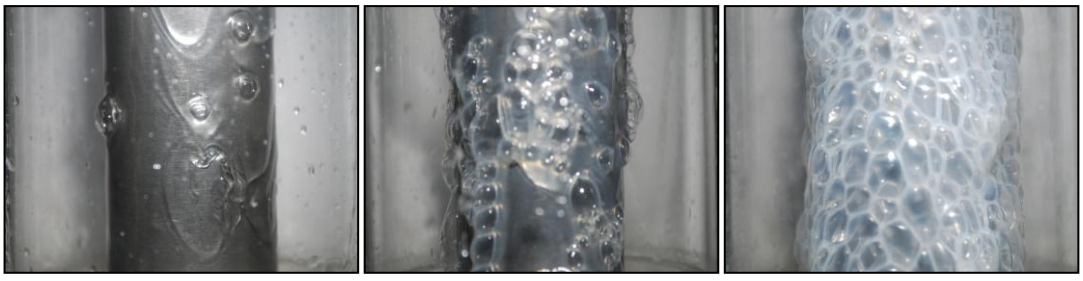

Figure 4.31 A series of photographs taken during the evaporation of sucrose-protein solution at 7L min^{-1} and 6.25kW m^{-2}. (a) 0 wt% MPC, (b) 0.6 wt% MPC and (c) 2.0 wt% MPC

A point to note, the change in appearance of sucrose-protein solution from transparent (0 wt% MPC) to white (2.0 wt% MPC) in color was due to the introduction of MPC into the sucrose solution.

The increase in bubble during boiling of sucrose-protein solution could be due to the following reasons. Firstly, the protein molecules introduced to the sucrose solution might have acted as nucleation sites for bubble to form during nucleation boiling. Secondly, the protein added lowers the surface tension of the sucrose-protein solution (see section 2.3), this enhances the stability of the bubbles formed. Therefore, the bubbles seen in the photograph could be an accumulation of bubbles formed at different time rather than instantaneous bubble formation.

4.4.3.2 Influence of flow rate

From Figure 4.32, the flow rate has the greatest effect on pure sucrose solution during the evaporation process where the HTC doubled from 1.35 kW $m^{-2}K^{-1}$ at 4 and 7 L min^{-1} to nearly 2.8 kW $m^{-2}K^{-1}$ at 10 L min^{-1}. As for the sucrose-protein solutions, only marginal improvement (maximum of 0.5 kW $m^{-2}K^{-1}$) in HTC was observed by increasing the flow rate and seems to plateau at around 3.0 kW $m^{-2}K^{-1}$. However, even with minute amount of protein added to the sucrose solution, the HTC improved, on average, by nearly 65% at 4 and 7 L min^{-1} but no significant difference was recorded at 10 L min^{-1}.

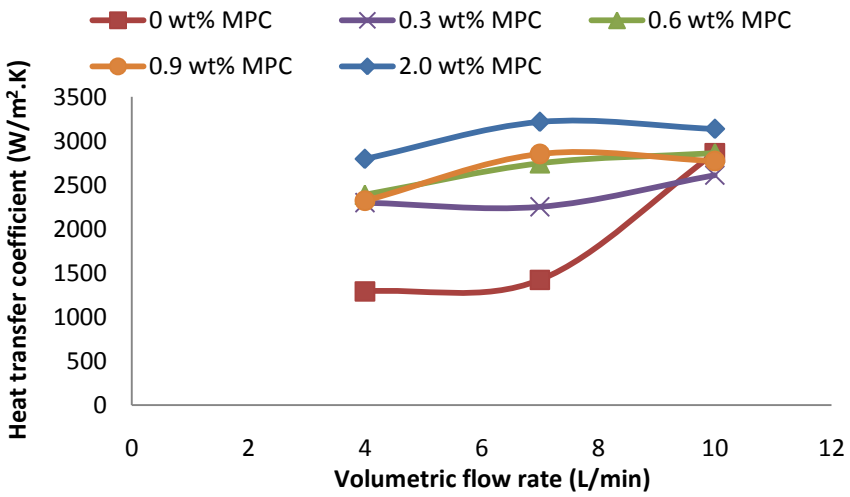

Figure 4.32 Heat transfer coefficient of electric-heated pilot evaporator with heat flux of 8.75kW m^{-2} at various flow rate and protein content

This indicates that similar enhancement of HTC by the adding protein can be replicated by creating more turbulence via increasing flow rate. Coincidentally, more bubbles were observed at 10 L min^{-1} than 4 and 7 L min^{-1} for pure sucrose solution as seen in Figure 4.33. These bubbles could be induced by the turbulence created by the higher flow rate.

(a) (b) (c)

Figure 4.33 A series of photographs taken during the evaporation of pure sucrose solution at 8.75kW m^{-2}. (a) 4 L min^{-1}, (b) 7 L $min^{-1}$and (c) 10 L min^{-1}

4.4.3.3 Influence of heat flux

The influence of heat flux on HTC is mild with pure sucrose solution where the HTC increased by merely 30% between 3.75 to 11.75 kW m^{-2}. On the other hand, sucrose-protein solution at 2.0 wt% MPC has shown an improvement in HTC by 2 folds, from 1.68 to 3.25 W m^{-2} K^{-1}.

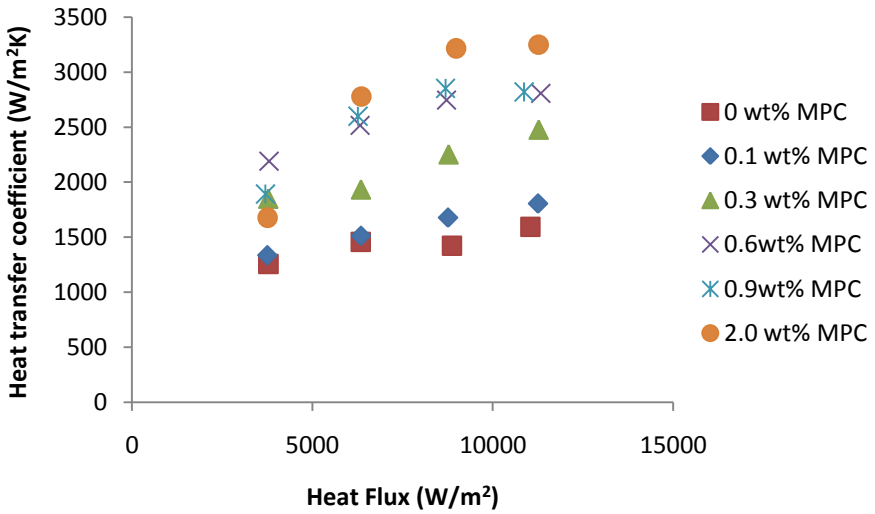

Figure 4.34 Heat transfer coefficient of electric-heated pilot evaporator with flow rate of 7 $Lmin^{-1}$ at various heat flux and protein content

With increasing protein content, the influence of heat flux becomes more apparent as the gradient of HTC with heat flux becomes steeper as illustrated in Figure 4.34.

The photographs also reveal the bubbling trend. Generally, the amount of bubbles increases with the heat flux for all solution tested. However, the increasing intensity of bubbling with rising heat flux was more obvious for sucrose-protein solution than pure sucrose as seen in Figure 4.35, Figure 4.36 and Figure 4.37.

(a) (b) (c)

Figure 4.35 A series of photographs taken during the evaporation of pure sucrose solution at 7 L min^{-1} (a) 3.75 kW m^{-2}, (b) 8.75 kW m^{-2} and (c) 11.25 kW m^{-2}

(a) (b) (c)

Figure 4.36 A series of photographs taken during the evaporation of sucrose-protein solution at 0.6 wt% MPC and 7 L min^{-1} (a) 3.75 kW m^{-2}, (b) 8.75 kW m^{-2} and (c) 11.25 kW m^{-2}

(a) (b) (c)

Figure 4.37 A series of photographs taken during the evaporation of sucrose-protein solution at 2.0 wt% MPC and 7 L min^{-1} (a) 3.75 kW m^{-2}, (b) 8.75 kW m^{-2} and (c) 11.25 kW m^{-2}

For the complete set of pictures on the bubbling trends with respect to the tested parameters, see Appendix A.5.

4.5 Conclusions

In this chapter, experimental investigations of heat transfer within falling film evaporator under various operation conditions were conducted. The design considerations and engineering requirements for effective measurement of heat transfer were also described in detail. The design of the electric-heated pilot evaporator was different compared to commercial falling film evaporator mainly due to the better direct measurement of the temperature difference between the heat transfer surface and the process fluid. Clear perspex shell of the evaporator enables visual observation of the boiling fluid within the evaporator.

The measurement of overall heat transfer coefficient (OHTC) of steam-heated pilot evaporator was based on the rate of condensation collected throughout the evaporation process. Boiling point elevation of milk at various solids content was taken into account when the temperature difference between the steam and boiling milk was calculated. The OHTC fell from 2.5 to 1.3 kW $m^{-2}K^{-1}$ during the evaporation of fresh medium heat treated skim milk from around 30wt% to 57wt% (see Figure 4.24). When Re is above 130, the OHTC maintained at 2.5 kW $m^{-2}K^{-1}$. This corresponded to the evaporation of skim milk concentrate up to 46wt%. Below Re 130, the OHTC decrease exponentially as Re reduces. The gear pump used in the steam-heated pilot evaporator was suppose to perform better than the centrifugal counterpart at high viscosity, yet, it still exhibited a 20% reduction in pump capacity when it was pumping skim milk concentrate from 50 to 57wt%. The high pressure drop across the preheater could be the cause of the reduction in pump performance. However, the deterioration of pump capacity at high solids content could be a potential problem if commercial evaporators continue to use centrifugal pumps, especially at the last few stages of the evaporation process.

The heat transfer investigation on the electric-heated pilot evaporator was separated into two sections.

Firstly, a comparison of heat transfer within the evaporator between reconstituted and fresh medium heat-treated skim milk was conducted. The difference in trends

between the heat transfer coefficients of both type of milk was apparent. The reconstituted skim milk maintained at around 3.75 kW $m^{-2}K^{-1}$ regardless of heat flux and Re. On the other hand, the fresh skim milk displayed a positive linear relationship between the HTC and Re. When 100 <Re<500 , the HTC rose from 3.0 to 6.0 kW $m^{-2}k^{-1}$. The difference in HTC trend between the milks could be due to the magnitude of turbulence created by bubbling during the evaporation process, which are affected by the states of the proteins involved.

The second part focused on the influence of protein content (milk protein concentrate was added), flow rate and heat flux has on the heat transfer within the evaporator. The HTC almost doubled when the protein content increased from 0 to 0.9wt. Only marginal improvement (less than 20%) in HTC was observed when the flow rate was increased from 4 to 10 L min^{-1} except for pure sucrose solution where HTC increased from 1.5 to 3.0 kW $m^{-2}k^{-1}$ between 7 to 10 L min^{-1}. However, the influence of heat flux becomes greater with increasing protein content. From the results, it was concluded that protein content overshadows the degree of influence by heat flux and flow rate have on the heat transfer. From the study of the photographs taken, the amount of bubbles formed generally increases with all the factors tested although level of increment differs with protein content.

4.6 Nomenclature

A	Area of heating surface	m^{-2}
$A_i \; and \; A_o$	Inner and outer surface area of the tube	m^2
A_m	Log mean area for heat transfer	m^2
F	Mass flow rate of feed	$kg.s^{-1}$
h_c	Enthalpy of condensate	$J.kg^{-1}$
h_f	Enthalpy of feed	$J.kg^{-1}$
$\bar{h}_{dc}$	Heat transfer coefficient of dropwise condensation	$W.m^{-2}\,K^{-1}$
h_{fg}	Latent heat	$J.kg^{-1}$
h_i	Heat transfer coefficient of evaporative side	$W.m^{-2}\,K^{-1}$
h_o	Heat transfer coefficient at the product side	$W.m^{-2}\,K^{-1}$

h_p	Enthalpy of product	J.kg^{-1}
h_s	Enthalpy of steam	J.kg^{-1}
h_s	Heat transfer coefficient at the heating (steam) side	W.m^{-2} K^{-1}
I	Current (Ampere)	A
k_L	Liquid thermal conductivity	W.m^{-1} K^{-1}
k_w	thermal conductivity of wall	W.m^{-1} K^{-1}
m, n	Constants	-
m_{evap}	Mass of water evaporated	kg
$\dot{m}_{\text{feed}}$	Mass flow rate of feed	kg.s^{-1}
m_{steam}	Mass of steam utilised	kg
N	Maximum numbers of effects	-
n_{tubes}	Number of tubes	-
P	Power	W
Pr	Prandtl number	-
q	Heat transfer	W
q"	Heat flux	W.m^{-2}
R_{wall}	Wall resistance	m^{2}K.W^{-1}
Re	Reynolds number	-
r_f	Resistance due to fouling on the heat transfer surface	m^{2}K.W^{-1}
T_e	Tempearature elevation	°C or K
T_p	Temperature of process milk	°C or K
T_s	Temperature of steam	°C or K
T_{sat}	Saturation temperature	°C or K
T_w	Wall temperature	°C or K
ΔT	Temperature difference between the heating medium and the boiling medium	°C or K
U	Overall heat transfer coefficient	W.m^{-2}K^{-1}
V	Mass flow rate of vapour	kg.s^{-1}
V	Voltage	V
x	Wall thickness	m

x_F	Solid mass fraction of feed	-
x_P	Solid mass fraction of product	-
η	Viscosity	Pa.s
η_L	Liquid viscosity	Pa.s
Γ	Mass flow rate per unit perimetric length	$kg.m^{-1}s^{-1}$
Γ_{min}	Minimum mass flow rate per unit perimetric length	$kg.m^{-1}s^{-1}$
Γ_T	Terminal flow rate	$kg.m^{-1}s^{-1}$
σ	Surface tension of liquid	$N.m^{-1}$

4.7 References

Al-Roubaie, S. M. &Burton, H. (1979). Effects of Free Fatty Acids on the Amount of Deposit from Milk on Heated Surfaces. *Journal of Dairy Research* 46: 463 - 471.

Angelletti, S. &Moresi, M. (1983). Modelling of multiple effect falling film evaporators. *J. Food Technol.* 18: 539.

Bansal, B. &Chen, X. D. (2006). Comprehansive Reviews in Food Science and Food Safety: A Critical Review of Milk Fouling in Heat Exchangers. *Institute of Food Technologists* 5: 27 - 33.

Belmar-Beiny, M. T., Gotham, S. M., Paterson, W. R., Fryer, P. J. &Pritchard, A. M. (1993). The Effect of Reynolds number and fluid temperature in Whey Protein Fouling. *Journal of Food Engineering* 19: 119 - 139.

Beuf, M., Rizzo, G., Leuliet, J. C., Muller-Steinhagen, H., Yiantsios, S., Karabelas, A. &Benezech, T. (2007). Fouling and Cleaning of Modified stainless Steel Plate Heat Exchangers Processing Milk Products. *2003 ECI Conference Proceedings*: 99 - 106.

Boland, M. (2003).Influences on Raw Milk Quality. In *Dairy Processing - Improving Quality*(Ed S. G). Woodhead Publishing.

Bott, T. R. (1995). *Fouling of Heat Exchangers.* Amsterdam: Elsevier Science.

Bouman, S., Waalewijn, R., De Jong, P. &Van Der Linden, H., J. L. J. (1993). Design of falling-film evaporators in the dairy industry. *International Journal of Dairy Technology* 46(3): 100-106.

Burdett, M. (1974). The Effect of Phosphates in Lowering the Amount od Deposit Formation during the Heat Treatment of Milk. *Journal of Dairy Research* 41: 123 - 129.

Burton, H. (1968). Deposits of Whole Milk in Treatment Plants: A Review and Discussion. *Journal of Dairy Research* 35: 317 - 330.

Bylund, G. (1995). *Dairy Processing Handbook.* Lund: Tetra Pak Processing Systems AB.

Changani, S. D., Belmar-Beiny, M. T. &Fryer, P. J. (1997). Engineering and Chemical Factors Associated With Fouling and Cleaning in Milk Processing. *Experimental thermal and fluid science* 14: 392 - 406.

Chen, S. C. &Hernandez, E. (1997).Design and performance evaluation of evaporators. In *Handbook of food engineering practice*, 211 - 252 (Eds K. J. Valentas, E. Rotstein and R. P. Singh). New York: CRC Press.

Chen, S. L., Gerner, C. L. &Tien, C. L. (1987). General film condensation correlations. *Experimental Heat Transfer* 1(2): 93 - 107.

Chun, K. R. &Seban, R. A. (1971). Heat Transfer to Evaporating Liquid Film. *Heat Transfer Trans. ASME Ser. C* 93: 391.

de Jong, P. (1997). Impact and Control of Fouling in Milk Processing. *Trends Food Sci Technol* 8: 401 - 405.

de Jong, P., van der Horst, H. C. &Waalewijn, R. (1998).Reduction of Protein and Mineral Fouling. In *Fouling and Cleaning in Food Processing*Luxembourg.

Deplace, F., Leuliet, J. C. &Levieux, D. (1997). A Reaction Engineering Approach to the Analysis of Fouling by Whey Proteins of Six-Channel-Per-Pass Plate Heat Exchangers. *Journal of Food Engineering* 34: 91 - 108.

Foster, C. L., Britten, M. &Green, M. L. (1989). A Model Heat-Exchanger Apparatus for the Investigation of Fouling of Stainless Steel Surfaces by Milk. *Journal of Dairy Research* 56: 201 - 209.

Fox, P. F. (1989).The Milk Protein System. In *Developments in Dairy Chemistry*New York: Elsevier Applied Science.

Fox, P. F. &Morrissey, P. A. (1977). Reviews of the Progress of Dairy Science: the Heat Stability of Milk. *Journal of Dairy Research* 44: 627 - 646.

Fryer, P. J. (1986).Modelling Heat Exchanger Fouling. Vol. PhD ThesisCambridge: Univ. Cambridge.

Fryer, P. J., Gotham, S. M. &Paterson, W. R. (1992).The Concentration Dependence of Fouling from Whey Protein Concentrates. In *CHEMECA 92*, Vol. 1, 368 - 375 Canberra: Proc. 20th Aust. Chem. Eng. Conf.

Garett, B. A., Ridges, P. &Noyes, N. J. (1985). *Fouling of Heat Exchangers: Characteristics, Cost, Prevention, Control and Removal.* Englewood Cliffs: Prentice-Hall.

Geankoplis, C. J. (1993).Evaporation. In *Transport Processes and Unit Operation* 489 - 519 New Jersey: Prentice Hall.

Georgiadis, M. C., Rotstein, G. E. &Machietto, S. (1998). Modeling and Simulation of Shell and Tube eat Exchangers under Milk Fouling. *AIChE Journal* 44(4): 959 - 971.

Gordon, K. P., Hankinson, D. J. &Carver, C. E. (1968). Deposition of Milk Solids on Heated Surfaces. *Journal of Dairy Science* 51: 520 - 526.

Gotham, S. M. (1990).Mechanisms of Protein Fouling of Heat Exchangers. Vol. PhD ThesisCambridge: Univ. Cambridge.

Gray, R. M. (1981). Subject: 'Skim milk' technology of skimmed milk evaporation. *Journal of the Society of Dairy Technology* 34(2): 53 - 57.

Gray, R. M. (1984).Evaporation: quality with economy In *Profitability of Food Processing*, 259 London: Institute of Chemical Engineers.

Gynning, K., Thime, K. E. &Samuelsson, E. G. (1958). Das Anbrennen in Plattenerhitzern. *Milchwissenschaft* 13: 62 - 70.

Hall, C. W. &Hedrick, T. I. (1971). *Drying of Milk and Milk Products.* Westport, Conn: AVI.

Hartel, R. W. (1992).Evaporation and Freeze Concentration. In *Handbook of Food Engineering*, 341 (Eds D. R. Heldman and D. B. Lund). New York: Marcel Dekker, Inc.

Hartley, D. E. &Murgatroyd, W. (1964). Criteria for the break-up of thin liquid layers flowing isothemally over solid surfaces. *Int. J. Heat and Mass Transfer* 7: 1003 - 1015.

Hege, W. U. &Kessler, H. G. (1986). Deposit Formation of Protein-Containing Dairy Liquids. *Milchwissenschaft* 41: 356 - 360.

Hegg, P. O., Castberg, H. B. &Lundh, G. (1985). The Fouling of Whey Proteins on Stainless Steel at Different Temperatures. *Journal of Dairy Research* 52: 213 - 218.

Holman, J. P. (1976). *Heat Transfer.* New York: McGraw-Hill Book Company.

Holt, C., Muir, D. D. &Sweetsur, A. W. M. (1978). Seasonal Changes in the Heat Stability of Milk from Creamery Silos in South-West Scotland. *Journal of Dairy Research* 45: 183 - 190.

Hui, Y. H. (2006). *Food Biochemistry & Food Processing.* Iowa: Blackwell Publishing.

Incropera, F. P. &DeWitt, D. P. (2002).Boiling and Condensation. In *Fundamental of Heat and Mass Transfer*, 593 - 640 Hoboken: John Wiley & Sons, Inc.

Jebson, R. S. &Chen, H. (1996). Performances of Falling Film Evaporators on the Whole Milk and a Comparison with performance on Skim Milk. *Journal of Dairy Research* 64: 57-67.

Jeurnink, T. J. M. (1991). Effect of Proteolysis in Milk on Fouling in Heat Exchanger. *Neth. Milk Dairy J.* 45: 23 -32.

Jeurnink, T. J. M. (1995a). Fouling of Heat Exchangers by Fresh and Reconstituted milk and the influence of Air Bubbles. *Milk Sci. Int.* 50(4): 189 - 193.

Jeurnink, T. J. M. (1995b). Fouling of Heat Exchangers in Relation to the Serum-Protein Concentration in Milk. *Milk Sci. Int.* 50(5): 257 - 260.

Kessler, H. G. (1981). *Food Engineering and Dairy Technology* Freising, Germany: Verlag A Kessler.

Kessler, H. G. (1986).Energy aspects of for preconcentration In *Concentration and Drying of Foods*, 147-163 London: Elsevier Applied Science.

Knipschildt, M. E. &Andersen, G. G. (1994).Drying of MIlk and MIlk Products. In *Modern Dairy Technology: Advance in Milk Processing*, Vol. 1(Ed R. K. Robinson). London: Chapman and Hall.

Lewis, M. &Heppell, N. (2000).Fouling, Cleaning and Disinfecting. In *Continuous Thermal Processing of Foods*Gaithersburg: Aspen Publishers.

Lyster, R. L. J. (1970). The Denaturation of Alpha-lactalbumin and Beta-Lactoglobulin in Heated Milk. *Journal of Dairy Research* 37: 233 - 243.

Marshall, R. J. (1986). Increasing Cheese Yields by Heat-Treatment of Milk. *Journal of Dairy Research* 53: 89 - 95.

McAdams, W. H. (1954). *Heat Transmission* New York: McGraw-Hill Book Company.

McKenzie, H. A. (1971). *Milk Proteins: Chemistry and Molecular Biology.* London: Academic Press.

Meili, A. &Stuecheli, A. (1987). *Chem. Eng.* 94(Feb. 16): 133.

Melo, L. F., Bott, T. R. &Bernardo, C. A. (1987). *Fouling Science and Technology.* Alvor: Kluwer Academic Publishers.

Minton, P. E. (1986a). *Handbook of evaporation technology.* Park Ridge, N.J., U.S.A: Noyes Publications.

Minton, P. E. (1986b).Heat Transfer in Evaporators. In *Handbook of Evaporation Technology*, 9 - 38 New Jersey: Noyes Publications.

Minton, P. E. (1986c).Mechanical Vapor Compression. In *Handbook of Evaporation Technology*, 186 - 205 New Jersey: Noyes Publications.

Minton, P. E. (1986d).Thermal Compression. In *Handbook of Evaporation Technology* 176 - 186 New Jersey: Noyes Publications.

Morison, K. R. &Hartel, R. W. (2007).Evaporation and Freeze Concentration. In *Handbook of Food Engineering*(Eds D. R. Heldman and D. B. Lund). Boca Raton: CRC Press.

Muir, D. D., Abbot, J. &Sweetsur, A. W. M. (1978). Changes in the Heat Stability of Milk Protein during the manufacture of Dried Skim Milk. *Journal of Food Technology* 13: 45 - 53.

Muir, D. D. &Sweetsur, A. W. M. (1976). The Influence of Naturally-Occuring Leveles of Urea on the Heat Stability of Milk. *Journal of Dairy Research* 43: 495 - 499.

Muir, D. D. &Sweetsur, A. W. M. (1977). Effect of Urea on the Heat Coagulation of Caseinate Complex in Skim Milk *Journal of Dairy Research* 44: 249 - 257.

Palen, J. W. (1986). *Heat Exchanger Sourcebook.* Berlin: Springer-Verlag.

Pelligreno, L., Resmini, P. &Luf, W. (1995).Assessment (indices) of heat treatment of milk. In *Heat Induced changes in milk*Brussels, Belgium: International Dairy Federation.

Pisecky, I. J. (1997).Evaporation and Membrane Filtration. In *Handbook of Milk Powder Manufacture*, 3-18 Copenhagen: Niro A/S.

Pyne, G. T. (1958). The Heat Coagulation of Milk. II. Variations in Sensitivity of Casein to Calcium Ion. *Journal of Dairy Research* 25: 467 - 474.

Rakes, P. A., Swartzel, K. R. &Jones, V. A. (1986). Deposition of Dairy Protein-containing Fluids on Heat Exchanger Surfaces. *Biotechnology Progress* 2(4): 210 - 217.

Robertson, N. M. &Dixon, A. (1969). The Nitrogen Fractions and the Heat Stability of Bovine Milk. *Agroanimalia* 1: 141 - 144.

Sandu, C. &Singh, R. K. (1991). Energy Incease in Operation and Cleaning Due to Heat Exchanger Fouling in Milk Pasteuration. *Food Technology* 23: 84.

Santos, O., Nylander, T., Rizzo, G., Muller-Steinhagen, H., Tragardh, C. &Paulsson, M. (2003).Study of Whey Protein Adsorption under Turbulent Flow Rate. In *Proceedings of Heat Exchanger Fouling and Cleaning - Fundamentals and Applications*New Mexico: Engineering Conferences International.

Saravacos, G. D. &Kostaropoulos, A. E. (2002).Food Evaporation Equipment. In *Handbook of Food Processing Equipment*, 297 - 329 New York: Klumer Academic/Plenum Publishers.

Sawyer, L. (2003).β-Lactoglobulin. In *Advanced Dairy Chemistry Vol.1, Proteins* (Eds P. F. Fox and P. L. H. McSweeney). New York: Kluwer Academic-Plenum Publisher.

Sawyer, W. H. (1968). Heat Denaturation of Bovine Beta-Lactoglobulins and Relevance of Disulphide Aggregations. *Journal of Dairy Science* 51: 3.

Schwartzberg, H. G. (1989).Food property effects in evaporation. In *Food Properties and COmputer-Aided Engineering of Food Processing Systems*(Eds A. Medina and R. P. Singh). Dordrecht, Netherlands: Kluwer.

Skudder, P. J., Brooker, B. E. &Bonsey, A. D. (1986). Effect of pH on the Formation of Deposit from Milk on Heated Surfaces during UHT Processing. *Journal of Dairy Research* 53: 75 - 87.

Skudder, P. J., Thomas, E. L., Pavey, J. A. &A.G., P. (1981a). Effects of adding Potassium Iodate to Milk before UHT treatment. I. Reduction in the amount of deposit on the heated surfaces *Journal of Dairy Research* 48: 99 - 113.

Skudder, P. J., Thomas, E. L., Pavey, J. A. &Perkin, A. G. (1981b). Effect of Potassium Iodate to Milk before UHT Treatment. *Journal of Dairy Research* 48: 99 - 113.

Standiford, F. C. (1963). Evaporation is a unit operation. *Chem. Eng.* 70(25): 158.

Sweetsur, A. W. M. &Muir, D. D. (1981). Role of Cyanate Ions in the Urea-Induced Stabilization of the Casinate Complex in Skim Milk. *Journal of Dairy Research* 48: 163 - 166.

Thijssen, H. A. C. (1970). Concentration Processes for liquid foods containing volatile flavors and aromas. *J.Food Technol.* 5: 211.

van Asselt, A. J., Visser, M. M. M., Smit, F. &de Jong, P. (2005).In-line control of fouling. In *Engineering Conference International*Germany.

Van Nostrand, W. L., Leach, S. H. &Haluska, J. L. (1981). *Fouling of Heat Transfer Equipment.* Washington: Hemisphere Publishing Corp.

Visser, J. &Jeurnink, T. J. M. (1997). Fouling of Heat Exchangers in Dairy Industry. *Exp Therm Fluid Sci* 14: 407 - 424.

Walstra, P., Wouters, J. T. M. &Geurts, T. J. (2006).Colloidal Particles of Milk. In *Dairy Science and Technology*, 109-157 Boca Raton: CRC Press.

Welty, J. R., Wicks, C. E. &Wilson, R. E. (1984). *Fundamentals of Momentum, Heat and Mass Transfer.* New York: John Wiley & Sons, Inc.

Westergaard, V. *Milk Powder Technology, Evaporation and Spray Drying.* Niro Hudson, Inc., Hudson, WI.

Westergaard, V. (1994).Evaporation. In *Milk Powder Technology: Evaporation and Spray Drying*: NIRO A/S, Copenhagen

Zimmer, A. (1980). *Chem. Eng. Progr.* 76(9): 37.

CHAPTER FIVE: MODELLING OF AN EVAPORATOR

5.0 MODELLING OF EVAPORATORS

In the previous chapters, the physical properties of milk and heat transfer within a falling film evaporator were investigated. They, together with other correlations, are the foundations of a model shown here for a falling film evaporator. The fundamental components that constitutes an evaporator model is illustrated in Figure 5.2. In this chapter, the process of building a mathematical model for the steam-heated pilot evaporator is described in detail. The applications of this model to the commercial evaporator are also discussed.

5.1 Pilot Evaporator Modelling Philosophy

The approach of creating a model that simulates the steam-heated pilot evaporator is to divide the length of the evaporation column into smaller sections where heat and mass transfer would be balanced. Within each section, the heat energy, mainly from the condensation of steam in the shell side, passes through the tube wall onto the flowing milk film on the tube side. This energy boils and evaporates water from the milk, hence concentrating the milk.

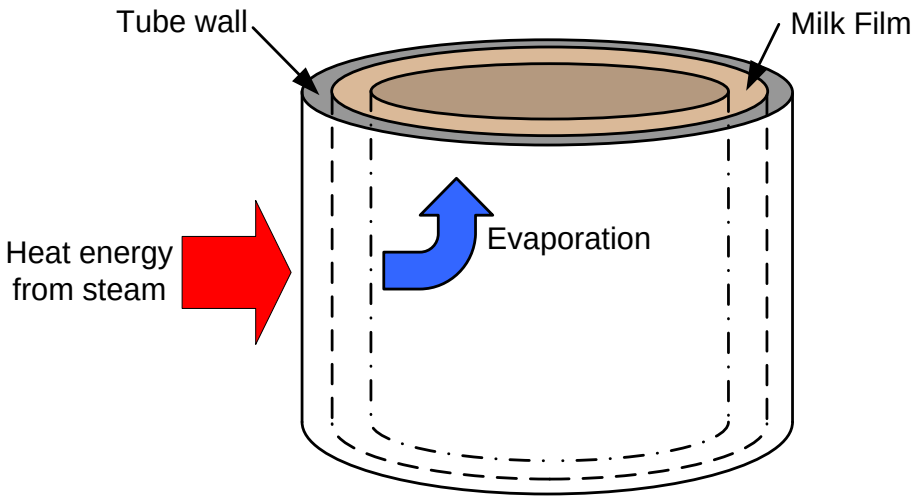

Figure 5.1 Illustration of heat and mass transfer in a section of an evaporation tube

As the steam-heated pilot evaporator is a batch process unit, the processing time instead of the location on the evaporator determines the total solids of the milk.

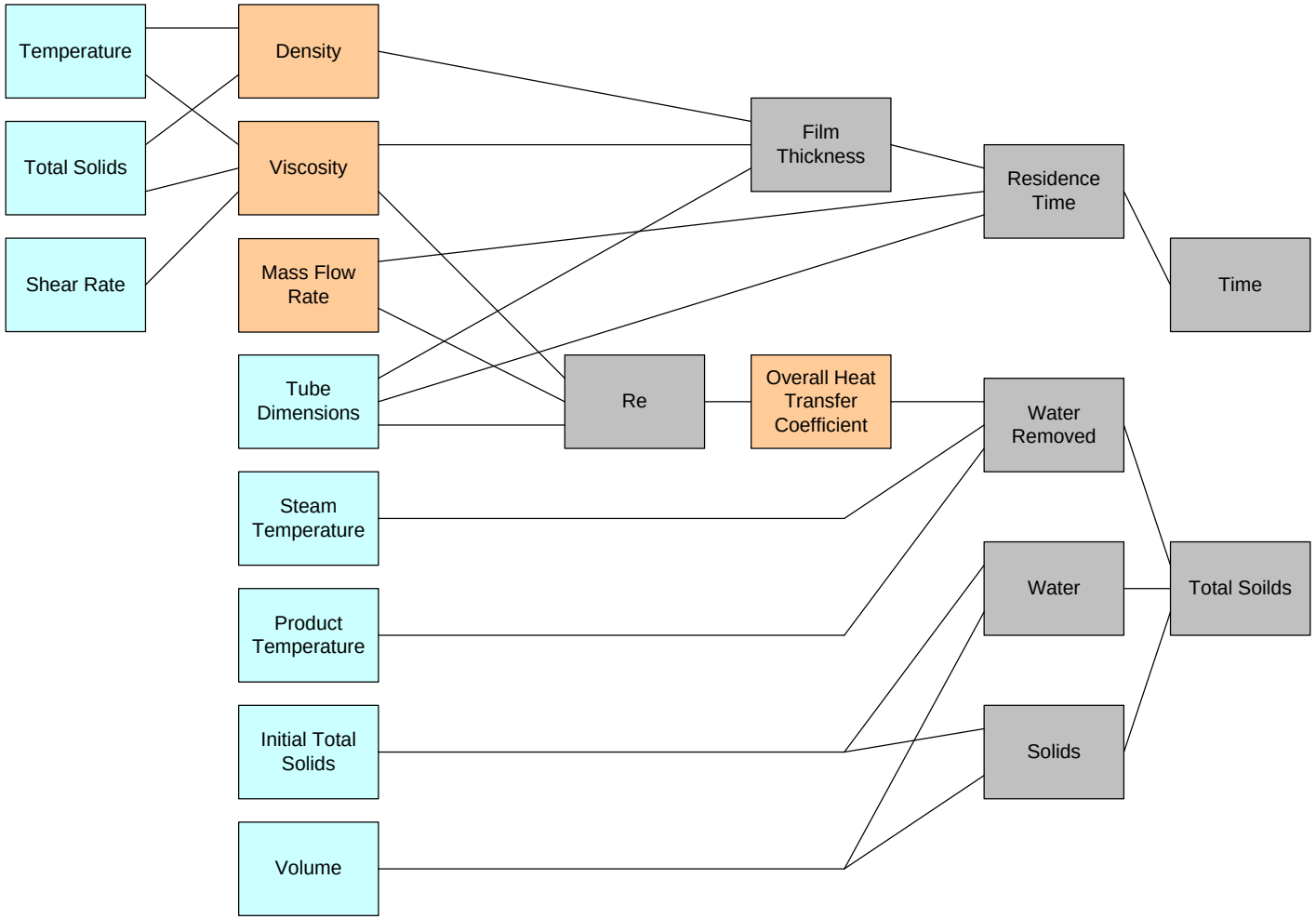

Figure 5.2 Relationship between the process parameters and structural dimensions in the modelling of an evaporator

5.2 Mass and Energy Balance

Figure 5.3 illustrates a material-balance diagram for a falling film evaporator. The column is fed with F kg/min of milk with total solid x_F and leaves the evaporator at P kg/min of milk with total solid x_P and V kg/min of water vapour. Two independent overall material balances can be written,

Total material balance

$$F = P + V \tag{5.1}$$

Water balance

$$F(1 - x_F) = P(1 - x_P) + V \tag{5.2}$$

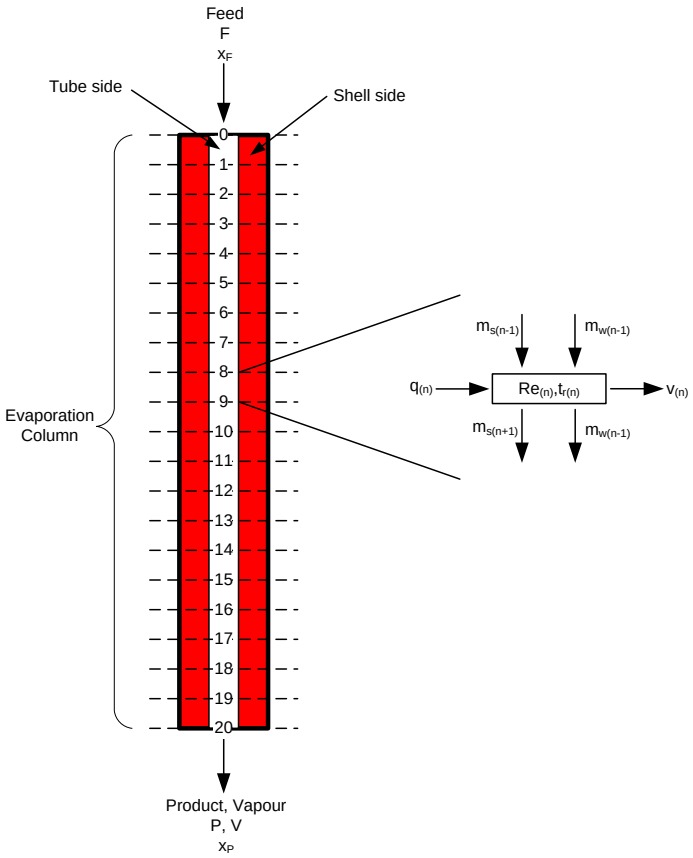

Figure 5.3 Step-wise heat and mass transfer model within a section of the evaporator

The 2m evaporation column is divided into 20 equal sections (100mm each). Within each section, heat energy transferred from the steam side of the evaporator, q, vaporises a small amount of water, v, as milk flows, Re, along the evaporation tube. The mass of water after each section, $m_{w(n+1)}$, can be calculated by

$$m_{w(n+1)} = m_{w(n-1)} + v_{(n)} \quad (5.3)$$

where n is the number of calculation steps

While the mass of solids remains the same after each section.

$$m_{s(n+1)} = m_{s(n-1)} \quad (5.4)$$

From the experimental data in section 4.4.1, the overall heat transfer of steam-heated pilot evaporator (kW $m^{-2}K^{-1}$) was related to Reynolds number, Re by the following correlation

$$U = -6223 \cdot Re^{-0.5993} + 2732 \quad (5.5)$$

With this correlation, the next stage of creating the model is to calculate the residence time within each section of the tube and the flow characteristic, Re, of skim milk concentrate.

5.3 Residence Time and Flow Characteristic

Residence time, t_r, is the amount of time the fluid stayed in a processing unit. In a batch evaporator, it is crucial to determine the residence time of liquid within the evaporator as milk gets concentrated over time.

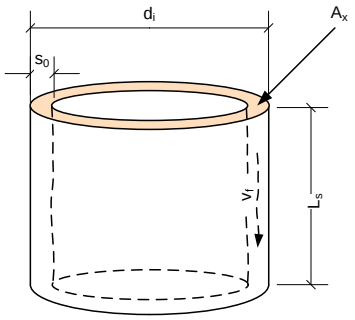

Figure 5.4 A section of the evaporation tube

The calculation of residence time, $t_r(s)$, in one section can be derived from

$$t_r = L_s/v_f \tag{5.6}$$

where L_s is the section length (m) and v_f is the film velocity (m s^{-1})

5.3.1.1 Liquid velocity

$$v_f = \left(\frac{m}{\rho_l}\right)/A_x \tag{5.7}$$

where m is mass flow rate (kg s^{-1}), ρ_l is the liquid density (kg m^{-3}) and A_x is the cross-section area of the liquid film (m^2).

5.3.1.2 Cross-section area

$$A_x = \left(\frac{\pi}{4}\right)[d_i^2 - (d_i - 2s_0)^2] \tag{5.8}$$

where $d_i$is the tube inner diameter (m) and s_0 is the film thickness (m).

5.3.1.3 Film thickness

The equation to determine the film thickness (s_0) is taken from Evaporation Technology: principles, applications, economics (Billet, 1989).

$$s_0 = \sqrt[3]{\frac{3\mu\Gamma}{3600\rho^2 g}} \tag{5.9}$$

where η is the viscosity of liquid (Pa.s), Γ is the liquid load on the tube ($kgs^{-1}m^{-1}$), ρ is the density of liquid and g is gravitational acceleration ($m\ s^{-2}$). The viscosity used in this equation is derived from the viscosity model in section 3.8.3.

5.3.1.4 Liquid load

Liquid load is the mass of the liquid flowing per unit length on the circumference of tube wall.

$$\Gamma = \frac{m}{\pi \cdot d_i} \tag{5.10}$$

Therefore, the residence time, t_r (s), within each section is a function of viscosity of milk, μ (Pa.s), mass flow rate, m ($kg\ s^{-1}$), tube diameter, d_i (m), section length, L_s (m), and liquid density, ρ_l ($kg\ m^{-3}$).

$$t_r = f(\mu, m_T, d_i, L_s \text{ and } \rho_l) \tag{5.11}$$

The residence time in each section of the tube varies as the viscosity, density and mass flow rate changes with time. The viscosity of milk rises with concentration.

The accumulation of residence time in each calculation steps is the processing time, t_c.

$$t_{c(n)} = \sum_{n=1} t_{r(n)} \tag{5.12}$$

5.3.2 Reynolds Number, Re

Reynolds number can be calculated by the following equation:

$$\mathrm{Re} = \frac{4\Gamma}{\eta} \tag{5.13}$$

where Γ is the liquid load (kg s^{-1} m^{-1}) on the tube and μ is the dynamic viscosity (Pa.s)

5.4 Calculation Logic of Pilot Evaporator Model

With the balance of heat and mass transfer and residence time in each section completed. The next step was to design a logic that organise the calculation steps. The logic behind a batch evaporator is slightly more complex than a single pass evaporator as the recirculation of milk in the steam-heated pilot evaporator would result in the concentration of milk over time. Therefore, the logic has to take account of the recirculation of milk and the increase in total solids over time. In contrast, the conditions of the milk entering a single pass falling film evaporator are the same during steady state operation.

In order for the model to work, some initial input parameters, such as initial concentration of milk, process volume, tube dimensions, flow rate, etc., are required. With the initial input parameters, the model can proceed to calculate Re, residence time and the amount of water evaporated within each section. When the calculation reaches the end of the evaporation column, it will restart from the first section again. This cycle repeats until the evaporation process finishes. The complete logic of the evaporator is illustrated in Figure 5.5.

Below are the assumptions were also made for the pilot evaporator model:

- Heat transfer along the entire evaporation tube is uniform
- Ideal mixing within the tank
- Feed of identical total solids level is fed to the evaporator within a cycle
- Liquid forms a thin uniform film along the entire evaporation tube

- All vapour evaporated condenses in the condenser and are collected for overall heat transfer coefficient calculation

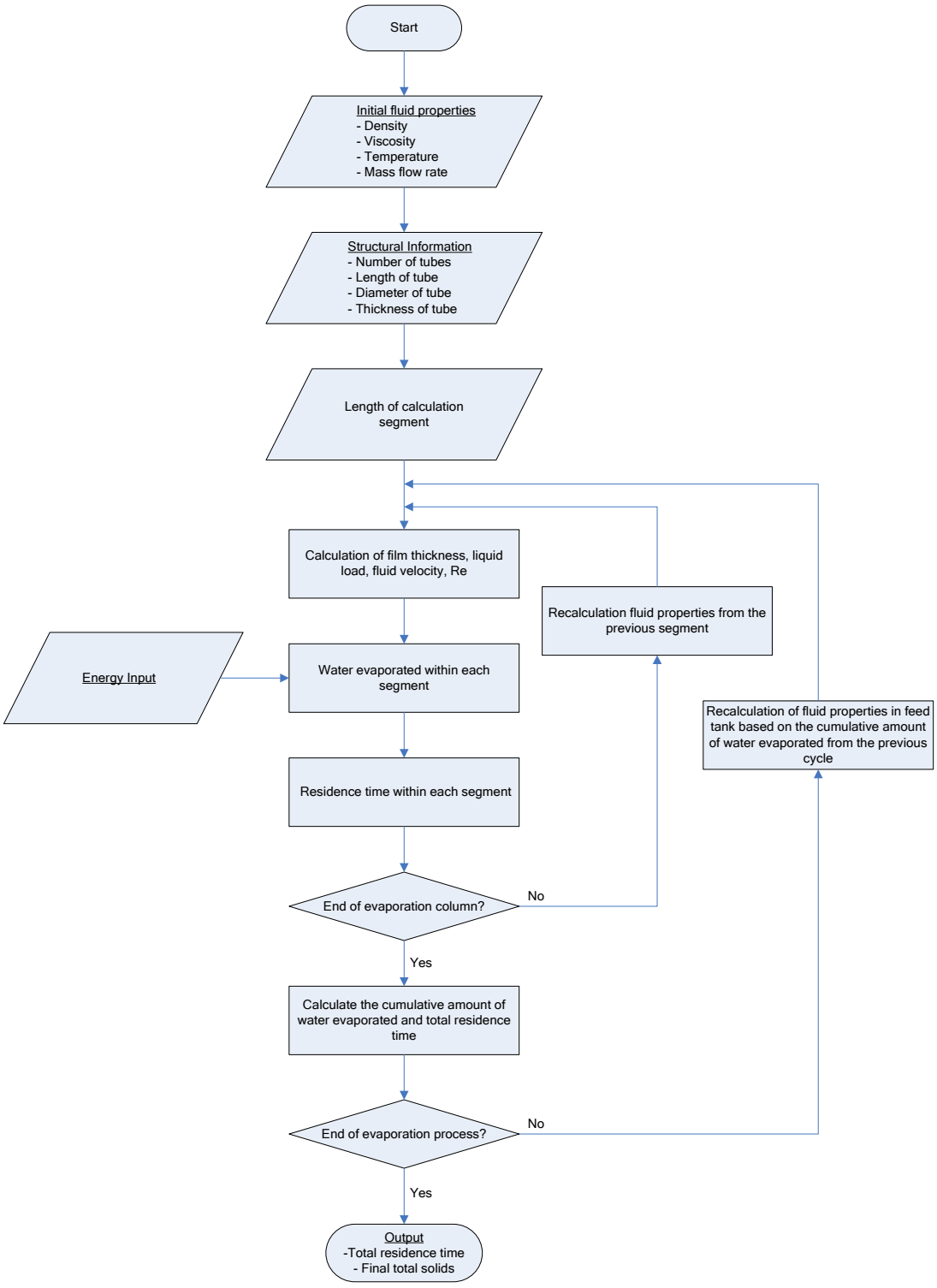

Figure 5.5 **Logic of the steam-heated pilot evaporator model**

5.4.1 Calculation of the amount of water evaporated and processing time

For every 21 calculation steps, it represents a complete cycle through the evaporator. The beginning of a new cycle is then fed with milk of slightly higher solids which is calculated based on the amount of water evaporated from the previous cycles. Figure 5.6 is a sample calculation sheet of the model and the cell highlighted in reds and greens have identical total solids and they indicate the beginning of a new calculation cycle.

To calculated the amount of water evaporated at any given number of calculation steps,

For n = 1 to 21, the milk is fed into the evaporator for the first time.

When n ≤ 21

$$\Delta v_n = \sum_{i=0}^{n} (n-i) v_{(i+1)} \tag{5.14}$$

For n >21, the process milk re-enters the evaporator.

When n > 21

$$\Delta v_n = \Delta m_{n-1} + \sum_{i=0}^{20} v_{(n-i)} \tag{5.15}$$

To calculated the processing time, t (s) at any given number of calculation steps,

$$\mathrm{t_{(n)}} = \sum_{\mathrm{i=1}}^{\mathrm{n}} \mathrm{t_{r(i)}} \tag{5.16}$$

	n	Length (mm)	Solid Content, X, (wt%)	Liquid Load, Γ, ($kg\ s^{-1}.m^{-1}$)	Product Density, ρ, ($kg\ m^{-3}$)	Viscosity, μ, (Pa.s)	Reynolds Number, Re	Film Thickness, s_0, (mm)	Overall Heat Transfer Coefficient, U, ($W/m^2.K$)	Heat Transfer Rate, q, (W)	Heat of Vaporisation, h_v, (J/kg)	Residence Time, t_r, (s)	Cumulative Residence Time, t_c, (s)	Water Evaporated, v, (kg)	Cumulative Water Evaporated, v_c,(kg)	Solids Load, ($kgs^{-1}.m^{-1}$)	Tank Concentration, (wt%)
	1	0	29.0300	0.6250	1095.83	0.00395	632.8	0.8567	2601.62	188.01	2355862.7	0.1376	0.1376	1.0980E-05	1.0980E-05	0.1814	29.03
	2	100	29.0814	0.6239	1096.06	0.00397	629.2	0.8572	2601.17	187.98	2355862.7	0.1377	0.2753	1.0986E-05	3.2945E-05	0.1814	29.03
	3	200	29.1329	0.6228	1096.29	0.00398	625.6	0.8577	2600.72	187.94	2355862.7	0.1378	0.4131	1.0993E-05	6.5905E-05	0.1814	29.03
	.	.	.	.	.	.	.	.	.	.	.	.	.	.	.	.	.
	.	.	.	.	.	.	.	.	.	.	.	.	.	.	.	.	.
	.	.	.	.	.	.	.	.	.	.	.	.	.	.	.	.	.
	.	.	.	.	.	.	.	.	.	.	.	.	.	.	.	.	.
	.	.	.	.	.	.	.	.	.	.	.	.	.	.	.	.	.
	19	1800	29.9821	0.6051	1100.14	0.00425	569.3	0.8663	2593.09	187.39	2355862.7	0.1397	2.6335	1.1110E-05	2.0942E-03	0.1814	29.03
	20	1900	30.0368	0.6040	1100.39	0.00427	565.8	0.8669	2592.58	187.36	2355862.7	0.1398	2.7733	1.1117E-05	2.3151E-03	0.1814	29.03
New cycle	21	2000	30.0916	0.6029	1100.64	0.00429	562.4	0.8674	2592.08	187.32	2355862.7	0.1399	2.9132	1.1125E-05	2.5472E-03	0.1814	29.03
→	22	0	29.0341	0.6250	1095.85	0.00395	632.6	0.8568	2601.60	188.01	2355862.7	0.1376	3.0508	1.0981E-05	2.7792E-03	0.1815	29.03
	23	100	29.0855	0.6239	1096.08	0.00397	629.0	0.8573	2601.15	187.97	2355862.7	0.1377	3.1885	1.0988E-05	3.0113E-03	0.1815	29.03
	24	200	29.1370	0.6228	1096.31	0.00398	625.4	0.8578	2600.70	187.94	2355862.7	0.1378	3.3263	1.0995E-05	3.2434E-03	0.1815	29.04
	.	.	.	.	.	.	.	.	.	.	.	.	.	.	.	.	.
	.	.	.	.	.	.	.	.	.	.	.	.	.	.	.	.	.
	.	.	.	.	.	.	.	.	.	.	.	.	.	.	.	.	.
	.	.	.	.	.	.	.	.	.	.	.	.	.	.	.	.	.
	.	.	.	.	.	.	.	.	.	.	.	.	.	.	.	.	.
	40	1800	29.9863	0.6051	1100.16	0.00425	569.1	0.8664	2593.06	187.39	2355862.7	0.1397	5.5470	1.1111E-05	6.9567E-03	0.1815	29.04
	41	1900	30.0410	0.6040	1100.41	0.00427	565.7	0.8670	2592.56	187.35	2355862.7	0.1398	5.6868	1.1118E-05	7.1888E-03	0.1815	29.04
New cycle	42	2000	30.0958	0.6029	1100.66	0.00429	562.2	0.8675	2592.05	187.32	2355862.7	0.1399	5.8268	1.1126E-05	7.4209E-03	0.1815	29.04
→	43	0	29.0419	0.6250	1095.88	0.00395	632.2	0.8570	2601.55	188.00	2355862.7	0.1376	5.9644	1.0983E-05	7.6530E-03	0.1815	29.04
	44	100	29.0933	0.6239	1096.11	0.00397	628.6	0.8575	2601.11	187.97	2355862.7	0.1377	6.1021	1.0990E-05	7.8851E-03	0.1815	29.04
	45	200	29.1449	0.6228	1096.35	0.00399	625.0	0.8580	2600.65	187.94	2355862.7	0.1378	6.2400	1.0997E-05	8.1172E-03	0.1815	29.04
	.	.	.	.	.	.	.	.	.	.	.	.	.	.	.	.	.
	.	.	.	.	.	.	.	.	.	.	.	.	.	.	.	.	.
	.	.	.	.	.	.	.	.	.	.	.	.	.	.	.	.	.
	.	.	.	.	.	.	.	.	.	.	.	.	.	.	.	.	.
	.	.	.	.	.	.	.	.	.	.	.	.	.	.	.	.	.
	61	1800	29.9944	0.6052	1100.19	0.00426	568.8	0.8666	2593.01	187.39	2355862.7	0.1397	8.4612	1.1113E-05	1.1831E-02	0.1815	29.05
	62	1900	30.0490	0.6041	1100.44	0.00427	565.3	0.8671	2592.51	187.35	2355862.7	0.1398	8.6010	1.1121E-05	1.2063E-02	0.1815	29.05
	63	2000	30.1039	0.6030	1100.69	0.00429	561.9	0.8677	2592.00	187.31	2355862.7	0.1400	8.7410	1.1128E-05	1.2295E-02	0.1815	29.05

Figure 5.6 Sample calculation spreadsheet

5.5 Verification of Pilot Evaporator model

The completed steam-heated pilot evaporator model was also verified with the 2 sets of randomly chosen experimental data to test its accuracy. The first set evaporates water from fresh medium heat-treated skim milk while the second set uses reconstituted medium heat-treated skim milk.

5.5.1 Case study 1

5.5.1.1 Input parameters

Table 5.1 shows the initial input parameters that are required to be specified for case study 1.

Table 5.1 Initial conditions and parameters for case study 1

Parameters/Dimensions	Value	Units
Initial Inlet Flow Rate	2.7	L min^{-1}
Initial Solid Content	29.03	wt%
Inlet Product Temp to Evaporator	62	°C
Initial Batch Volume	15.5	L
Saturated Steam Temp. in Evaporator	70	°C
Saturated Product Vapour Temperature	60	°C
Tube Length	2000	mm
Number of Tube	1	
Wall Thickness	1.2	mm
Inner Tube Diameter	23	mm
Outer Tube Diameter	25.4	mm
Calculation Section Length	100	mm

The specification of the initial conditions and parameters enables the calculation of the following list of properties in Table 5.2.

Table 5.2 Additional processing information for case study 1

Inlet feed density	1117.89	kg m^{-3}
Initial feed flow rate	0.0503	kg s^{-1}
Solid mass in initial batch of milk	5.8618	kg
Water mass in initial batch of milk	11.4655	kg
Saturated steam pressure	31.25	kPa
Saturated product pressure	19.88	kPa

The model then calculates the increase in total solids over time from the evaporator as shown in Figure 5.7.

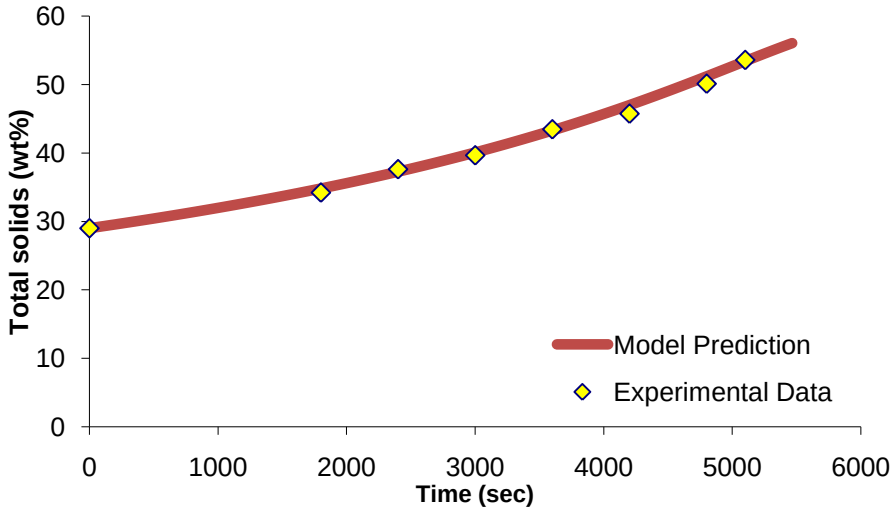

Figure 5.7 Comparison between the steam heated pilot evaporator model and the experimental data in case study 1

The model works very well in the predicting the total solids at any given time with a R^2 of 0.9935. In total, 30680 step calculations were required to create the plot in Figure 5.7.

5.5.2 Case study 2

5.5.2.1 Input parameters

In case study 2, there is a slight different in initial solid content and batch volume as compared with case study 1. In Table 5.3 are the initial input parameters that are required to be specified for case study 2, followed by the additional processing information in Table 5.4.

Table 5.3 Initial conditions and parameters for case study 2

Parameters/Dimensions	Value	Units
Initial Inlet Flow Rate	2.7	L min^{-1}
Initial Solid Content	31.54	wt%
Inlet Product Temp to Evaporator	62	°C
Initial Batch Volume	19.5	L
Sat. Steam Temp. in Evaporator	70	°C
Sat. Product Vapour Temp.	60	°C
Tube Length	2000	mm
No. of Tube	1	
Wall Thickness	1.2	mm
Inner Tube Diameter	23	mm
Outer Tube Diameter	25.4	mm
Calculation Section Length	100	mm

Table 5.4 Additional processing information for case study 2

Inlet Product Density	1107.2620	kg m^{-3}
Initial Product Mass Flow	0.04983	kg s^{-1}
Solid Mass	6.8010	kg
Water Mass	14.7816	kg
Sat. Steam Pressure	31.25	kPa
Sat. Product Pressure	19.88	kPa

The model will then proceed to calculate the increase in total solids over time from the evaporator as shown in Figure 5.8.

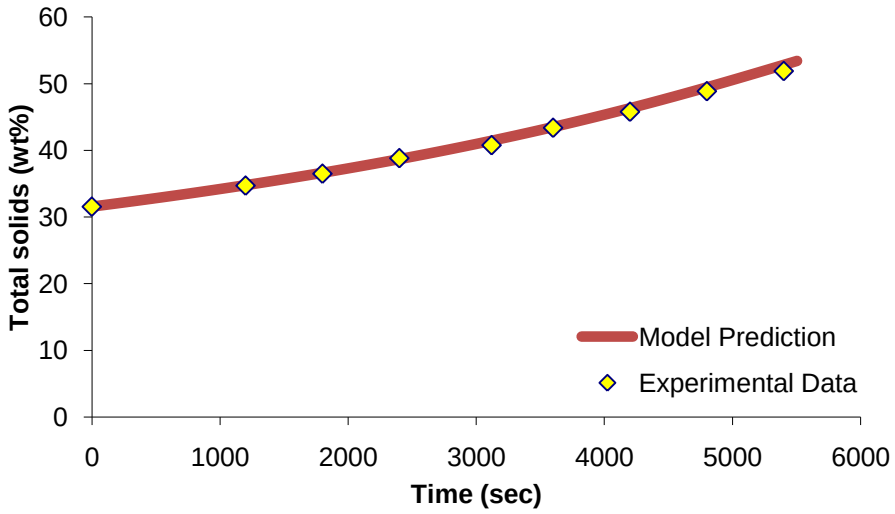

Figure 5.8 Comparison between the steam heated pilot evaporator model and the experimental data in case study 2

Once again the pilot evaporator model fitted the experimental data rather accurately with R^2 of 0.9990. In total, 31107 step calculations were required to create the plot in Figure 5.8

From the 2 case studies above, they have proven that the steam-heated pilot evaporator model is working well. The model is able to predict the total solids at any given processing time accurately given that the initial conditions and parameters are provided. Also, the modelling of milk viscosity and the correlation of overall heat transfer coefficient with flow characteristic played important roles in calculating the residence time and the rate of water evaporated.

5.6 Influence of viscosity on film thickness and average flow velocity

At this stage, the changes of film thickness and average velocity within the tube with solids content are illustrated in Figure 5.9. The progression of the average fluid velocity and the film thickness with apparent viscosity are based on the conditions found in section 5.5.1.

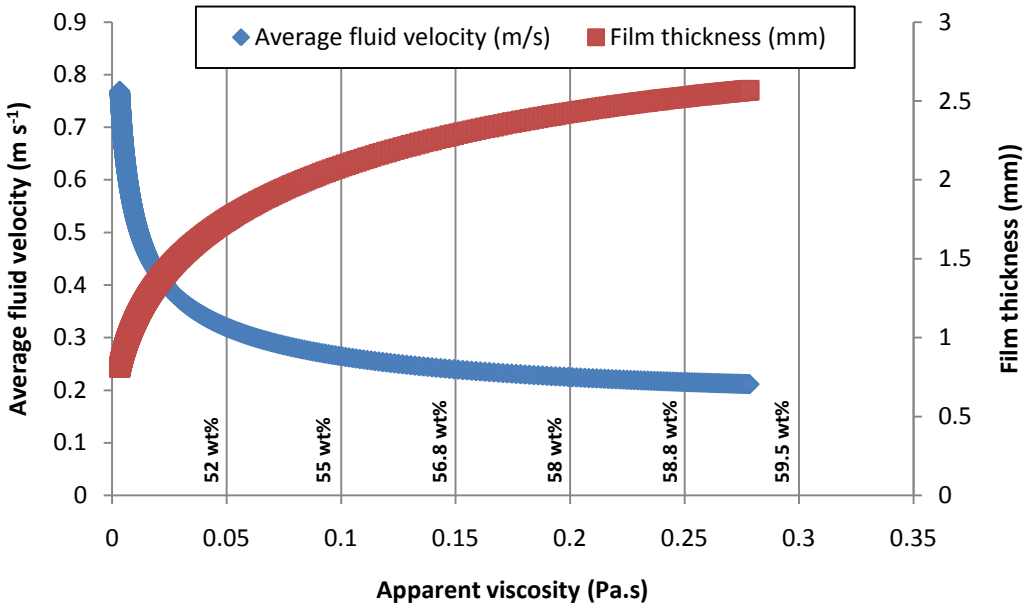

Figure 5.9 Influence of viscosity on average fluid velocity and film thickness with a evaporation tube.

In Section 4.4.1, shows that the mass flow rate of the feed is influenced by the viscosity considerably and the reduction in mass flow rate would bring about decrease in liquid load. According to Equation (5.9), the decrease in liquid load should result in thinner film. However, the rate of increase in viscosity surpassed that of decreasing liquid load. Therefore, this results in the overall thickening of film. The consequence of a thicken film reduces the fluid velocity within the evaporation tube as well. Based on the trend in Figure 5.9, the film thickness should plateau close to 3mm while fluid velocity stabilise at around 0.8 m s^{-1}.

5.7 Applications to commercial evaporator

The fundamental principles of the steam-heated pilot evaporator model are identical with the commercial falling film evaporators. The difference lies on the logic behind the sequence of calculations. In a commercial evaporator, milk normally passes through each effect only once; therefore, no recirculation needs to be incorporated into the calculation logic. This made the logic of a single pass falling film evaporator simpler as illustrated in Figure 5.10. For a multi-effect evaporator, the logic in Figure 5.10 is arranged in series, where the end of one effect would be the beginning of the other. A similar model on commercial multi-effect evaporator was created by Dr Sean Lin based on the same principles (unpublished software).

A point to note, the heat transfer within each effect varies in a multi-effect evaporator as the quality of steam (that ultimately affects the temperature difference) and the concentration of milk differs. Heat transfer assessment is required to be conducted on each individual effect to establish the overall heat transfer coefficient relationship with the flow characteristics of milk in order to create a more accurate model.

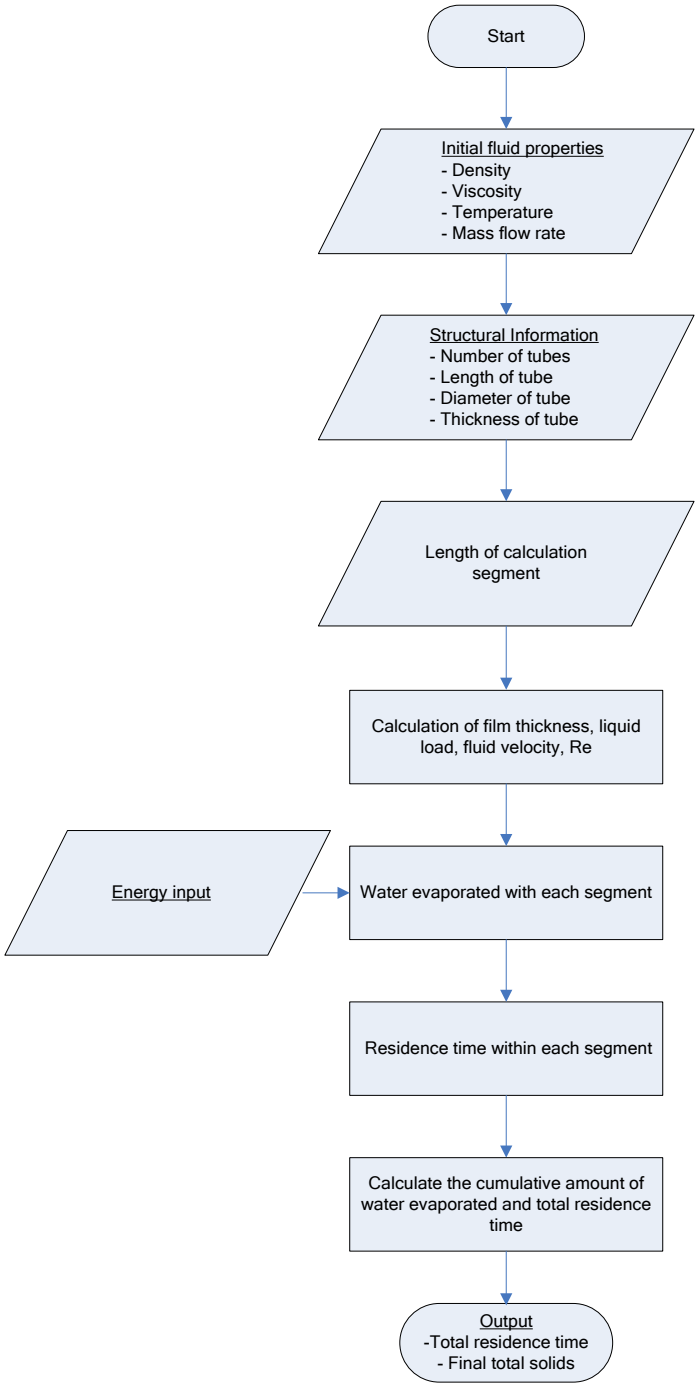

Figure 5.10 Schematic diagram of the calculation flowsheet of a single effect single pass falling film evaporator mode

5.8 Conclusions

To conclude, a simple model established on the steam-heated pilot evaporator was able to accurately predict the total solids of skim milk concentrate at any given time provided that the initial conditions and parameters are given. The viscosity models and the heat transfer coefficient relationship with flow characteristic found in earlier chapters were also proven to be valid as they worked flawlessly in the evaporator model. The fundamental principles of the pilot evaporator model can be directly applied to a commercial multi-effect falling film evaporator with minimal changes to the calculation flowsheet.

5.9 Nomenclature

A_x	Cross-sectional area	m^2
d_i	Tube inner diameter	m
F	Mass flow rate of feed	$kg.s^{-1}$
g	Gravitational acceleration	$m.s^{-2}$
L_s	Section length	M
m	Mass flow rate	$kg.s^{-1}$
m_s	Mass of solids	kg
m_w	Mass of water	kg
s_0	Film thickness	M
t_c	Accumulative residence time	s
t_r	Residence time	s
U	Overall heat transfer coefficient	$W.m^{-2}K^{-1}$
V	Mass flow rate of vapour	$kg\ s^{-1}$
v_f	Film velocity	$m\ s^{-1}$
x_F	Solid mass fraction of feed	-
x_P	Solid mass fraction of product	-
η	Viscosity	Pa.s
Γ	Mass flow rate per unit perimetric length	$kg.m^{-1}s^{-1}$
ρ	Density	$kg.m^{-3}$

5.10 References

Billet, R. (1989). *Evaporation technology : principles, applications, economics* New York: VCH Publishers.

CHAPTER SIX: CONCLUSIONS

6.0 CONCLUSIONS

The objectives of the studies from this research project are to improve the understanding of the rheological behaviour of skim milk under various conditions and their influence on the heat transfer and operation of a falling film evaporator. The results have proven that the viscosity measurements are repeatable and producible. This ensures that the reliability of the measurements and the accuracy of the viscosity models derived from them. The influence of flow characteristics on heat transfer within a falling film evaporator was also assessed using a custom made electric-heated pilot evaporator. With the viscosity models and heat transfer information gathered from the earlier chapters, a model for the steam-heated evaporator emerged and verified. Overall summary and conclusions based on the studies in this thesis and recommendations for future work are described here for individual chapters.

CHAPTER 2

Conclusions

- Milk in general is classified as a suspension where protein (mainly casein) and fat globules suspended in lactose solution.
- Majority of the physical properties of milk are highly sensitive to concentration and temperature.
- The protein in milk induces the lowering of surface tension of milk, this in turn results in a more stable bubble formed during the evaporation process.
- In previous studies where milk substitutes (predominantly reconstituted milk) were used, some of the milk substitutes may have different properties compared to the fresh milk. Therefore, the use of milk substitute has to be thoroughly evaluated before commencing experiments with the intention of illustrating a representation result of fresh milk.

CHAPTER 3

Conclusions

- The viscosity measurement protocol discussed in this thesis has proven to be reproducible and repeatable.
- The solids content measurement method used in the earlier part of this project (a method adopted from IDF standard 21B: 1987) is only accurate up to 40wt%. Beyond 40wt%, the Australian standard AS2300.1.1, which involved with the use of sand when drying, has been demonstrated to be more suitable.
- Fresh skim milk concentrate subjected to 24 hours of cold storage prior to evaporation may produce different viscosity profiles as compared to fresh milk that is evaporated immediately.
- Results has proven that skim milk concentrate of less that 30wt% produces no significant difference in viscosity profiles even when they are subjected to 24 hours of cold storage.
- The preliminary viscosity measurements results from the “pot” evaporator shows that the viscosity profile of are almost the same for UHT, reconstituted and market milk but fresh milk from the factory seems to produce a higher viscosity profile.
- The viscosity measurements gathered from the “pot” evaporator may not be representative as the milk concentrate were subjected to prolong heating and they remain stagnant throughout the entire experiment which may induce age-thickening.
- The custom made steam-heated pilot evaporator is able to operate as low as -85 kPa (gauge) on the product side and -70 kPa (gauge) on the steam side with ease. These operation conditions mimic the actual commercial evaporators.
- The steam-heated pilot evaporator is also able to produce skim milk concentrate of consistent viscosity profiles and reach total solids of 58wt%.

- Viscosity models that correlate influencing factors like total solids, temperatures and shear rates were created for reconstituted and fresh skim milk. They were verified with the experimental data and have proven to be accurate ($R^2 > 0.97$).
- On the whole, the viscosity of reconstituted skim milk remains almost identical to the fresh milk up to 43wt%, there after, the viscosity of reconstituted skim milk reaches twice as high as fresh skim milk. This shows that reconstituted skim milk does not display the true viscosity of fresh skim milk and it may not be suitable to be used as a milk substitute.
- On the other hand, the viscosity profiles of medium and low heat-treated fresh skim milk do not have any significant differences.
- The influence of temperature and shear rate becomes increasingly significant to the viscosity measurement with rising solids content.

CHAPTER 4

Conclusions

- The overall heat transfer coefficient (OHTC) of the steam–heated pilot evaporator ranged from 1.3 to 2.5 $kW.m^{-2}K^{-1}$ during the evaporation of fresh medium heat treated skim milk from 30wt% to 57wt%.
- When Re is above 130, the OHTC maintained at 2.5 $kW.m^{-2}K^{-1}$. This corresponded to the evaporation of skim milk concentrate up to 46wt%. Below Re 130, the OHTC decrease exponentially.
- The design of the electric-heated pilot evaporator is more complex than the steam-heated counterpart as the entire system is subjected to pressure as low as -85kPa (gauge). The film distribution system has to be redesigned because the film has to flow on the outer wall of a electric heater instead of flowing inside a conventional tube.
- With the film flowing outside the electric heater, the evaporation process can be observed through the perspex casing of the evaporation column.

- On the electric-heat pilot evaporator, reconstituted medium-heat treated skim milk displayed a difference heat transfer coefficients to Re trend compared to the fresh counterpart. The reconstituted skim milk maintained at around 3.75 $kW.m^{-2}k^{-1}$ regardless of heat flux and Re. On the other hand, the fresh skim milk displayed a positive linear relationship between the HTC and Re. When 100 <Re<500 , the HTC rose from 3.0 to 6.0 $kW.m^{-2}k^{-1}$. This has again indicated that reconstituted milk may not be suitable to represent heat transfer of fresh milk in a evaporator.
- The HTC almost doubled when the protein content of the sucrose-protein solution increased from 0 to 0.9wt. Furthermore, the influence of heat flux becomes greater with increasing protein content. Only minor improvement in HTC was observed when the flow rate was increased from 4 to 10 $L.min^{-1}$ except for pure sucrose solution where HTC doubled from 1.5 to 3.0 $kW.m^{-2}k^{-1}$ between 7 to 10 $L.min^{-1}$. From the results, it was concluded that protein content determines the degree of influence by heat flux and flow rate have on the heat transfer.
- The study of the photographs taken indicates that the amount of bubbles formed generally increases with protein content, flow rate and heat flux although level of increment differs with protein content as well.

CHAPTER 5

Conclusions

- A evaporator simulation model on the steam-heated pilot evaporator was created based on fundamental principles of heat and mass transfer. This simulation model incorporates the skim milk viscosity model and the overall heat transfer coefficient correlation from chapter 3 and 4.
- The simulation model is verified with the experimental data and is able to predict the total solids and calculate the flow conditions within the evaporation tube at any given time during the evaporation process.
- This simulation model, with some changes to the calculation logic, can be used onto a commercial falling film evaporator. This simulator will be

helpful to simulate the flow conditions and heat transfer within a falling film evaporator.

APPENDIX

A.1 VISCOSITY CONVERSION

Viscosity

Traditional cgs Unit:	poise (P)
	1 centipoise (cP) = 0.01 poise
SI Metric Unit:	pascal second (Pa.s)
Conversion Factors:	1P = 0.1 Pa.s
	1 Pa.s = 10 P
	1 cP=0.001 Pa.s = 1 mPa.s
	1 Pa.s = 1000cP

Kinematic Viscosity

Traditional cgs Unit:	stokes (St)
	1 centistokes (cSt) = 0.01 stokes
SI Metric Unit:	square metres per second ($m^2.s^{-1}$)
Conversion Factors:	1 St = 1×10^{-4} $m^2.s^{-1}$
	1 $m^2.s^{-1}$ = 10 000 St
	1 cSt = 1×10^{-6} $m^2.s^{-1}$ = 1 $mm^2.s^{-1}$
	1 $m^2.s^{-1}$ = 1 000 000 cSt

Viscosity in centipoise = kinematic viscosity in centistokes × density of fluid being measured, all measured at the same temperature.

A.2 CONTROL SOLUTIONS

Type of Milk Powder

Medium heat skim milk powder (34% Protein (Dry Basis) and 1.1% Fat) from Warrnambool Cheese & Butter Factory

Moisture content of Milk Powder

4.44 wt% (see Section 3.4.3.5)

Total solids of Milk Powder

$$TS\ (wt\%) = \frac{\left(\frac{(100 - MC)}{100}\right) \cdot P}{S} \tag{3.2}$$

	1	2	3	4
Powder (g)	225.98	273.06	178.33	375.68
Beaker (g)	295.01	295.06	212.18	295
Total (g)	1043.08	903.13	586.86	941.6
Water (g)	522.09	335.01	196.35	270.92
Total Solids (wt%)	28.87	42.91	45.48	55.52
Error (wt%)	0.12	0.18	0.19	0.23

Control solution (28.82 wt%)

	Drying Hours					
Sample	**2**	**3**	**4**	**5**	**6**	**24**
1	29.2527	29.0309	28.90521	28.9140	28.8354	28.4458
2	29.0243	28.9354	28.7138	28.7316	28.6477	28.2918
3	29.1266	28.8978	28.8550	28.7239	28.6675	28.2659
4	29.1354	29.0163	28.9057	28.8525	28.7686	28.3239
Std Dev	0.093	0.064	0.091	0.093	0.088	0.080
1.96 σ	0.183	0.125	0.178	0.183	0.173	0.156
Average	29.135	28.970	28.845	28.805	28.730	28.332

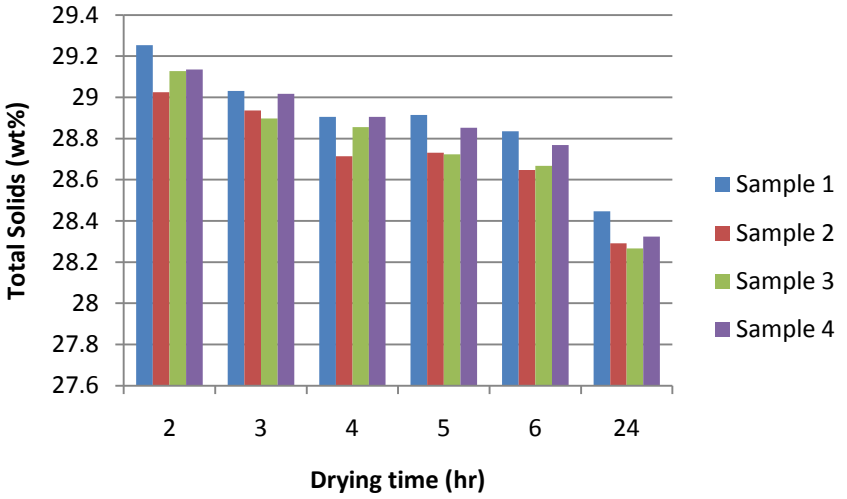

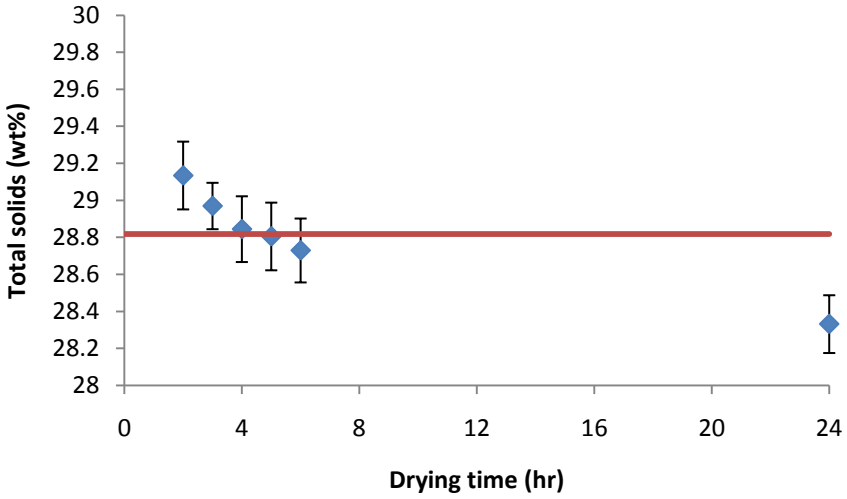

Control solution (42.84 wt%)

	Drying Hours					
Sample	**2**	**3**	**4**	**5**	**6**	**24**
1	43.0630	42.8444	42.7021	42.6248	42.5238	41.8843
2	43.3681	43.1215	43.0037	42.8800	42.8383	42.0919
3	43.5892	43.2167	43.0895	42.9136	42.7800	42.0137
4	43.9406	43.5515	43.3110	43.1732	43.0416	42.0479
Std Dev	0.370	0.292	0.252	0.224	0.213	0.089
1.96 σ	0.725	0.572	0.494	0.440	0.418	0.175
Average	43.490	43.184	43.027	42.898	42.796	42.009

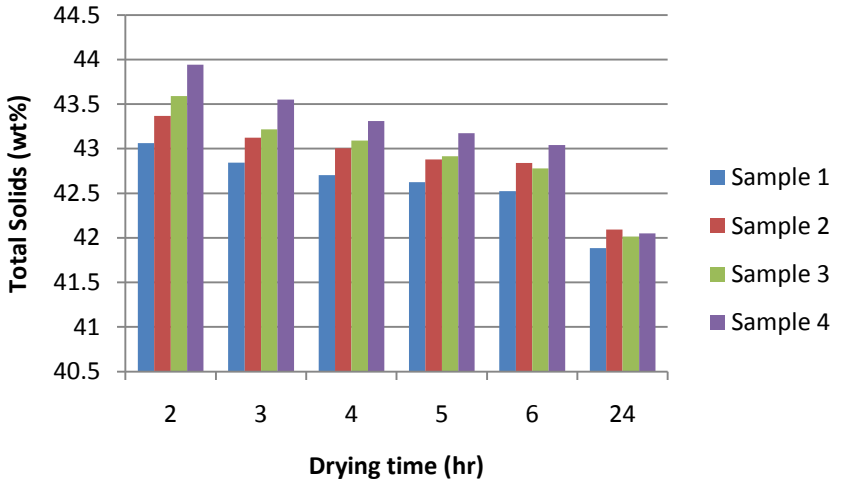

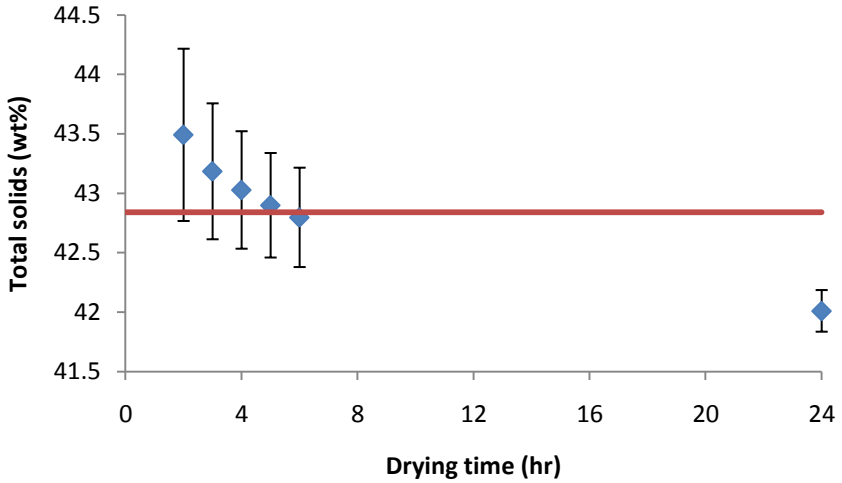

Control solution (45.26 wt%)

	Drying Hours					
Sample	**2**	**3**	**4**	**5**	**6**	**24**
1	45.6672	45.6526	45.6321	45.4772	45.4988	44.8010
2	45.8441	45.7613	45.4900	45.3875	45.3061	44.7873
3	46.1558	45.8030	45.6254	45.4667	45.4211	44.7441
4	46.4332	46.0626	45.7752	45.5785	45.4819	44.6220
Std Dev	0.339	0.174	0.116	0.078	0.087	0.081
1.96 σ	0.664	0.341	0.228	0.154	0.171	0.160
Average	46.025	45.820	45.631	45.477	45.427	44.739

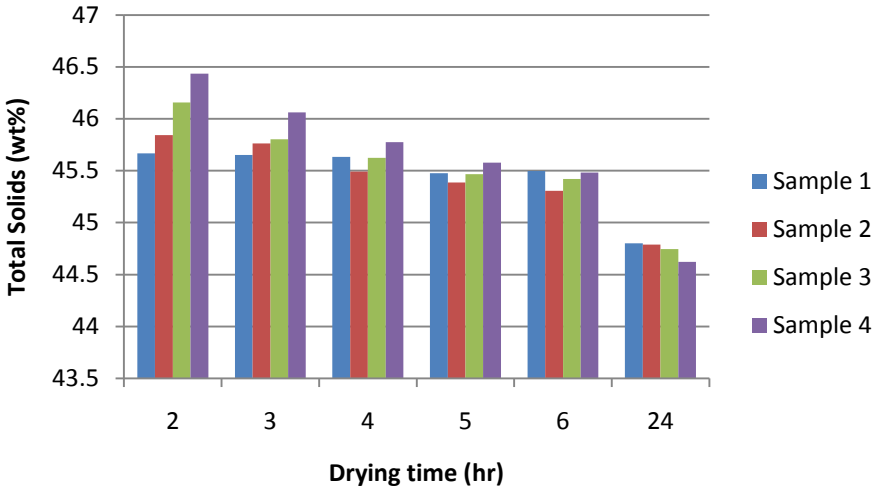

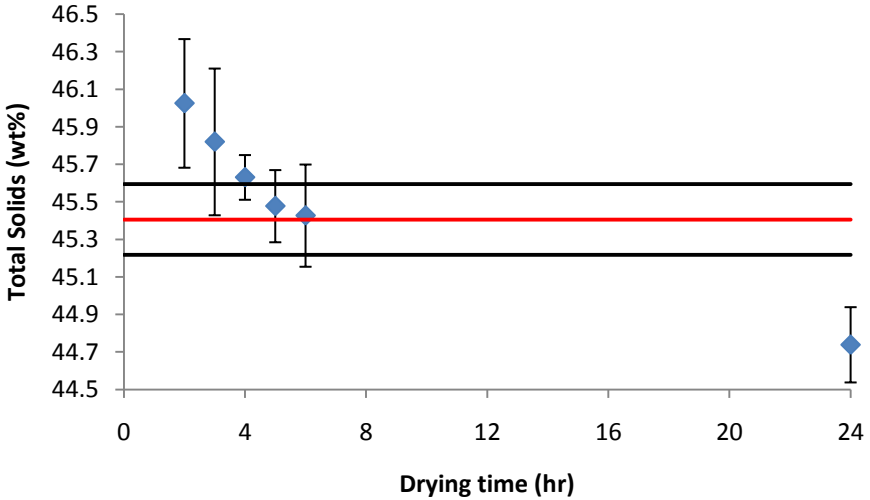

Control solution 55.43 wt%

	Drying Hours					
Sample	**2**	**3**	**4**	**5**	**6**	**24**
1	57.25079822	57.11533138	57.12345201	57.06956056	57.12086817	56.23055202
2	57.30281568	57.20761331	57.19571301	57.19535239	57.21338315	56.37495312
3	57.30476457	57.09959557	57.05745913	56.99445138	57.0409196	56.27025601
4	57.6323269	57.52820193	57.17071748	56.98146101	56.88547609	56.12743269
Std Dev	0.174895409	0.19945216	0.060811937	0.098109632	0.1389813	0.102342573
1.96 σ	0.342795001	0.390926233	0.119191396	0.192294879	0.272403348	0.200591444
Average	57.37267634	57.23768554	57.13683541	57.06020634	57.06516175	56.25079846

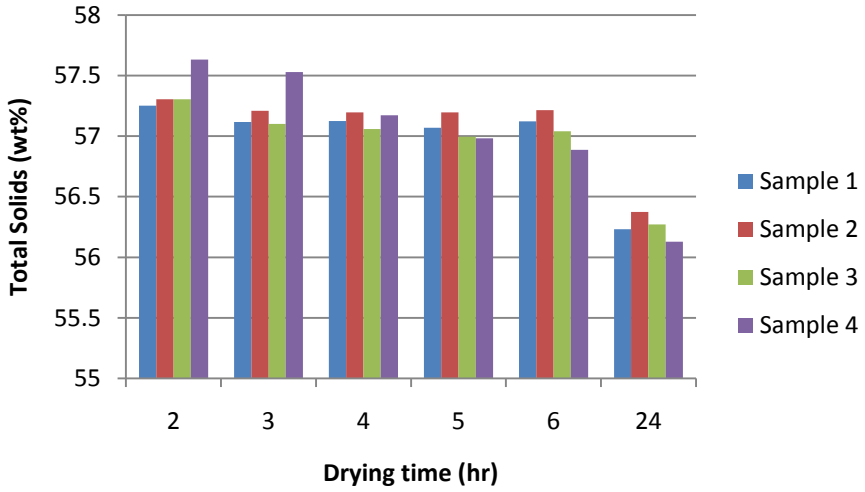

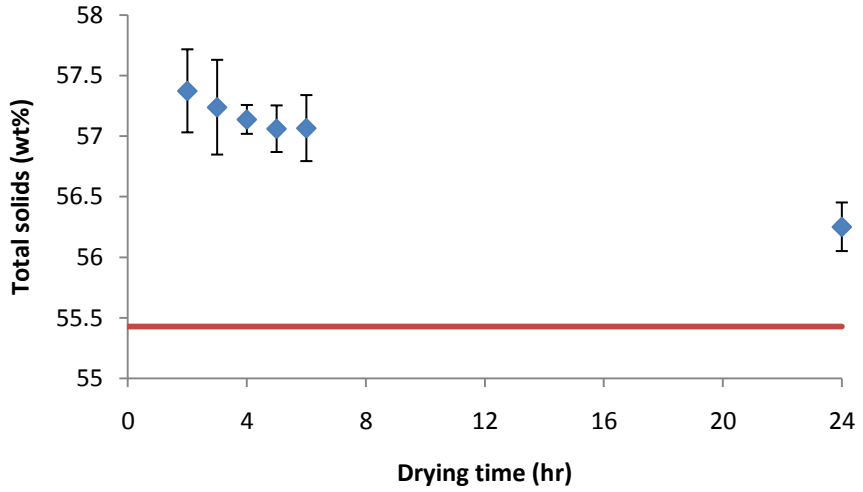

A.3 PRESSURE DROP CALCULATION EQUATIONS ACROSS PREHEATER

Reynolds Number, Re

$$Re = \frac{dV\rho}{\mu}$$

where d is the inner diameter of the tube (m), V is the average velocity (m.s^{-1}), ρ is the density of experimental fluid (kg.m^{-3}) and μ is the viscosity of experimental fluid (Pa.s)

Euler Number, Eu

$$Eu = \frac{\Delta P}{2\rho V^2}$$

where ΔP is the pressure drop across the spiral tube (N.m^{-2}).

Equivalent diameter, D_{eq}

$$D_{eq} = \frac{L_c}{n\pi}$$

where L_c is the length of the spiral tube (m) and n is the number of turns in the spiral tube

Geometrical number of a regular-helical coil, G_{rhc}

$$G_{rhc} = \frac{d^{0.85} D_{eq}^{0.15}}{L_c}$$

The correlations

$$EuG_{rhc} = 21.88Re^{-0.9} \quad \text{Re} < 500$$

$$EuG_{rhc} = 5.25Re^{-2/3} \quad 500 < \text{Re} < 6300$$

$$EuG_{rhc} = 0.56Re^{-0.4} \quad 6300 < \text{Re} < 10{,}000$$

$$EuG_{rhc} = 0.09Re^{-0.2} \quad 5\text{Re} > 10{,}000$$

Reference:

Ali, S. (2000). Pressure drop correlations for flow through regular helical coil tubes. *Fluid Dynamics Research* 28: 295 - 310.

A.4 BENCH TOP EVAPORATOR

The aim was to design a bench top evaporator (about 5 litres) that is able to operate under similar conditions as the industrial evaporators and measure the heat transfer coefficient during the evaporation process before scaling it up into pilot scale.

To mimic an actual falling film evaporation process, the milk can no longer remain static like the "pot" evaporator. A circulation system was required to keep a constant flow of milk along the heat transfer surface. Conventional design of a falling film evaporator has its heat source, usually steam, on the shell side while the product liquid film flows on the tube side of the evaporator. With this configuration, the measurement of wall temperatures on product side became a difficult task as the welding of thermocouples on the inside wall of a tube was virtually impossible. Therefore, the position of heat source and product stream were inverted (product film flows on the outside of the tube whereas the heat source stays in the tube) in the bench top evaporator design. With this design, thermocouples can be attached on the wall easily and boiling mechanism could be observed from the transparent casing.

Steam heating was not considered in the design as it was not practical to be incorporated into such a small evaporator. Hence, a electric cartridge heater (Helios cartridge heater, Ø 20mm × 200mm of heating length, 600W) was chosen as the heat source. The amount of energy released by the heater was controlled by a variac (also know as variable transformer). A custom made 316 stainless steel sleeve wraps around the heater that forms the heat transfer surface for the product and a small well on top of the heater (as shown in Figure 0.1). An overflow mechanism was applied to the distribution system where the process fluid floods the well on top of the heater and overflows onto the sleeve. This creates a flowing film of process fluid on the sleeves that imitates the falling film in a falling film evaporator.

The key challenges of designing this evaporation system lies on the ability to pump liquid out of a high vacuum environment (-80 kPa gauge) and the material of construction. In the early stages of the design, the storage tank was intended to be kept under atmospheric pressure while the evaporator operates at –80 kPa (gauge). The means of pumping the process liquid out of the evaporator was through a peristaltic pump (Masterflex L/S Ecomomy Digital Console Pump System). To observe of the boiling mechanism in the evaporator, the casing of the evaporator had to be transparent. Therefore, only glass and clear plastic were taken into consideration when the design of evaporator casing. At first, glass was preferred over plastic due to its high thermal resistivity (well over 1000°C) and the glass tube (Monash Scientific, 110mm OD and 100mm ID × 300mm length) withstood the initial pressure test (-80 kPa gauge) on the bench top evaporator.

When the bench top evaporator was assembled and tested, problems emerged. Firstly, the peristaltic pump was unable to drain the liquid out of the evaporator fast enough and the performance of the pump deteriorate with time as the tube in the peristaltic pump got worn off. Secondly, the glass tube cracked during the evaporation process. It was observed that the cracks propagate from the bottom of the glass tube where it was in contact with the process fluid. The possible reason for the structural failure of the glass tube could be due to the non-uniform thermal expansion where it was in contact with the process fluid.

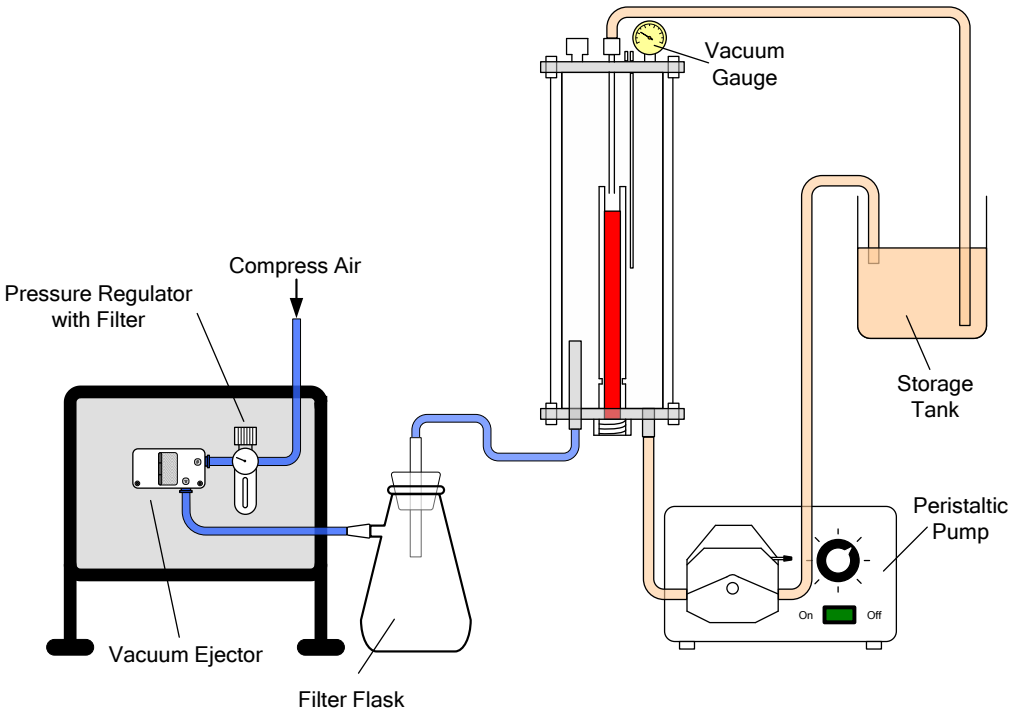

Initial design of the bench top evaporator

Thereafter, the design of the bench top evaporator was revised. The storage tank was then integrated into the evaporator so that the entire system operates under vacuum. Since the differential in pressure was eliminated from the system, the only requirement for the pump was to have air tight casing (March Pump, AC-2CP-MD). The glass tube was also replaced with perspex tube which proved to be more duration than the glass counterpart.

After the preliminary trials on the bench top evaporator were satisfactory, 6 thermocouples were installed into the evaporator as illustrated in Figure 0.1. Two thermocouples were soldered onto the sleeve to monitor the wall temperature and another two thermocouples were inserted between heater and the sleeve to keep track of the heater temperature. The temperatures of the process fluid inlet and ambient temperature around the sleeve were also monitored.

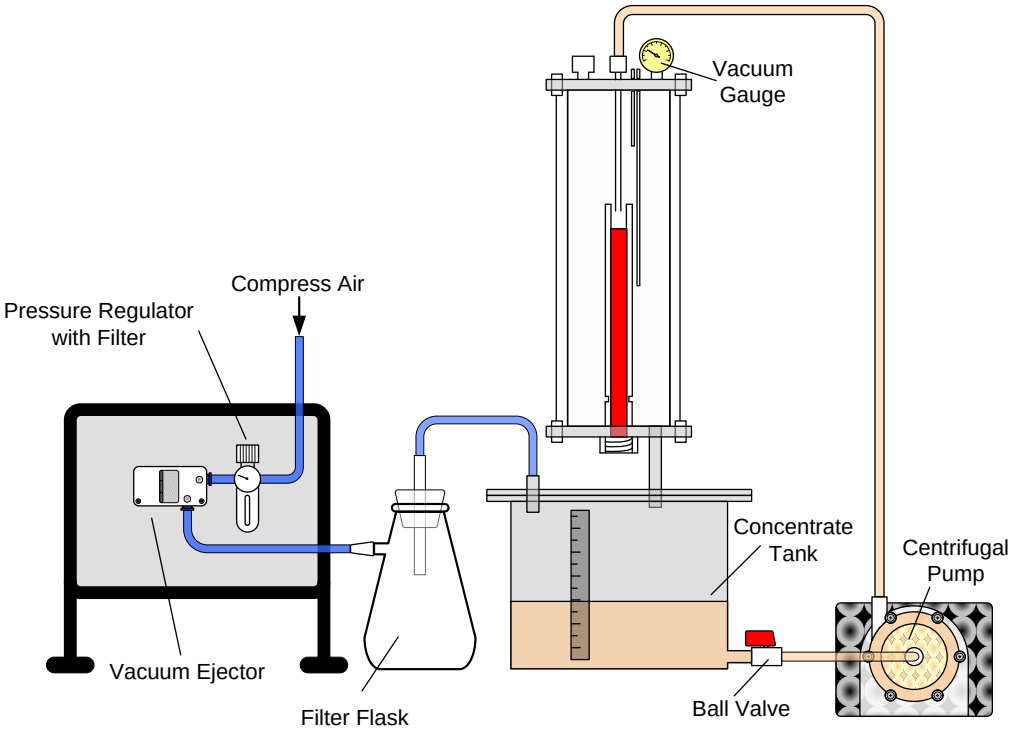

Layout of the bench top evaporator

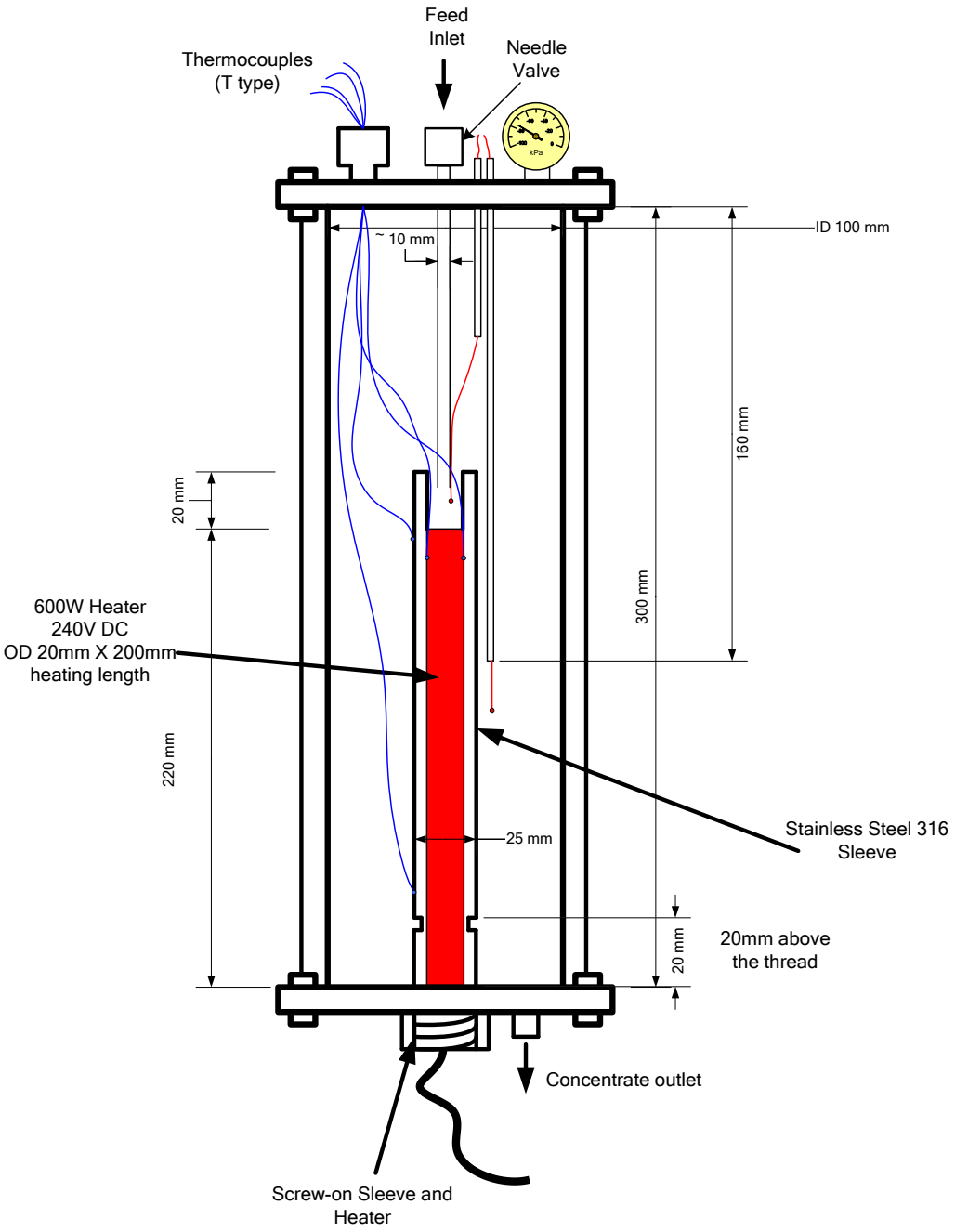

Figure 0.1 Schematic drawing of evaporation chamber

Operation of bench top evaporator

About 3-5L of milk was poured in concentrate tank. The vacuum ejector and the centrifugal pump were then turned on. Once the milk starts to circulate, the heater was switched on. As the milk reaches its boiling point, the mixture of steam and milk from the evaporator chamber travels to the concentrate tank. The steam would be pull out by the vacuum ejector and condense in the filter flask while the milk gets recirculated back into the system.

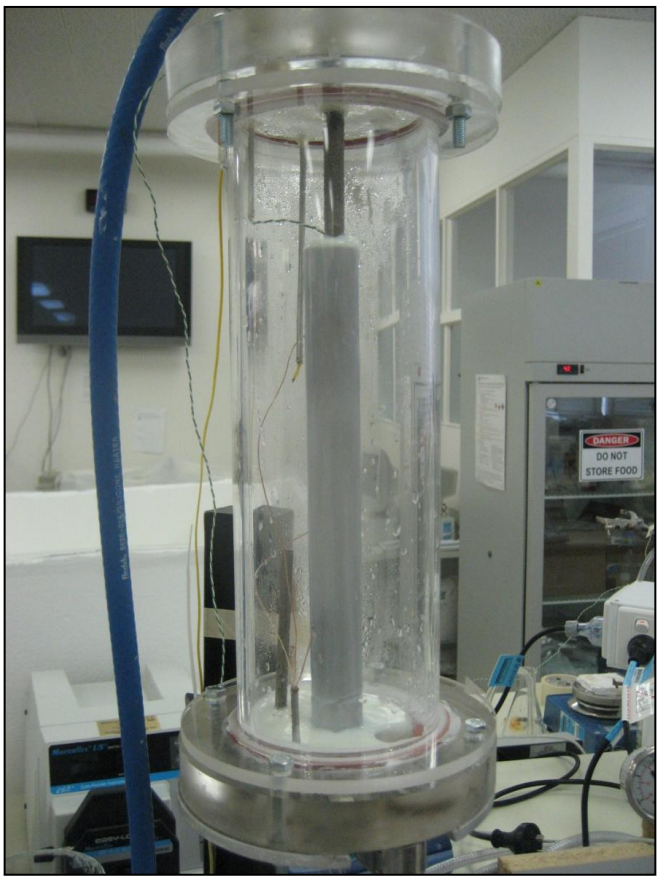

Evaporation chamber of bench top evaporator

No experimental data was collected as the scale of this evaporator was too small to measure any reliable information. However, the bench top evaporator had demonstrated the feasibility of some of the design ideas. These ideas include the uniform liquid film formation and most importantly, the evaporation of water from the system. A scaled up and improved version of the bench top evaporator was later constructed (See section 4.3.1).

A.5 BUBBLING TRENDS

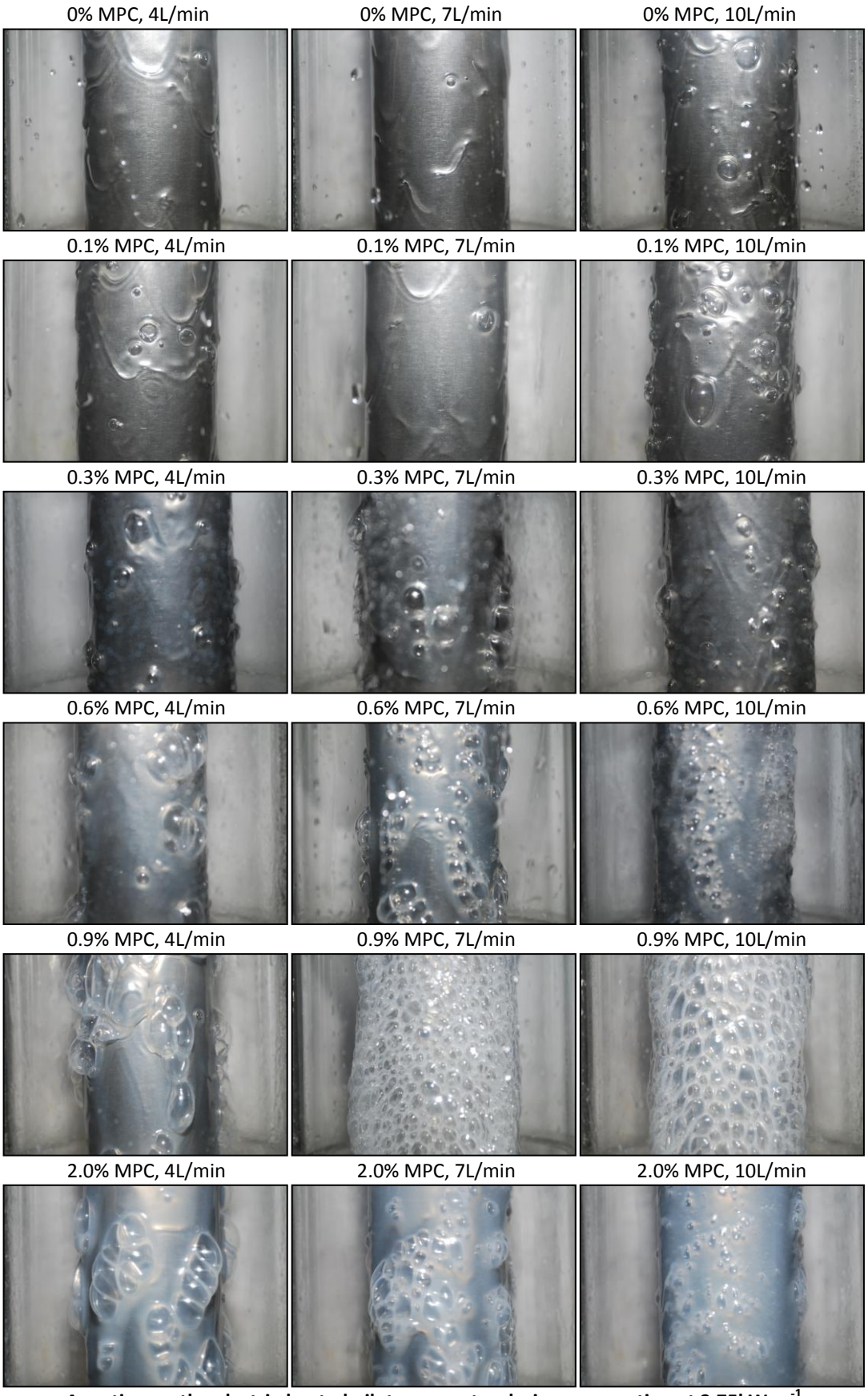

A section on the electric-heated pilot evaporator during evaporation at 3.75kW m^{-1}

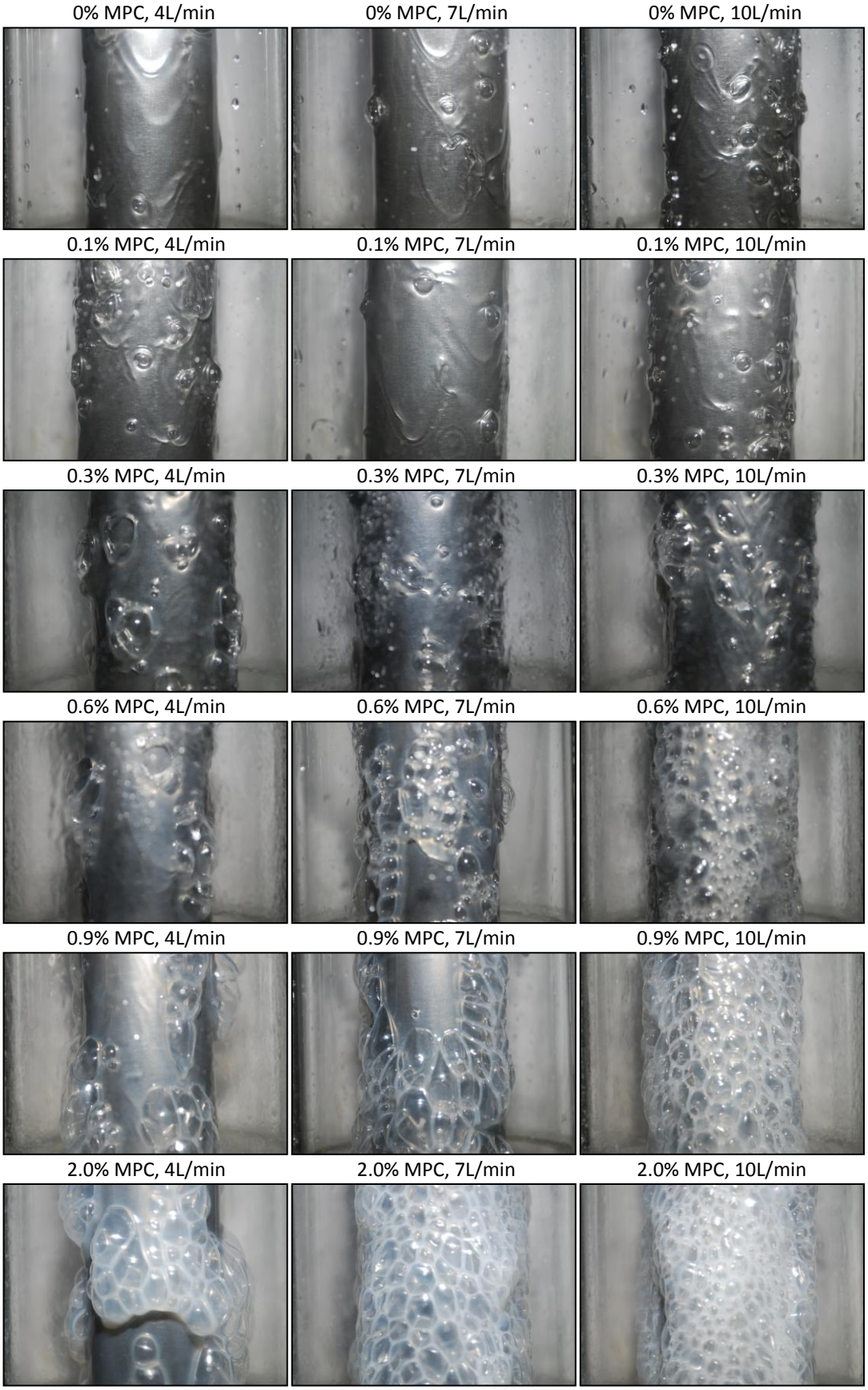

A section on the electric-heated pilot evaporator during evaporation at 6.25kW m^{-2}

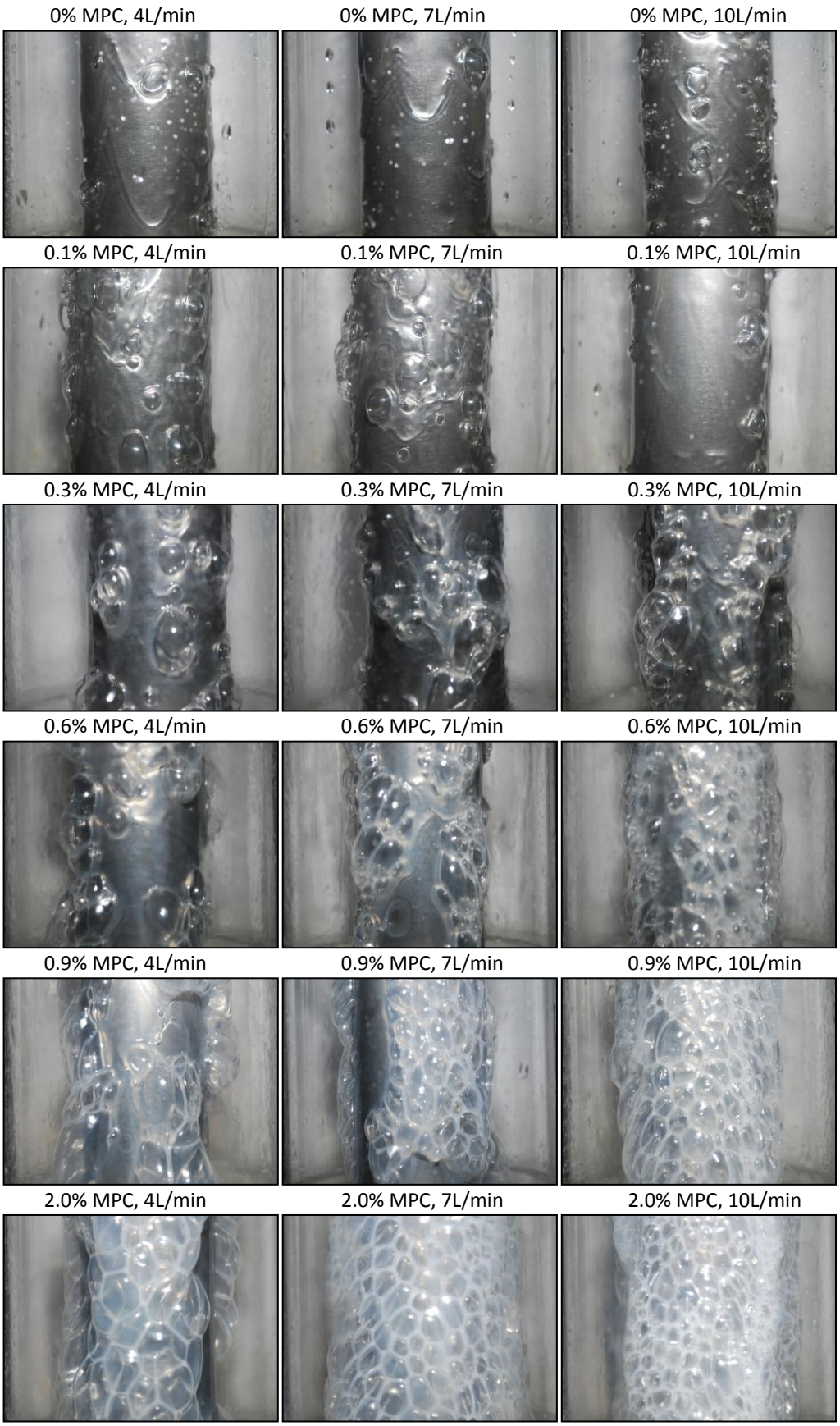

A section on the electric-heated pilot evaporator during evaporation at 8.75kW m^{-2}

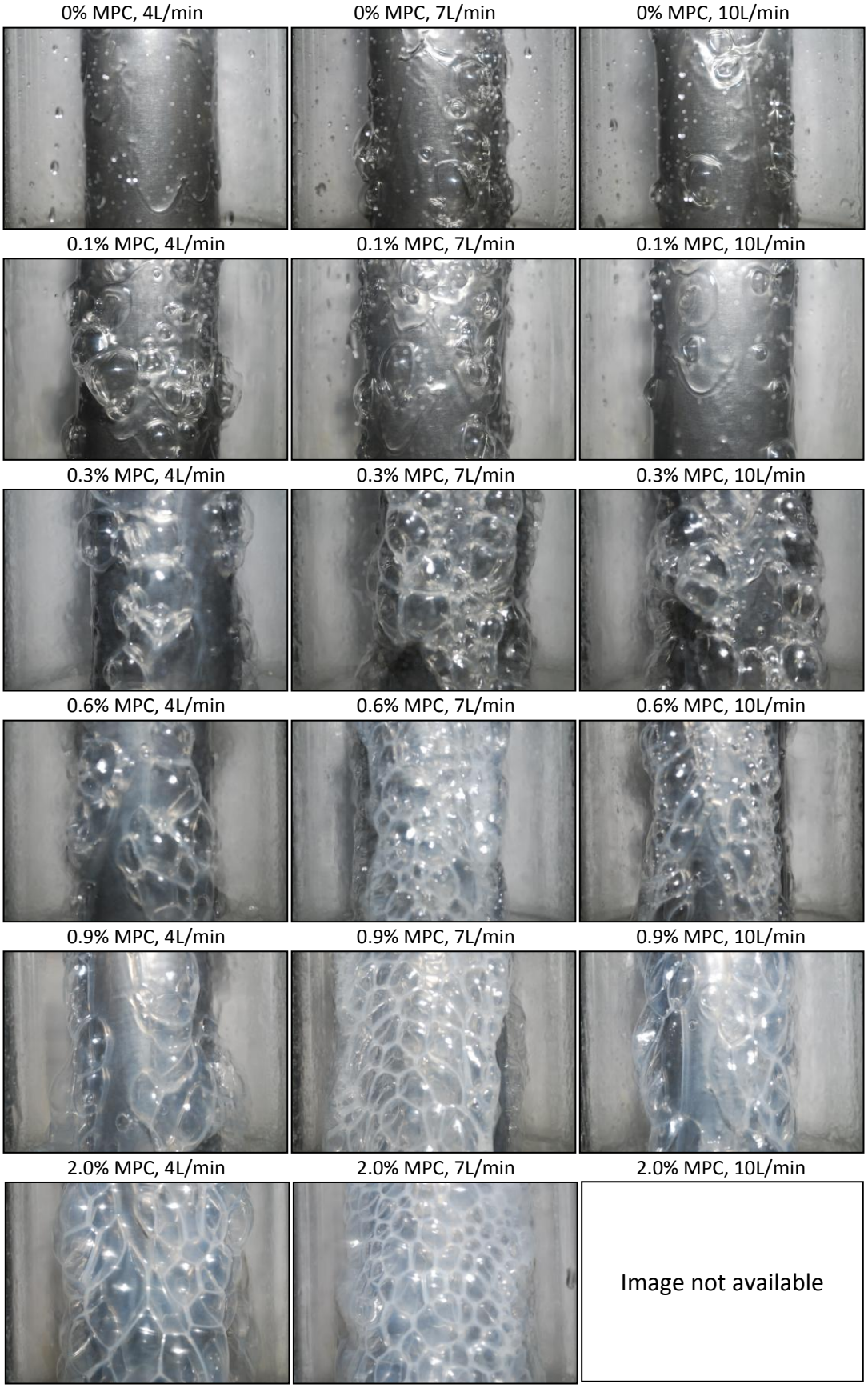

A section on the electric-heated pilot evaporator during evaporation at 11.25kW m^{-2}